DIFFUSIONAL INFLUENCES ON CATALYST ACTIVITY AND SELECTIVITY DURING CATALYST DEACTIVATION IN STEAM DEALKYLATION OF TOLUENE ON RHODIUM/ALUMINA CATALYST

A Thesis Submitted
In Partial fulfilment of the Requirements
for the Degree of
DOCTOR OF PHILOSOPHY

by

OMAR SALIM AL-AYED

to the

DEPARTMENT OF CHEMICAL ENGINEERING
INDIAN INSTITUTE OF TECHNOLOGY, KANPUR

JULY, 1989

ACKNOWLEDGEMENT

I wish to express my profound gratitude to Professor Deepak Kunzru. He has been a constant source of inspiration and help at every stage of this work. I will never be able to find the words which will express my feelings to him.

This work will not be complete without thanking Professor D.N.Saraf for allowing me to use the HP-1000 computer at any time and Professor Anil Kumar who asked every morning "how is your work",his help is acknowledged and not to be forgotten.

Those who have been to me more than parents are not to be forgotten and must be remembered all the time, Uncle, Aunty,Sarita and Raju, and those who don't want their names to be written here. I acknowledge and appreciate the help rendered to me by friends,Babji and his wife. Also I must thank Mr. Sohan Lal and Dada for their kind help at each stage of this work.

The help and freedom rendered to me by the Department of Chemical Engineering will remain in my heart for ever.

Omar Al-Ayed

CONTENTS

LIST OF TABLES

LIST OF FIGURES

NOMENCLATURE

a_i Activity of reaction i, dimensionless.

B(i,j) Collocation matrix

C_{Ab} Bulk concentration of a component A ,kmol/m^3

C_{p_i} Heat capacity of component i , J/(mol.K.)

$C_{i,j}$ 25x25 Matrix defined in equation (4.87)

d_i Activity order of reaction i.

$D_{eff,i}$ Effective diffusivity of component i, m^2/h.

$\bar{E}_i$ Parameter defined in equation (4.20).

E_i Activation energy of reaction i , kJ/kmol.

E_j Heat of adsorption of component j , kJ/kmol.

$\bar{E}_{ad,i}$ Heat of adsorption of component i.,kJ/kmol, defined in eqn. (4.21).

F_{jo} Inlet flow rate of component j ,kmol/h.

$(\Delta H)_{overall}$ Overall heat of reaction ,J/kmol.

$(\Delta H)_i$ Heat of reaction i, J/kmol.

k_i Reaction rate constant of reaction i, kmol/(kgcat) (h)/ $(atm)^n$.

k_{io} Preexponential frequency factor of reaction i. kmol/kgcat.h

K_j, K'_j, K''_j Equilibrium adsorption constants, J/kmol. (atm)

$K_{jo}, K'_{jo}, K''_{jo}$ Preexponential frequency factor of equilibrium adsorption constant. $(atm)^{-1}$

k_d Deactivation reaction rate constant. $(atm.\ h)^{-1}$

K Equilibrium of water gas shift reaction defined in equation (4.42).

k_{eff} Catalyst pellet thermal conductivity, W/(m)(K).

$\bar{K}_{io}$ Parameter defined in eqn (4.19).

M_j Molecular weight of component j .

P_j Partial pressure of component j,atm.

$p_j(i)$ Partial pressure of component j at the ith collocation point ,atm.

(p_j^e) Exit partial pressure of component j, atm.

r Radial distance,m.

R Inlet molar feed ratio of water/toluene.

r_c parameter defined in equation 4.65

R_i Reaction rate of reaction i, kmol/(kgcat)(h).

R_i^o Initial rate of reaction i, kmol/(kgcat)(h).

S_X Total external surface area of catalyst pellet, m^2.

S_j Selectivity of component j.

S Active site.

t Time,h.

T Temperature, K.

$\bar{t}$ Residence time in reactor,min, defined in eqn. (4.1) .

T^* Dimensionless temperature defined in eq. (4.22).

TOF_i Turnover frequency of reaction i., $(h)^{-1}$

V_P Pellet total volume, m^3.

W Weight of catalyst,kg.

x_T total conversion of toluene.

$\bar{X}$ Column vector matrix defined in equation (4.88).

GREEK SYMBOLS

β Thermicity factor defined in equation (4.66).

δ Moles of water/moles of toluene reacted .

ψ_i Deactivation function or reaction i.

Θ_j Fraction metal coverage of component j.

SUBSCRIPT

B	Benzene
b	Bulk
C	Carbon dioxide
CO	Carbon monoxide
H	Hydrogen
i	Reaction No., i= 1,2,3
j	Component number No., j=1,2,3,4,5,6
o	Reactor inlet conditions
T	Toluene
W	Water

SUPERSCRIPT

e	Exit
-	Average value
o	Fresh catalyst

SYNOPSIS

For the design of any catalytic reactor not only are the kinetics and selectivity of the main reaction important,but the effect of various process variables on the catalyst deactivation have also to be considered.Catalyst deactivation is important in any reactor design and optimization procedure and the interest in the area is reflected by the increase in recent years in the number of publications dealing with this subject. Intraparticle mass transport limitations combined with catalyst deactivation have a significant effect on the activity ,selectivity and life of the catalyst. Although the intrinsic deactivation kinetics has been determined for several single reactions,the experimental data for complex reactions,both in the diffusion-free and diffusion-influenced regime, is very limited. Even for simple reactions,the diffusion-deactivation interaction has been studied by very few investigators. To shed more light on the diffusion-deactivation interaction, this study was undertaken to experimentally measure the deactivation reaction kinetics of a complex reaction,under both diffusion-free and diffusion influenced conditions. The objective was to model the variation in activity and selectivity with time on stream for the diffusion-influenced pellet and compare this with the experimental values.The model reaction was taken to be steam dealkylation of toluene, a reaction of potential industrial significance.

The catalyst used in this study was rhodium on alumina.The metal loading was kept fixed at 0.4 wt% .The catalyst was prepared from rhodium trichloride by the method of excess solution. To provide uniform metal deposition,hydrochloric acid was used as a co-impregnant. For the intrinsic kinetic studies, the 3.2X3.2 mm

cylindrical pellets were impregnated, oxidized and then crushed to the desired size .

All the experimental runs were conducted in a gradientless, internal recycle reactor (Berty reactor) at atmospheric pressure in the temperature range of 663-723 K .The inlet water/toluene ratio and space time were varied from 1.11-14.8 mole water/mole toluene and 2.89-65.4 kgcat/kmol/h, respectively. The reactor effluent was quenched and the gas and liquid samples analyzed separately on 3 different columns using 2 gas chromatographs. The main reaction products were benzene,hydrogen, carbon monoxide and carbon dioxide together with traces of methane.

The catalyst deactivated with run time and the intrinsic kinetics for the main reactions were determined by extrapolating the data on crushed pellets to zero time.The experimental product distribution could be satisfactorily explained by the following three reactions:

$$CH_3-C_6H_5 + H_2O \longrightarrow C_6H_6 + CO + 2H_2 \quad (1)$$

$$CH_3-C_6H_5 + 7H_2O \longrightarrow 7CO + 11H_2 \quad (2)$$

$$CO + H_2O \rightleftharpoons CO_2 + H_2 \quad (3)$$

It was found that on increasing the inlet water partial pressure,the benzene selectivity (moles of benzene produced /mole of toluene reacted) showed a maximum. On the other hand,the rate of the reforming reaction (reaction 2) monotonically increased within creasing water partial pressure. Carbon monoxide had a marked inhibition effect on the rate of benzene formation.The rates of the the above three reactions were observed to be insensitive to the hydrogen partial pressure and decreased slightly with increasing benzene partial pressure.

The intrinsic kinetics of the three reactions were modeled using Langmuir-Hinshelwood rate expressions. For the dealkylation reaction, the model which assumed that water and toluene were adsorbed on different sites gave the best fit.The model choice was based on the findings of earlier workers,where it has been suggested that the support is the principal site for water activation,and the rate determining step is the migration of the hydroxyl group to the metal site, to react with the adsorbed toluene. It was observed that both the catalyst activity and product selectivities varied with time due to coke deposition. In order to explain the change in product selectivities,it was necessary to independently account for the activity of each of the three reactions. The intrinsic deactivation kinetics of this selective deactivation model were determined from the variation of conversion and product selectivities with time on-stream on crushed pellets. For modeling the rate of deactivation of these reactions, process time, rather than the coke content,was taken to be the independent variable.The decrease in the deactivation rate of the reforming reaction was negligible.The rates of deactivation of the other two reactions were of the form:

$$\frac{da_i}{dt} = f(p_A, p_B, p_C, .., T) \cdot a_i^d \qquad (4)$$

where a_i refers to the activity of reaction i,f is the deactivation function and d is the order of deactivation.

The rate of deactivation of reaction (1) increased with increasing partial pressures of carbon monoxide and aromatics whereas water partial pressure had an opposite effect.The rate of deactivation of the water gas shift reaction increased with

increasing partial pressures of benzene , toluene and water.

To study the diffusion deactivation interaction , runs were conducted on cylindrical pellets. Calculation and preliminary runs with different catalyst sizes showed that at these conditions, the pellets were operating in the diffusion-influenced regime. In the presence of diffusional limitation, both the toluene conversion and benzene selectivity were reduced whereas the rate of deactivation for the pellet was higher than that for the crushed pellets.

To model the pellet behavior, the intrinsic kinetic equations together with the intrinsic deactivation models were combined with the catalyst pellet mass balance equations for each of the six components of the reaction mixture. Since the experiments were conducted in a gradientless reactor, the external mass transfer gradients were negligible and the partial pressures of the components at the catalyst surface were the same as the exit values. Since the exit partial pressures are not known a priori , at each time interval initial guess values were supplied and the pellet mass equations were solved using a five point orthogonal collocation method. The average reaction rates for the pellet for each of the three reactions were then evaluated. With these average rates and the known inlet reactant flow rates and mass of catalyst, the exit partial pressures were calculated and checked with the assumed values. The new values for the exit partial pressures were updated using successive substitution method without convergence problems.The calculated and the experimental rates of the three reactions were compared at different run times and very good agreement was obtained at several temperatures.

The results of this study show that a selective deactivation model can satisfactorily model the variation of reaction rates with time on diffusion influenced catalyst pellets during the steam dealkylation of toluene. Such models should also be useful in modeling the deactivation-diffusion interaction in other complex reactions.

Chapter 1

INTRODUCTION

1.1 INTRODUCTION

Ever since Taylor, in 1932, put forward his theory of catalysis, based on active sites, several investigators have studied the nature of catalysts, and catalyst deactivation and have proposed various models to account for the effect of transport resistances of heat and mass transfer on the rates of reaction on porous catalyst pellets (Aris, 1975 ; Satterfield, 1970). Deactivation of catalysts frequently encountered in the petroleum, petrochemical and other industries, significantly affect not only the reactor design, but also its operation and optimization (Lee and Butt , 1982a). Quite often, the choice of the reactor for any process is dictated by the rate and mode of deactivation. For instance, systems in which the rate of catalyst deactivation is very fast, such as cracking of petroleum feedstocks where catalyst life is of the order of few seconds, a fluidized or moving bed would be a better choice so that the catalyst can be regenerated continuously. On the other hand, a fixed bed reactor with periodic generation is more suitable for slowly deactivating processes such as ammonia synthesis or naphtha reforming (Hughes, 1984). Normally, design procedures of catalytic reactors are based on fresh catalyst parameters, even when catalyst deactivation is known to occur (Lee and Butt,1982b). Due to lack of quantitative information about deactivation, it is the usual practice in industry to over design reactors or adjust the operating conditions so as to maintain a constant outlet conversion (Lee and Butt, 1982b).

Although deactivation is an inevitable process, with a proper understanding of the deactivation phenomenon, methods can be developed to include the effect of deactivation in the design of reactors which can lead to improved catalyst performance(Bartholomew ,1982). The effect of catalyst deactivation was first recognized by Voorhies (1945) and the effect of intraparticle diffusion on catalyst deactivation was first studied by Wheeler (1955).

The early work on catalyst deactivation has been elegantly reviewed by Butt (1972) and Levenspiel (1972). Generally,catalyst deactivation mechanisms have been classified a poisoning, fouling or sintering, in which the first two are essentially chemical in nature and the latter is physical (Lee and Butt, 1982a). Poisoning is the strong chemisorption of reactants,products, intermediates,or impurities on the active sites of the catalyst. Poisoning can be selective or nonselective and reversible or irreversible. A common example of poisoning is the deactivation of nickel reforming catalyst by sulphur (Hegedus and McCabe, 1980) and the poisoning of cracking catalysts by organometallic constituents of petroleum (Parera, 1968; Newson,1975). In sintering, catalyst and/or the support suffers a loss in the specific surface area or a modification in the chemical nature (Bartholomew,1984). Sintering is a consequence of the local high temperature and in some instances the nature of the oxidizing or reducing agent atmosphere. Of the three deactivation mechanisms,fouling is the most commonly encountered. Fouling is the physical deposition of any species on the catalyst which covers the active sites and, if it is excessive, can reduce the diffusional transport through the catalyst pores (Ramser and Hill,

1958). In the extreme case ,it can lead to pore blockage. In contrast to poisoning,which is usually associated with an impurity in the feed, the foulant precursors are formed from reactions involving the reactants and/or products. Due to the complex mechanism,it is usually very difficult to identify the particular species responsible for catalyst fouling.The most common form of catalyst fouling is the deposition of carbonaceous material,termed as coke,on the catalyst surface. Catalyst deactivation due to coke formation is commonly encountered in the petroleum and petrochemical industries such as catalytic cracking of gas oil, catalytic reforming of naphtha and hydrocracking of various petroleum fractions (Beuther et al. 1980). Such coke deposition is always associated with the main reaction, therefore, it is usually not possible to eliminate it, although it can be often substantially reduced by modifying the catalyst and/or the operating conditions so as to improve the catalyst selectivity.Such methods of coke reduction include the addition of alkali to reduce the acidity of the catalyst to suppress the side reactions (Rostrup-Neilsen, 1975; [illegible], Bridger,1970); addition of steam, hydrogen or inert to reduce the coke deposition rate and/or enhance the gasification of coke (Bartholomew, 1982) or regeneration of the catalyst at appropriate intervals. On the other hand, if the fouling material is an impurity in the feed such as metal sulfide, further purification will reduce the catalyst deactivation rate (Newson, 1975; Davies, 1978).

The nature of the coke precursors is still subject to some dispute (Wojciechowski ,1974 ; Beuther et al., 1980).Cracking reactions, polymerization and cyclization of

olefins through carbonium ion mechanism (Langer and Meyer,1980) and formation of polynuclear aromatics Mclaughlin and Anthony, 1985) have been suggested as the likely coke precursors. A number of investigators (Haldeman and Botty 1959; Trimm , 1977;Baker and Chludzinski , 1980) have examined the nature of the coke deposits on the catalyst, and have established that, with metal and supported metal catalysts,various forms of coke can be deposited. Deactivation reactions can be either in parallel and/or in series with the main reaction. For instance, fouling of alumina-boria catalyst during disproportionation of toluene to xylene is an example of parallel deactivation, whereas catalyst fouling during the dehydrogenation of aldehyde to coke in the dehydrogenation of primary alcohols is an example of series deactivation (Murakami et al., 1968).

Several workers have investigated the intrinsic kinetics of deactivation of simple reactions. Excellent reviews on the deactivation of simple systems have been given by Froment (1980),and Hughes (1984). Two approaches have been developed to model the intrinsic deactivation kinetics due to coke deposition. One approach utilizes the concept of activity in which the coke deposition is not explicitly accounted for in the model equations(Szepe and Levenspiel, 1968; Butt 1972 ; Corella and Asua,1982a,b), whereas in the second method, the activity is empirically related to the coke content of the catalyst and the coke content in turn is related to the process variables such as partial pressures ,temperature and space time (Froment and Hofschoff,1961;Dumez and Froment ,1976 ;dePauw and Froment ,1975). The first approach where catalyst activity is related directly to the run time has been employed to model the deactivation kinetics

of several reaction such as dehydrogenation of methyl cyclohexane on Pt catalyst (Wolf and Petersen ,1977a , b) ;dehydrogenation of cyclohexane on a nickel catalyst (Al-Ayed and Kunzru , 1988); disproportionation of cumene on a hydrocracking catalyst (Corella et al. ,1986) ; dehydration of isoamyl alcohol over silica-alumina catalyst (Corella and Asua , 1981). The second approach where catalyst activity is related to the coke content has been used successfully to model the deactivation kinetics of several reactions such as in cracking of ethylene over a silica-alumina catalyst (Ozawa and Bischoff, 1968),hydrogenation of acetylene to 1-butene on a cobalt catalyst (Bernardo and Lobo, 1980) and dehydrogenation of isobutene (Takeuchi et al.,1966).

Although the intrinsic deactivation kinetics of several simple reactions have been investigated in detail, very meager experimental data is available on catalyst deactivation of complex systems, and on the effect of the diffusional influences on catalyst activity and selectivity during catalyst deactivation. For the modeling of intrinsic deactivation kinetics of complex reactions, a number of investigators have used the non-selective model which assumes that at any time,the activity for each of the reactions is identical (Weekman and Nace,1970; Campbell and Wojciekowski,1969). Such an approach cannot account for the change in product selectivity with time on-stream. To explain the variation in product selectivities with time , selective deactivation models, which independently account for the activity of each of the reactions, have been used to model the deactivation kinetics in the catalyst cracking of gas oil (Jacob et al., 1976; Corella et al.,1989), catalytic reforming of naphtha (Schipper et al., 1984), and isobutylene oxidation reaction

(Corella et al. ,1985a,b).

Due to pressure drop limitations in industrial reactors,the catalysts are usually used in the form of pellets,where diffusional resistances can affect the reaction rate and selectivity.Very little attention has been given to the problem of both deactivation and diffusion limitation in the design and analysis of catalytic reactors. The first attempt to analyze the effect of deactivation-diffusion interaction on catalyst performance was by Wheeler (1955). In 1955, Wheeler proposed three different deactivation reaction mechanisms in order to explain the selectivity of complex reactions. The first study on the theoretical analysis of deactivation in single catalyst pelletswas by Masamune and Smith (1966). These workers numerically solved the mass balance equations for an isothermal pellet and first order kinetics,assuming that deactivation occurred by either parallel or series mechanisms. Their work was later extended by Sagara et al.(1967) to account for the non-isothermality in the pellet. Kam et al. (1975, 1977a, b) have theoretically modeled the deactivation-diffusion interaction using Langmuir- Hinshelwood kinetics. Experimental studies on diffusional influences on activity and selectivity have been very meager and limited to simple reaction systems. Dumez and Froment (1976) investigated the effect of diffusional limitation on coking rates for dehydrogenation of butene to butadiene over a Cr_2O_3-Al_2O_3 catalyst.The intrinsic kinetics of the main reaction were combined with the pellet mass balance equations and solved numerically. Excellent agreement was reported between the experimental and calculated values. Similarly, good agreement between the calculated and experimental activities was reported by Lee and

Butt (1982b) for poisoning of nickel catalyst during benzene hydrogenation. Wojciechowski and Pachovsky (1971) studied the diffusion-deactivation interaction during catalytic cracking of gas oil whereas Pachovsky and et. al, (1973) reported that,the diffusional resistances resulted in an increase in the gasoline selectivity.There has been no experimental work reported on the diffusion-deactivation interaction for complex reactions.To shed more light on the diffusion-deactivation interaction ,this study was undertaken to experimentally measure the deactivation reaction kinetics of a complex reaction under both diffusion-free and diffusion-influenced regime.

1.2 OBJECTIVE OF THIS WORK

The objective of this study was to model the variation in activity and selectivity with time on-stream for the diffusion-influenced pellet and compare this with the experimental values.The model reaction was taken to be steam dealkylation of toluene,a reaction of potential commercial importance. This reaction produces, rather than consumes hydrogen, in addition to the production of benzene, which is an industrially important finished product.Half of the total benzene consumption in the United States is produced by hydrodealkylation of toluene (White ,1986).In addition ,this reaction is of a complex nature since there are at least three competitive reactions taking place simultaneously. Moreover,not much information is available on the kinetics of this reaction.

Initially, the intrinsic kinetics of the main reaction together with the intrinsic deactivation kinetics was investigated in a gradientless internal recycle reactor

(Berty reactor). The effect of temperature and partial pressures of reactants and products on the the main kinetics and on deactivation rates was investigated. Models were then developed for the diffusion-free kinetics of the main and deactivation reactions.Experimental studies were then conducted on cylindrical pellets to investigate the effect of diffusion limitations on the selectivity and activity of the three reactions viz. dealkylation, reforming and water shift reaction. The pellet mass balance equations for the different species were solved and the calculated rates at various times for the three reactions compared with those experimentally measured.

Chapter 2

LITERATURE REVIEW

2.1 INTRODUCTION

Catalyst deactivation due to fouling occurs to some extent in most organic reactions which are conducted at moderate or high temperatures. The most common cause for catalyst fouling is coke deposition, although catalyst fouling can also be the result of other precursors formed from the reactants. The term coking and fouling are often used interchangeably. However, it should be emphasized that in general, there is no direct relationship between the catalyst activity and the coke content. The earliest work to correlate the coke formation to process variables such as time on-stream was by Voorhies (1945) who studied the rate of coke deposition during catalytic cracking of gas oil feedstocks. Since then, a number of investigators have studied catalyst fouling including different aspects of catalyst deactivation such as possible mechanisms and precursors for coke formation (Rostrup-Nielsen and Trimm , 1977 ; Bartholomew ,1982 , 1984 ; Albright and Baker ,1982 ; Beuther et al. ,1980), structure of the deposited coke (Haldeman and Botty , 1959 ; Trimm and Baker , 1977; McLaughlin and Anthony ,1985), intrinsic deactivation kinetics (Corella and Asua , 1980) and the effect of diffusional influences on catalyst activity and selectivity (Dumez and Froment 1976). Excellent reviews on catalyst deactivation which cover the work till the early seventies are available (Levenspiel, 1972 ; Butt ,1972). More recently, Hughes (1984) , Petersen and Bell (1987) and Wojciechowski and Corma (1986) have reviewed the latest

advances in deactivation kinetics.

2.2 MECHANISM OF CATALYST FOULING

Catalyst fouling reactions are always associated with the main reaction and the foulant precursors can be formed either from the reactants and/or products. Fouling is classified as parallel or series depending on the reaction(s) responsible for the formation of the precursors. In parallel fouling , the foulant is mainly formed from the reactants whereas in series deactivation,the products further react to yield the coke precursors as shown below

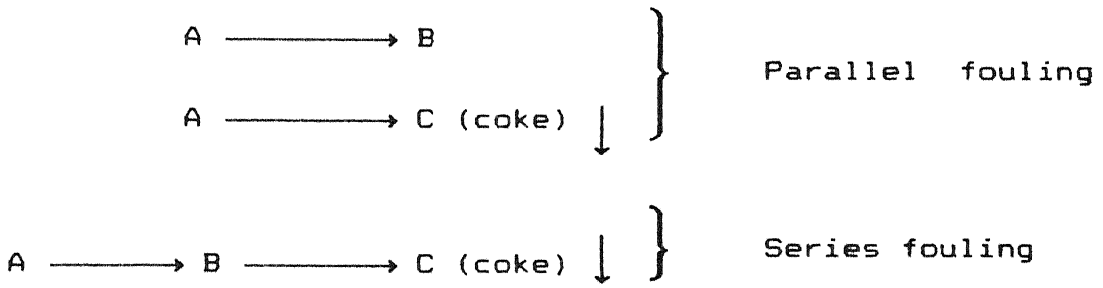

Examples of parallel deactivation include isomerization of n-pentane on platinum/alumina catalyst (Hosten and Froment, 1971), deactivation of copper/silica catalyst during conversion of benzyl alcohol to benzaldehyde (Romero et al., 1981) and the disproportionation of toluene to xylene , benzene and coke on alumina-boria catalyst (Murakami et al., 1968). Series deactivation has also been reported for several systems such as dehydrogenation of cyclohexane on nickel/alumina catalyst (Al-Ayed and Kunzru, 1988), dehydrogenation of isopentane over chromia-alumina (Noda et al.,1974) and the dehydrogenation of primary alcohols to aldehyde (Murakami et al.,1968). In addition, for several reactions it has been observed that both reactants as well

as products can lead to the coke precursors. Such parallel-series deactivation has been reported during the dehydrocyclization of n-heptane on supported-platinum bimetallic catalyst (Mahoney , 1974), catalytic cracking of gas oil (Corella et al., 1989 , John et al. 1974) and catalytic reforming of naphtha (Schipper et al. 1984).

Although a number of investigators have modeled the catalyst deactivation due to fouling, the available information on mechanisms of coke formation is very limited and is restricted to catalytic cracking and steam reforming reactions on metal and metal oxide catalysts. Depending on the reaction conditions and nature of the catalyst and/or support, various coke morphologies have been reported (Trimm ,1983; Bell, 1987). The structure and the nature of coke deposits on the catalyst surface have been investigated by Haldeman and Botty (1959), Trimm (1977); Baker and Chludizinski (1980); and Wojciechowski (1974).

Coke deposits may originate from molecules having an unsaturated electronic structure such as CO , NO , HCN or from successive dehydrogenation of aromatic or high molecular weight compounds (Bartholomew ,1984). Bell (1987) reviewed the various aspects of coke formation processes, such as the different methods of coke formation , the nature and the structural forms of the deposited coke. He has pointed out that coke can be formed from different pathways either from carbon monoxide or hydrocarbons. The overall processes of coke formation on the catalyst surface were summarized as shown in Figure 2.1

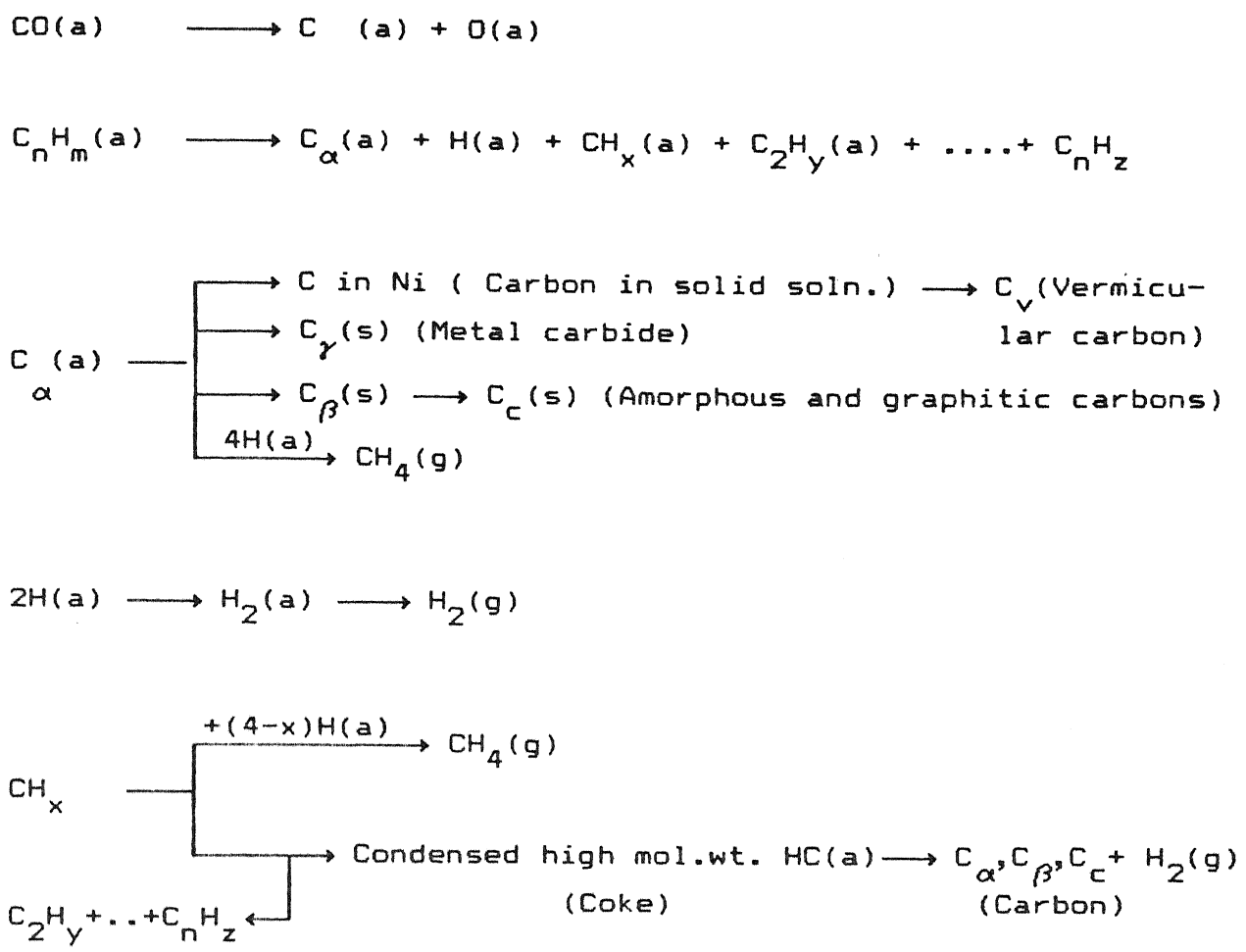

Figure 2.1 Possible Pathways for Coke Formation

In Figure 2.1 a, g and s refer to adsorbed,gaseous and solid respectively.

As shown in Figure 2.1,carbon monoxide can disproportionate to produce elemental carbon, $C_\alpha(a)$. These carbon atoms can polymerize to form either amorphous, $C_\beta(a)$, and/or graphitic carbons ,$C_c(s)$, which in turn dissolve into the bulk of the metal resulting in precipitation and formation of vermicular carbon, C_v. The dissolved carbon can also react to form metal carbide, $C_\gamma(s)$. For example, during the steam reforming process, carbon monoxide can disproportionate to carbon and carbon dioxide. Similarly, it is known that carbon atoms are important

intermediates during methanation reaction (McCarty and Wise, 1979). Several workers(Blue and Engle, 1951 ; Wojciechowski , 1974 ; Bakulen et al.,1978) have suggested that coke can also be formed from olefins. They postulated that olefins dimerize to give diolefins which undergo Diels-Alder reaction to form large polynuclear aromatic compounds. A similar mechanism has been also given by Wolf and Petersen (1977b) and Schipper et al. (1984). The other possible pathway for coke formation is the dehydrogenation of hydrocarbons . The coke originating from the hydrocarbons is more complex in nature than elemental carbon. The adsorbed species dehydrogenate in a series of successive steps leading to partially dehydrogenated species ($P_1, P_2 \ldots P_n$) with average molecular formula of the coke varying between $C_1 H_1$ - $C_1 H_{0.4}$ (Hughes , 1984) . This scheme can be represented as

$$P_1 \xrightarrow{-H_2} P_2 \xrightarrow{-H_2} P_3 \ldots P_n \xrightarrow{-H_2} \text{Coke} \downarrow$$

From the above discussion , it is clear that the mechanism of coke formation is still not properly understood. It seems that any hydrocarbon, in particular olefins and aromatics can dehydrogenate to form coke. The available evidence indicates that, most likely, aromatics are the immediate precursors. This is supported by the fact that many coke aggregates have aromatic condensed rings (Hughes , 1984). Most recently, McLaughlin and Anthony (1985) analyzed the solvent extractable portion of the residue from spent zeolite catalyst during methanol to hydrocarbon reaction. They found that the coke consisted mainly of naphthene, anthracene and its alkylated derivatives, toluene, xylene and

polynuclear aromatics upto tetracyclic pyrene . Similarly ,Langer and Meyer (1980) analyzed the coke formed during butadiene cracking and found that, polynuclear aromatics constituted the major portion of the deposited coke. X-ray and microscopic examination of the coke residue during catalytic cracking has also established that approximately 50 % of the coke deposits are in the form of pseudo-graphitic structure and the remainder probably in the form of condensed polynuclear aromatic structures (Haldeman and Botty , 1959).

From the above discussion, it is quite clear that, it is difficult to ascribe coke formation to any particular precursor. The available evidence indicates that , all hydrocarbons, from paraffins to aromatics, can result in coke formation under appropriate experimental conditions.

2.3 MODELING OF INTRINSIC DEACTIVATION KINETICS

Due to the industrial importance of catalyst fouling, numerous attempts have been made to model the intrinsic fouling kinetics of several reacting systems. In the classical work of Voorhies (1945), it was shown that the coke content of the catalyst during catalytic cracking of gas oil could be correlated as a function of the process time. Since then, two distinct approaches to model the fouling kinetics have been developed . In one approach, the decrease in the activity is related to the catalyst coke content, which is in turn is related to the process variables such as the partial pressure of the reactants and/or products , space time and temperature (Froment and Bischoff , 1961). In the second approach, (Szepe and Levenspiel, 1968, Kam et al. 1975,1977 ; Jodra et al. 1976, Corella and Asua , 1982) the

coke content is not explicitly accounted for, rather the decrease in the rate of the main reaction is related to the activity whereas the rate of change of activity with time is related to the partial pressures of the reacting species ,temperature and the remaining activity.

2.3.1 Coke Content Approach

The classical work of Voorhies in 1945 was the first attempt to investigate and account for the deactivation kinetics. The coke deposited on the catalyst surface in parallel,series or combination thereof with the main reaction, was correlated to the time on-stream . The coke deposited over a wide range of cracking reactions of petroleum fractions was represented by the following empirical equation:

$$C = A\, t^{n} \qquad (2.1)$$

where C is coke content of the catalyst, t is the time-on stream, A is the constant of proportionality and n is the time on-stream exponent with n generally between 0 and 1. In Voorhies's work, the value of n was approximately 0.5 . He explained eqn. (2.1) on the basis that, the diffusion of the reactant into the catalyst pellet was limited by the thickness of the deposited coke layer. For n equal to 0.5 , eqn.(2.1) can be interpreted as the solution of the following differential equation:

$$\frac{dC}{dt} = \frac{A}{C} \qquad (2.2)$$

Although, Voorhies's formula was developed for cracking of gas oil feedstocks, under diffusion-influenced conditions, it has been used by many investigators beyond the original scope to also model the intrinsic deactivation kinetics of several reactions. For example, Ruderhausen and Watson (1954) investigated the coke formation during dehydrogenation of cyclohexane over a Co-Mo catalyst and found that, Voorhies type of equation with time exponent of about 0.61 could fit their data. The high temperature dependency of the coking rate ruled out the possibility of diffusional influence on the coking rate. This form of intrinsic coking kinetics can be explained if it is assumed that the coking proceeds by the addition of the reactant to the already adsorbed species, i.e.

$$A_n + A \longrightarrow A_{n+1} \downarrow \qquad (2.3)$$

where A_n is the adsorbed coke precursor,A is the adsorbed reactant and A_{n+1} is the coke product. If in addition, it is assumed that , the rate of coking reaction is surface controlled and can be expressed using a Langmuir-Hinshelwood rate expression, then the coke formation rate can be written as follows:

$$r_c = \frac{K' C_{An} P_A}{(1 + K_A P_A + K_R P_R + C_{An})^2} \qquad (2.4)$$

where C_{An} is the concentration of coke on the catalyst surface, p_A and p_R are the partial pressures of the coke precursor and reactant, respectively, and K_A, K_R and K' are the usual Langmuir-Hinshelwood constants. If the coke adsorption is the controlling

step, then C_{An} term is predominant and the denominator of the above eqn.(2.4) reduces to

$$r_c = \frac{K' C_{An} P_A}{C_{An}^2} = \frac{K' P_A}{C_{An}} \qquad (2.5)$$

If the partial pressure of the reactant is in excess i.e P_A does not vary with time , equation (2.5) and (2.2) become identical.

Similarly ,Ozawa and Bischoff (1968) correlated the coke formation during ethylene cracking over a silica-alumina spherical catalyst pellet and obtained time exponent value varying between 0.55-0.91 . Butt et al.(1975) adopted the coke content approach to investigate coke deposition during cracking of cumene over H-mordenite catalyst. Eberly et al. (1966) studied coke formation for n-hexadecane cracking and reported time on-stream exponent value between 0.41-0.97 . The deactivation kinetics of catalyst was studied by Uchida (1975) and the deposited coke was found to increase linearly with time on stream.

Although number of investigators have utilized Voorhies correlation, it has been questioned by Richardson (1972) supported by the earlier works of Levinter et al. (1967) on the basis that the coke deposition is not uniform on the catalyst surface. This kind of equation ignores the coke formation dependence on space time, temperature and partial pressures of the reacting species,in addition to the implicit assumption that, the process of coke deposition is diffusion controlled. Moreover, this equation is not very useful in predicting the catalyst activity because , in general , there is no direct proportionality between the amount of coke deposited and the catalyst activity. To model the effect

of coke formation on the intrinsic rates of the main reaction , more detailed models are necessary.

Froment and Bischoff (1961) modeled the deactivation kinetics in a fixed bed reactor by assuming that the rate of coke formation was related to the partial pressures of the reacting species and temperature. The catalyst coke content approach was generalized and developed by dePauw and Froment (1975) and Dumez and Froment (1976) to model the deactivation kinetics. The method of analysis was based on Langmuir-Hinshelwood rate expressions for the main and the deactivation reactions. The deactivation reaction kinetics was deduced in a similar manner as the main reaction. The method developed by Froment and co-workers is summarized below for the simple reaction $R \rightleftarrows P$ in which the surface reaction is assumed to be the controlling step. The elementary steps for the main reaction can be represented as :

$$\left.\begin{array}{ll} R + S \longrightarrow R.S & \\ R.S \longrightarrow P.S & \\ P.S \rightleftarrows P + S & \end{array}\right\} \qquad (2.6)$$

where S, represents a vacant active site. Assuming that some coke precursor , C , competes for the active sites and ultimately forms coke, we have

$$C + S \longrightarrow C.S \qquad (2.7)$$

Then, the rate for the main reaction can be written as follows:

$$r_R = k_1 K_R C_S \left[C_R - \frac{C_P}{K} \right] \qquad (2.8)$$

where C_R ,C_P ,C_S are the concentrations of R ,P and the vacant sites,respectively.The total concentration of active sites, C_t is given by

$$C_t = C_S + C_{RS} + C_{PS} + C_{CS} \qquad (2.9)$$

where C_{RS} and C_{PS} are the equilibrium concentrations of reactant and product, respectively, and these may be eliminated through the usual adsorption equilibrium relations. C_{CS} is the concentration of active sites occupied by the coke, which cannot be measured directly. Substituting eqn. (2.9) in eqn. (2.8), the kinetics of the main reaction can be expressed as :

$$r_R = \frac{k_1 C_t K_R \left(C_R - \frac{C_P}{K}\right)}{\left(1 + K_R C_R + K_P C_P + \frac{C_{CS}}{C_S}\right)} \qquad (2.10)$$

Since the coke concentration C_{CS} and C_S are not amenable to direct measurements,Froment and Bischoff (1961) proposed several empirical correlations where the ratio C_{CS}/C_S is related to catalyst coke content or deduced form eqn. (2.9) as follows:

$$C_t - C_{CS} = C_S \left(1 + K_R C_R + K_P C_P \right) \qquad (2.11)$$

Substituting for C_t into equation (2.10) leads to:

$$r_R = \frac{k_1 C_t K_R \phi_R \left(C_R - \frac{C_P}{K} \right)}{\left(1 + K_R C_R + K_P C_P \right)} \qquad (2.12)$$

where $\phi_R = \left[C_t - C_{CS} \right) / C_t \Big]$ is the fraction of active sites remaining active. A more generalized form of ϕ_R has been proposed (Froment, 1980) to account for the number of active sites involved in the main reaction, n . Thus

$$\phi_R = \left[\frac{C_t - C_{CS}}{C_t} \right]^n \qquad (2.13)$$

The deactivation function ,ϕ_R, is empirically related to the catalyst coke content. Several workers have proposed different forms of deactivation functions, such as

$$\left.\begin{aligned} \phi_R &= \exp(-\alpha C_c) \\ \phi_R &= 1 - \alpha C_c \\ \phi_R &= 1/(1 + \alpha C_c) \end{aligned}\right\} \qquad (2.14)$$

The origin of the coking precursors are not specified in eqn. (2.7). The coke precursor can result either from the reactants and/or products. If the coke formation reaction is in parallel with the main reaction and, if it is further assumed that

the coke precursor adsorption is the controlling step ,then the rate of coke formation can be written as:

$$\frac{dC_{CS}}{dt} = k_C' C_{RS} \qquad (2.15)$$

Equation (2.15) can be expressed in terms of catalyst coke concentration and the rate of coke formation ,r_C, can be written as:

$$r_C = \frac{dC_c}{dt} = k_c' K_R C_R C_S \qquad (2.16)$$

Using the expression for C_S (eqn. 2.11), eqn. (2.16) can be reduced to a form similar to equation (2.12) as follows:

$$r_C = r_C^o \phi_C = \left[\frac{k_c C_t K_R C_R}{(1 + K_R C_R + K_P C_P)} \right] \phi_C \qquad (2.17)$$

where $\phi_C = (C_t - C_{CS} / C_t)$ is the deactivation function for the coking reaction, and, r_C^o , is the rate of coke formation on a fresh catalyst. ϕ_C can be same or different from ϕ_R depending upon the number of active sites involved in the main or the deactivation reactions.

This approach has been used by several investigators to model the intrinsic coking kinetics. For instance, Dumez and Froment (1976) investigated the main and the deactivation kinetics of the dehydrogenation reaction of 1-butene to butadiene on a Cr_2O_3-Al_2O_3 catalyst. These authors have found that the exponential form of the deactivation function could represent the catalyst coke content. The kinetics of the main reaction together with the intrinsic coking kinetics was used to model the catalyst

pellet behavior and the integral reactor performance. Cooper and Trimm (1980), reported a hyperbolic or exponential relationship for coke deposition on the catalyst surface during catalytic reforming. Similarly, an exponential form of deactivation function was found to give the best fit to the catalyst coke content in reforming of C_7 hydrocarbons on a sulfided platinum on alumina catalyst (Van Trimpont et al. 1988) and dehydrogenation of n-heptane (Van Trimpont et al., 1986).Similar studies were conducted by Marin and Froment (1982) on dehydrogenation of methyl cyclohexane to toluene on sulfided commercial Pt/Al_2O_3 catalyst, and many others (Hosten and Froment,1971; Lambrecht and Froment, 1972) utilizing the catalyst coke content approach to model the deactivation of simple reactions.

In complex reactions systems, catalyst fouling can not only affect the activity but also alter the product distribution with time. The experimental data on the deactivation kinetics of complex reactions using the coke content approach is very limited. Weekman and Nace (1970) studied the deactivation kinetics of catalytic cracking of gas oil into gasoline, dry gas and coke with rate equations of power law type. The reactants and products were lumped into three pseudo-components. In their study, the product selectivities were independent of the process time and the deactivation functions for the three reactions were equal at any time. On the other hand, in the study of isomerization of n-pentane on a Pt/Al_2O_3 catalyst (dePauw and Froment, 1975), the product selectivities were found to vary with run time and the deactivation functions for the isomerization and hydrocracking reactions were different. Since the respective amount of coke deposited on the Pt and Al_2O_3 sites could not be determined

accurately, the distribution of coke over the two sites was assumed constant, i.e. independent of time or coke content. The rate of coke deposition of each deactivating reaction was related to the total coke content of the catalyst through an adjustable parameter. They found that an exponential form of deactivation function could model their data.

The coke content approach has the limitation that it assumes a relationship between activity and coke content where none might exist because multilayered coke may also be formed. In addition, for dual functional catalyst, it is difficult to experimentally determine the separate amounts of coke formed on the two different type of sites.

2.3.2 Activity Approach

Another approach to analyze the deactivation kinetics during catalyst fouling has been developed by many investigators (Szepe and Levenspiel,1968; Wolf and Petersen, 1977a,b; Levenspiel,1972; Corella et al., 1985a,b ; Corella and Asua, 1982) , and has been widely used to correlate catalyst deactivation kinetics of various reacting systems.

In general, the rate of a reaction catalyzed by a solid surface can be written as:

$$r_A = f_1(S, p_i, T) \qquad (2.18)$$

where r_A is the reaction rate at any time, S is the number of active sites, p_i is the partial pressure of component i in the bulk gas stream and T is the reaction temperature.When the previous equation can be written as:

$$r_A = f_2(p_i, T)\ f_3(S) \qquad (2.19)$$

then, the equation is termed 'separable'. $f_3(S)$ is related to the concentration of the catalytically active sites. Butt and co-workers (Butt et al., 1978 ; Onal and Butt, 198[illegible] ; Butt, 1984) have shown that the concept of separability is only valid for ideal surfaces. However, Gavalas (1971) has argued that this is not a restrictive assumption. For separable kinetics, eqn. (2.19) can be written as:

$$r_A = r_{Ao}\ f_3(S) \qquad (2.20)$$

where r_{Ao} is the reaction rate for a fresh catalyst i.e. in the absence of catalyst fouling. The activity is defined as r_A/r_{Ao} , so that eqn. (2.20) can be expressed as:

$$r_A = r_{Ao}\ a \qquad (2.21)$$

where in general:

$$-\frac{da}{dt} = f_4(p_i, T)\ f_5(a) \qquad (2.22)$$

Szepe and Levenspiel (1968) proposed the following separable form t

model fouling deactivation kinetics:

$$-\frac{da}{dt} = f_6(T)\, f_7(p_i)\ a^d \qquad (2.23)$$

In addition, the main kinetics was assumed to be of the separable

$$r_A = f_8(T) \cdot f_9(p_i) \cdot a \qquad (2.24)$$

On the basis of Szepe and Levenspiel's analysis, several investigators have modeled the deactivation kinetics of various reaction systems. Jodra et al.(1976) extended the deactivation formulation where the kinetics of the main reaction are of the Hougen-Watson type, and are of the form:

$$r_A = f_2(T,p_i) \cdot a \qquad (2.25)$$

where $f_2(T,p_i)$ represent a nonseparable expression. Theoretical and experimental investigations by Jodra et al (1976), Butt et al. (1978) and Corella and Asua ,(1982), have shown that in some cases equation (2.23) fails to model the deactivation kinetics. Instead, they suggested a more flexible deactivation rate equation as follows:

$$-\frac{da}{dt} = f(p_i,T) \cdot f_3(a) \qquad (2.26)$$

where the function $f(p_i, T)$ is of nonseparable nature and can be deduced or assumed (Corella and Asua ,1982).

Corella and Asua (1982) generalized theoretically the deactivation kinetics and proposed various mechanisms for coke formation, which included catalyst fouling by reactant and/or product degradation , polymerization reactions , condensation of molecules adsorbed on adjacent sites and also blocking of active sites by steric effect. The proposed mechanisms consisted mainly

of the following three steps:

(i) adsorption of reactants or products on the catalyst surface. The adsorption equilibrium constant for this step was assumed to be the same or different from the main reaction.

(ii) formation of the coke precursor from the adsorption species . This could be either due to reaction between the adsorbed species or between the adsorbed species and the gas phase components.

(iii) further reaction of the coke precursors to form different and perhaps more stable forms of coke.

Depending upon the proposed mechanism and the rate controlling step, different expressions for the rate of deactivation were obtained. Their analysis for the reaction

$$A \rightleftharpoons B + C \qquad (2.27)$$

$$M \longrightarrow P$$

where M is either the reactant or the product, and P is the coke precursor,is given below for one of the possible mechanisms. For this analysis, the proposed mechanism is

Step 1:
$$M + S \rightleftharpoons M.S \qquad (2.28)$$

Step 2:
$$nM(g) + hM.S \rightleftharpoons P_1S_h \qquad (2.29)$$

where n = 0,1,2 and h = 1,2. For an elementary reaction, $n + h \leq 3$

Step 3:
$$P_1S_h \rightleftharpoons P_2S_h \rightleftharpoons P_3S_h \qquad (2.30)$$

where P_1, P_2, P_3 are coke precursor intermediates.

Any of the three steps can be rate controlling and in the subsequent analysis, step 2 has been assumed to be the slowest step. The coke deposition rate from equation (2.29) can be written as:

$$\frac{dC_{PS_h}}{dt} = k_d \cdot p_M^n \cdot C_{MS}^h \qquad (2.31)$$

Since step 1 is at equilibrium, we have

$$K_M = C_{MS} \; / \; p_M \cdot C_S \qquad (2.32)$$

Hence, eqn. (2.31) can be written as

$$\frac{dC_{PS_h}}{dt} = k_d \cdot K_M^h \; p_M^{n+h} \cdot C_S^h \qquad (2.33)$$

$$\text{where } PS_h = P_1 S_h + P_2 S_h + P_3 S_h + \ldots\ldots \qquad (2.34)$$

The total active sites concentration is given by the following equation:

$$S_o = C_S + C_{AS} + C_{BS} + C_{CS}(m-1) + hC_{PS_h} \qquad (2.35)$$

where m is the number of active sites involved in the controlling step of the main reaction. Substituting for C_{AS} , C_{BS} and C_{CS} from equilibrium relations in equation (2.32) and eliminating for C_S, we obtain

$$C_S = \frac{S_o - hC_{PS_h}}{1 + K_A P_A + K_B P_B + (m-1)K_C P_C} \qquad (2.36)$$

Substituting C_S from eqn. (2.36) in equation (2.33), we obtain

$$\frac{dC_{PS_h}}{dt} = \frac{k_d K_M^h P_M^{n+h} (S_o - hC_{PS_h})^h}{(1 + K_A P_A + K_B P_B + (m-1)K_C P_C)^h} \qquad (2.37)$$

If we rearrange and integrate equation (2.37) for $h \neq 1$, we have:

$$-\frac{S_o^{1-h}}{h(1-h)} \left[\left(\frac{S_o - hP_{S_h}}{S_o} \right)^{(1-h)} - 1 \right] = \int_0^t \frac{k_d K_M^h P_M^{n+h}}{(1 + K_A P_A + K_B P_B + (m-1)K_C P_C)^h} dt \qquad (2.38)$$

The activity is defined as:

$$a = \left[\frac{S_o - C_{PS}}{S_o} \right]^m \qquad (2.39)$$

Introducing equation (2.39) into equation (2.38) and taking the differential form for any given value of h , we obtain:

$$-\frac{da}{dt} = \frac{mhS_o^{h-1}k_d K_M^h P_M^{n+h}}{(1 + K_A P_A + K_B P_B + (m-1)K_C P_C)} \cdot a^{(m+h-1)/m} \qquad (2.40)$$

The derived equations for all the proposed mechanisms by Corella and Asua (1982) were of the above typeand a general form of deactivation rate equation could be written as:

$$-\frac{da}{dt} = \frac{(\text{kinetic term})(\text{pressure gradient})^{n+h}}{(\text{chemisorption strength term})^h} \cdot (\text{activity})^d \qquad (2.41)$$

where d =(m+h-1)/m , m and h are the number of active sites involved in the controlling steps of the main and deactivation reactions, respectively ; while n is an adjustable exponent in such a way that $n + h \leq 3$. The above equation was also extended to encompass the case of simultaneous coke deposition where gradient terms for each coke precursor have to be included in the deactivation equation.

It has been suggested by many workers that the order of deactivation can change with time on-stream in systems where the catalyst activity decline is very fast such as fluid catalytic cracking units. Similarly , the deactivation energy for deactivation reaction and the coking mechanism can also change with time (Corella et al.,1985a,b ; Corella et al., 1989).

The activity approach analysis has been utilized to model various deactivation kinetics of several simple and complex reaction systems. The experimental data for various systems shows that the order of deactivation is generally in the range of Ø to 3 (Corella et al., 1985b).The classical work of Blanding (1953) was the first attempt to model fouling kinetics using the concept of

activity.The activity decline of cracking of hydrocarbons over natural and synthetic catalyst was very rapid and the slope of activity vs. time curve was found to be some what greater than 0.5. Jodra et al.(1976) studied the deactivation kinetics of dehydrogenation of benzyl alcohol over Cu-Cr_2O_3/asbestos catalyst. Carbucicchio et al.(1980) adopted the activity concept to model the deactivation kinetics of Fe_2O_3-MoO_3 catalyst supported on silica in the oxidation of methanol to formaldehyde. The activity function used was of the exponential form and of the type :

$$a = \exp(-\lambda t) \qquad (2.42)$$

where $\lambda = k_d f(p_i)$ and p_i is the partial pressure of either the reactant and/or product. The deactivation order of the activity decline was assumed and derived as an extension of the model proposed by Szepe and Levenspiel (1968). Similarly, the deactivation kinetics of a 10%Cu-0.5% Cr_2O_3/asbestos catalyst for benzyl alcohol dehydrogenation was investigated and modeled by Corella and Asua (1980). The activity function was nonseparable type and the activity order was unity. Corella and Asua (1981) investigated the deactivation kinetics of dehydration of isoamyl alcohol over a silica alumina catalyst.The deactivation data was explained by utilizing the Langmuir-Hinshelwood rate expressions for the deactivation kinetics to model series fouling reaction in an isothermal reactor. In another study, Corella and Asua (1982) determined the deactivation kinetics of a 5 wt% HgCl on active charcoal catalyst during oxidation of isobutene to methylacrolein. Similarly, Corella et al. (1986) modeled the deactivation kinetics of a commercial hydrocracking catalyst in the reaction of cumene

disproportionation. Petersen and coworkers (Wolf and Petersen, 1977b;Jossens and Petersen, 1982a,1982)studied the dehydrogenation of methyl cyclohexane (MCH) to toluene on a commercial reforming catalyst having 0.6% Pt supported on γ-alumina in a single pellet diffusion reactor. The activity was found to be a function of both the MCH and toluene partial pressures as well as time on stream. The deactivation order was unity. Al-Ayed and Kunzru (1988) modeled the deactivation kinetics of dehydrogenation of cyclohexane to benzene on a nickel catalyst using the activity concept. The rate of deactivation was found to increase with increasing benzene partial pressure and decrease with increasing hydrogen partial pressure. The deactivation order of 1.6 gave the best fit to the data.The deactivation kinetics of benzyl alcohol conversion to benzaldehyde on Cu supported on SiO_2 catalyst was studied by Romero et al.(1981). The activity function used was similar to that of Wolf and Petersen.

To account for the changes in product selectivities with time on-stream, selective deactivation approach which independently accounts for the rate of deactivation of each of the reactions has been utilized by several investigators to explain the deactivation kinetics of complex reactions. Such models have been developed by Campbell and Wojciechowski (1969) Jacob et al. (1976) and Corella et al. (1989) for catalytic cracking of gas oil. Similarly, Schipper et al. (1984) modeled the deactivation kinetics during the catalytic reforming of naphtha over a platinum catalyst. Due to the complexity of the process and the deactivation kinetics, each kinetic constant or reaction rate in the network was multiplied by a different activity or function dependent on time on-stream. Corella and Asua (1982a studied the

deactivation kinetics during oxidation of isobutene to methylacrolein reaction. Selective deactivation model was used with nonseparable deactivation function to model the activity for each reaction.

Most of the complex reaction deactivation kinetics modeling has been limited to petroleum fractions and related reactions since it is of prime interest to the industry. Very little information is available for other complex reactions.

2.4 DIFFUSION DEACTIVATION-INTERACTION

When reactions are affected by both deactivation and diffusion, the diffusional influences on the intrinsic deactivation kinetics have to be included in any model of the catalyst pellet.

The first attempt to study the effect of diffusional influences on the catalyst activity was made by Wheeler (1951). He studied the variation of activity with the fraction of active sites deactivated for uniform and pore mouth deactivation. Wheeler showed that the interaction of intrapellet diffusion on the rate of the main and deactivation reaction can lead to a variety of relations between the activity and the fraction of active sites deactivated. Wheeler's analysis of deactivation kinetics was extended by Carberry (1966) and by Weisz and Hicks (1962) to include external mass transfer and nonisothermal effects. It was shown in their analysis, that the effectiveness factor can have values greater than unity. Furthermore, it was also shown that, at certain values of the Thiele modulus, more than one value of the effectiveness could be obtained.

Generally, the rate of deactivation is much slower than the

rate of the main reaction and most authors have made the pseudosteady state assumption in solving the pellet equations for a deactivating catalyst. With this assumption, for a single reaction, the conservation equations which govern the behavior of any diffusion-influenced deactivation can be expressed as

$$D_{eff} \nabla^2 C_i = \rho_p r_{int} \cdot a \qquad (2.43)$$

$$k_{eff} \nabla^2 T = \rho_p (\Delta H) r_{int} \cdot a \qquad (2.44)$$

$$- \frac{da}{dt} = k_d f(C_i, T) \cdot a^d \qquad (2.45)$$

where r_{int} is the rate of reaction in the absence of diffusion limitations in kmol/(kgcat)(h) , ρ_p is pellet density in kg/m^3 , k_{eff} is the effective thermal conductivity in J/(m)(K)(h), D_{eff} is the effective diffusivity of the catalyst pellet in m^2/h and C_i is the concentration of the reactant in k mol/m^3.

In the above equation , it has been assumed that, the heat of reaction of the deactivation reaction is negligible. Masamune and Smith (1966) solved these differential equations by numerical techniques for an isothermal pellet with first order kinetics. Their analysis showed that, a catalyst with the lowest intraparticle diffusion resistance gave the maximum activity when series deactivation was involved; on other hand, for parallel deactivation,a catalyst with intermediate diffusion resistance was

more selective and less easily deactivated. Later on , this work was extended by Smith and co-workers (Sagara et al. 1967) to include non-isothermal systems. Murakami et al.(1968) extended the analysis further to include film resistances.They also provided experimental verification of coking profiles in parallel and series fouling. Carberry and Gorring (1966) simulated the deactivation-diffusion interaction as a non-catalytic gas-solid reaction to correlate the fraction of catalyst deactivated with the process time.

In another approach, Khang and Levenspiel (1973) extended the power law formulation to include the effect of intrapellet diffusional resistances for parallel, independent, simultaneous and consecutive reaction-deactivation networks. The intrinsic kinetics was assumed to be first order and of the following form :

$$r_A = k.C_A .a \qquad (2.46)$$

$$r_d = -\frac{da}{dt} = f(C_A, C_B, C_P) \cdot a^d \qquad (2.47)$$

where C_A, C_B, C_P are the concentration of reactants and/or products; d is the activity exponent and C_p is the poison concentration.

They solved the pellet equations to calculate the average activity of the pellet and showed that the intrinsic deactivation order of unity can change due to the effect of diffusional resistances. d values varied between 1 and 3 depending upon the mechanism of deactivation and the Thiele modulii of the main and deactivation reactions.

Several investigators have attempted to simulate the deactivation kinetics of catalyst pellets. Recently Kam et al. (1977 a,b) extended the isothermal analysis of Masamune and Smith (1966) to include the external film resistances in nonisothermal pellets, transient behavior and finally a full Langmuir-Hinshelwood (L-H) analysis of fouling. In their analysis, it was assumed that fouling could occur by a reaction in parallel or series with the main reaction. Since many deactivation reactions take place by a complex series of reaction pathways involving both mechanisms, the possibility of simultaneous fouling by parallel and/or series process was also included. Lee and Butt (1982a) developed a general expression for time-dependent activity of a catalyst pellet affected by both diffusion and deactivation. Specific results were given for both uniform and pore-mouth poisoning,with parallel and series fouling mechanisms. Satisfactory agreement was obtained between the theoretical and experimental results. A pellet effectiveness representing the combined effect of diffusion-deactivation was also developed by them in a form suitable for direct inclusion in reactor conservation equations. Kumbilieva et al. (1987) studied the combined effect of intraparticle diffusion and catalyst deactivation and found that, catalyst deactivation under diffusional influence could prolong the operation time of the catalyst, and hence, increase the total yield of the product. These authors studied the isoprene production over a commercial catalyst deactivated by series deactivation.

Although several investigators have modeled coke formation in the presence of diffusion, the published literature on the experimental verification of these models is very limited. Dumez

and Froment (1976) investigated the effect of diffusional limitations on coking rates for dehydrogenation of butene to butadiene, and the coking profiles could be predicted from models developed from intrinsic deactivation kinetics. A good agreement was obtained between the predicted and the measured values.Lee and Butt (1982b) modeled the poisoning of nickel catalyst during benzene hydrogenation in the presence of transport limitations. The agreement between theory and experimental data obtained for parallel pore-mouth poisoning was satisfactory, although the model was found to be sensitive to the value of the effective diffusivity.Krishnaswamy and Kittrell (1981) used concentration-independent deactivation kinetics to model deactivation-diffusion interactions. Krishnaswamy and Kittrell (1982) extended their earlier results to model decomposition of hydrogen peroxide deactivation-diffusion kinetics and found good agreement between the predicted and experimental results.

Several investigators have found that coke deposition can also reduce the total catalyst surface area as well as the effective diffusivity. Appleby et al. (1962) observed reduction in catalyst surface area of 22 % and 33 % , depending upon the amount of deposited coke during cracking of n-butane and phenanthrene. Ramser and Hill (1958) reported a 27 % decrease in the catalyst surface area for 2.2 wt % of deposited coke. Similarly, Levinter et al. (1967) observed a reduction in the surface area of different silica-alumina catalyst for styrene benzene reaction mixture. Nemits et al.(1988) reported a decrease in the effective diffusivity during dehydrogenation of butane to butene over a platinum based catalyst. Reduction in the total

available catalyst surface area and pore blockage can have a significant effect on the product selectivity with time on stream.

In contrast to the above findings, several investigators reported no changes in the catalyst total surface area or the effective diffusivity. Ozawa and Bischoff (1968) and Haldeman and Botty (1959) found no changes in either the surface area or the effective diffusivity. It should be noted that, the effective diffusivity and total surface area might be affected under severe coking conditions or due to catalyst sintering.

2.5 STEAM DEALKYLATION OF TOLUENE

Very little information is available on the kinetics of this reaction. The first studies of this reaction on rhodium/ alumina catalyst were reported by Rabinovich and coworkers, (Rabinovich et al.,1971 Rabinovich and Mozhaiko , 1975). Several other workers (Kochloefl, 1976; Grenoble, 1978a,b; Beltrame et al. 1984 ;Duprez et al. 1986) investigated the kinetics of this reaction under various conditions and different rhodium loading on different supports. The temperature range of investigations has varied from 648 to 898 K. The main products of this reaction are benzene, carbon monoxide ,carbon dioxide ,hydrogen and methane. Most of the workers have reported benzene selectivity in the range of 70 to 90 % . Toluene steam dealkylation reaction is a complex reaction and several reactions can occur simultaneously on the catalyst surface. The product distribution in this system has generally been explained on the basis that toluene steam dealkylation (benzene formation), toluene steam reforming (complete destruction of the aromatic ring) and the water gas shift reaction are occurring simultaneously. Some workers have

suggested additional reactions also such as methanation reaction , hydrodealkylation reaction (Kochloefl, 1976 ,Beltrame et al , 1984) to explain the product distribution.

Grenoble (1978a) studied this reaction over Group VIII noble metals and found that in comparison to Pt, Pd, Ni, Os, Ir, Ru,rhodium was the most active catalyst. Similar results have also been reported by other investigators (Rabinovich et al. 1971 ; Kochloefl, 1976). The selectivity to benzene decreased with increasing Rh content (Kochloefl, 1976) whereas the catalyst activity was maximum for Rh content of approximately Ø.8 wt % . They also reported that rhodium content of Ø.7 wt % gave the highest catalyst activity on Cr_2O_3-Al_2O_3 support. Similar results were also reported by Duprez et al. (1985) who found that Ø.6 wt.% Rh showed the highest exploitation of the noble metal. In another study, Kocholoefl (1976) investigated the effect of various supports such as Cr_2O_3 ,SiO_2, ZnO, MgO and Al_2O_3 . His results show that both the activity and selectivity of the rhodium catalyst is affected by the nature of the support. Similar studies were carried out by Grenoble (1978b).

The mechanism and kinetics of this reaction has been investigated by relatively few investigators. Rabinovich and coworkers suggested a reaction mechanism based on the assumption that water was activated on the hydrophilic surface of the alumina and the hydrocarbon on the metal sites. The migration of the hydroxyl group to the metal site was assumed to be the controlling step. Dydykina et al.(1972) investigated the role of support oxygen in the reaction mechanism , and concluded from IR studies that the hydroxyl groups on the alumina support were the source of oxygenated species for the formation of carbon oxides. The

experimental investigations suggested that the water cleaves on the support as follows:

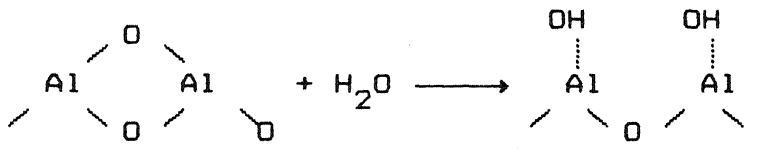

(2.48)

Similar explanations were also given by Grenoble (1978a) and other workers supported by the fact that alumina is a better support than silica which has tightly bound oxygen sites. Kochloefl (1976) studied this reaction in the temperature range 649-898 K and a total pressure between 1 to 22 atm. The catalyst was 0.6 wt% rhodium on γ-alumina. The main reactions identified were toluene steam dealkylation , toluene hydrodealkylation and toluene steam reforming,where toluene steam dealkylation reaction was considered to consists of two steps as follows:

$$C_6H_5CH_3 + H_2O \longrightarrow C_6H_6 + CO + 2H_2 \qquad (2.49)$$

$$CO + H_2O \rightleftharpoons CO_2 + H_2 \qquad (2.50)$$

For their experimental conditions ,it was found that, the water gas shift reaction eqn. (2.50) was much faster than the dealkylation reaction eqn.(2.49).The reaction rate of toluene steam dealkylation reaction was modeled using Langmuir-Hinshelwood rate expressions and could be described as

$$r = \frac{k\, K_T K_W\, P_T P_W}{(\,1 + K_T P_T + K_W P_W\,)^2} \qquad (2.51)$$

The form of the rate expression used by him assumes that water and toluene are chemisorbed on the same type of active sites, which is in disagreement with the experimental findings of other investigators. Kochloefl (1976) also investigated the mechanism of benzene formation in a separate experiment, and concluded, that the hydroxyl group of the support was the source of the carbon oxides in the product.

Grenoble (1978b) proposed a kinetic model based on the assumption that water and toluene are adsorbed on different sites. The Langmuir-Hinshelwood expression for the initial rate of the water/toluene reaction derived by him was

$$r = bk\, P_T^n \left[\frac{(K_W P_W)^{\frac{1}{2}}}{(1 + (K_W P_W)^{1/2}} \right]^{1-n} \qquad (2.52)$$

where b is a constant, k is the reaction rate constant and n lies between 0 and 1 . If the equilibrium constant ,K_W, for water adsorption and/or the partial pressure of water is small, then eqn. (2.52) is reduced to:

$$r = bk\, p_T^n\, (K_W P_W)^{(1-n)/2} \qquad (2.53)$$

The reaction orders with respect to toluene and steam were determined to be 0.08 and 0.42 ,respectively. In another study, Duprez et al. (1982) modified the noncompetitive mechanism proposed earlier by Grenoble to account for the recovery of the support active sites, giving rise to a different reaction rate

equation.

Several investigators have also studied this reaction on supports other than alumina (Kim, 1978; Beltrame et al.,1984;Forni et al ,1984). Beltrame et al. (1984) modeled this reaction for $Rh/Cr_2O_3/\gamma\text{-}Al_2O_3$ catalyst. In their analysis, the water toluene reaction was represented by an overall equation as follows:

$$C_6H_5CH_3 + 4.9H_2O \longrightarrow 0.7C_6H_6 + 0.3CO + 2.3CO_2 + 0.2CH_4 + 6.4H_2O \quad \text{.....(2.54)}$$

They found that the rate of benzene formation increased with increasing partial pressures of toluene and water. In addition , carbon monoxide had a very strong inhibition effect whereas benzene had a mild inhibition effect on the rate of toluene steam dealkylation reaction. Their data could be represented by a Langmuir-Hinshelwood rate expression of the following type:

$$r = \frac{k\, p_T\, p_W}{(1 + K_W p_W)(1 + K_T p_T + K_R p_R)} \qquad (2.55)$$

This model assumes that toluene and steam are adsorbed on different sites. In all these kinetic studies, only a single rate expression has been reported for this complex reaction.

Pressure also has an effect on the product distribution. Kochloefl (1976) studied this reaction in the pressure range of 1.0 to 22.0 atmospheres. His results show that the hydrodealkylation reaction increases as the total operating pressure is increased.In his study, the methane content in the

gaseous products increased from 2.1 vol% at atmospheric pressure to 34.8 vol% at 21.0 atm. Similar results were also reported by Rabinovich et al. (1973) who studied this reaction at a total pressure ranging from 1.0 to 16.0 atmospheres.

The available information indicates that the activity of the catalyst for the water gas shift reaction significantly affects the rate of toluene conversion. Mori and Mesoa (1976) studied steam dealkylation of toluene on Rh/Al_2O_3 system promoted by urania. They observed a three fold increase in toluene conversion as compared to unpromoted catalyst with no change in benzene selectivity. This was attributed to the role of urania in catalyzing the shift reaction and diminishing the adsorbed CO which inhibits further dealkylation . Kim (1978) found VO_x to be a strong promoter for this reaction on Rh/Al_2O_3 catalyst and observed no significant variation in the amount of carbon monoxide in the product as compared to the unpromoted Rh/Al_2O_3 catalyst. Beltrame et al. (1979) studied the effect on α-Cr_2O_3 on the rate of steam dealkylation of toluene reaction, and found, that α-Cr_2O_3 was a better catalyst support than silica-stabilized alumina for rhodium catalyst.

The available evidence indicates that the activity of the unpromoted rhodium on γ-alumina support declines fairly rapidly. Duprez et al. (1985) studied the variation of conversion with time at 713 K and 1 atm and reported a sharp activity decline initially and a slow or negligible deactivation rate later on. This was attributed to the coke formation . Duprez et al. (1986) have shown that the coke is an essential poison particularly during the early period of the reaction (0 - 1h). Duprez et al. (1986) studied the effect of feed sulphur content and coke

deposition during steam reforming of toluene on rhodium/alumina catalyst. From the EPMA analysis, it was concluded that the catalyst was affected markedly by sulphur concentration and the coke deposited. The results showed that the coke content of the catalyst increased with the depth of the catalyst bed suggesting a series deactivation. Kochloefl (1976) also reported a rapid decline in the activity of all rhodium/γ-alumina catalysts both for the toluene steam dealkylation as well as the toluene hydro-dealkylation reaction. He attributed this deactivation to the strong adsorption of polynuclear aromatics hydrocarbons formed by the dehydrocondensation reaction of benzene and toluene. Francis (1980) studied the deactivation kinetics of alkyl phenols on Rh supported on different alumina phases, and observed a rapid rate of deactivation for all γ-Al_2O_3 supported catalyst. It was suggested that the dehydrogenation function of the catalyst may at least partially contribute to the rapid rate of deactivation . Forni et al.(1984) studied the variation in the catalyst activity and selectivity of rhodium supported on α-Cr_2O_3. They observed a progressive loss in the reaction selectivity which was presumed to be due to the change conferred by Rh^{3+} ions on the properties of the chromia.

The above literature survey shows that very little information is available on the intrinsic deactivation kinetics of this reaction on rhodium/γ-alumina catalyst and no information is reported on the diffusion-deactivation interaction on this system.

Chapter 3

EXPERIMENTAL SET-UP AND PROCEDURE

3.1 INTRODUCTION

Both the diffusion-free and diffusion-influenced kinetics of the steam dealkylation of toluene were investigated in a gradientless internal recycle reactor (Berty reactor) at atmospheric pressure. The catalyst used in this investigation was rhodium on γ-alumina. The temperature was varied in the range 663-723 K , the inlet water to toluene mole ratio in the range of 1.11-14.8 and the space time from 2.78- 64.5 kg cat/(kmol)(h) .

3.2 CATALYST PREPARATION

The method of excess solution was used to impregnate the required percentage of rhodium on the catalyst support. The catalyst support used for all the runs was γ-alumina (Al-4183T 1/8", Harshaw) in the form of 3.2x3.2 mm cylindrical pellets. The bidisperse support had a total pore volume of 1.09 cm^3/g ,a surface area of 200 m^2/g and an average micro and macro pore sizes of 50 A^o and 6500 A^o ,respectively.

Since the objective of this study was to model the deactivation kinetics on pellets, the catalyst for the intrinsic kinetics studies was prepared by crushing the impregnated pellets rather than by impregnating the crushed support. The rhodium was deposited on the catalyst in the form of rhodium trichloride ($RhCl_3.xH_2O$; min. rhodium content 38.5 wt%). Some exploratory runs were conducted with different metal loading, but for all the main runs the rhodium content on alumina was fixed at 0.4 wt % . Figure

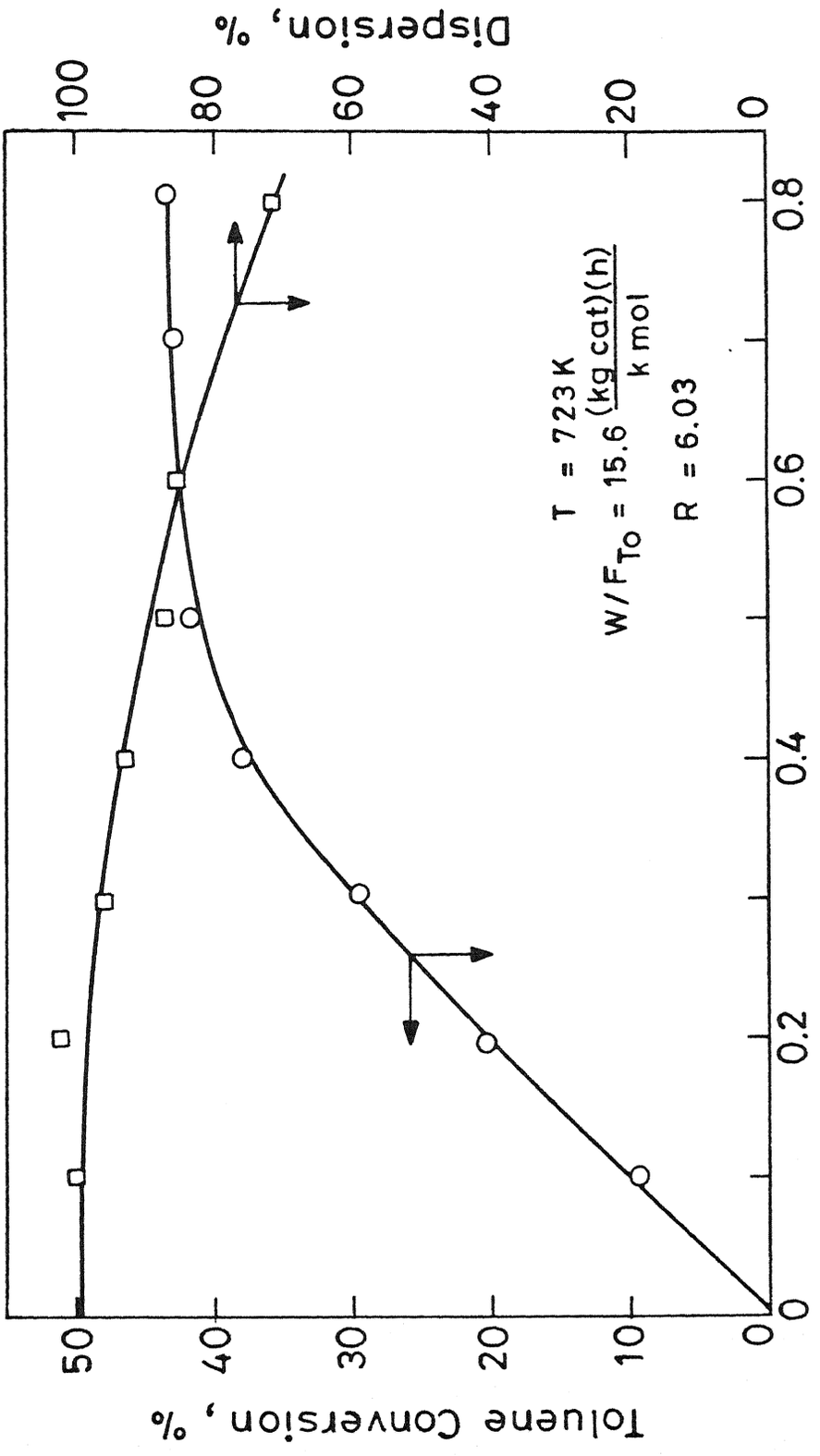

Fig. 3.1 Variation of toluene conversion and Rh dispersion with metal loading.

3.1 depicts the effect of metal loading and the metal fraction exposed on the toluene conversion and benzene selectivity . On basis the of these findings , it was decided to fix the rhodium at 0.4 wt. % for all the main runs. Preliminary runs indicated that, due to the strong chemisorption ,the rhodium deposited nonuniformly on the untreated alumina pellets.

A number of trial runs had to be made in order to develop a suitable impregnation procedure for obtaining a catalyst with a uniform activity profile. To achieve uniform rhodium distribution inside the catalyst pellet, sequential impregnation with hydrochloric acid was employed. Since hydrochloric acid is more strongly chemisorbed on alumina than rhodium, pretreatment of the alumina with hydrochloric acid results in the rhodium penetrating deeper into the pellet. The catalysts were prepared in 30 g batches, by, first treating the alumina pellets with 0.03 N solution of hydrochloric acid (pH = 1.56) for four hours at room temperature and then dried overnight. To obtain a loading of 0.4 wt.% rhodium,the treated alumina pellets were impregnated with 120 cm^3 of 0.15 M rhodium trichloride solution. The initial pH of the aqueous rhodium trichloride solution was maintained at 0.03 N by adding hydrochloric acid to the aqueous solution. Due to the continuous evaporation of water from the solution, deionized water was added to the impregnation solution. To increase the diffusion rate of the rhodium metal into the pellets, the impregnation temperature was maintained at 343K . The impregnation time was approximately 24 hours. After the impregnation was completed, the catalyst pellets were again dried at room temperature. The dried pellets were calcined for five hours at 773 K. The catalyst was crushed, and the 0.2 - 0.4 mm fraction was retained, for the

intrinsic kinetic studies. The catalyst (crushed or pellets) was reduced in-situ in flowing hydrogen for six hours at 723 K.

3.3 CATALYST CHARACTERIZATION

The catalyst was characterized with respect to total surface area and metal dispersion

3.3.1 Total Surface Area

The total surface area of the alumina support was determined using BET technique and the total surface area was found to be 200 m^2/g .

3.3.2 Metal Dispersion

The rhodium dispersion on the catalyst was determined from H_2 chemisorption on a Micromeritics Pulse Chemisorb 2700 catalyst characterization unit using the dynamic pulsing technique. The metal dispersion for the 0.4 wt% rhodium on alumina catalyst was found to be 92 % .

3.3.3 X-Ray Diffraction

In order to determine the lattice parameter , X-ray diffraction was carried out for the following samples i) uncalcined and unreduced catalyst ii) calcined and unreduced iii) calcined and reduced . No rhodium peak was detected for any of the investigated samples indicating high dispersion as confirmed by the metal dispersion measurement.

3.4 EXPERIMENTAL APPARATUS

As mentioned earlier,the experimental work was carried out in an internal recycle catalytic reactor (Berty reactor), and the schematic diagram of the reactor is shown in Figure 3.2. The 3" I.D. Berty reactor (supplied by Autoclave Engineers Inc.,

U.S.A) was made of 316 SS ,with available reactor volume of 96.7 cm^3. The reactor was heated by a furnace with three heating zones,the top and the middle heaters had rating of 1.1 kW whereas the bottom zone had a maximum rating of 1.8 kW. The mixing in the reactor was provided by an impeller ,driven by a magnetic coupling ,which eliminates the usual problems encountered in conventional packed drives. The impeller was driven by 1/4 hp DC motor ,and had a maximum speed of 3000 rpm. A schematic diagram of the experimental set up is shown in Figure 3.3 . The water and toluene liquid feed were separately vaporized and then mixed. The combined vaporized feed was then heated to the reaction temperature in a preheater before entering the reactor. Water and toluene were injected continuously by a syringe pump (Model 351,Sage Instruments, USA),which could be adjusted in the range of 0.02 to 100 cm^3 per minute,depending on the size of the syringe used. With a syringe of 50 cm^3capacity,the range of flow rates was 0.09 to 60 cm^3 per minute. The vaporizer and preheater were constructed by winding Kanthal wire on a ceramic tube, and then insulated with magnesia powder. The vaporizer and the preheater had maximum heating capacities of 2.8 kW and 2.0 kW , respectively.

To avoid any temperature drop between the vaporizer and the preheater, a line heater was placed in between. Similarly, a line heater was also placed between the preheater and the reactor inlet. The temperature of the catalyst bed was monitored by two iron-constantan thermocouples, one measured the bottom temperature of the bed and the other one recorded the top zone temperature of the reactor. The reactor was maintained at the desired temperature by controlling the heat input to the bottom zone using a PI controller (Model No. 400-D Indotherm, India).The

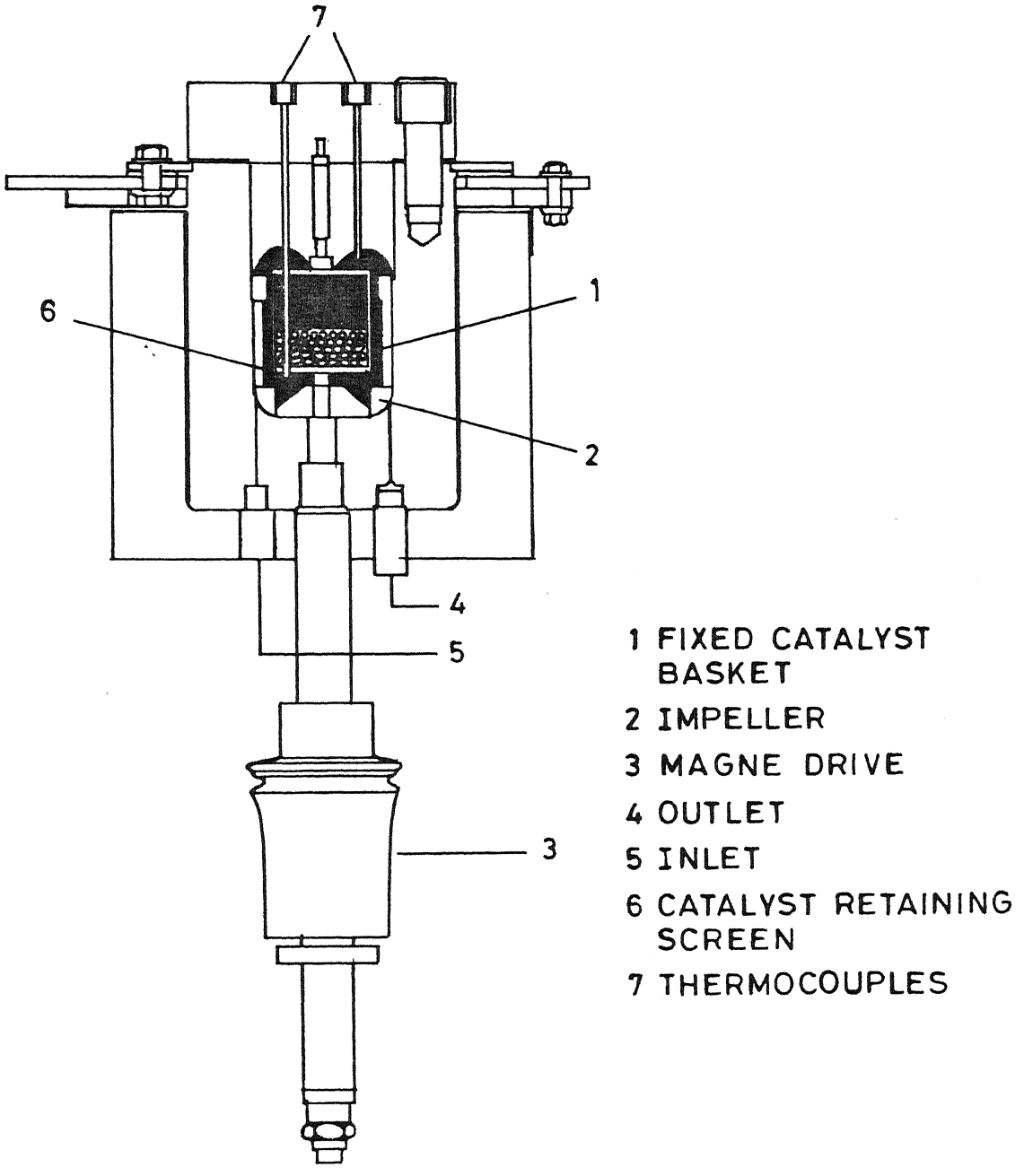

Fig. 3.2 Schematic diagram of Berty reactor.

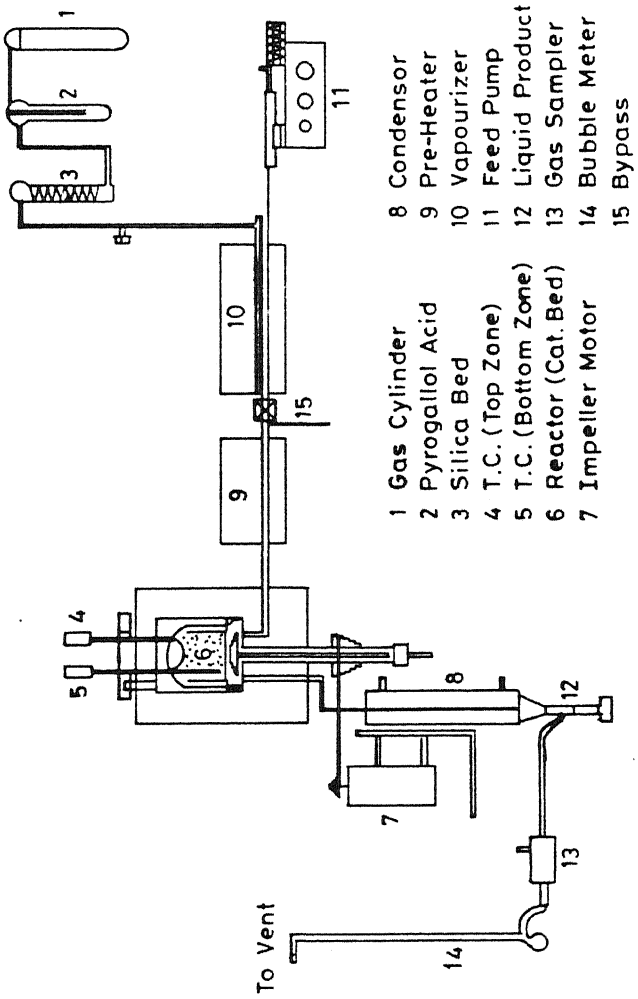

Fig. 3.3 Schematic diagram of the experimental set up.

unconverted liquid reactants and products were quenched in a condenser which was cooled by a circulating water-glycerin solution maintained at 278 K. The condensables were collected in a measuring cylinder and the noncondensables were passed through a gas sampling valve and flow-meter and then vented.

3.5 EXPERIMENTAL PROCEDURE

Each experimental run was initiated by placing a known amount of fresh impregnated alumina catalyst inside the reactor basket.To ensure good flow pattern distribution and a generation of pressure head inside the reactor ,the basket was filled with an inert material of the same size as the catalyst . The catalyst was reduced in-situ by passing hydrogen during the heating process.The hydrogen gas was passed through alkaline pyrogallol solution to remove traces of oxygen followed by a silica gel bed to absorb any water carried by the gas from the alkaline solution. After the required reaction temperature had been attained,the hydrogen flow was stopped and steam was passed through the reactor for a period of 30 minutes. The flow of the reactants were stabilized before the inlet to the reactor,and when the required reaction temperature had stabilized, the reactants were introduced into the reactor. The liquid and gas product samples were analyzed as a function run time. The gas flow rate was measured by a soap bubble meter, and the condensed liquid containing the water and the organic fraction was collected in a measuring cylinder. Initially , when the rate of deactivation was high ,sampling duration was 10 minutes for a period of one hour and then at 20 minute interval for another hour, and then every half an hour till the completion of the run. At the

end of each run, the reactor was purged with nitrogen to avoid burning of any coke deposited on the catalyst surface. After the run was over the catalyst bed was taken out and replaced with fresh catalyst for the next run.

3.5.1 Gas and Liquid Analysis

The gaseous and the liquid products of the toluene steam dealkylation reaction ,together with the unconverted reactants were analyzed as function of run time on 3 different columns using two gas chromatographs. The chromatograms were recorded on a hewlett Packard reporting integrator (Model 3390A, Hewlett Packard ,U.S.A.). For all the analysis, thermal conductivity detector was used. The CO, CO_2, CH_4 in the product gases. were analyzed on a Poropak Q column (3 mm i.d., 3 m long) using hydrogen as carrier gas at a flow rate of 30 cm^3 per minute. The injector ,oven temperature and detector were fixed at 323K, 313K and 373K, respectively. Since the H_2 and CO could not be separated on the Poropak Q column, a Molecular Sieve 5A column (3 mm i.d and 3 meters long) was used to separate H_2 ,CO and CH_4 .The carrier gas was nitrogen at a flow rate of 20 cm^3 per minute at 403 K and the oven and detector temperatures were maintained at 373 K. The benzene and toluene in the organic fraction of the condensed reactor effluent were analyzed on a 3 mm i.d., 2.5 meter long diethylene glycol succinate (DEGS) on Chromsorb P column.The carrier gas was nitrogen at a flow rate of 30 cm^3 per minute .The injector temperature was fixed at 403 K and the oven and the detector temperature at 373 K . The detector bridge current was fixed at 120 mA.

The peak areas were converted to weight or mole percent using calibration curves prepared from pure components . The

Chapter 4

RESULTS AND DISCUSSION

The effect of deactivation-diffusional influences on catalyst activity and selectivity during steam dealkylation of toluene on rhodium/alumina catalyst was investigated in a gradientless (Berty reactor) reactor at a total pressure of one atmosphere in the temperature range of 663 - 723 K. The space time and the molar ratio of water to toluene were varied from 2.8 - 64.5 kg cat./(kmol)(h) and 1.11 - 14.8 (mol/mol), respectively.

4.1 PRELIMINARY RUNS

Various preliminary runs were conducted to determine the residence time distribution (RTD) in the reactor as well as the experimental conditions where external mass transfer resistances and pore diffusional resistances did not affect the reaction rate. In addition, preliminary runs were also made to investigate the influence of the reduction time and temperature on the catalyst activity.

4.1.1. Interphase Mass Transfer Effects

To study the effect of external mass transfer resistances on the conversion , experiments were performed for different rpm values of the impeller speed ranging form 1200 to 3000 rpm , keeping the other variables constant. The results are shown in Figure 4.1 . The conversion of toluene increased with increasing impeller speeds till about 2000 rpm, beyond which rpm did not affect the conversion. Therefore, for all the subsequent runs, the impeller rpm was kept more than 2000 , ensuring that external mass

transfer resistances did not affect the conversion.

4.1.2. Intraphase Mass Transfer Effects

The effect of pore diffusion was studied by conducting runs at a constant W/F_{To} (kg catalyst per kg mole of toluene per hour), temperature and inlet molar ratio of water/toluene for different catalyst particle sizes ranging from 0.2 to 3.2 mm . The effect of catalyst particle size on the toluene conversion is shown in Figure 4.2 . As shown in this figure, conversion increased with decreasing particle size till 1.2 mm. For catalyst sizes below 1.2 mm diameter, conversion was not affected by the particle size. Thus, for determining the intrinsic kinetics of the main as well as the deactivation reactions, a catalyst size of 0.2 -0.4 mm was used. To study the diffusion-deactivation interaction on the catalyst activity and selectivity, the size was either 1.68 or 3.2 mm.

4.1.3. RTD of The Berty Reactor

To determine the degree of mixing in the reactor, a step change in concentration was made at the inlet of the reactor and the resultant reactor outlet concentration measured continuously. The reactor basket was filled with inert ceramic material to provide greater pressure head inside the reactor to increase the internal recycle ratio (Berty, 1974). Initially, a nitrogen flow rate in the range of 30 to 90 cm^3/min was passed through the reactor which was kept at room temperature. When the flow had stabilized hydrogen at flow rates varying from 3 to 10 cm^3/min was introduced with the help of a toggle valve and the hydrogen concentration in the outlet stream monitored on a thermal conductivity detector. This was performed at a impeller speed of

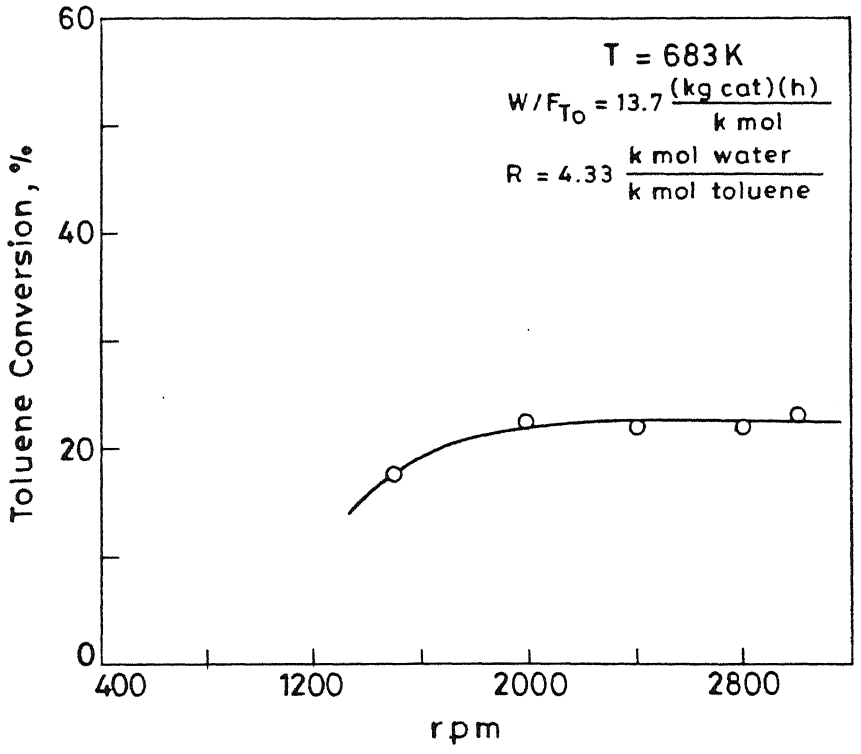

Fig. 4.1 Effect of impeller speed on toluene conversion.

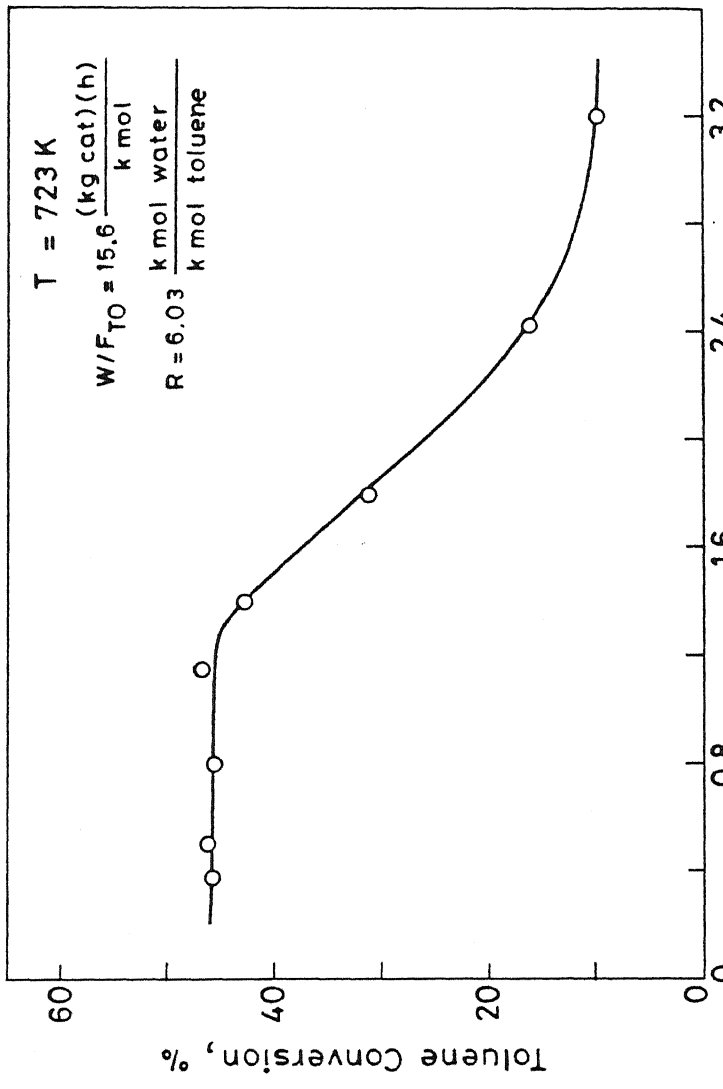

Fig. 4.2 Effect of catalyst size on the toluene conversion.

2800 rpm.

For an ideal CSTR behavior, it can be shown that (Levenspiel, 1972),

$$\ln (1 - C/C_o) = -t/\bar{t} \qquad (4.1)$$

conductivity detector. This was performed at a impeller speed of 2800 rpm.

where C : exit concentration of hydrogen at any time ,mol/cm^3.

C_o: initial concentration of hydrogen , mol/cm^3.

$\bar{t}$: residence time in the reactor ,min.

Thus, for an ideal CSTR a plot of ln (C/C_o) versus time should give a straight line. For all the experiments, the semilog plots of hydrogen concentration in the outlet stream versus time showed a good linearity . This indicated that the gas within the reactor was well mixed.

4.1.4 Effect of Reduction Temperature and Time

From the published literature available for this reaction, it was observed that there is a wide variation in the reduction conditions employed by different investigators. Grenoble (1978b) reduced the supported rhodium catalyst for one hour in flowing H_2 at 775 K. For ni et al. (1984) studied the kinetics of toluene steam dealkylation over chromia-alumina support. The catalyst was reduced for a period of two hours at 603 K. Similar conditions were employed by Beltrame et al. (1984). Duprez et al.(1986) reduced the catalyst for 14 hours in hydrogen atmosphere at 723 K.

Runs were conducted to investigate the effect of reduction temperature and time on the catalyst activity. The catalyst was reduced at different temperatures varying from 663 to 733 K for a fixed reduction time of 2 hours. The results are shown in

Figure 4.3. As can be seen from this figure, over this temperature range, the catalyst activity is independent of the reduction temperature which implies that the catalyst was completely reduced even at 663 K. Similarly, for the next set of runs, the reduction temperature was kept constant at 683 K and the reduction time was varied from 1 to 12 hours. As can be seen from Figure 4.4 ,over this range , there is no effect of the reduction time on the catalyst activity. Thus, throughout this study, the reduction temperature was kept fixed at 723 K and the catalyst was reduced at this temperature for 2 hours.

4.2 INTRINSIC KINETICS OF THE TOLUENE STEAM DEALKYLATION REACTIONS

To study the intrinsic kinetics of the steam dealkylation reaction in the temperature range of 663-723 K and a total pressure of one atmosphere, various runs were conducted to determine the effect of temperature, reactant(s) and product(s) partial pressures on the main reaction rate. Toluene and water partial pressures were varied in the range 0.04 to 0.35 and 0.18 to 0.90 atm, respectively. Carbon monoxide, hydrogen and benzene partial pressure were varied in the range 0.01 to 0.27 , 0.05 to 0.20 and 0.03 to 0.18 atm, respectively, by adding these components to the feed. For all the runs, the overall material balance and the carbon , hydrogen and oxygen balances were made and these were usually 100 ± 3% .

Preliminary runs conducted on γ-alumina support without any rhodium impregnation confirmed that, no reaction occurred on the alumina support.

The products of toluene steam dealkylation were mainly benzene, carbon monoxide , carbon dioxide, hydrogen together

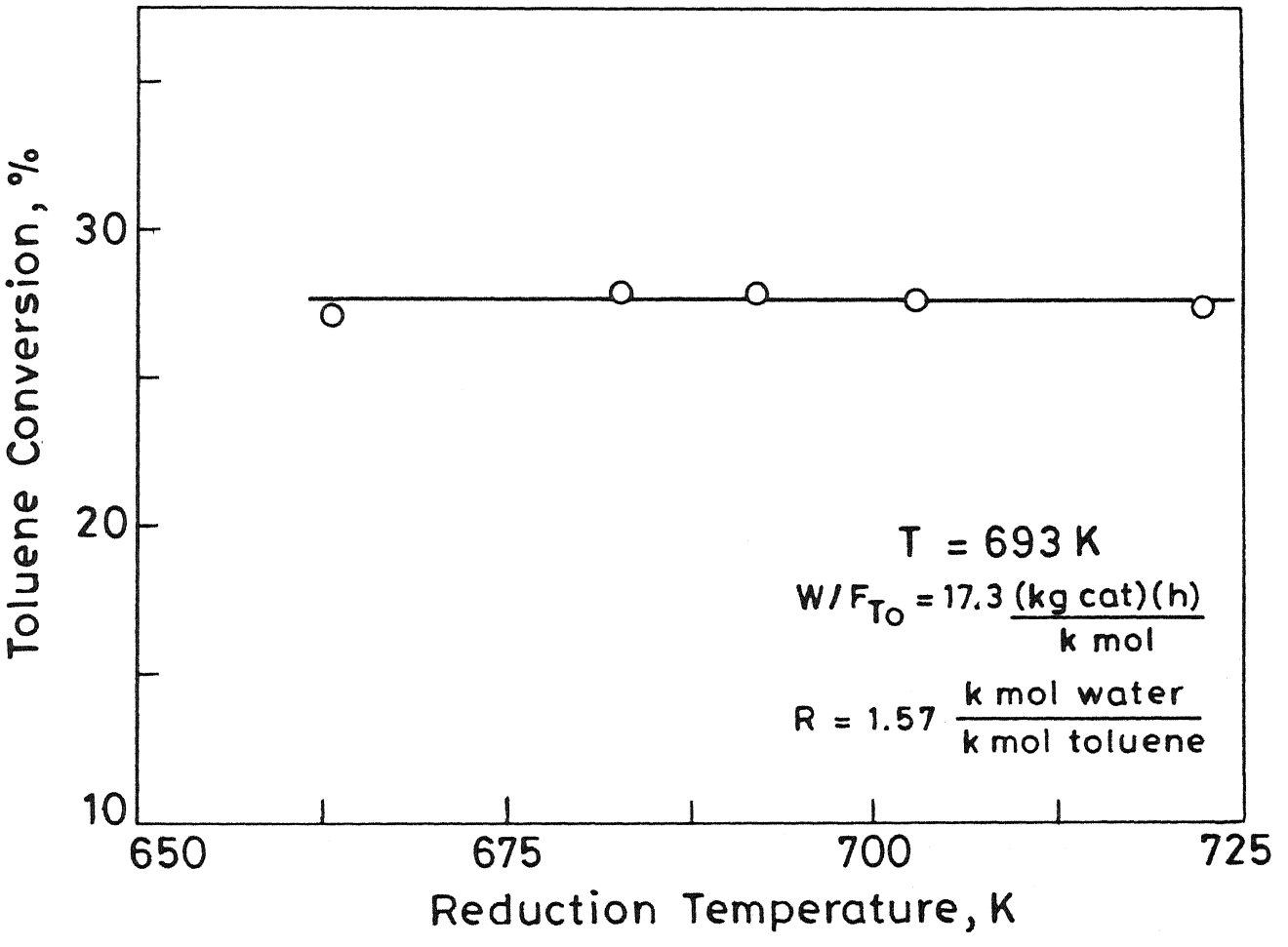

Fig. 4.3 Effect of reduction temperature on toluene conversion.

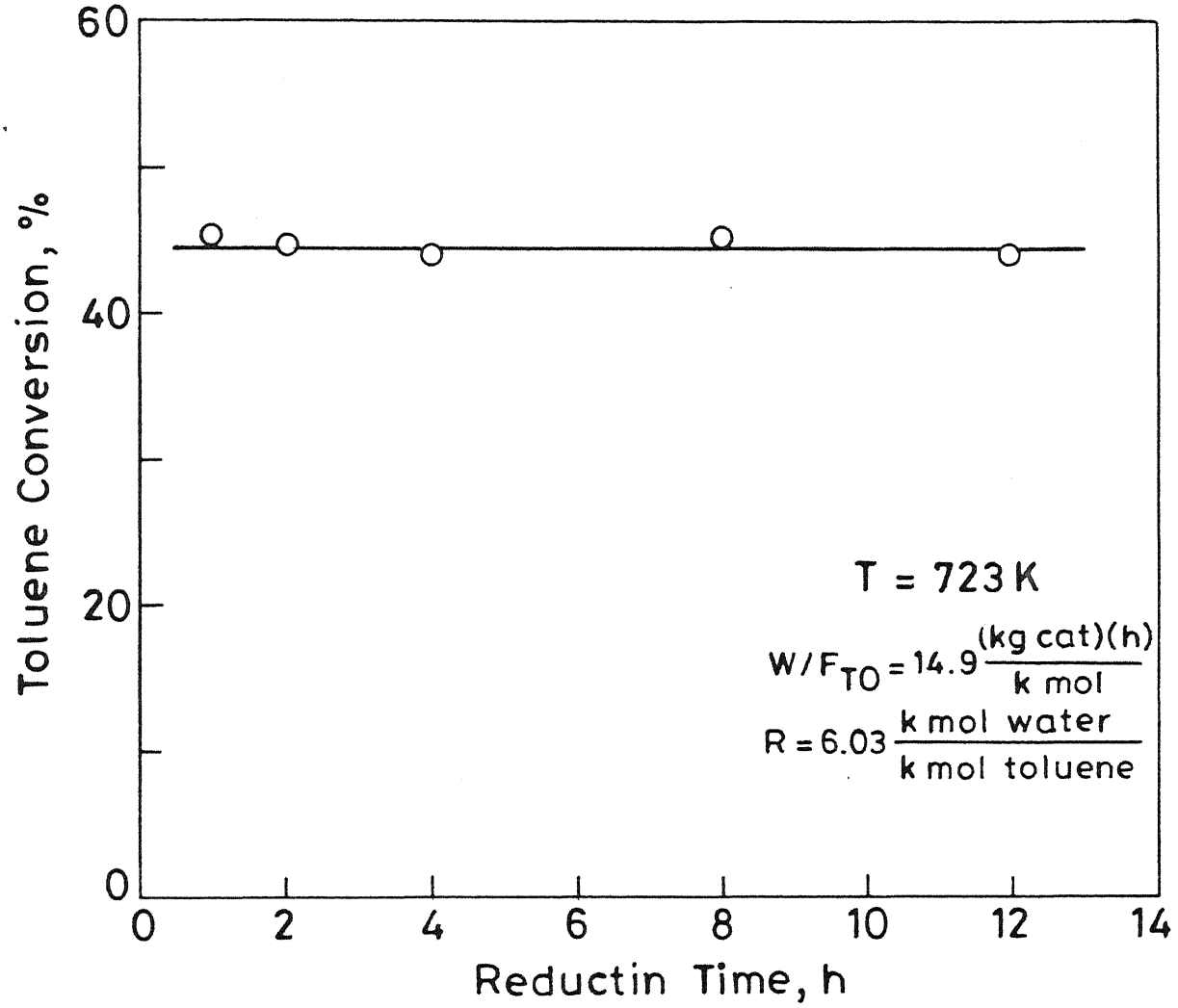

Fig. 4.4 Effect of reduction time on toluene conversion.

with traces of methane. The activity of the catalyst decreased with time and the initial conversion and selectivities were determined by extrapolating the data to zero time. A typical plot of the variation of conversion with run time is shown in Figure 4.5 . For all the runs, the conversion showed a rapid decline till a run time of 1 to 2 hour followed by a slower rate of catalyst deactivation. These results are in good agreement with the findings of Duprez et al.(1986) and Grenoble (1978b). Duprez et al.(1986) have reported that the metal coverage of the coke increased from 0 to 65% in 1 hour whereas from a run time of 1 to 8 hours, the increase was very gradual, the metal coverage by coke increasing to 70 % in 8 hours. The deactivation kinetics is discussed in detail later (Section 4.4).

Depending on the space time , temperature and the partial pressure of the reactants, the initial toluene conversion varied from 6 to 50 % . The toluene conversion, selectivities of benzene, S_B, carbon monoxide, S_{CO}, carbon dioxide, S_{CO2}, hydrogen, S_{H2}, and the moles of water consumed per mole of toluene reacted at 713 K and various values of the inlet molar ratio of water/toluene, R, are given in Table 4.1. As can be seen from Table 4.1, at a constant W/F_{To} , for R less than 8 the toluene conversion increased with an increase in R. On the other hand, for R greater than 10 (refer Table 4.1,runs R7,R8,and R22),the toluene conversion decreased with increasing R. It should be emphasized that this is a combined effect of changes in both the toluene and water partial pressures. At high values of R, the surface concentration of the adsorbed toluene would be lowered decreasing the rate of reaction. Since the total pressure was fixed at 1 atm ,for partial pressure of water in the reactor approaching unity, the rate of the

Table 4.1: Typical product distribution of toluene/water reaction

T = 713 K

Run No.	$\frac{W}{F_{To}}$, $\left[\frac{kgcat}{kmol/h}\right]$	R	X_T ,%	δ	S_B	S_{CO}	S_{CO2}	S_{H2}
R6	15.61	1.11	10.8	1.93	0.98	1.06	0.05	2.22
R5	15.61	1.57	22.5	1.15	0.98	1.04	0.11	2.31
R11	21.41	1.57	20.5	1.55	0.90	1.37	0.24	3.16
R10	21.44	2.47	22.8	1.86	0.89	1.49	0.20	3.21
R4	15.61	2.79	30.6	1.83	0.88	1.30	0.16	3.21
R15	07.23	2.79	17.5	2.21	0.84	1.31	0.46	3.55
R14	21.45	3.32	22.6	2.21	0.84	1.75	0.26	3.67
R3	15.61	3.76	29.6	2.15	0.87	1.41	0.38	3.53
R2	15.61	4.40	38.8	2.49	0.84	1.45	0.53	3.97
R13	21.44	5.93	25.0	3.11	0.72	1.91	0.38	4.40
R1	15.61	6.03	43.1	2.85	0.81	1.16	0.83	4.50
R24	12.26	7.79	50.6	2.72	0.82	1.22	0.77	4.33
R9	22.79	9.34	44.4	2.90	0.86	1.08	0.75	4.04
R8	16.41	10.57	34.4	2.56	0.83	1.50	0.54	4.07
R7	16.33	12.56	19.4	3.01	0.73	2.10	0.49	4.84
R22	32.81	14.22	33.4	3.02	0.79	1.70	0.71	4.60

R : inlet molar ratio of water to toluene.

S_B, S_{CO}, S_{CO_2}, S_{H_2} : moles of benzene, CO , CO_2 , H_2 formed per mole of toluene reacted, respectively.

X_T : conversion of toluene, % .

δ : moles of water consumed per mole of toluene reacted.

dealkylation reaction tends to zero.

The initial benzene selectivity, (moles of benzene produced per mole of toluene reacted) varied from 70 - 90 %), which is in good agreement with the results reported by several other investigators (Grenoble, 1978b ; Kochloefl , 1976 ; Beltrame et al. 1984). It is well established that for toluene steam dealkylation , the benzene selectivity depends on the nature of the support, metal dispersion and the rhodium content of the catalyst. Different investigators have reported benzene selectivity in the range of 50 - 95 % . Higher metal dispersion generally result in a higher benzene selectivity. Duprez et al. (1985) reported an increase in benzene selectivity from 72 to 80 % as the metal dispersion of $Rh/\gamma-Al_2O_3$ increased from 20 to 90 %.

Another observation which can be made from Table 4.1 is that the moles of water consumed per mole of toluene reacted , δ, increased as the benzene selectivity, decreased. This is due to the fact, that, compared to the benzene formation reaction, the complete destruction of the toluene ring requires more water. As shown in Table 4.1 , the moles of carbon monoxide , carbon dioxide and hydrogen formed per mole of toluene reacted increased as R was increased. Depending upon the inlet water partial pressure, the moles of carbon monoxide produced per mole of toluene reacted varied between 1.1 to 3.2 whereas the number of moles of carbon dioxide produced per mole of toluene reacted varied from 0.1 to 0.8 . For the intrinsic kinetics runs in this study, the molar ratio of CO/CO_2 in the gaseous product varied from 1.8 to 7.5.This CO/CO_2 ratio was mainly a function of the water partial pressure and temperature. As Beltrame et al. (1984) have reported, the CO/CO_2 molar ratio in the gaseous product depends on the nature of

the support. The sequence for the CO/CO_2 ratio at a temperature of 733 K reported by them was as follows: silica-stabilized γ-alumina , 2.2 ; γ-alumina ,0.3-0.5; Cr_2O_3-Al_2O_3,0.13; α-Cr_2O_3 , 0.016 (equilibrium value). The low value of CO/CO_2 ratio reported for chromia was attributed to the role of the support in promoting the water gas shift reaction . It seems that the γ-alumina support used in this study is not as effective in catalyzing the water gas shift reaction. A possible reason could be the different catalyst preparation method and/or support. Dictor (1987) reported that extensive oxidation of rhodium/ γ-alumina resulted in a rapid loss in the water gas shift activity. His data suggests that there is some intermediate oxidation treatment that gives the greatest activity for the water gas shift reaction.

The hydrogen produced in the toluene/water reaction constituted about 60 vol.% of the total gaseous product, and the hydrogen selectivity, S_{H2} increased from 2.2 to 4.8 as R was increased from 1.1 to 14.2 .

The toluene steam dealkylation is a complex reaction in which several consecutive and parallel reactions can take place. The dealkylation of toluene is generally accompanied by the steam reforming and water gas shift reactions. There is some controversy regarding the exact stoichiometry of these reactions. For instance, Kochloefl (1976), considered the following reactions in his study:

toluene steam dealkylation reaction (TSD):

$$C_6H_5CH_3 + 2H_2O \longrightarrow C_6H_6 + CO_2 + 3H_2 \qquad (4.2)$$

toluene hydrodealkylation reaction (THD):

$$C_6H_5CH_3 + H_2 \longrightarrow C_6H_6 + CH_4 \qquad (4.3)$$

toluene steam reforming reaction (TSR):

$$C_6H_5CH_3 + 14H_2O \longrightarrow 7CO_2 + 18H_2 \qquad (4.4)$$

where toluene steam dealkylation reaction (4.2) was considered to consists of two steps as follows:

$$C_6H_5CH_3 + H_2O \longrightarrow C_6H_6 + CO + 2H_2 \qquad (4.5)$$

$$CO + H_2O \rightleftharpoons CO_2 + H_2 \qquad (4.6)$$

In addition, depending upon the conditions and the properties of the catalyst , he also suggested the possibility of methanation reaction and the reaction of CH_4 with CO_2 . From his study, he concluded that, on rhodium/γ-alumina catalyst, methane produced during toluene steam dealkylation reaction is formed mainly by hydrodealkylation reaction. On the other hand, Duprez et al. (1982) did not include the hydrodealkylation reaction, and for the toluene steam reforming they used a stoichiometric coefficient of water as seven . They represented the toluene/water reactions in the following way:

$$C_6H_5CH_3 + H_2O \longrightarrow C_6H_6 + CO + 2H_2 \qquad (4.7)$$

$$C_6H_5CH_3 + 7H_2O \longrightarrow 7CO + 11H_2 \qquad (4.8)$$

$$CO + H_2O \rightleftharpoons CO_2 + H_2 \qquad (4.9)$$

$$CO + 3H_2 \longrightarrow CH_4 + H_2O \qquad (4.10)$$

Reaction (4.10) generally takes place at pressures well above one atm.

In this study, for all the runs , the amount of methane produced was negligible (maximum amount of CH_4 measured at 723 K was less than 1 % of the total gaseous product) and hence reaction (4.10) was not taken into account in further calculations. For all the runs in this study, reactions (4.7) , (4.8), and (4.9) could satisfactorily explain the experimentally measured product distribution.

To check the applicability of this reaction scheme, the extent of steam dealkylation reaction (4.7) was calculated from the amount of benzene experimentally measured. The extent of the steam reforming reaction (4.8) was determined from the difference between the total toluene reacted and the benzene formed. The total toluene reacted was determined from the reactor mass balance equation. It was assumed that CO_2 was produced only in the water gas shift reaction (4.9).Then, based on the above stoichiometry, the moles of H_2 and CO produced together with moles of water consumed per mole of toluene reacted were calculated. A comparison of the experimental values with those calculated as detailed above, is shown in Table 4.2 for some representative runs. The details of these runs are given in Table 4.1. As can be seen from Table 4.2 ,very good agreement was obtained between the experimental values and those calculated using the reaction

Table 4.2: Comparison of experimental selectivities and selectivities calculated from the assumed reaction stoichiometry.

Run no.	water consumed per mole toluene reacted		moles carbon monoxide formed per mole toluene reacted		moles hydrogen formed per mole toluene reacted	
	exptl.	calcd.	exptl.	calcd.	exptl.	calcd.
R5	1.15	1.12	1.10	1.09	2.23	2.21
R4	1.83	1.88	1.55	1.57	3.21	3.25
R24	2.72	2.79	1.32	1.31	4.35	4.39
R7	3.15	3.11	2.10	2.13	4.84	4.92

scheme given by reactions (4.7) to (4.9). Similar agreement was obtained for the other runs also. Thus, for all the runs in this study it was assumed that only these three reactions were occurring to any appreciable extent.

4.2.1 Effect of Partial Pressures of Reactants and Products on Reaction Rates

The effect of reactant(s) partial pressures on each of the three reactions occurring simultaneously in this system was investigated. A gradientless internal recycle reactor was used in this study, and therefore the partial pressures inside the reactor were the same as the exit partial pressures. Thus, based on the total toluene converted, the combined rates of the toluene steam dealkylation (TSD) and toluene steam reforming (TSR) reactions, at any time, were calculated from the reactor mass balance equation as follows:

$$(R_1 + R_2) = \frac{F_{To}\, X_T}{W} \qquad (4.11)$$

where R_1 and R_2 represent the rates of the TSD and TSR reactions, respectively. The rate of toluene steam dealkylation reaction was calculated from the experimental measured rate of benzene formation as shown below:

$$R_1 = S_B \frac{F_{To} X_T}{W} \qquad (4.12)$$

Similarly,the rate of water gas shift reaction (WGS) was calculated from the experimentally measured rate of carbon dioxide formation, as follows:

$$R_3 = S_{CO2} \frac{F_{To} X_T}{W} \qquad (4.13)$$

In equation (4.13), R_3 is the rate of the water gas shift reaction. Equations (4.11) to (4.13) are valid for any run time and for the intrinsic kinetics of the fresh catalyst, the conversion and selectivities at zero time were used.

The effect of water partial pressure on toluene steam dealkylation , steam reforming and water gas shift reactions was investigated and some of the results at 713 K are shown in Figures 4.6 and 4.7. One of the usual problems encountered in gradientless reactor studies is the difficulty in isolating and investigating the effect of a particular component on the reaction rates. Although , a number of experimental measurements at this temperature were made (refer Appendix II) in most of these runs, partial pressure of all the components changed simultaneously. For the sake of qualitative representation, some runs in which the partial pressures of the other species were approximately constant have been identified and these have been shown in these figures. Needless to mention, for the purpose of subsequent model development (Section 4.3) , all the data shown in Appendix II were utilized.

As shown in Figures 4.6 and 4.7 for water partial pressure in the range of 0.2 to 0.6 atm, the initial rates of the three reactions increased with increasing water partial pressure. The toluene steam dealkylation reaction rate increased from 0.012 to 0.018 kmol/(kgcat)(h) as the partial pressure of water was increased three fold from 0.2 to 0.6 atm . For these runs, the exit toluene partial pressure was approximately constant (0.14 ±

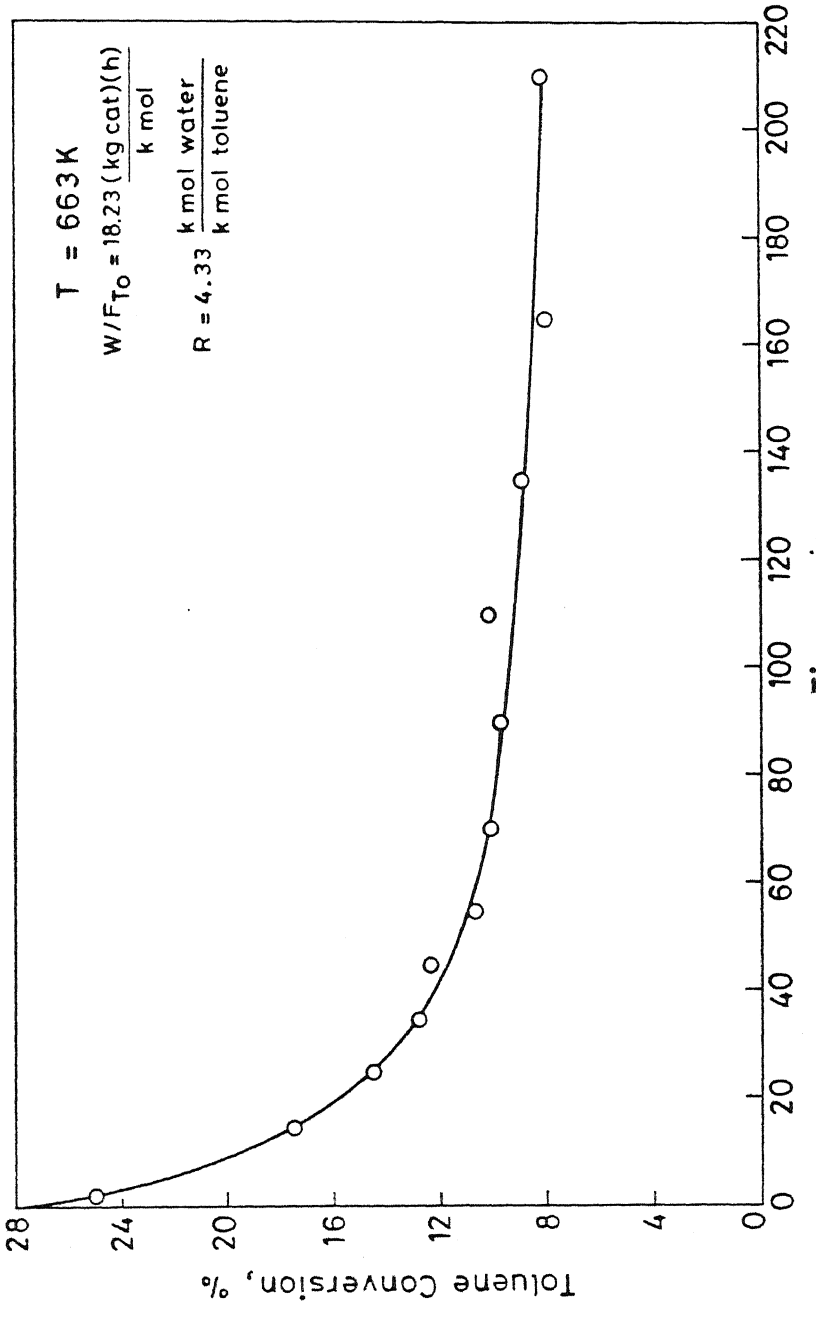

Fig. 4.5 Variation of toluene conversion with run time.

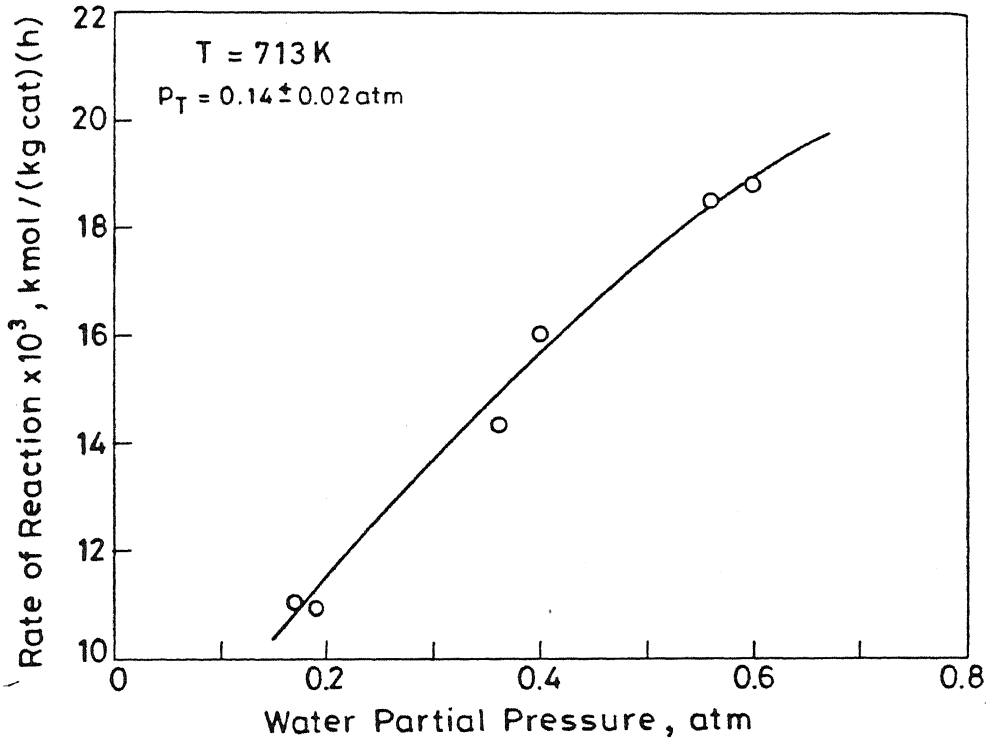

Fig. 4.6 Effect of water partial pressure on rate of toluene steam dealkylation reaction.

0.02 atm) . In these runs, nitrogen was added as an inert and the partial pressures of CO, CO_2 and benzene inside the reactor was less than 0.06 atm while hydrogen partial pressure was less than 0.11 atm. On the other hand, as shown in Table 4.3 , the benzene formation rate declined for water partial pressures greater than 0.85 atm. It should be noted that for the data shown in Table 4.3, the partial pressures of the other components are also varying ; and , the effect of the variation of other components could be significant since water is in excess. The data in this table show that for higher water partial pressures (and consequently lower toluene partial pressure), the rate of toluene steam dealkylation reaction decreased significantly. A comparison of Figures 4.6 and 4.7 shows that the benzene selectivity decreased with increasing steam partial pressure. For instance, at a partial pressure of 0.2 atm, S_B was 0.96 and decreased to 0.86 at a partial pressure of 0.6 atm. As shown in Table 4.3 , for water partial pressure greater than 0.85 atm, the rate of toluene steam dealkylation reaction decreased whereas the rate of steam reforming reaction did not show any decline. Thus, the benzene selectivity decreased with increasing steam partial pressure.

The results obtained in this study are in good agreement with those reported by Kochloefl (1976) who found a considerable increase in the total conversion of toluene with increasing inlet molar ratio of water to toluene. Moreover, the benzene selectivity was found to decrease because the steam reforming reaction increased at a faster rate than the dealkylation reaction with increasing partial pressure of water. Grenoble (1978b) also reported similar results at 1 atm and 713 K for

Table 4.3 : Variation of initial reaction rates with partial pressures.

Partial pressures are in atmosphere.

R_1^o, R_2^o, and R_3^o are in kmol/(kgcat)(h).

Temperature : 713 K

run No.	$R_1^o \times 10^3$	$R_2^o \times 10^3$	$R_3^o \times 10^3$	P_T	P_B	P_H	P_{CO}	P_{CO2}	P_W
R6	13.5	3.1	13.8	0.07	0.050	0.145	0.043	0.033	0.68
R5	16.0	3.0	10.0	0.11	0.053	0.160	0.043	0.033	0.60
R11	15.6	2.7	7.6	0.12	0.051	0.148	0.039	0.030	0.56
R10	18.0	1.5	3.0	0.13	0.052	0.150	0.030	0.033	0.40
R14	13.8	5.0	9.0	0.06	0.012	0.047	0.015	0.011	0.85
R3	17.2	3.4	11.0	0.05	0.025	0.090	0.039	0.013	0.78
R2	16.8	2.8	14.5	0.04	0.04	0.150	0.035	0.034	0.69
R13	14.0	4.7	8.2	0.03	0.070	0.031	0.013	0.008	0.91
R24	15.9	1.8	4.2	0.26	0.067	0.165	0.047	0.032	0.41
R9	10.2	0.6	6.6	0.03	0.110	0.250	0.072	0.068	0.27

Rh/γ-alumina catalyst. In his study, the rate of toluene reaction increased as the square root of the steam partial pressure. Although the power law kinetics used by Grenoble (1978b) was not adopted in this study, an approximate order with respect to the water partial pressure was calculated using our data and found to be 0.45 , which is in good agreement with his results. In another study of this reaction on Rh/γ-alumina/Cr_2O_3, Beltrame et al. (1984) also reported an increase in toluene reaction rate due to increasing water partial pressure in the range of 0.13 to 0.77 atm.

The effect of toluene partial pressure on the rates of the three reactions was studied and some of the results are shown in Figures 4.8 and 4.9 . Figure 4.8 depicts the effect of partial pressure of toluene on the rate of toluene steam dealkylation reaction at 713 K. As the toluene partial pressure was increased from 0.07 to 0.28 atm,the rate of benzene formation increased from 0.014 to 0.019 kmol/(kgcat)(h) . As can be seen from this figure, the increase in the rate was approximately linear till a toluene partial pressure of 0.18 atm and then leveled off. The benzene selectivity was not significantly affected by the partial pressure of toluene. Due to experimental limitations, the maximum value of toluene partial pressure studied in this investigation was 0.35 atm. As shown in Figure 4.9 , the effect of toluene partial pressure on the rate of toluene reforming reaction was similar to that for the dealkylation reaction . On the other hand, the rate of water gas shift reaction decreased slightly with increasing toluene partial pressure.The effect of toluene pressure on water gas shift reaction rate was not unexpected since the increase in the partial pressure of toluene would decrease the

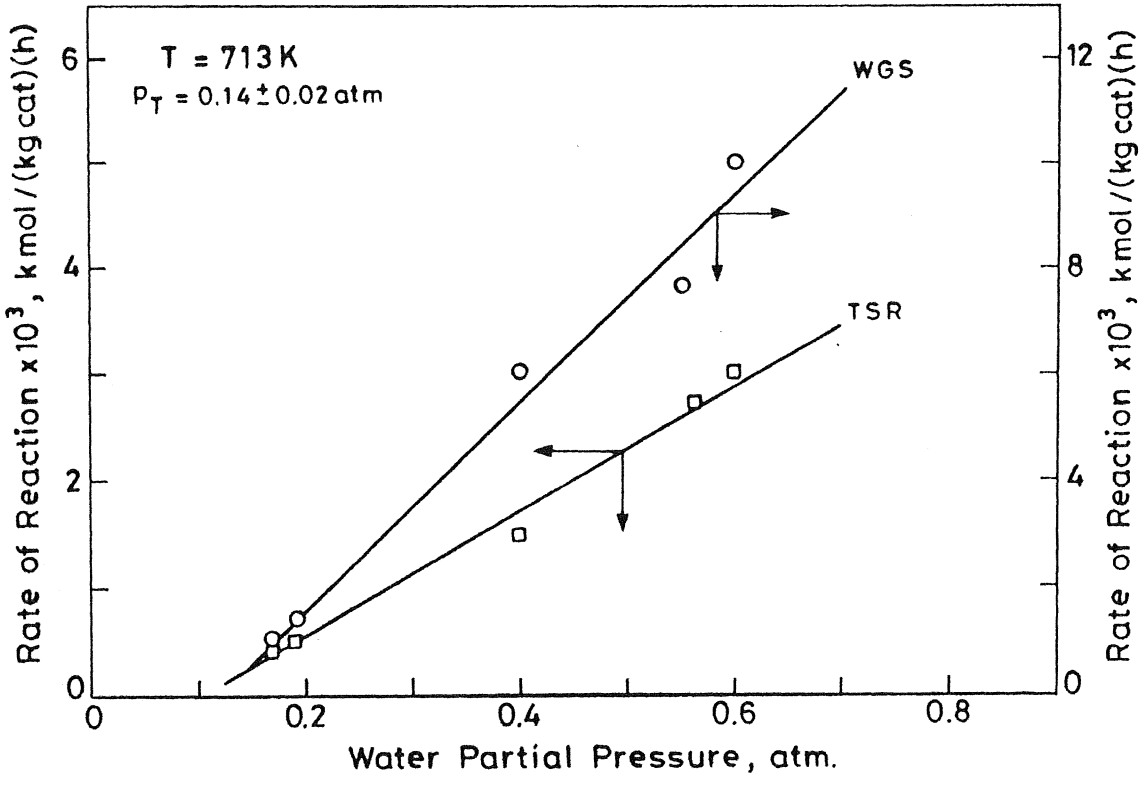

Fig. 4.7 Effect of water partial pressure on toluene steam reforming and water gas shift reactions.

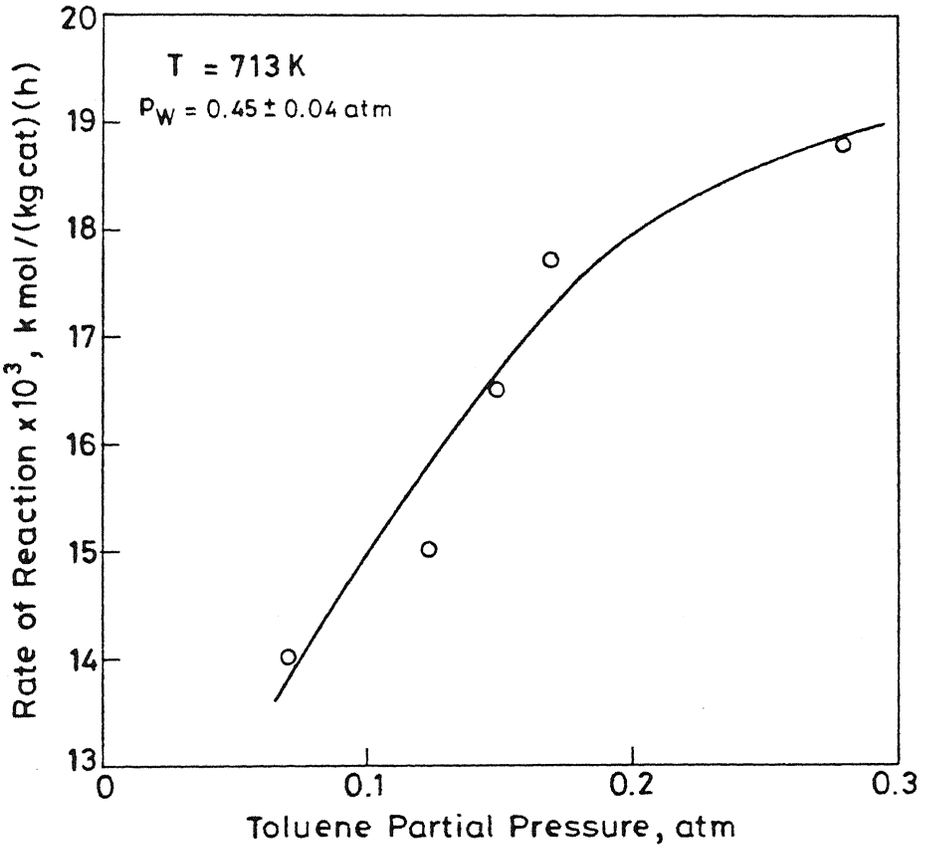

Fig. 4.8 Effect of toluene partial pressure on rate of toluene steam dealkylation reaction.

concentration of adsorbed carbon monoxide and water , thus , decreasing the rate of the water gas shift reaction .

The published work on the kinetics of toluene water reaction is very limited and only a few workers have investigated the effect of toluene partial pressure on the reaction rates. These results are consistent with the kinetic models developed by Kochloefl (1976) and Beltrame et al. (1984). Grenoble (1978b) used power law kinetics to model the total toluene conversion and reported an order of 0.1 with respect to toluene partial pressure.From the data shown in Figure 4.8 , an approximate order with respect to toluene partial pressure was calculated and found to be 0.2 . This is also in agreement with the results of Duprez et al. (1985) who correlated the rate of toluene steam dealkylation reaction on rhodium/alumina catalyst and reported the exponent of toluene partial pressure to be 0.3 .

The effect of carbon monoxide on the initial rates, R_1^o, R_2^o and R_3^o was investigated, and the results are shown in Figures 4.10 and 4.11. Figure 4.10 shows the strong inhibition effect of carbon monoxide on the rate of the toluene steam dealkylation reaction . The benzene formation rate decreased from 0.012 to 0.003 kmol/(kgcat)(h) as the exit carbon monoxide partial pressure was increased from 0.10 to 0.27 atm. As is also shown in this figure, the rate of toluene steam reforming reaction also decreased with increasing partial pressure of carbon monoxide ; however, the effect was much less than that on the toluene steam dealkylation . As a result, the selectivity of benzene decreased with increasing partial pressure of carbon monoxide. On the other hand, increasing the carbon monoxide partial pressure increased the water gas shift reaction rate as shown in Figure 4.11. The

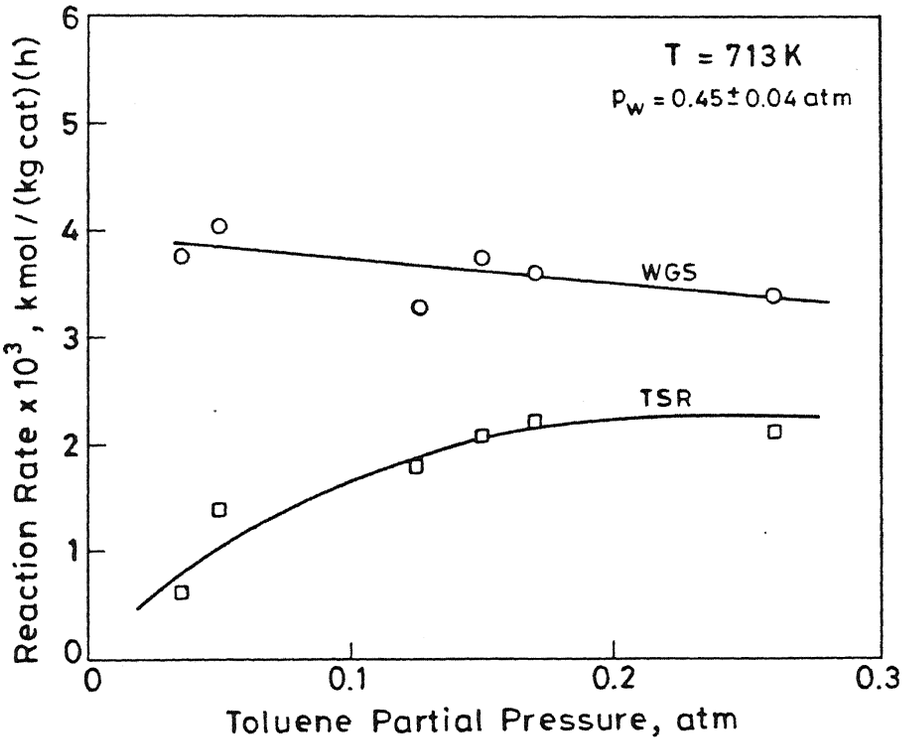

Fig. 4.9 Effect of toluene partial pressure on toluene steam reforming and water gas shift reactions.

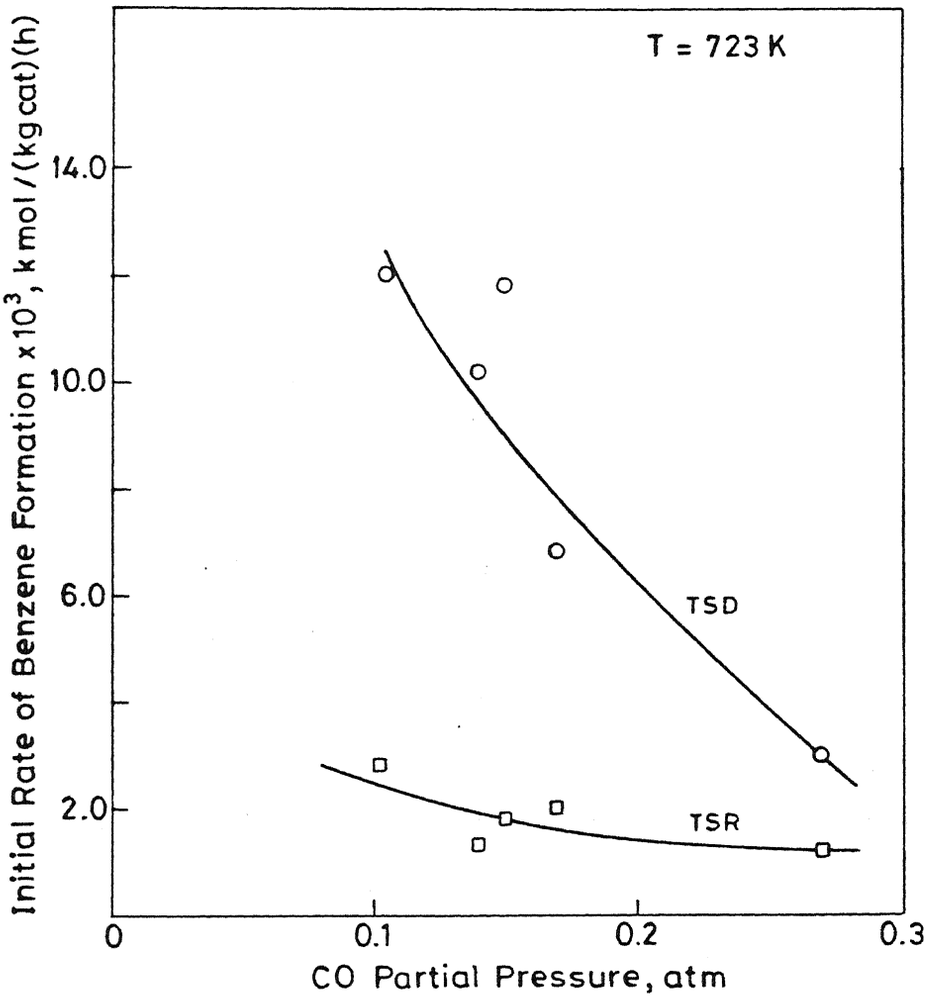

Fig. 4.10 Effect of carbon monoxide partial pressure on the rate of benzene formation.

findings of this study are in good agreement with the results reported by Beltrame et al. (1984), who studied the effect of carbon monoxide on the rate of toluene steam dealkylation and benzene selectivity. They observed a strong inhibition effect by carbon monoxide on the dealkylation reaction rate. However , no change in selectivity due to the increase in the partial pressure of carbon monoxide was reported. Grenoble et al. (1981) studied the water gas shift reaction kinetics over a number of metals of Group VIIB, VIII and Ib on alumina support, and found that rhodium and iridium metals have the lowest turnover numbers at 573 K. They also reported the rate of the reaction to be more or less independent of carbon monoxide partial pressure. In their study , the carbon monoxide partial pressure was 0.24 atm. This range of partial pressure lies on the right side of Figure 4.11 where the effect of the carbon monoxide partial pressure on the rate of rate reaction is not appreciable. Hence, it can be concluded that the results of this study are consistent with their findings. On the contrary, Duprez et al.(1985), reported a marginal increase in the benzene selectivity with conversion and attributed this to the greater inhibition by carbon monoxide of the steam reforming reaction compared to the inhibition of the dealkylation reaction.

The effect of benzene partial pressure on the reaction rates was also investigated and some of the results are shown in Figure 4.12 . As can be seen from this figure , increasing the benzene partial pressure decreased the rates of the three reactions. Although the effect is clearly evident for the toluene steam dealkylation and toluene steam reforming reactions, there is some scatter in the data for the water gas shift reaction. It

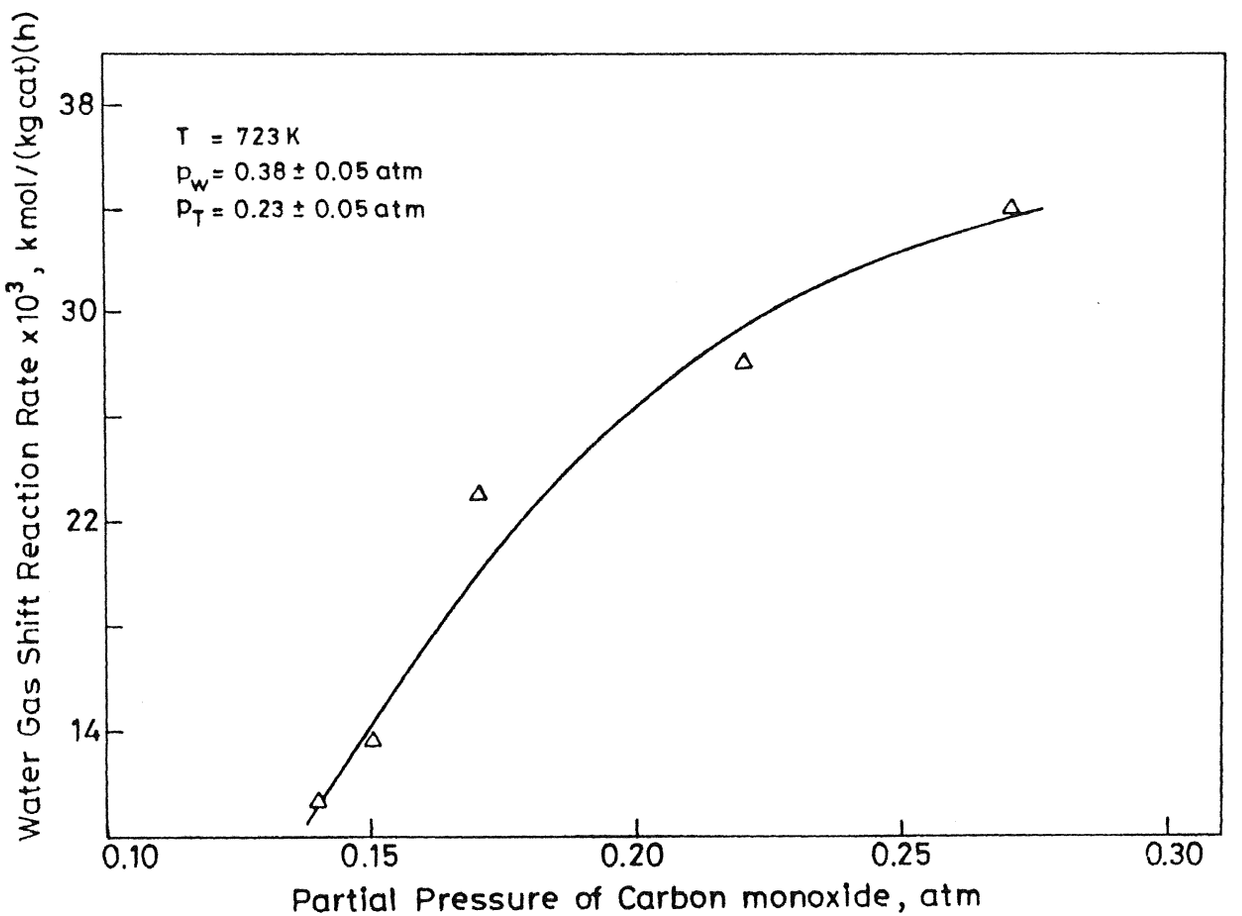

Fig. 4.11 Effect of carbon monoxide partial pressure on the water gas shift reaction.

should be again emphasized that all these rates are not measured at the same partial pressure of the other components and a possible reason for the scatter could be the simultaneous change in the partial pressure of water and carbon monoxide. Beltrame et al.(1984) also investigated the effect of benzene on the water/ toluene reaction and reported a decrease in the toluene conversion with increasing benzene partial pressure.

The effect of hydrogen partial pressure on the reaction rates was also investigated. The hydrogen partial pressure was varied from 0.10 to 0.39 atm at 713 K. Under the present experimental conditions, no significant effect on the rates of any of the three reactions could be detected (refer Appendix II, runs 15 to 18) . Special attention was given to methane formation and it was found that no significant CH_4 was formed upon increasing the hydrogen partial pressure.

4.2.2 Effect of Temperature on Reaction Rates

To investigate the temperature effect on the rates of the three simultaneous reactions occurring in the toluene water system, various runs were conducted at different reaction temperatures in the range 663 -723 K. The detailed variation of the reaction rates with temperature at different partial pressures is given in Appendix II, and some of these results are shown in Figures 4.13 to 4.15. The effect of temperature on the rates of steam dealkylation reaction at various partial pressures of water is shown in Figure 4.13. As can be seen from this figure, the rate of benzene formation increased with increasing reaction temperature . For example, the rate of dealkylation reaction increased from 0.008 to 0.02 kmol/(kgcat)(h) as the temperature was increased from 663 to 723 K. Similarly, as shown in Figure

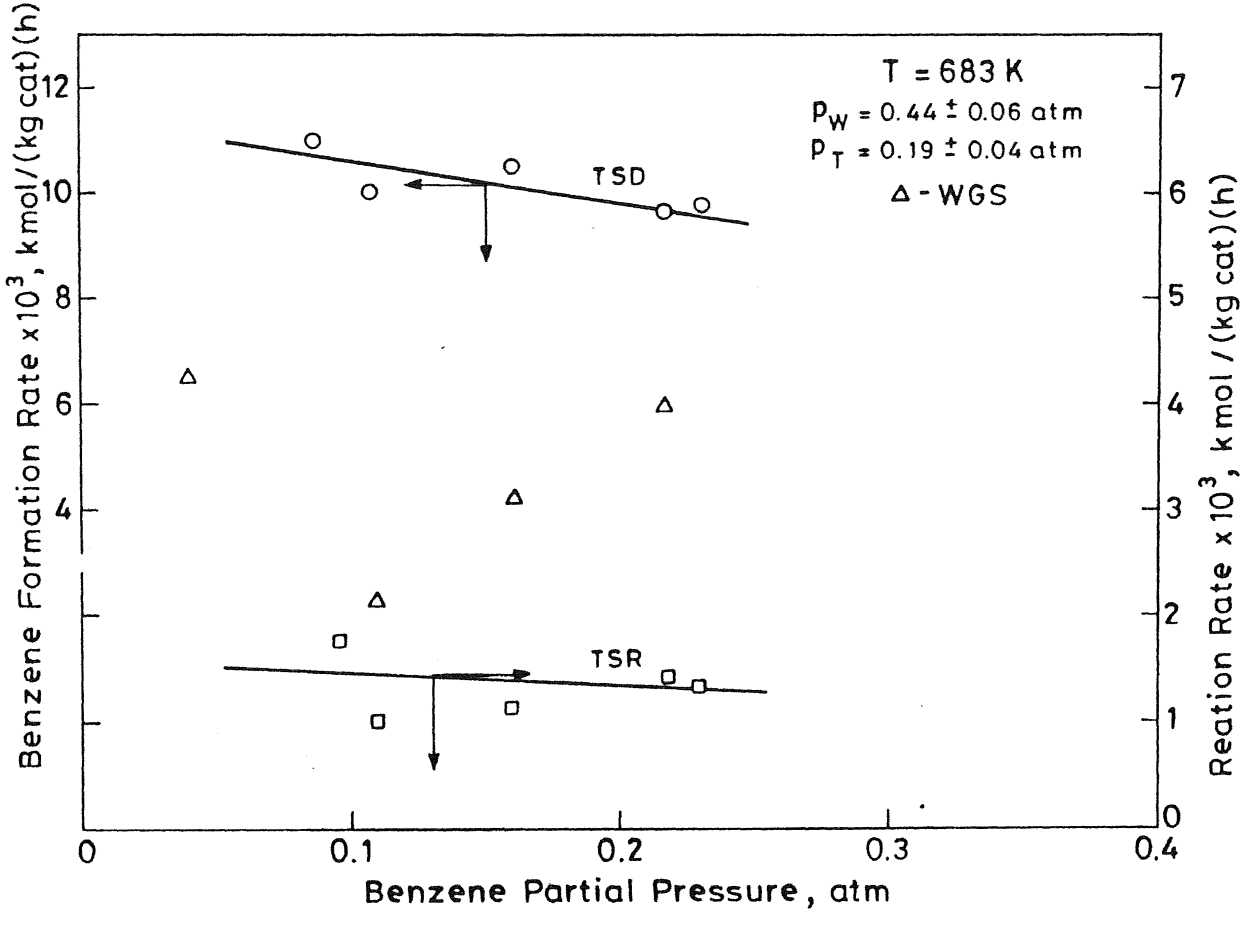

Fig. 4.12 Effect of benzene partial pressure on the rates of the three reactions.

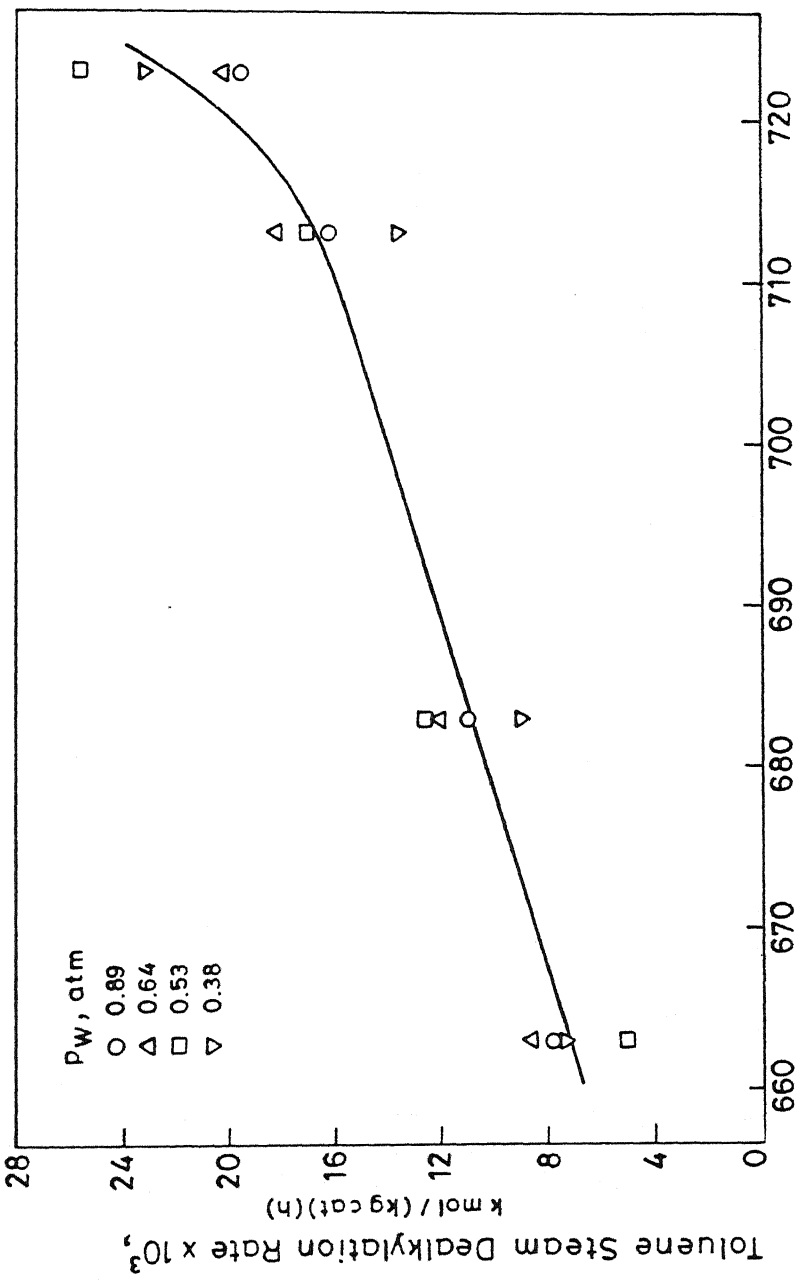

Fig. 4.13 Effect of temperature on the rate of toluene steam dealky - lation reaction.

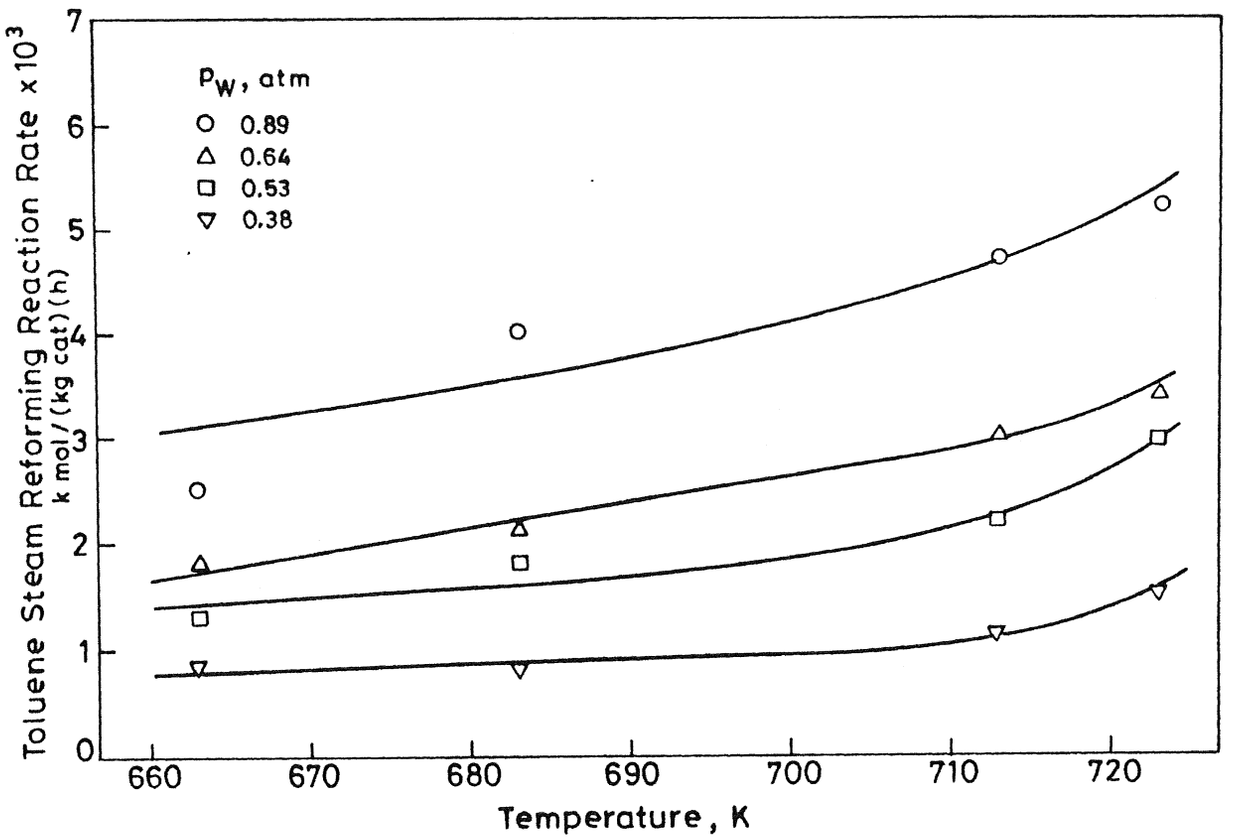

Fig. 4.14 Effect of temperature on the rate of steam reforming reaction.

4.14 , the rate of the toluene steam reforming reaction increased with increasing temperature. A comparison of Figure 4.13 and Figure 4.14 shows that the benzene selectivity increased with increasing temperature. For example, at 0.64 atm partial pressure of water the selectivity increased from 80 % to 89 % when the temperature was increased from 663 to 723 K. This implies that the activation energy for the toluene steam dealkylation reaction is higher than that of the toluene steam reforming reaction. As shown in Figure 4.15, the effect of temperature on the water gas shift reaction was quite different from that on the toluene steam dealkylation and toluene steam reforming reactions. For the WGS reaction, the reaction rate leveled off at higher temperatures . Since the water gas shift reaction is a reversible exothermic reaction (ΔH = -41.73 kJ/mol, at T = 700 K), the reverse reaction begins to affect the reaction rate at the higher temperature.

The rates measured for the toluene steam dealkylation and water gas shift reactions were compared on the basis of the turnover frequency (TOF) data available in the published literature. No information on TSR is available for this system . The turnover frequency is defined as follows:

TOF = molecules produced or reacted per catalyst exposed metal atom per hour.

For the toluene steam dealkylation reaction, the turnover frequency $(TOF)_1$ was calculated from the rate of benzene formation rate, whereas the turnover frequency for the toluene steam reforming reaction $(TOF)_2$ was calculated from the difference between the rate of total toluene consumption and benzene formation. The turnover frequency for the water gas shift reaction

Table 4.4 : Comparison of turnover frequencies

Temp. K	TOF_1 h^{-1}	TOF_2 h^{-1}	TOF_3 h^{-1}	P_T atm	P_B atm	P_H atm	P_{CO} atm	P_{CO2} atm	P_W atm	Remarks
713	279.8	16.8	204.1	0.03	0.11	0.25	0.07	0.07	0.27	this study
713	226.4	—	—	0.08	—	—	—	—	0.26	a
713	200	—	—	0.14	—	—	—	—	0.86	b
713	329.8	—	—	na	—	—	—	—	na	c
713	97.6	—	——	na	—	—	—	—	na	d
723	86.7	33.6	950.7	0.14	0.01	0.15	0.27	0.11	0.33	this study
723	——	——	2005	——	—	—	0.24	——	0.31	e

na: not available

a : Grenoble (1978a)

b : Duprez et al. (1985)

c : Rabinovich and Mozhaiko (1975)

d : Kochloefl (1976)

e : Grenoble et al. (1981)

$(TOF)_3$ was calculated from the rate of carbon dioxide formation. As shown in Table 4.4, $(TOF)_1$ is within the range reported by other investigators.

The various turnover frequencies for toluene steam dealkylation reaction reported in Table 4.4 were either reported at the same temperature or corrected to 713 K. The extrapolation was performed using the reported apparent activation energy. For instance, the results reported by Rabinovich and Mozhaiko (cited by Grenoble 1978a), were generated from their conversion data at 703 K and corrected to 713 K. Similarly, the data of Kochloefl (1976) were corrected from 723 to 713 K.

No data is available for the water gas shift reaction in the presence of benzene and toluene. The turnover frequency reported by Grenoble et al. (1981) for the reaction of pure carbon monoxide and water , was corrected to 723 K using their reported apparent activation energy.The lower value of $(TOF)_3$ obtained in this study at comparable conditions could be due to the inhibiting effect of toluene and benzene.

4.3. KINETIC MODELING OF THE MAIN REACTIONS

Very few studies have been reported on the modeling of complex reactions. The mathematical and statistical tools for parameter estimation and model discrimination in complex kinetic models have been reviewed by Froment (1987). For this study , the rates for the toluene steam dealkylation , toluene steam reforming and water gas shift reactions were modeled separately, rather than by using a multiresponse objective function. As mentioned earlier, the reaction scheme given by equations (4.7) to (4.9) gave the best fit to the product distribution. A total of 94

Table 4.5 : Effect of water partial pressure on the initial reaction Rates

Partial pressures are in atmospheres.

R_1^o, R_2^o, and R_3^o are in kmol/(kgcat)(h).

Temp. K	$R_1^o \times 10^3$	$R_2^o \times 10^3$	$R_3^o \times 10^3$	P_T	P_B	P_H	P_{CO}	P_{CO2}	P_W
723	26.0	06.0	06.3	0.12	0.090	0.060	0.020	0.055	0.78
723	24.0	05.4	16.1	0.11	0.021	0.064	0.042	0.014	0.75
723	24.0	05.9	13.0	0.06	0.011	0.040	0.018	0.007	0.87
723	25.5	05.7	13.2	0.12	0.016	0.053	0.038	0.010	0.77
723	17.1	03.5	23.1	0.05	0.038	0.121	0.037	0.028	0.72
723	23.0	05.4	15.0	0.07	0.020	0.070	0.028	0.011	0.80
723	18.8	04.7	12.0	0.03	0.014	0.035	0.012	0.008	0.90
723	19.9	05.2	14.9	0.04	0.010	0.035	0.016	0.005	0.91
723	20.0	04.0	18.0	0.08	0.050	0.130	0.046	0.028	0.66
693	15.6	02.7	03.1	0.22	0.023	0.096	0.030	0.018	0.61
693	12.0	00.9	03.0	0.26	0.068	0.180	0.044	0.040	0.39
693	10.2	02.6	15.6	0.05	0.041	0.093	0.038	0.022	0.76
693	14.0	02.3	05.2	0.12	0.040	0.137	0.033	0.029	0.62
663	05.0	01.3	08.1	0.35	0.013	0.053	0.032	0.009	0.53
663	08.6	01.8	01.5	0.23	0.026	0.067	0.025	0.012	0.64
663	07.8	02.5	02.8	0.06	0.006	0.023	0.013	0.029	0.89
663	09.1	02.3	04.2	0.12	0.020	0.047	0.022	0.015	0.78
663	06.8	00.8	01.8	0.37	0.055	0.115	0.045	0.024	0.38

experimental points were available. Table 4.5 shows the initial rates of the three reactions with partial pressures at different reaction temperatures for some of the runs. The details of the other measured rates at various partial pressures and temperatures is given in Appendix II.

The simplest kinetics to use is the power law rate expression. This was not adopted here due to the fact that, in general, for heterogeneous catalytic reactions, this type of rate equation cannot model the data over the whole conversion range unless the reaction orders are assumed to vary with conversion. In this study, models based on the Langmuir-Hinshelwood formulation were used to correlate the reaction rates for the three reactions.

4.3.1 Modeling of Toluene Steam Dealkylation Reaction

The rate data was tested against various models shown in Table 4.6. Except model I, all the models are based on the assumption that, the surface reaction between the adsorbed water and the adsorbed toluene was the controlling step.

The general form of the rate expression for the various models was:

$$R_i^o = \frac{k\ p_W p_T}{(\text{ Adsorption Term})} \qquad (4.14)$$

The adsorption terms differed by the number of product terms introduced, the type and the number of active sites involved in the reaction.

In Table 4.6 , model I is based on the assumption that the rate controlling step is the reaction between adsorbed toluene and

water in the gas phase. In model II , it is assumed that the surface reaction between water and toluene, both adsorbed on the same type of active site is controlling. This model has been utilized by Kochloefl (1976) to correlate his data. However, this model is not supported by the experimental evidence that water is adsorbed on the alumina site and toluene on the metal site. (Grenoble, 1978b ; Dydykina et al., 1972). Model III is based on the assumption that surface reaction occurs between water and toluene adsorbed on different sites and that the products do not compete for the active sites. The only difference between model IV and model III is that, in model IV it has been assumed water can adsorb on both types of sites. Model V is similar to model IV with an additional adsorption term for the products which are assumed to compete with toluene and water for the same active site. To reduce the number of adjustable parameters, the partial pressures of carbon monoxide, carbon dioxide, hydrogen and benzene were lumped together. Model VI is derived on the assumption that water adsorbs on one type of site whereas the toluene and the other products (CO , CO_2, H_2 , benzene) compete for the second type of active site. Model VII differs from model VI in that the adsorption equilibrium constant of carbon monoxide is taken to be different from that of the other products. In contrast to model VII , in model VIII it has been assumed that the adsorption of carbon monoxide on the site occurs as follows:

$$2CO + M \rightleftharpoons CO - M - CO \qquad (4.15)$$

where M is one type of active site. This is supported by the experimental evidence reported by Yates et al. (1979) and Solymosi et al. (1980). These workers proposed that there are three

Table 4.6: Various Langmuir-Hinshelwood kinetic expressions tested

model no.	kinetic equation
I	$R_1^o = \dfrac{k\ K_W\ K_T\ p_W\ p_T}{(\ 1 + K_W p_W + K_T p_T\ )}$
II	$R_1^o = \dfrac{k\ K_W K_T\ p_W\ p_T}{(\ 1 + K_W p_W + K_T p_T\ )^2}$
III	$R_1^o = \dfrac{k\ K_W\ K_T\ p_W\ p_T}{(\ 1 + K_W p_W\ )(\ 1 + K_T p_T\ )}$
IV	$R_1^o = \dfrac{k\ K_W\ K_T p_W\ p_T}{(\ 1 + K_W p_W\ )(\ 1 + K_T p_T + K_W p_W\ )}$
V	$R_1^o = \dfrac{k\ K_W\ K_T\ p_W\ p_T}{(\ 1 + K_W p_W\ )(\ 1 + K_T p_T + K_W p_W + K_R(p_R + p_{CO}))}$
VI	$R_1^o = \dfrac{k\ K_W\ K_T\ p_W\ p_T}{(\ 1 + K_W p_W\ )(\ 1 + K_T p_T + K_R(p_R + p_{CO}\ ))}$
VII	$R_1^o = \dfrac{k\ K_W\ K_T\ p_W\ p_T}{(\ 1 + K_W p_W\ )(\ 1 + K_T p_T + K_{CO} p_{CO} + K_R p_R\ )}$
VIII	$R_1^o = \dfrac{k\ K_W\ K_T\ p_W\ p_T}{(\ 1 + K_W p_W\ )(\ 1 + K_T p_T + K_{CO} p_{CO}^2 + K_R p_R\ )}$

where $p_R = p_B + p_{CO_2} + p_H$

structural forms of the adsorbed carbon monoxide on rhodium metal. A twin structure (gem-dicarbonyl) in which two carbon monoxide molecules are adsorbed on one metal site ; a linear structure in which one carbon monoxide molecule is adsorbed on a metal site and a bridged form in which one molecule of carbon monoxide is adsorbed in a bridge shape between two rhodium atoms. It is also well established that the twin structure (gem-dicarbonyl) is favored at high dispersion values of the rhodium metal (Wang and Yates,1984 ; Solymosi and Pasztor, 1985;

At first, the initial rates for the toluene steam dealkylation reaction at each temperature were analyzed separately. The adsorption and reaction rate constants at different temperatures, were estimated by means of a non-linear least square fit of the experimental and calculated rates. These computed values were then used to estimate the activation energies, heats of adsorption and the preexponential factors. Subsequently, the temperature dependence of the various parameters was included in the model and the rate data for all the temperatures analyzed by non-linear regression analysis. Due to the strong correlation between the preexponential factor and the activation energy or heats of adsorption, a reparameterization was necessary. The reparameterization was introduced for the reaction rate constant and the adsorption equilibrium constant as follows:

$$k_i = k_{io} \exp(-E_i/RT) \qquad (4.16)$$

$$= \bar{k}_{io} \exp(-\bar{E}\, T^*/R) \qquad (4.16a)$$

and

$$K_i = K_{io} \exp (E_{ad,i} T/R) \qquad (4.17)$$

$$= \bar{K}_{io} \exp (\bar{E}_{ad,i} T^*/R) \qquad (4.17a)$$

where

$$k_{io} = \bar{k}_{io} \exp(\bar{E}/R) \qquad (4.18)$$

$$K_{io} = \bar{K}_{io} \exp(-\bar{E}_{ad,i}/R) \qquad (4.19)$$

$$\bar{E}_i = E_i/\bar{T} \qquad (4.20)$$

$$E_{ad,i} = E_{ad,i}/\bar{T} \qquad (4.21)$$

$$T^* = \bar{T}/T - 1 \qquad (4.22)$$

and $\bar{T}$ is the average temperature for all the runs.

The models of Table 4.6 were tested against the rate data. The estimation of the parameters was done by a nonlinear regression analysis of the data for finding the minimum sum of squares of M non-linear functions in N variables using Gauss-Newton algorithm. The details of the computer programme are given in Appendix IV. Approximate 95 percent confidence intervals for the various model parameters were calculated from the estimate of their individual variances.

Although, all the parameters of model I were positive, it was rejected because some of the estimated constants were not significantly determined at the 95 % confidence level. The average absolute error was 38 % . Models II to VI were rejected because either some of the estimated parameters were negative or on the basis of statistical tests (95 % confidence limits; residual sum of squares).

For model VII , although all the parameters were positive, the model could not satisfactorily represent the strong inhibition effect of carbon monoxide on the rate of reaction. The average absolute error was 11.8 %. The fit to the experimental data was

improved upon the introduction of the square exponent for the carbon monoxide partial pressure (Model VIII). Model VIII fitted the data very satisfactorily. Thus, the experimental rate data could be modeled using the following expression :

$$R_1^o = \frac{k_1 K_W K_T P_W P_T}{(1 + K_W P_W)(1 + K_T P_T + K_{CO} P_{CO}^2 + K_R P_R)} \qquad (4.23)$$

where $k_1 = k_o \exp(-E_1/RT)$

$K_W = K_{Wo} \exp(E_W/RT)$

$K_T = K_{To} \exp(E_T/RT)$

$K_{CO} = K_{(CO)o} \exp(E_{CO}/RT)$

$K_R = K_{Ro} \exp(E_R/RT)$

The best estimates of the various parameters for model VIII together with the 95% confidence limits are shown in Table 4.7.The average absolute error between the calculated and the experimental rates for toluene steam dealkylation reaction was 3.8 percent.

From Table 4.7, it can be seen that there exist a very strong correlation between the preexponential factor and the heat of adsorption of the product term. When this adsorption constant was assumed to be independent of temperature, the average absolute error was decreased from 3.8 to 3.6 percent. Thus the product equilibrium constant could be assumed to be independent of temperature without any appreciable effect on the reaction rate. The comparison of the calculated and the experimental rates are shown in Figure 4.16. As shown in Figure 4.16 , very good agreement between the experimentally measured and the calculated values is achieved. Thus, model VIII ,with K_R independent of

Table 4.7 : Kinetic parameters for the steam dealkylation reaction

parameter	Model VIII	Model VIII*
k_{1o} (kmol/(kgcat)(h)	(2.72 ± 0.02)x10^{5}	(3.05 ± 0.023)x10^{5}
E_1 (kJ/mol)	(95.8 ± 20.2)	(93.7 ± 20.5)
K_{Wo} $(atm)^{-1}$	(3.6 ± 1.0)x10^{-2}	(3.9 ± 1.1)x10^{-2}
E_W (kJ/mol)	(25.6 ± 12.2)	(24.9 ± 12.5)
K_{To} $(atm)^{-1}$	(9.3 ± 3.1)x10^{-2}	(9.1 ± 2.7)x10^{-2}
E_T (kJ/mol)	(36.5 ± 12.12)	(36.6 ± 10.2)
$K_{(CO)o}$ $(atm)^{-2}$	(2.16 ± 1.39)	(2.1 ± 0.36)
E_{CO} (kJ/mol)	(32.5 ± 24.4)	(31.9 ± 20.5)
K_{Ro} $(atm)^{-1}$	(2.8 ± 0.8)x10^{-7}	———
E_{Ro} (kJ/mol)	(90.3 ± 45.6)	———
K_R		(1.7 ± 0.9)
average absolute error	3.8 %	3.6 %

* K_R independent of reaction temperature.

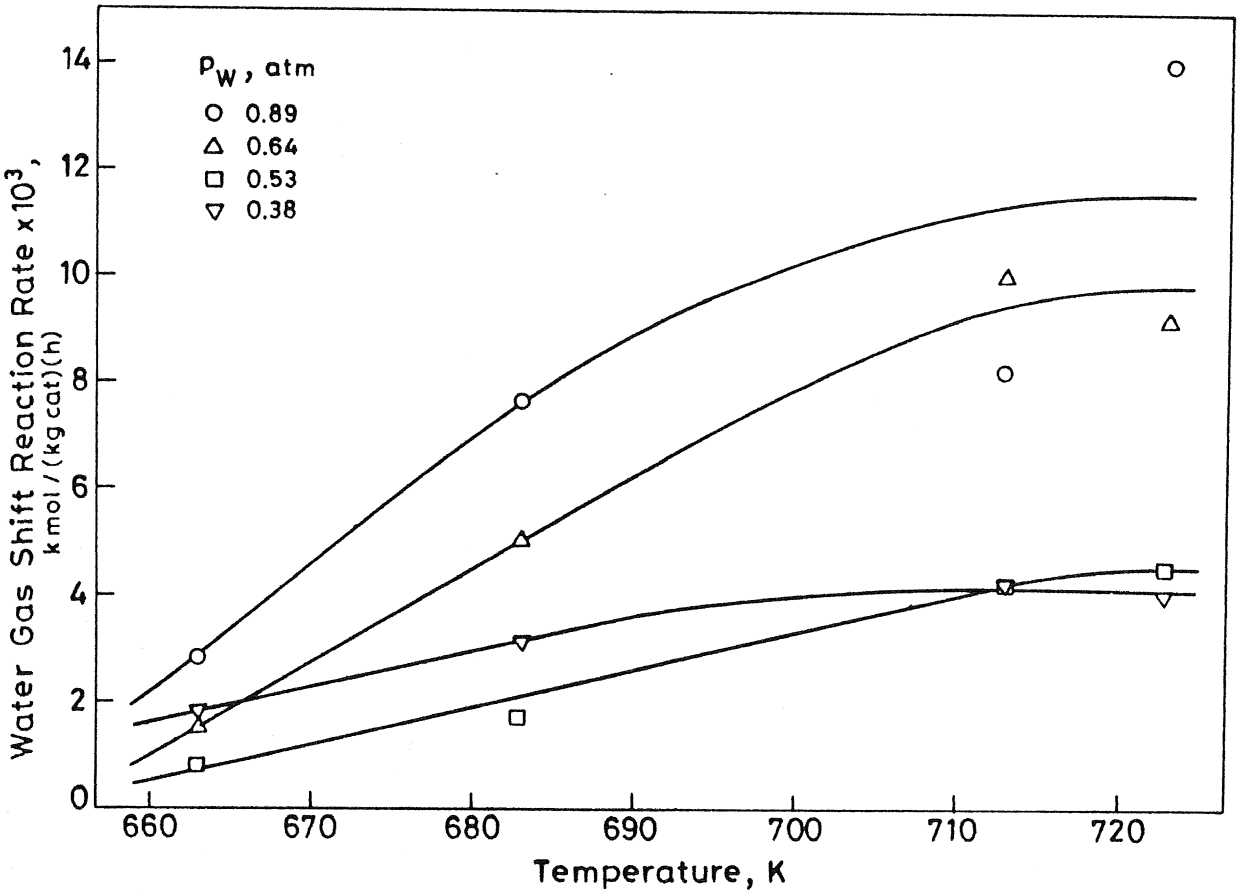

Fig. 4.15 Effect of temperature on the rate of water gas shift reaction.

temperature, was used in the subsequent modeling of the pellet.

For this reaction, Grenoble (1978b) and Kochloefl (1976) have reported apparent activation energy of 138.6 and 102.1 kJ/mol, respectively. For the sake of comparison, an apparent activation energy was calculated using model VIII with K_R independent of temperature. To do this, R^o_1 was calculated from the model at a fixed partial pressures of the reacting components: p_{CO} = 0.03, p_{CO2} = 0.04 , p_H = 0.09 , p_B = 0.08 , p_W = 0.61, and p_T = 0.15 atm and different temperatures. From the slope of $\ln(R^o_1)$ vs. 1/T , the apparent activation energy was found to be 98.7 kJ/mol, which is in excellent agreement with the reported literature values.

4.3.2. Modeling of Toluene Steam Reforming Reaction

As discussed earlier (Section 4.2), the rate of toluene steam reforming reaction continuously increased with increasing water partial pressure and was not as strongly inhibited by carbon monoxide partial pressure as the rate of TSD. Moreover, the benzene selectivity decreased with increasing partial pressure of water. The rate data for all the runs is given in Appendix II whereas some selected data are shown in Table 4.5 . According to the Langmuir-Hinshelwood formulation, the denominator of the rate expression accounts for the sites occupied by the various components in the reaction mixture. Therefore, for a complex reaction, if the same number and type of active sites are involved in the controlling step for each reaction, then the denominator of the different rate expressions should be the same. In case different number and/or type of active sites are involved in the controlling steps, then although the exponent of the

denominator will be different, the magnitude of the adsorption equilibrium constants should be the same. For instance, Steijns and Froment (1981) modeled their kinetic data on hydroisomerization and hydrocracking by a common adsorption term for the various reactions. Similarly, Jacob et al.(1976) correlated their data on catalytic cracking by the same adsorption terms for the different reactions. On the other hand, other workers have had to use different adsorption terms to model their data. Dixon and Cresswell (1987) modeled an industrially significant complex reaction of a hydrocarbon with an oxidant to form the partial oxidation desired product and complete oxidation to the undesired product. The rates of the two reactions were modeled using different adsorption terms. Similarly, Corella and Asua (1982) used different adsorption terms to model isobutene oxidation. Klugherz and Harriott (1971) modeled the kinetics of ethylene oxidation to form either ethylene oxide or ethane and carbon dioxide on supported silver oxide catalyst by Langmuir-Hinshelwood rate expressions with different adsorption constants for each reaction.

As a first step in the modeling of this reaction, the exponent of the water partial pressure in the numerator of model VIII (Table 4.6) was squared to account for the effect of water partial pressure on the toluene steam reforming reaction. The adsorption constants were kept fixed at the values determined earlier for toluene steam dealkylation reaction and the modified model VIII tested against the data. Using this model, there was a large discrepancy between the calculated and the experimental rates. The average error was 13.8 % . To improved the model prediction, the adsorption constants were also estimated together

with the rate constant from the rate data of the toluene steam reforming reaction. With this modification, although all the estimated parameters were positive, heats of adsorption of carbon monoxide and the lumped product terms (E'_{CO} , E'_{R}) were not significant at the 95% level. Moreover, the absolute error between the calculated and experimental rates was rather high, especially for the runs in which carbon monoxide had been added in the feed. Since the above model could not satisfactorily correlate the data, the denominator of the rate expression for the toluene steam reforming reaction was allowed to be different than that for the toluene steam dealkylation reaction. In order to account for the effect of carbon monoxide partial pressure in the model formulation, the square exponent of carbon monoxide partial pressure in model VIII was removed. The following model could correlate the rate data satisfactorily for all the runs:

$$R_2^o = \frac{k_2 K'_T K'_W P_T P_W^2}{(1 + K'_W P_W)(1 + K'_T P_T + K'_{CO} P_{CO} + K'_R P_R)} \qquad (4.24)$$

where $k_2 = k_{2o} \exp(-E_2/RT)$

$K'_T = K'_{To} \exp(E'_T/RT)$

$K'_W = K'_{Wo} \exp(E'_W/RT)$

$K'_{CO} = (K'_{CO})_o \exp(E'_{CO}/RT)$

$K'_R = K'_{Ro} \exp(E_R/RT)$

In equation (4.24), R_2^o is the initial reaction rate of toluene steam reforming reaction, K'_is are the various adsorption equilibrium constants and k_2 is the reaction rate constant. The

parameter estimation procedure was similar as that for estimating toluene steam dealkylation reaction parameters. Table 4.8 shows the different adsorption and reaction rate constants with their approximate 95 % confidence limits. The average absolute error between the experimental and calculated rates for the toluene steam reforming was 4.9 percent. Just as for toluene steam dealkylation reaction, to reduce the number of adjustable parameters in the model eqn. (4.24), K'_R was assumed to be independent of temperature and the model parameters redetermined. When K'_R was assumed to be independent of temperature, the average absolute error decreased to 4.8 %. These parameters together with the 95 % confidence limits are also shown in Table 4.8. Figure 4.17 shows the comparison between the rates experimentally measured and those calculated using the above model.As can be seen from this figure, good agreement between the predicted and the measured rates was achieved for all runs.Thus, equation (4.24) with K'_R independent of temperature was used to represent the initial rate data.

The activation energy estimated for toluene steam reforming reaction was 76.3 kJ/mol as compared to 93.7 kJ/mol for the toluene steam dealkylation reaction. Since no kinetic study has been reported for this reaction in the presence of TSD, no comparison with published values could be made. The heats of adsorption for water and toluene for the TSR reaction were 18.9 and 42.9 kJ/mol, compared to 24.9 and 36.6 kJ/mol, respectively. Comparison of the adsorption constants at different temperatures for the TSD and TSR reactions (Table 4.9) shows that the estimated adsorption parameters for water and toluene were within a factor of 2 of each other.

Table 4.8 : Kinetic parameters for the steam reforming and water gas shift reactions

parameter	Model (4.28)	Model* (4.28)
k_{2o} (kmol)(kgcat.h.atm)$^{-1}$	(5.56 ± 0.15)x10^{3}	(5.56 ± 0.26)x10^{3}
E_2 (kJ/mol)	(76.3 ± 40.6)	(76.3 ± 43.9)
K'_{Wo} (atm)$^{-1}$	(5.9 ± 3.1)x10^{-2}	(5.9 ± 0.02)x10^{-2}
E'_W (kJ/mol)	(18.9 ± 3.8)	(18.9 ± 7.4)
K'_{To} (atm)$^{-1}$	(3.0 ± 1.5)x10^{-2}	(3.1 ± 1.4)x10^{-3}
E'_T (kJ/mol)	(42.9 ± 3.2)	(42.9 ± 3.7)
$K'_{(CO)o}$(atm)$^{-1}$	(3.1 ± 1.16)x10^{-8}	(3.0 ± 2.3)x10^{-8}
E'_{CO} (kJ/mol)	(113.4± 106.5)	(113.3 ± 102.4)
K'_{Ro} (atm)$^{-1}$	(5.9 ± 1.20)x10^{-8}	———
E'_{Ro} (kJ/mol)	(89.3 ± 64.9)	———
K'_R		(0.32 ± 0.27)
average absolute error	4.9 %	4.8 %
k_{3o} (kmol)/(kgcat)(h)	(2.80 ± 0.4)x10^{12}	(3.45 ± 0.5)x10^{12}
E_3 (kJ/mol)	(156.9± 22.2)	(158.1± 22.2)
average absolute error	7.64 %	7.59 %

* K_R is independent of temperature in steam reforming reaction.

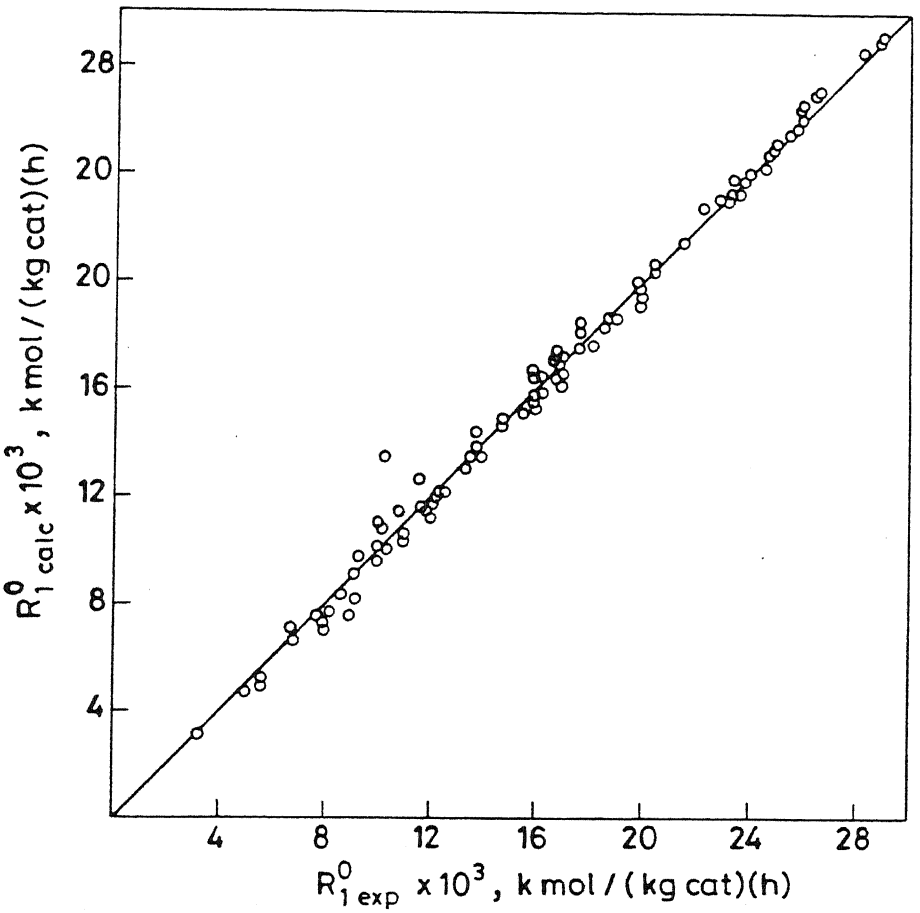

Fig. 4.16 Comparison of calculated and experimental rates of TSD reaction.

Table 4.9 : Comparison of adsorption constants estimated for toluene steam dealkylation toluene and steam reforming reactions.

Temperature K	K_W,(atm)$^{-1}$		K_T,(atm)$^{-1}$	
	TSD	TSR	TSD	TSR
723	2.38	1.32	39.0	47.83
693	2.85	1.52	50.75	65.08
663	3.47	1.76	67.53	91.04

4.3.3. Modeling of Water Gas Shift Reaction

The water gas shift reaction was also modeled using a Langmuir-Hinshelwood rate expression. There is no available literature on the modeling of this reaction in the presence of toluene steam dealkylation and steam reforming reactions; very few workers have modeled this reaction on $Rh/\gamma-Al_2O_3$ catalyst. Grenoble et al. (1981) and Dictor (1987) modeled the intrinsic kinetics of this reaction at different temperatures. Grenoble et al.(1981) reduced his L-H kinetic model to a simple power law rate equation. Similarly, Dictor (1987) also used a power law rate expression to model the intrinsic kinetics. In both of these investigations, the reaction rate was independent of the carbon monoxide partial pressure and the reaction order of approximately 0.44 was observed for water. Grenoble et al. (1981) investigated the kinetics of this reaction at 573 K and partial pressures of carbon monoxide and water of 0.24 and 0.31 atm, respectively. On the other hand, Dictor (1987) modeled the kinetics of this reaction at higher temperature (773 K) and the carbon monoxide and water partial pressures were 0.012 and 0.12 atm, respectively. Their results are not directly applicable to this study because they not only used pure carbon monoxide and water as the reactants but the reaction conditions were also different. However, Grenoble et al.(1981) proposed a reaction sequence which was modified in the present work to account for the presence of the toluene and benzene and the reversibility of the reaction.

The model assumes that carbon monoxide reacts to form carbon dioxide through an intermediate.Assuming that CO is adsorbed only on the metal site and water is activated on the

support site by nondissociative adsorption , we have:

$$\text{step 1} \qquad CO + M \rightleftharpoons CO\text{–}M \qquad (4.25)$$

$$\text{step 2} \qquad W + S \rightleftharpoons W\text{–}S \qquad (4.26)$$

where M is the vacant metal site and S represent the vacant support site.

The next step is assumed to be the reaction of adsorbed carbon monoxide on the metal site with adsorbed water on the alumina site to give an adsorbed intermediate as follows:

$$\text{step 3} \qquad CO\text{–}M + W\text{–}S \rightleftharpoons I\text{–}S + M \qquad (4.27)$$

where I-S represents the adsorbed intermediate on the support site .

There is experimental justification for the above sequence. It has been established that formic acid is an intermediate in the water gas shift reaction (Amenomiya, 1978,1979). Amenomiya (1979) identified the presence of formate ions in both the forward and the reverse WGS reaction. Depending on the direction of the water gas shift reaction , these formate ions can react further on the metal or on the Lewis acid sites to form either carbon dioxide and hydrogen or carbon monoxide and water, respectively. As proposed by Grenoble et al. (1981), the next step is assumed to be the transport and adsorption of the intermediate from the support site adjacent to the metal site as follows:

step 4 $$I\text{–}S + M \underset{k_{-4}}{\overset{k_4}{\rightleftharpoons}} I\text{–}M + S \qquad (4.28)$$

The intermediate on the metal site can then dehydrogenate to carbon dioxide and hydrogen according to the following steps :

step 5 $$I\text{–}M + M \rightleftharpoons CO_2\text{–}M + H_2\text{–}M \qquad (4.29)$$

step 6 $$CO_2\text{–}M \rightleftharpoons CO_2 + M \qquad (4.30)$$

step 7 $$H_2\text{–}M \rightleftharpoons H_2 + M \qquad (4.31)$$

If step 4 is assumed to be rate controlling, as proposed by Grenoble et al. (1981), we have :

$$R_3^o = k_4 \Theta_{I-S} \Theta_M - k_{-4} \Theta_{I-M} \Theta_S \qquad (4.32)$$

where k_4 : forward reaction rate constant for step 4

k_{-4} : reverse reaction rate constant for step 4

Θ_{I-S}: fraction of support sites occupied by the intermediate

Θ_M : fraction of vacant metal sites

Θ_{I-M}: fraction of the metal sites occupied by intermediate

Θ_S : fraction of vacant support sites

Since the other steps in the above reaction scheme are assumed to be fast and at equilibrium, we have:

$$K'_{CO} = \frac{\Theta_{CO}}{P_{CO}\,\Theta_M} \qquad (4.33a)$$

$$K'_W = \frac{\Theta_W}{P_W \Theta_S} \qquad (4.33b)$$

$$K_3 = \frac{\Theta_{I-S} \Theta_M}{\Theta_{CO} \Theta_W} \qquad (4.33c)$$

$$K_5 = \frac{\Theta_{CO_2} \Theta_{H_2}}{\Theta_{I-M} \Theta_M} \qquad (4.33d)$$

$$K_6 = \frac{P_{CO_2} \Theta_M}{\Theta_{CO_2}} \qquad (4.33e)$$

$$K_7 = \frac{P_{H_2} \Theta_M}{\Theta_{H_2}} \qquad (4.33f)$$

In equation (4.33), Θ_W is the fraction of support sites occupied by water, Θ_{H_2},is the fraction of sites covered by hydrogen, Θ_{CO} is the fraction of metal site occupied by carbon monoxide, Θ_M is the fraction of vacant metal sites and Θ_{CO_2} is the fractional coverage of the metal site by carbon dioxide. K'_W , K'_{CO} , K_3, K_4, K_5, K_6 and K_7 are the various equilibrium adsorption constants in the proposed reaction scheme . Substituting (4.33a) to (4.33f) in equation (4.32) , we have

$$R_3^o = k_4 K_3 K'_W K'_{CO} P_W P_{CO} \Theta_S \Theta_M - \frac{k_{-4}}{K_5 K_6 K_7} P_H P_{CO_2} \Theta_S \Theta_M \qquad (4.34)$$

$$R_3^o = k_4 K_3 K'_W K'_{CO} (P_W P_{CO} - \frac{P_H P_{CO_2}}{K}) \Theta_S \Theta_M \qquad (4.35)$$

where K is the equilibrium constant for the water gas shift reaction.

As for the toluene steam dealkylation and toluene steam reforming reactions , if it is assumed that only water is adsorbed on the support sites and no water is adsorbed on the metal sites, we have:

$$\Theta_S = \frac{1}{(1 + K'_W P_W)} \qquad (4.36)$$

and

$$\Theta_M = \frac{1}{(1 + K'_T P_T + K'_{CO}P_{CO} + K'_R P_R)} \qquad (4.37)$$

The fractional coverage of the metal sites will account for the occupancy by the different species of the toluene water reaction. These include the coverage by toluene , benzene, carbon monoxide , carbon dioxide and hydrogen. Thus, equation (4.35) can be expressed as :

$$R^o_3 = \frac{k_3 K'_{CO} K'_W \left[P_W P_{CO} - \frac{P_H P_{CO2}}{K} \right]}{(1 + K'_W P_W)(1 + K'_T P_T + K'_{CO}P_{CO} + K'_R P_R)} \qquad (4.38)$$

where $k_3 = k_4 K_3$

Similarly, other rate expressions based on different controlling steps in the above reaction scheme were derived and tested against the rate data.

To reduce the number of adjustable parameters, the adsorption constants of the tested models were kept the same as for the toluene steam reforming reaction. The equilibrium constant for

the water gas shift reaction was calculated by standard methods (Levenspiel, 1972) and can be expressed as:

$$K = K_o \exp\left[\frac{1}{R}\left\{\Delta\alpha \ln(T/T_o) + \Delta\beta/2(T - T_o) + \Delta\gamma/6(T^2 - T_o^2) + \left[- \Delta H_{ro} + \Delta\alpha T_o + \Delta\beta T_o^2 + \Delta\gamma T_o^3 \right]\left[\frac{1}{T} - \frac{1}{T_o} \right]\right\}\right] \qquad (4.39)$$

where K_o and ΔH_{ro} are the equilibrium constant and the heat of reaction , respectively, evaluated at the standard temperature, T_o. At T_o = 298 K, K_o = 22.875 and ΔH_{ro} is = -9835 cal/mol

heat capacities are expressed as

$$C_{P_i} = \alpha + \beta T + \gamma T^2 \qquad (4.40)$$

From Reid et al.(1977), the heat capacities for carbon monoxide , carbon dioxide, water (g), and hydrogen are

$$C_{P_{CO_2}} = 5.14 + 15.4\times10^{-3}T - 9.94\times10^{-6}\,T^2$$

$$C_{P_{H_2}} = 6.88 - 0.022\times10^{-3}T + 0.21\times10^{-6}\,T^2$$

$$C_{P_{CO}} = 6.92 - 0.65\times10^{-3}T + 2.80\times10^{-6}\,T^2$$

$$C_{P_{H_2O}} = 8.10 - 0.72\times10^{-3}T + 3.36\times10^{-6}\,T^2$$

where C_{P_i} are in cal/(mol)(K) and T is in K

In equation (4.39) ,

$$\Delta\alpha = (\alpha_{CO_2} + \alpha_{H_2}) - (\alpha_{CO} + \alpha_{H_2O}) \qquad (4.41a)$$

$$= -3.0 \text{ cal/(mol)}$$

$$\Delta\beta = (\beta_{CO_2} + \beta_{H_2}) - (\beta_{CO} + \beta_{H_2O}) \qquad (4.41b)$$

$$= 16.7\times10^{-3} \text{ cal/(mol)(K)}^2$$

$$\Delta\gamma = (\gamma_{CO_2} + \gamma_{H_2}) - (\gamma_{CO} + \gamma_{H2O}) \qquad (4.41c)$$

Substituting equation (4.41a) to (4.41c) in equation (4.39) , the variation of the equilibrium constant with temperature can be expressed as:

$$K = K_o \exp\left\{\frac{1}{R}\left[37.71 - 31\ln(T) + 8.374\times10^{-3} T - 2.6933\times10^{-6} T^2 + \left[9542.09\right]\left[\frac{1}{T} - \frac{1}{298}\right]\right]\right\} \qquad (4.42)$$

As mentioned earlier, nonlinear least square optimization technique was used to estimate the preexponential factor and the activation energy of the reaction rate constant. The procedure of determining these constants was similar as that used for the toluene steam dealkylation and toluene steam reforming reactions. This included the estimation of the reaction rate constant at different temperatures and then a reparameterization. The above model with step 4 as the controlling step was found to give the best fit. The estimated parameters together with their 95 % confidence limits are also shown in Table 4.8. The average absolute error between the experimentally measured rates and the calculated rates from the model was 7.64 percent. Where K'_R was

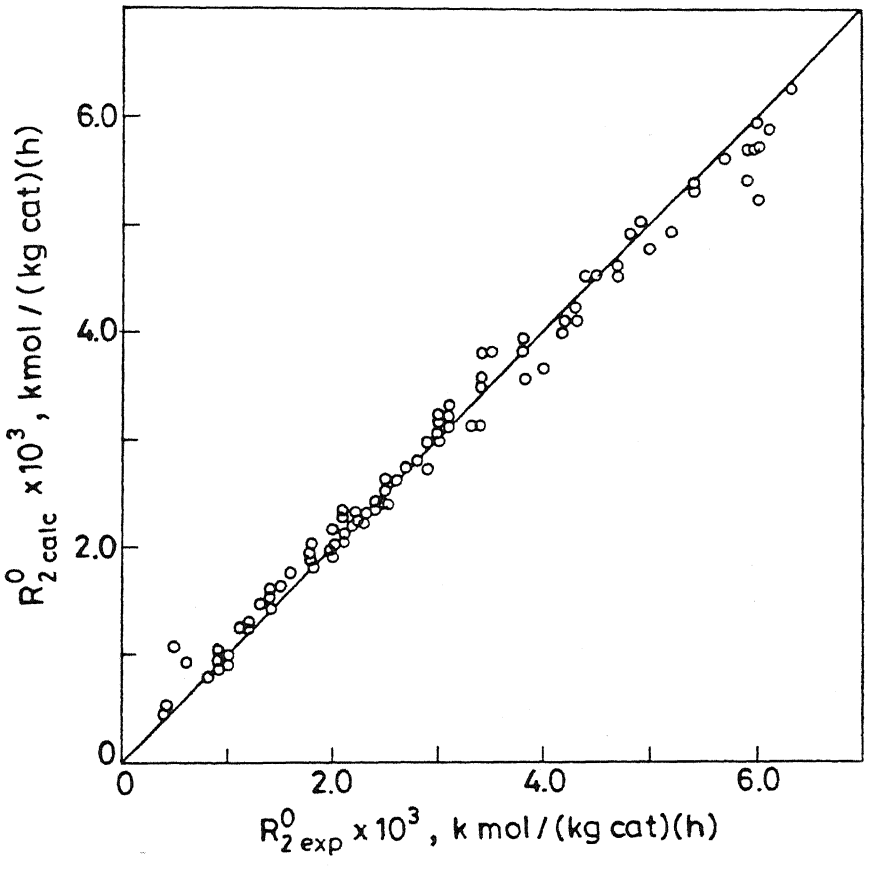

Fig. 4.17 Comparison of calculated and experimental rates of TSR reaction.

assumed to be independent of temperature, the average absolute error decreased slightly to 7.59 % and the parameters values for this case are also given in Table 4.8. As shown in Figure 4.18, the agreement between the experimentally measured and the predicted rate data from the model assuming K'_R to be independent of temperature was very good.

It should be noted that, the estimated value of E_3 (158.1 kJ/mol) , is a contribution of two activation energies. To compare our results with the value of apparent activation energy reported in the literature, a plot of $\ln(R^o_3)$ vs. 1/T at a constant partial pressures i.e. $p_{CO} = 0.3, p_{CO2} = 0.04$, $p_H = 0.09$, $p_B = 0.08$, $p_W = 0.61$, and $p_T = 0.15$ atm was generated using the model parameters and a value of 73.08 kJ/mol was obtained from the slope of the plot. This is in good agreement with the apparent activation energy of 96.6kJ/mol reported by Grenoble et al. (1981) and Dictor (1987).

From the above discussion , it can be seen that the rates of the toluene steam dealkylation , toluene steam reforming and water gas shift reactions can be modeled using the following rate equations:

$$R^o_1 = \frac{1.083\times10^3 \exp(-3851/T)\ p_T\ p_W}{(1+0.04\exp(2993/T)p_W)(1+0.09\exp(4383/T)p_T+2.1\exp(3616/T)p^2_{CO}+1.7p_R)} \qquad (4.43)$$

$$R_2^o = \frac{56.3\exp(-1740/T)\,p_T\,p_W^2}{(1+.6\exp(2266/T)p_W)(1+.03\exp(5142/T)p_T+3.1\times10^{-8}\exp(13582/T)p_{CO}+.32p_R)} \quad (4.44)$$

$$R_3^o = \frac{72.9\exp(-714/T)\left(p_{CO}p_W - \frac{p_H\,p_C}{K}\right)}{(1+0.6\exp(2266/T)p_W)(1+.03\exp(5142/T)p_T+3.1\times10^{-8}\exp(13582/T)p_{CO}+.32p_R)} \quad (4.45)$$

4.4. INTRINSIC DEACTIVATION KINETICS

As mentioned earlier (section 4.1), for all the runs the toluene conversion and product selectivities varied with run time. Typical plots of variation of toluene conversion with run time for some runs is shown in Figure 4.19, whereas the variation of conversion with run time for all the runs is given in Appendix II. As can be seen from this figure, the decrease in toluene conversion is initially rapid followed by a slower decrease. There is no quantitative data available on the rate of deactivation for this reaction; however, it has been reported that the rate of deactivation of the toluene steam dealkylation reaction is rapid (Grenoble, 1978b ; Beltrame et al. 1984 ; Duprez et al. 1982). Duprez et al. (1986) reported a fast deactivation in the early periods of the reaction (0 - 1 h) after which the toluene conversion did not show any significant decrease with run time. In this study, as shown in Figure 4.19 , the toluene conversion continuously decreased even for runs in which the run time was as large as 16 hours. The variation of product selectivities , S_B , S_{CO} , and S_{CO2} with run time at a temperature of 723 K , W/F_{To} = 20.51 (kgcat)(h)/kmol and R = 9.34 , are shown in Figure 4.20a , whereas Figure 4.20b shows the corresponding variation of reaction rates with run time. For this run, the benzene and the carbon dioxide selectivities decreased from 0.78 to 0.60 and 1.1 to 0.61 respectively, while carbon monoxide selectivity increased from 1.25 to 2.9 as run time increased from 0 to 7.0 hours. For all the runs, S_B and S_{CO2} decreased whereas S_{CO} increased with run time (refer Appendix II). As can be seen from Figure 4.20b and Appendix II , the rate of toluene steam dealkylation reaction decreased

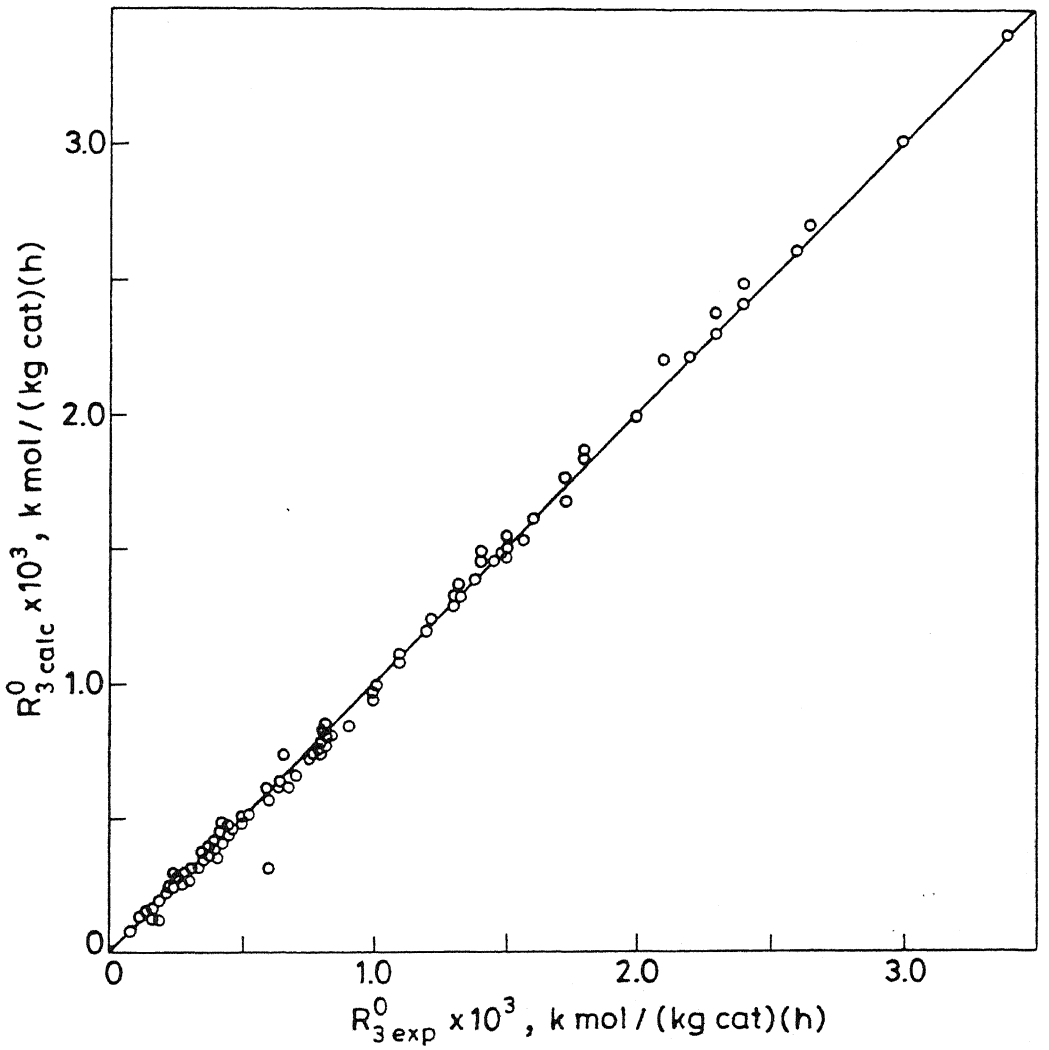

Fig. 4.18 Comparison of calculated and experimental rates of WGS reaction.

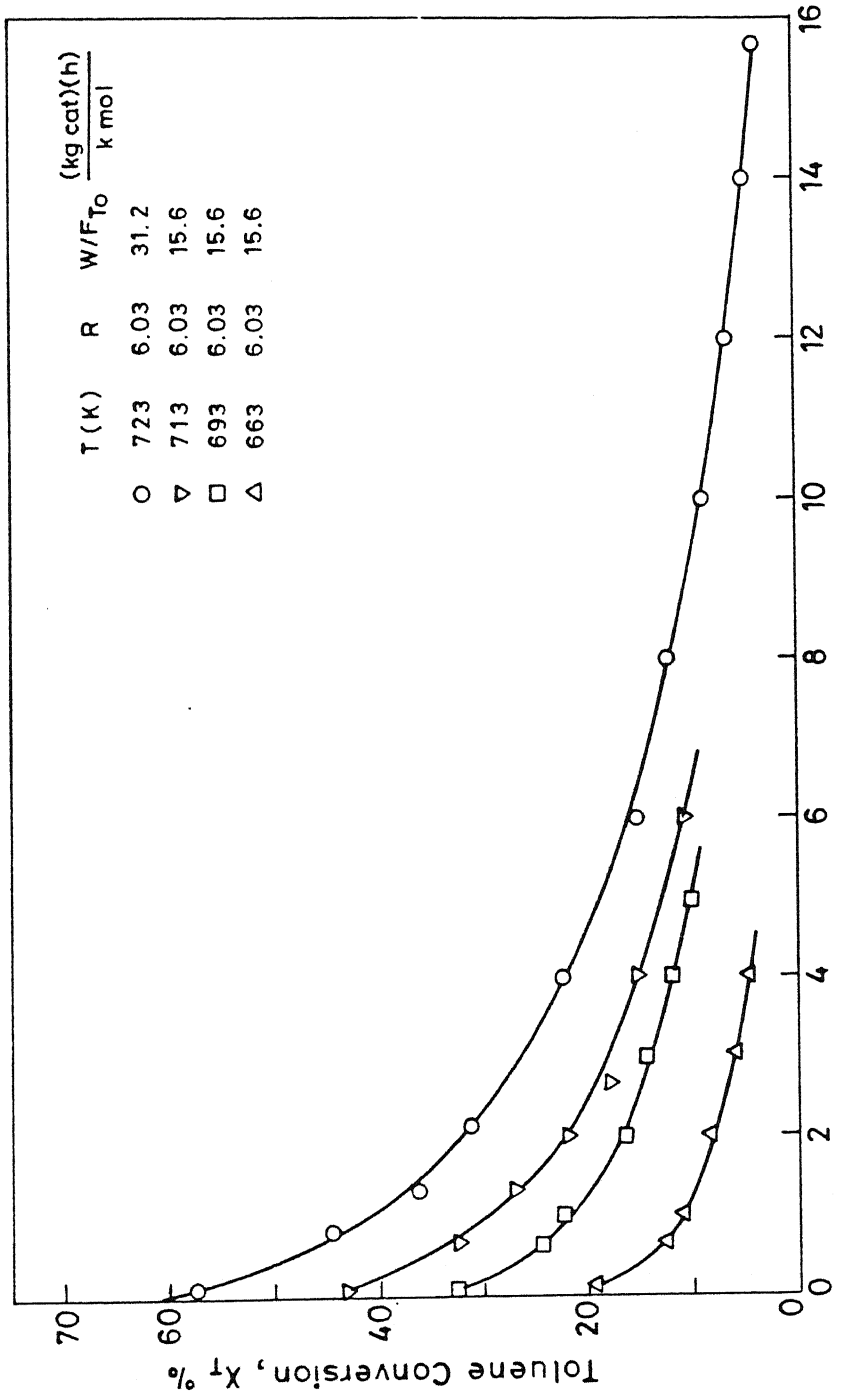

Fig. 4.19 Variation of toluene conversion with run time.

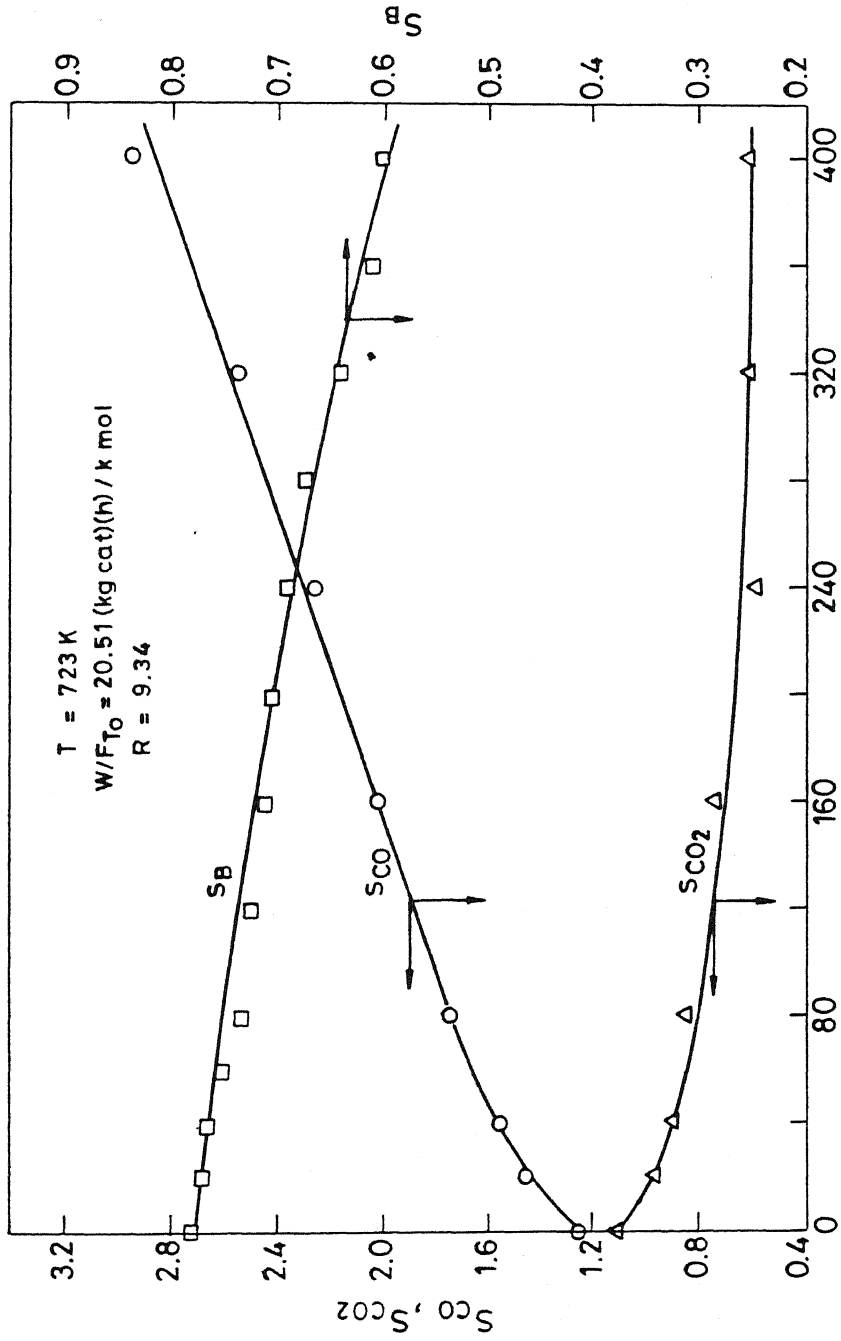

Fig.4.20a Variation of product selectivities with run time.

significantly with run time whereas there was hardly any change in the rate of toluene steam reforming reaction. Hence, benzene selectivity decreased continuously with run time.

Although this study did not focus on the actual deactivation mechanism(s), the decrease in the catalyst activity is most likely due to the fouling of the catalyst by coke deposition. For some runs , the spent catalyst was oxidized in a Thermogravimetric Analyzer (TGA) and the loss in weight recorded. The loss in weight for most of the runs was of the order of 0 - 0.2 wt%. For the 16 hour run shown in Figure 4.19, the weight loss was approximately 0.7 %. In addition, the noncondensable gases during the oxidation of the deactivated catalyst were also monitored and found to contain mainly carbon monoxide and carbon dioxide. These results are in good agreement with those of Kochloefl (1976) and Duprez et al. (1986) who reported that coke deposition or deposition of polynuclear aromatics on the catalyst surface were the main cause for catalyst deactivation.

As is clear from Figure 4.20b ,the coke deposition affects the rate of the three reactions differently. Thus, it is not appropriate to use nonselective deactivation kinetics which assumes that the activity for all reactions is the same at any time. Therefore, selective deactivation kinetics was adopted and the rates of the three reactions were expressed as :

$$R_i = R_i^o \, a_i \qquad ; \qquad i = 1,2,3 \tag{4.46}$$

$$-\frac{da_i}{dt} = \psi_i(p_W, p_T, p_B, \ldots, T)\, a_i^{d_i} \qquad ; \quad i = 1,2,3 \tag{4.47}$$

where R_i is the rate of ith reaction at any time; a_i is the

activity of the ith reaction , ψ_i is the deactivation function of the ith reaction and d_i is the order of deactivation of the ith reaction.

It should be emphasized that in equation (4.46), R_i and R_i^o have to be evaluated at the same conditions of partial pressures and temperature. For low conversions , since the exit partial pressures do not vary significantly with run time, the activity of each reaction can be calculated as the ratio of the rate at any time to the rate at time zero for the same run. For high conversions , due to catalyst deactivation , the exit partial pressures at the start and end of the run can be significantly different . Therefore, the activity of each reaction has to be calculated as the ratio of the reaction rate at any time to the rate of reaction for a fresh catalyst at the existing partial pressures and temperature at that time (Corella and Asua , 1982).

In this study, except for runs conducted at 723 K, the exit partial pressures at the start and end of the run were within 10 % (refer Appendix II) , and eqn. (4.46) was used for calculating the activity for each reaction. For the high conversion runs at 723 K, the reaction rates for the fresh catalyst at any partial pressure were calculated from the model equations and the activity evaluated as the ratio of the experimental rate to the rate of the fresh catalyst.

4.4.1 Effect of Partial Pressures of Reactants and Products on the Rates of Deactivation

In general, the deactivation function which accounts for the loss in the intrinsic activity of the catalyst can be function of the reactant and/or product partial pressures and temperature.

As mentioned earlier , since a completely mixed internal recycle reactor was used , it was not possible to study the effect of individual partial pressures on the rates of deactivation. However, from the data listed in Appendix II, runs have been identified in which only the partial pressure of one component varied significantly. This was done to obtain a qualitative understanding of the effect of the various components on the rates of deactivation. However,for the model development (Section 4.4.2) all the data listed in Appendix II was utilized.

The effect of partial pressure of water on the variation of activity with run time for the toluene steam dealkylation ,toluene steam reforming and water gas shift reactions is shown in Figures 4.21 to 4.23, respectively. As can be seen from Figure 4.21, with increasing partial pressure of water, the rate of deactivation of TSD , as measured from the slope of the activity vs. time plot, decreased. This is most probably a result of the reduction in the coke deposition due to the removal of coke by the carbon-steam reaction. The effect of water in reducing catalyst fouling has been reported in several catalytic reactions.

The effect of increasing the partial pressure of water on the activity of the toluene steam reforming reaction is shown in Figure 4.22. As can be seen from this figure, the activity does not change significantly with reaction time for any of the runs. Moreover, no change in the rate of the TSR reaction was observed due to the increase in the partial pressure of any of the water/ toluene reaction components. A possible reason for the large difference in the deactivation characteristics of the toluene steam dealkylation and toluene steam reforming reactions could be due to the existence of active sites with different strengths.

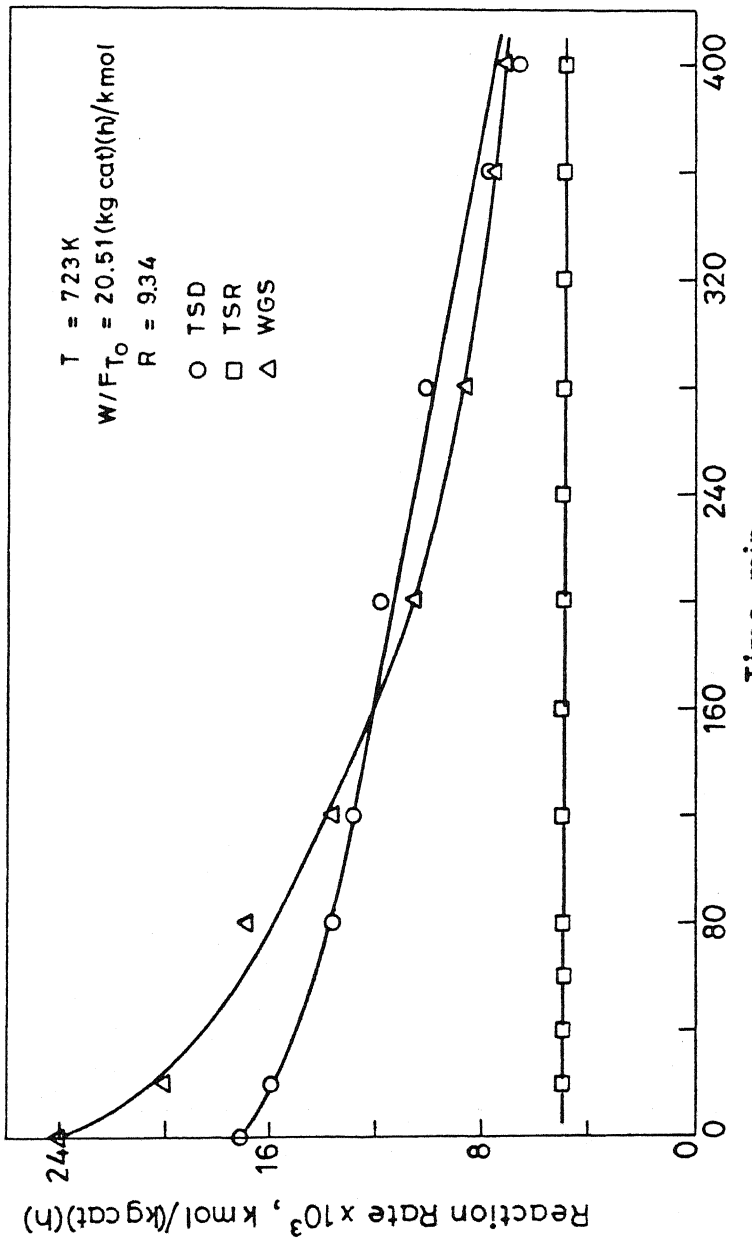

Fig. 20b Variation of reaction rates with run time.

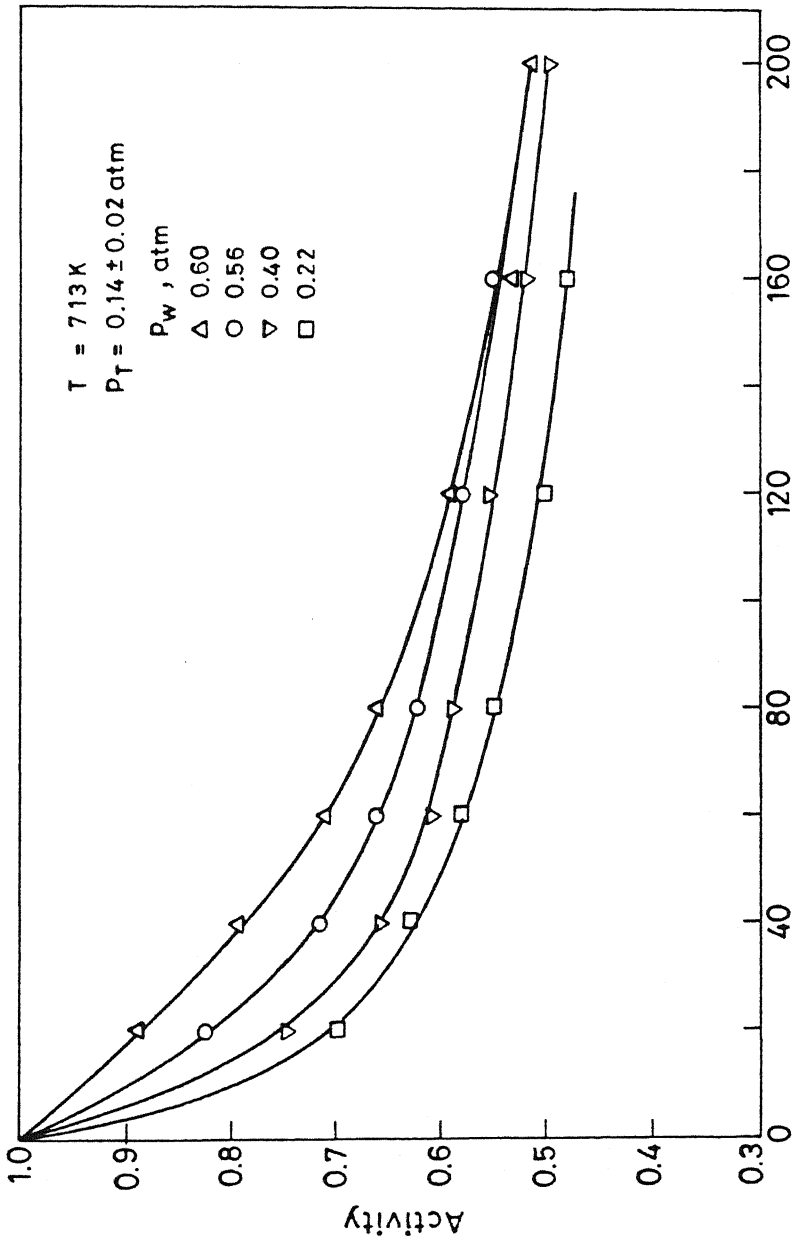

Fig. 4.21 Effect of water partial pressure on the activity of toluene steam dealkylation reaction.

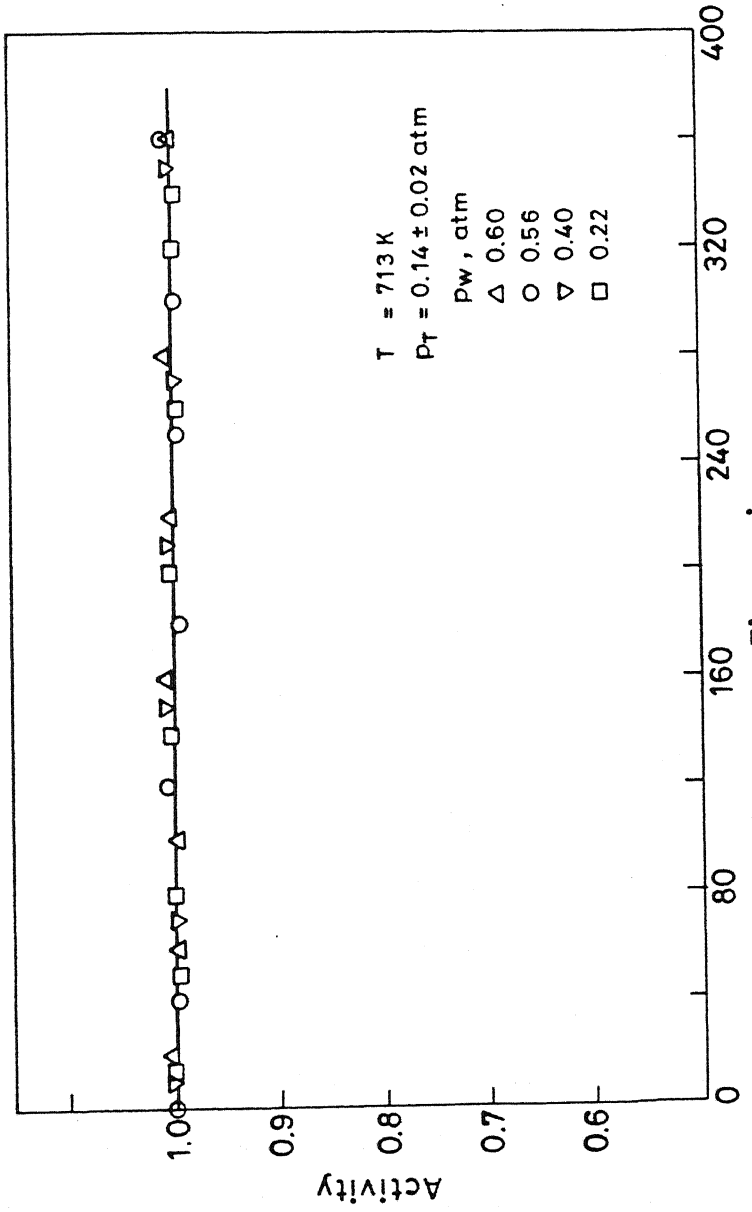

Fig. 4.22 Effect of partial pressure of water on the activity of toluene steam reforming reaction.

Kochloefl (1976) found that the ratio of the rates of TSD to TSR increased from 10.1 to 27.1 as the metal loading of the catalyst support was decreased from 0.9 to 0.15 wt % rhodium. This suggests that the toluene steam dealkylation and steam reforming reaction rates are related in a complex manner to the structure and geometry of the rhodium metal on the support surface. It is known that the metal rhodium tends to form large crystallite sizes at higher loading, and this is probably the reason for the increase in the TSD/TSR ratio with increasing catalyst concentration on the support.

According to Somorjai and Blakely (1975), carbon formation proceeds rapidly on smooth catalyst faces where the metal atoms have a high coordination, whereas the metal atoms situated on edges and corners resist fouling better and stay active longer. As mentioned earlier, the most probable site for steam reforming reaction is the crystallite rather than the individual rhodium atoms, and the results indicate that in the presence of steam these sites are not fouled significantly.

The effect of increasing the partial pressure of water on the activity of the water gas shift reaction is shown in Figure 4.23. From this figure, it can be seen that the rate of deactivation increased with increasing water partial pressure. As mentioned earlier, carbon monoxide can adsorb on Rh/Al_2O_3 as either a twin structure, a linear structure or in bridge form. It has been reported that the infrared spectra of CO adsorbed on Rh/Al_2O_3 catalysts are altered by the introduction of water (Dictor, 1987), and the results obtained suggest that at the conditions of our study, the adsorbed carbon monoxide phase which results in the formation of carbon dioxide and hydrogen is

deactivated in the presence of water, thus decreasing the rate of water gas shift reaction.

The effect of toluene partial pressure on the rates of deactivation of toluene steam dealkylation and water gas shift reactions are shown in Figures 4.24 and 4.25, respectively. It is very clear form these figures that the activity of TSD and WGS reactions decreased as the toluene partial pressure was increased Similarly, as shown in Figures 4.26 and 4.27, increasing the benzene partial pressure increased the rate of deactivation of the toluene steam dealkylation and the water gas shift reactions. The most likely reason for the increase in the rate of catalyst deactivation of both TSD and WGS reactions is that benzene and toluene can dehydrogenate on the catalyst surface to form unsaturated hydrocarbon compounds which on further reaction can lead to coke deposition. It is not clear at this stage whether the catalyst deactivation is due to coke deposition or due to the condensation of polynuclear aromatics on the catalyst surface. Kochloefl (1976) attributed the drop in the catalyst activity on acidic carriers such as Al_2O_3 and SiO_2-Al_2O_3 due to the blocking of Rh active sites by bulky aromatic molecules formed from reactions such as

$$C_6H_5CH_3 + C_6H_6 \longrightarrow C_6H_4CH_2C_6H_4 + 2H_2 \qquad (4.48)$$

The extent of reaction (4.48) and similar reactions depends on the temperature and toluene and benzene partial pressures. In Kochloefl's study, at 798 K and $R < 7$, the conversion of toluene or benzene into biphenyl , flourene, and anthracene reached a maximum of 1.6 wt %.

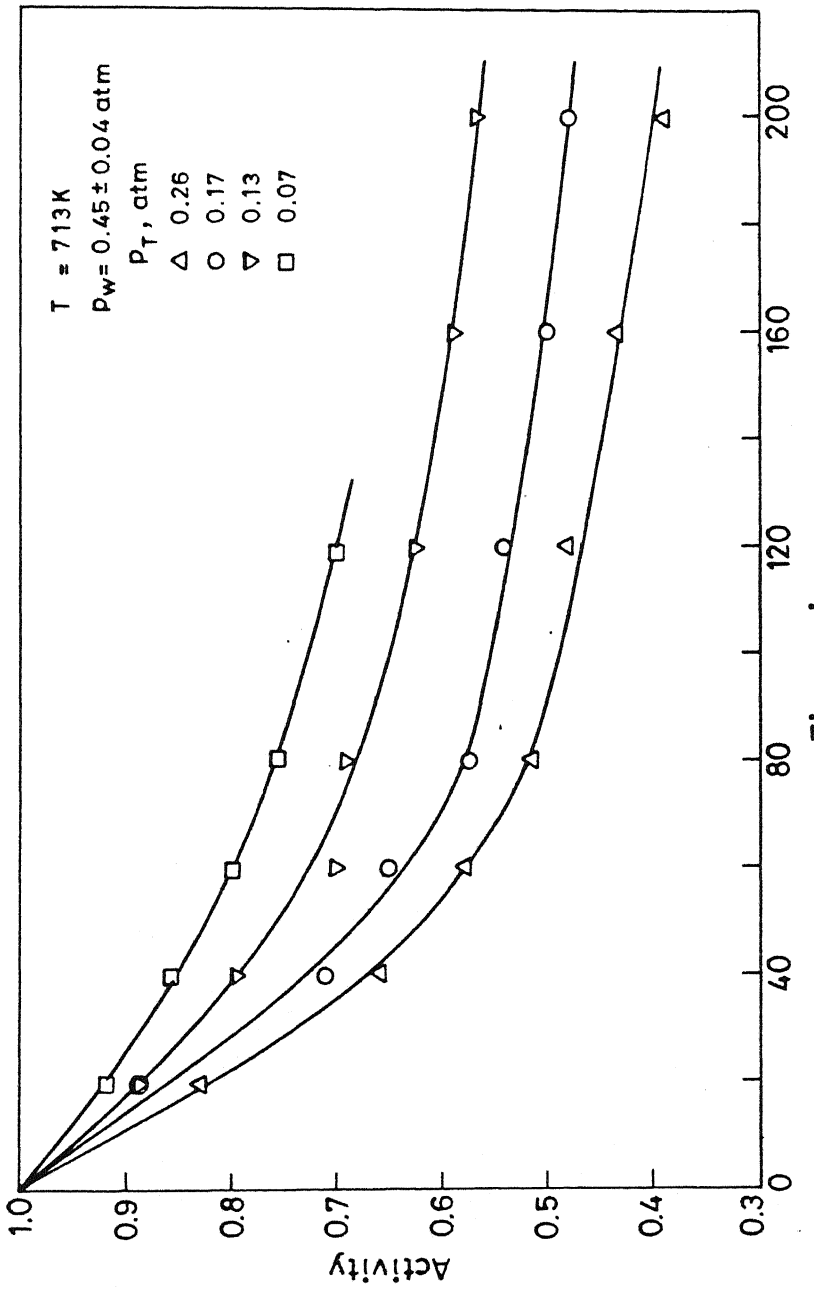

Fig. 4.24 Effect of toluene partial pressure on the activity of toluene steam dealkylation reaction.

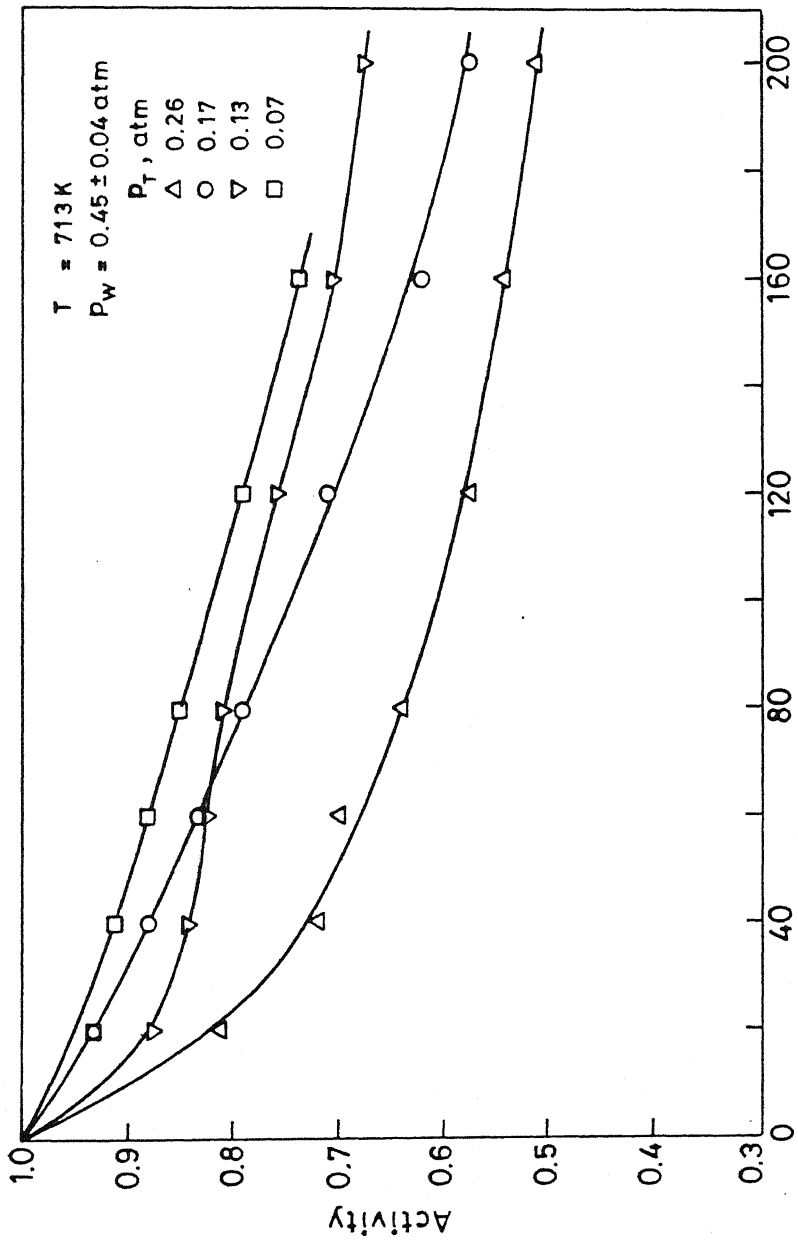

Fig. 4.25 Effect of toluene partial pressure on the activity of water gas shift reaction.

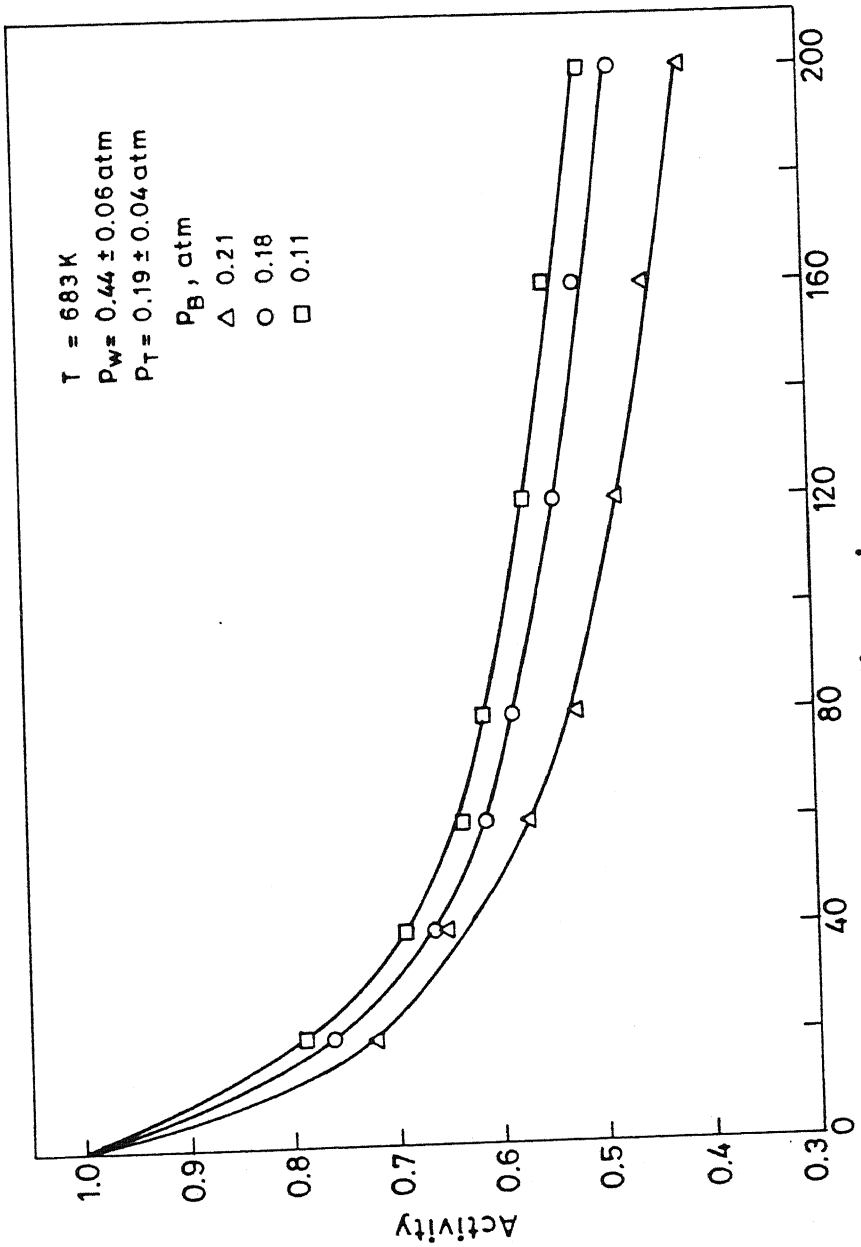

Fig. 4.26 Effect of benzene partial pressure on the activity of toluene steam dealkylation reaction.

The effect of carbon monoxide on the activity of toluene steam dealkylation and the water gas shift reactions is shown in Figures 4.28 and 4.29, respectively. It can be seen from Figure 4.28 that for runs in which carbon monoxide was added in the feed, the activity declined rapidly with run time. Moreover, the activity of the TSD reaction decreased as the carbon monoxide partial pressure was increased. As shown in Figure 4.29, with increasing partial pressure of carbon monoxide, the activity of the water gas shift reaction also decreased. However, compared to the toluene steam dealkylation reaction , the rate of deactivation was slower.Disproportionation or dissociation of carbon monoxide can lead to coke deposition on the catalyst surface (Petersen and Bell, 1987; Bartholomew, 1982) as follows:

$$2CO \longrightarrow C + CO_2 \qquad (4.49)$$

$$CO \longrightarrow C + O \qquad (4.50)$$

Thus, the increase in the rate of deactivation of toluene steam dealkylation and water gas shift reactions with increasing carbon monoxide partial pressure is most likely due to coke deposition by the above reactions.

Runs in which the effect of increasing partial pressure of hydrogen (refer Appendix II runs S15 -S18) was investigated did not show any effect on the rate of deactivation of either of the main reactions. Thus, for the range of hydrogen partial pressures investigated in this study, the deactivation rates of TSD ,TSR, and WGS reactions were taken to be independent of the hydrogen partial pressure.

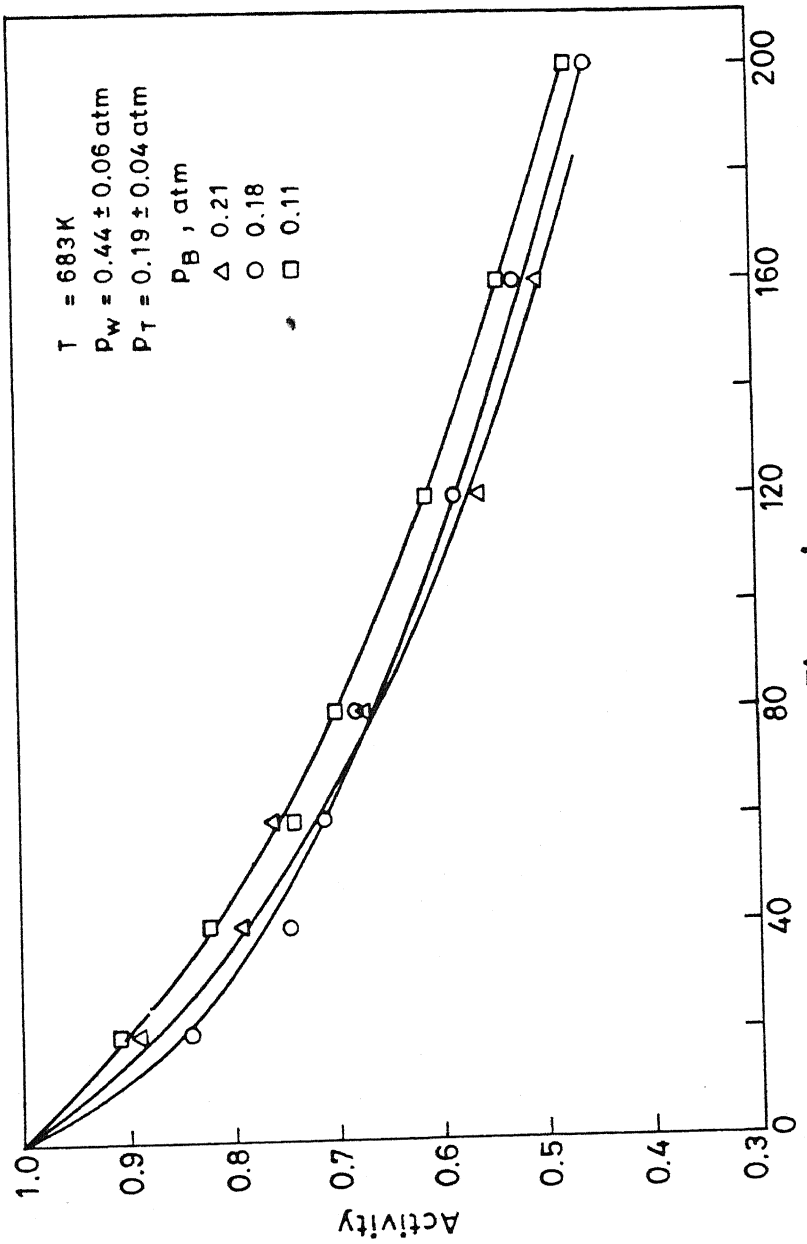

Fig. 4.27 Effect of benzene partial pressure on the activity of water gas shift reaction.

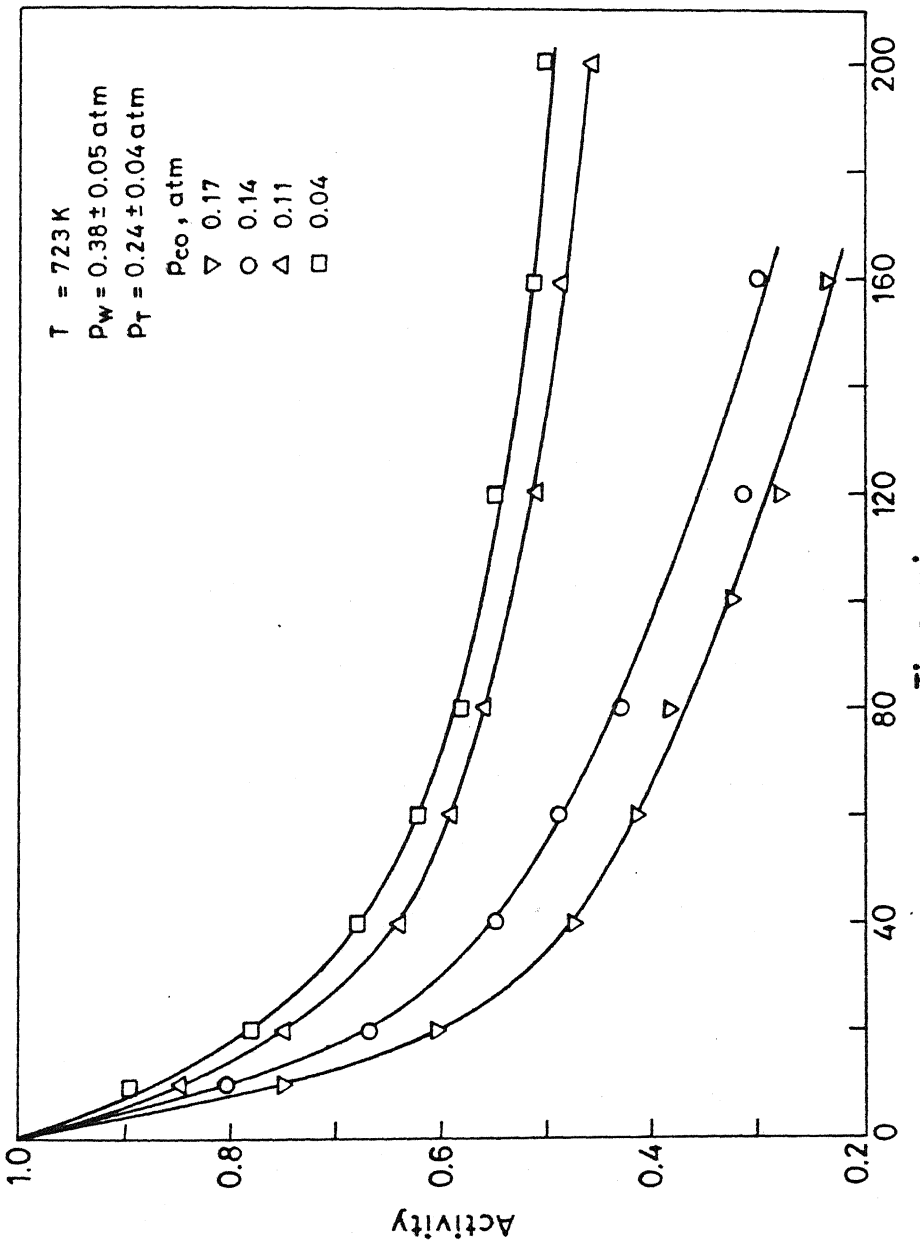

Fig. 4.28 Effect of carbon monoxide partial pressure on the activity of toluene steam dealkylation reaction.

4.4.2 Modeling of Deactivation Kinetics

The intrinsic deactivation kinetics of the main reactions were modeled using the activity concept. Generally, the deactivation function, ψ_i of any reaction is a function of temperature and the partial pressures of the reactants and/or products. For the three main reactions, the kinetic constants for the deactivation equations, eqn. (4.47) must be calculated separately. Either, the differential or integral method of analysis can be used to determine the deactivation kinetics. Regardless of the method adopted , the variation of the activities with run time is required.

For low conversion , it can be assumed that the variation in the partial pressures inside the reactor is negligible and , therefore, for an isothermal reactor, eqn. (4.47) can be integrated to give:

$$a_i = \exp[-\psi_i(P_W , P_T , P_B , \ldots,T)t] \quad ; d_i = 1 \qquad (4.51)$$

$$[a_i^{(1-d_i)} - 1] = (d_i - 1)\psi_i(P_W,P_T,P_B,\ldots,T)t \; ; \; d_i \neq 1, \qquad (4.52)$$

On the other hand, for high conversions, since the change in partial pressure during the run can be significant; ψ_i can change during the course of a run and therefore, eqns.(4.51) and (4.52) are valid over small intervals of the activity vs time plots.

As mentioned earlier, the rate of the toluene steam reforming reaction did not show any decrease with run time for the conditions of the study (refer Appendix II). Therefore, for the toluene steam reforming reaction,

$$-\frac{da_2}{dt} = 0 \qquad (4.53)$$

To determine the deactivation orders for the toluene steam dealkylation and water gas shift reactions, eqns. (4.51) and (4.52) with various values of d_i were tested. The deactivation order was determined from the low conversion data as well as the initial part of the high conversion data. As shown in Figure 4.30 for the low conversion data, the $(\text{activity})^{-1}$ vs time plots for the toluene steam dealkylation reaction were linear for the whole range, which shows that deactivation order for TSD is 2 . The deactivation function at different partial pressures and temperatures was calculated as the slope of these plots and the variation of ψ_i with temperature and partial pressures for all the runs is shown in Table 4.10. It should be mentioned that for the high conversion data, the $(1/a_i)^{-1}$ vs. time plots were linear till a run time of approximately two hours where the changes in partial pressures with time were negligible. For these runs, the activity was calculated on the basis of reaction rate at any time to that of fresh catalyst at the existing conditions. The deactivation function for these runs was calculated from the initial slopes. Similarly, as shown in Figure 4.31 , for the water gas shift reaction also, $(1/a_i)^{-1}$ vs. time plots were linear for all the runs; and therefore the deactivation order was also 2 for the reaction. The ψ_1 and ψ_3 , based either on the Langmuir-Hinshelwood formulation (Corella and Asua, 1982) or empirical were tested against the data shown in Table 4.10. These models included several deactivation functions as follows:

Table 4.10 : Variation of ψ_1 and ψ_3 with temperature and partial pressures

Average partial pressures are in atmospheres,(atm)

ψ_1,$(h)^{-1}$	ψ_3,$(h)^{-1}$	P_T	P_B	P_H	P_{CO}	P_C	P_W	Temp. K
0.27	0.22	0.136	0.030	0.030	0.015	0.026	0.810	723
0.41	0.20	0.100	0.026	0.100	0.031	0.024	0.710	723
0.19	0.63	0.070	0.001	0.017	0.009	0.002	0.900	723
0.97	0.35	0.430	0.011	0.060	0.030	0.001	0.430	723
0.53	0.31	0.230	0.020	0.060	0.035	0.016	0.640	723
0.73	0.36	0.340	0.026	0.080	0.040	0.019	0.490	723
0.76	0.35	0.350	0.020	0.055	0.031	0.013	0.520	723
0.40	0.27	0.110	0.016	0.060	0.041	0.013	0.760	723
0.21	0.16	0.061	0.072	0.035	0.017	0.006	0.870	723
0.37	0.23	0.125	0.050	0.041	0.031	0.009	0.785	723
0.28	0.19	0.060	0.025	0.010	0.028	0.022	0.760	723
0.30	0.23	0.062	0.023	0.097	0.029	0.022	0.760	723
0.23	0.19	0.070	0.020	0.080	0.025	0.015	0.790	723
0.27	0.21	0.078	0.013	0.052	0.022	0.009	0.830	723
0.24	0.17	0.081	0.008	0.050	0.026	0.007	0.83	723
0.23	0.17	0.076	0.013	0.060	0.020	0.009	0.820	723
0.12	0.50	0.042	0.020	0.013	0.008	0.002	0.930	723
0.46	0.28	0.181	0.020	0.045	0.030	0.010	0.720	723
0.37	0.26	0.044	0.037	0.130	0.034	0.034	0.710	723
0.35	0.24	0.060	0.030	0.110	0.032	0.022	0.750	723
0.12	0.57	0.060	0.003	0.020	0.009	0.004	0.910	723
0.44	0.23	0.235	0.011	0.070	0.020	0.014	0.650	723
0.11	0.10	0.040	0.007	0.025	0.010	0.006	0.910	723

0.51	0.23	0.233	0.018	0.050	0.018	0.011	0.670	723
0.10	0.12	0.041	0.032	0.016	0.012	0.003	0.920	723
0.12	0.12	0.034	0.009	0.040	0.013	0.006	0.900	723
0.46	0.25	0.240	0.020	0.040	0.012	0.085	0.680	723
0.39	0.20	0.185	0.006	0.033	0.014	0.007	0.740	723
0.39	0.27	0.100	0.030	0.093	0.040	0.021	0.720	723
0.39	0.28	0.050	0.030	0.135	0.038	0.031	0.710	723
0.36	0.25	0.043	0.037	0.150	0.033	0.035	0.700	723
0.73	0.33	0.300	0.042	0.133	0.041	0.025	0.450	723
0.85	0.37	0.370	0.056	0.116	0.045	0.018	0.390	723
0.79	0.36	0.115	0.030	0.170	0.130	0.090	0.470	723
2.33	0.65	0.140	0.004	0.150	0.290	0.100	0.300	723
1.27	0.57	0.200	0.009	0.110	0.182	0.060	0.440	723
1.50	0.55	0.300	0.010	0.110	0.160	0.060	0.365	723
1.44	0.55	0.285	0.015	0.140	0.133	0.050	0.350	723
1.80	0.23	0.310	0.030	0.190	0.170	0.096	0.185	723
0.44	0.28	0.095	0.032	0.102	0.030	0.021	0.700	713
0.43	0.23	0.125	0.040	0.130	0.035	0.025	0.640	713
0.42	0.16	0.140	0.033	0.120	0.033	0.023	0.600	713
0.54	0.13	0.150	0.030	0.121	0.040	0.025	0.420	713
0.41	0.12	0.155	0.025	0.100	0.030	0.020	0.220	713
0.11	0.14	0.180	0.012	0.040	0.010	0.009	0.185	713
0.33	0.47	0.062	0.006	0.033	0.012	0.007	0.870	713
0.24	0.18	0.064	0.016	0.050	0.020	0.007	0.830	713
0.11	0.13	0.055	0.030	0.130	0.025	0.030	0.720	713
0.49	0.23	0.037	0.004	0.022	0.010	0.003	0.820	713
0.77	0.29	0.190	0.031	0.118	0.031	0.023	0.470	713
0.23	0.12	0.292	0.044	0.150	0.040	0.030	0.440	713
0.33	0.17	0.080	0.013	0.075	0.021	0.016	0.525	713

0.51	0.21	0.145	0.017	0.096	0.026	0.020	0.495	713
0.48	0.20	0.147	0.013	0.370	0.050	0.018	0.370	713
0.18	0.16	0.160	0.020	0.090	0.030	0.014	0.235	713
0.31	0.20	0.170	0.016	0.200	0.031	0.007	0.465	713
0.39	0.25	0.048	0.107	0.185	0.046	0.041	0.360	713
0.51	0.23	0.058	0.350	0.040	0.030	0.011	0.520	713
0.66	0.20	0.047	0.300	0.160	0.055	0.044	0.370	713
0.76	0.37	0.030	0.170	0.230	0.065	0.060	0.280	713
0.45	0.17	0.047	0.013	0.060	0.018	0.009	0.850	713
1.15	0.17	0.090	0.035	0.120	0.034	0.024	0.680	713
0.37	0.33	0.049	0.012	0.051	0.017	0.008	0.860	713
0.64	0.23	0.226	0.018	0.090	0.027	0.017	0.620	693
0.59	0.31	0.285	0.050	0.170	0.044	0.035	0.410	693
0.75	0.28	0.350	0.015	0.075	0.030	0.012	0.520	693
0.27	0.27	0.360	0.056	0.144	0.040	0.033	0.260	693
0.11	0.14	0.030	0.025	0.075	0.032	0.018	0.810	693
0.32	0.19	0.056	0.060	0.028	0.013	0.006	0.890	693
0.30	0.20	0.145	0.023	0.105	0.030	0.025	0.660	693
0.66	0.31	0.125	0.013	0.043	0.022	0.011	0.790	683
0.17	0.16	0.380	0.045	0.120	0.050	0.030	0.373	683
0.17	0.25	0.056	0.006	0.030	0.016	0.006	0.880	683
0.59	0.27	0.352	0.015	0.067	0.033	0.005	0.520	683
0.65	0.31	0.243	0.008	0.060	0.025	0.011	0.654	683
0.33	0.22	0.022	0.015	0.074	0.015	0.023	0.850	683
0.13	0.15	0.132	0.035	0.122	0.025	0.031	0.655	683
0.29	0.19	0.075	0.024	0.104	0.022	0.027	0.750	683
0.56	0.27	0.082	0.010	0.050	0.017	0.070	0.830	683
0.47	0.27	0.200	0.175	0.096	0.038	0.023	0.460	683
0.18	0.16	0.175	0.205	0.075	0.031	0.020	0.485	683

0.14	0.12	0.270	0.080	0.125	0.032	0.026	0.450	683
0.20	0.14	0.218	0.145	0.126	0.040	0.035	0.425	683
0.39	0.28	0.360	0.010	0.045	0.027	0.008	0.540	663
0.17	0.10	0.055	0.006	0.032	0.018	0.008	0.880	663
0.13	0.10	0.025	0.014	0.050	0.020	0.010	0.666	663
0.28	0.18	0.345	0.016	0.060	0.027	0.011	0.525	663
0.46	0.25	0.065	0.004	0.020	0.010	0.005	0.891	663
0.14	0.14	0.095	0.011	0.040	0.021	0.013	0.820	663
0.16	0.17	0.120	0.016	0.050	0.022	0.013	0.781	663
0.15	0.15	0.160	0.017	0.064	0.023	0.014	0.720	663
0.24	0.20	0.407	0.030	0.096	0.040	0.021	0.405	663
0.56	0.30	0.270	0.070	0.022	0.0120	0.007	0.880	663

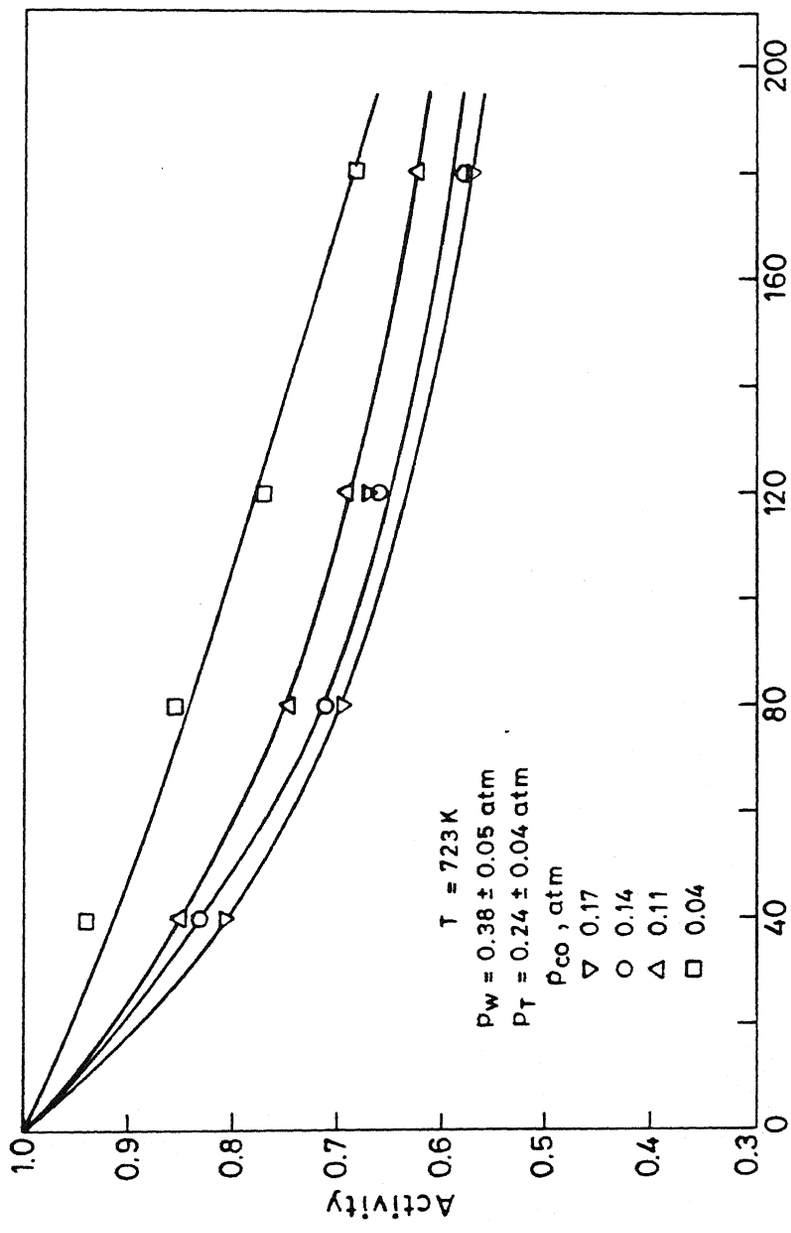

Fig. 4.29 Effect of carbon monoxide partial pressure on the activity of water gas shift reaction.

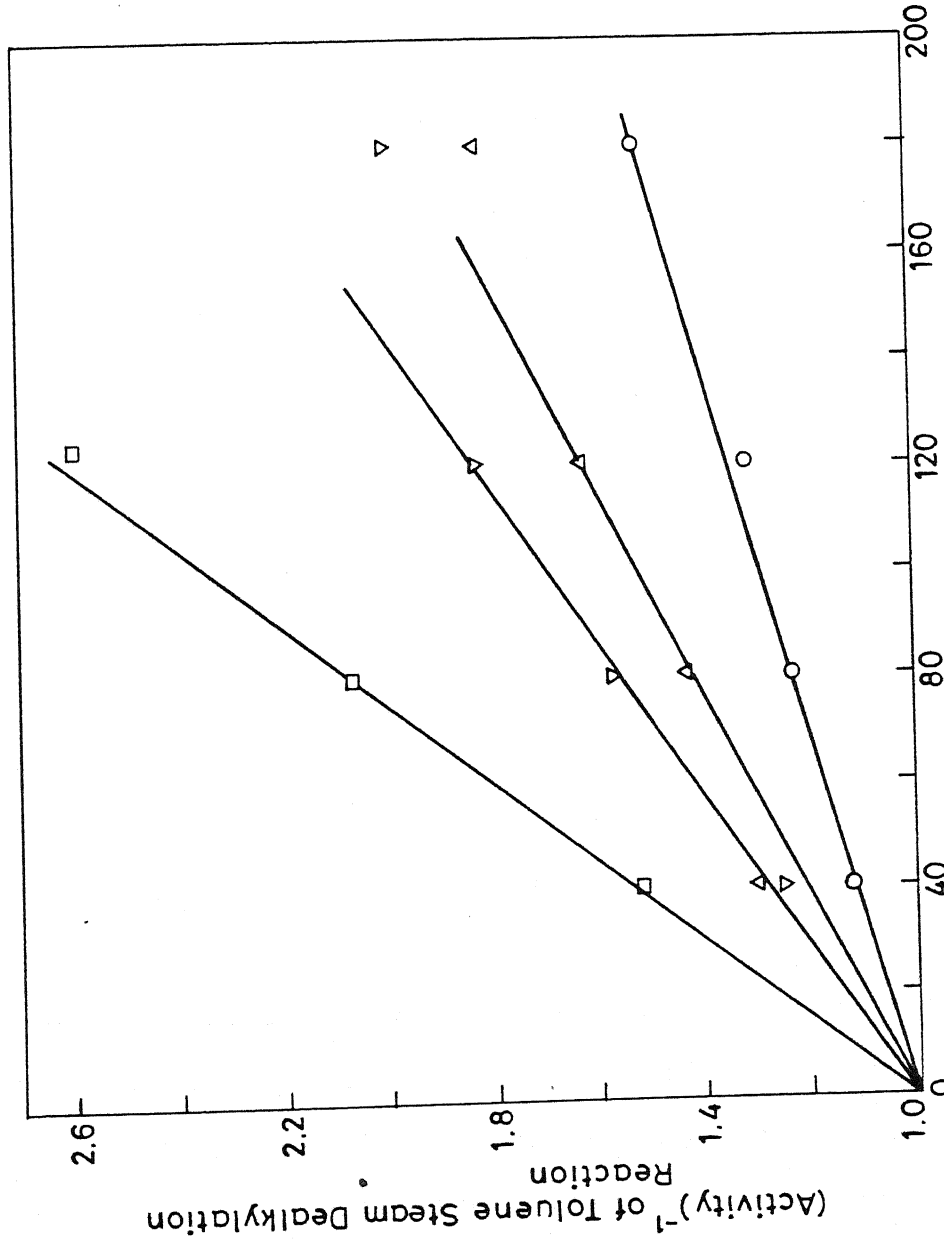

Fig. 4.30 Variation of (activity)$^{-1}$ of TSD with run time.

$$\psi_1 = \frac{k_{d1}(P_{CO} + P_C) + k_{d2}(P_T + P_B)}{(1 + K''_W P_W)} \quad (4.54)$$

$$\psi_1 = \frac{k_{d1}P_{CO} + k_{d2}P_T + k_{d3}P_B}{(1 + K''_W P_W)} \quad (4.55)$$

$$\psi_1 = \frac{k_{d1}P_{CO} + k_{d2}(P_T + P_B)}{(1 + K''_H P_H)} \quad (4.56)$$

$$\psi_1 = \frac{k_{d1}P_{CO} + k_{d2}(P_T + P_B)}{(1 + K''_W P_W)} \quad (4.57)$$

$$\psi_3 = k_{d3}P_{CO} + k_{d4}(P_T + P_B) \quad (4.58)$$

$$\psi_3 = k_{d3}P_{CO} + k_{d4}P_T + k_{d5}P_B \quad (4.59)$$

$$\psi_3 = k_{d3}P_{CO}P_W + k_{d4}P_T + k_{d5}P_B \quad (4.60)$$

$$\psi_3 = (k_{d3}P_{CO}P_W + k_{d4}(P_T + P_B)/(1 + K_H P_H) \quad (4.61)$$

These expressions were tested against the experimental mesured deactivation function data. Some of these models were rejected on the basis of either the average absolute error is large or some of the estimated parmeters were negative. The deactivation function for toluene steam dealkylation reaction was best represented by equation (4.57). On the other hand , equation (4.61) was found to give the best fit for the water gas shift reaction deactivation function. The best estimates of the various

Table 4.11: Deactivation kinetic parameters for steam dealkylation reaction

Kinetic parameter	Value
$k_{d1}(atm.h)^{-1}$	$(1.2 \pm 0.4)\times10^{2}$
$E_{d1}(kJ/mol)$	(16.2 ± 4.6)
$k_{d2}(atm.h)^{-1}$	$(1.18 \pm 0.2)\times10^{3}$
$E_{d2}(kJ/mol)$	(38.4 ± 3.0)
$K''_W\ (atm)^{-1}$	$(9.6 \pm 2.8)\times10^{-2}$
$E''_W\ (kJ/mol)$	(12.8 ± 2.2)
average absolute error	7.6 %.

deactivation reaction rate constants and equilibrium adsorption constants for toluene steam dealkylation reactions, with approximate 95% percent confidence limits are shown in Table 4.11. The average absolute error was 7.6 %. A comparison of the calculated deactivation function and the experimental deactivation data is shown in Figure 4.32. As can be seen from this figure, good agreement is obtained.

Similarly, the deactivation function for water gas shift reaction was tested against several empirical models (eqn. 4.58 to 4.61). The experimentally measured deactivation functions data was best represented by equation (4.61). The estimated parameters with their 95 % confidence limits are shown in Table 4.12. The average absolute error was 7.4 %. A comparsion of the calculated deactivation function and the experimental deactivation data is shown in Figure 4.33. As can be seen from this figure, good agreement is obtained.

Thus the intrinsic deactivaiton kinetics of the three reactions could be best represented by the following equation:

$$-\frac{da_1}{dt} = \left[\frac{1.2\times10^{2}\exp(-1940/T)p_{CO} + 1.2\times10^{3}\exp(-4598/T)(p_T + p_B)}{(1 + 0.096\exp(1529/T)p_W}\right]a_1^2 \qquad \text{.....(4.62)}$$

$$-\frac{da_2}{dt} = 0 \qquad (4.63)$$

$$-\frac{da_3}{dt} = \left[14.13\exp(-601/T)p_{CO}p_W + 57.1\exp(-3232/T)(p_T + p_B)\right] a_3^2 \qquad \text{.....(4.64)}$$

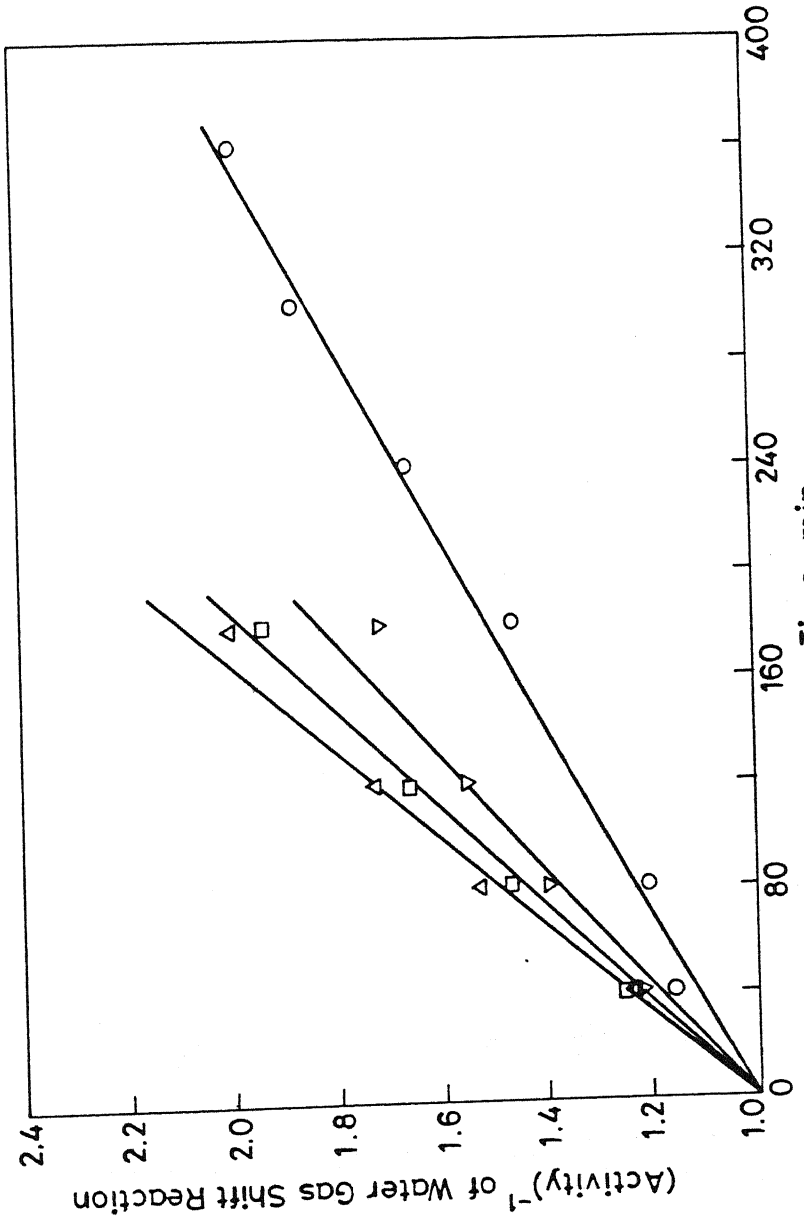

Fig. 4.31 Variation of (activity)$^{-1}$ of WGS with run time.

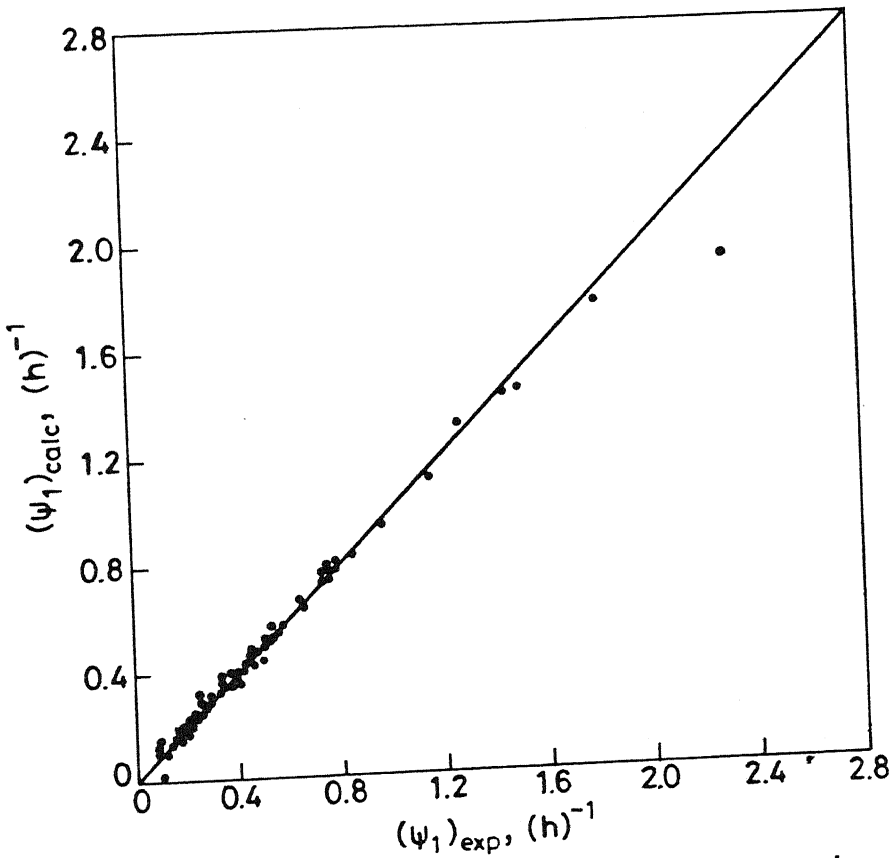

Fig. 4.32 Comparison of calculated and experimental deactivation function of TSD reaction.

Table 4.12: Deactivation kinetic parameters for water gas shift reaction

Kinetic parameter	Value
$k_{d3}(atm)^{-2}(h)^{-1}$	(14.1 ± 3.5)
$E_{d3}(kJ/mol)$	(5.0 ± 0.2)
$k_{d4}(atm.h)^{-1}$	(57.1 ± 6.6)
$E_{d4}(kJ/mol)$	(27.0 ± 3.8)
average absolute error	7.4 %.

4.5 DIFFUSION-DEACTIVATION INTERACTION

4.5.1 Diffusion Influenced Experimental Data

Intraparticle mass transport has a significant effect on the rate of reaction inside the catalyst pellet. For simple reactions in which the intrinsic rate of reaction increases with increasing partial pressure of the reactants, the average reaction rate in an isothermal catalyst pellet, compared with diffusion free kinetics, decreases due to the diffusional limitations of the reactants. However, in complex reactions the average reaction rate under diffusion influenced conditions can be more than for diffusion-free conditions. Normally, deactivation reactions are either in parallel or in series with the main reactions. For parallel deactivation, the rate of deactivation will be reduced under the influence of diffusional limitations, whereas, the catalyst will deactivate faster if the deactivation is in series with the main reaction.

To study the effect of diffusional influences on the activity, selectivity and the rate of catalyst deactivation, the toluene/water reaction was carried out over 3.2x3.2 mm cylindrical pellets as well as on crushed pellets of 1.68 mm average diameter in the temperature range 663 - 723 K.Preliminary runs indicated that diffusional influences were present for a catalyst size larger than 1.2 mm (refer Figure 4.2).The influence of the catalyst size on the average reaction rates of the main reaction was investigated and the data for the diffusional influenced runs are shown in Appendix III.

For both sizes, for the same inlet conditions (i.e. same W/F_{To} ,T and R) , the conversion , selectivity and rate of deactivation were different than the intrinsic kinetics runs (e.g

refer Runs no,P1,M6,P2,M2,P6,M3) .However, it is more appropriate to compare the results for the three catalyst sizes at identical exit conditions. Since data at exactly the same outlet partial pressures was not available , for the sake of comparison, runs in which the partial pressures were approximately the same have been identified and the effect of catalyst size on the reaction rates of toluene steam dealkylation , toluene steam reforming and water gas shift reactions is shown in Figures 4.34 to 4.39. As can be seen from Figure 4.34 and 4.35, the rate of toluene steam dealkylation reaction decreased as the catalyst pellet diameter was increased from 0.20 to 3.2 mm. Similarly, as shown in Figure 4.36 and 4.37, the rate of toluene steam reforming reaction also decreased with increasing catalyst size. On the other hand, (Figures 4.38 and 4.39) , the rate of water gas shift reaction under diffusion-influenced conditions was higher than that for the diffusion-free case and increased as the catalyst size increased.The rate of reaction of water gas shift reaction is mainly dependent on the partial pressures of carbon monoxide and water. Due to diffusional influences the partial pressure of the carbon monoxide would be higher and water partial pressure lower inside the pellets. Presumably, for the catalyst pellet, the decrease in rate due to the decrease in water partial pressure is more than compensated for by the corresponding increase in the carbon monoxide partial pressure inside the pellet.

The diffusional resistances in the catalyst not only affected the initial rates of the reaction, but also influenced the variation of catalyst activity with time. As shown in Figure 4.36 and 4.37 and Appendix III, the rate of the steam reforming reaction did not significantly change with time for any size.

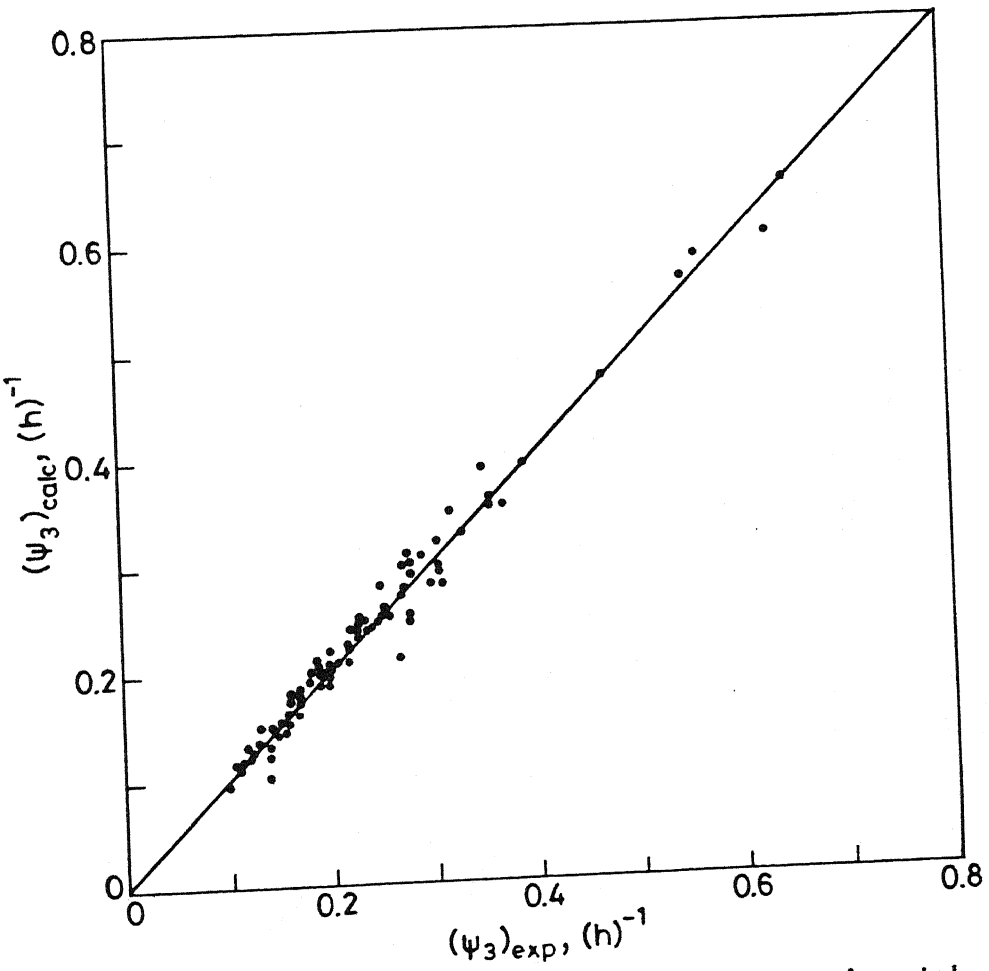

Fig. 4.33 Comparison of calculated and experimental deactivation function of WGS reaction.

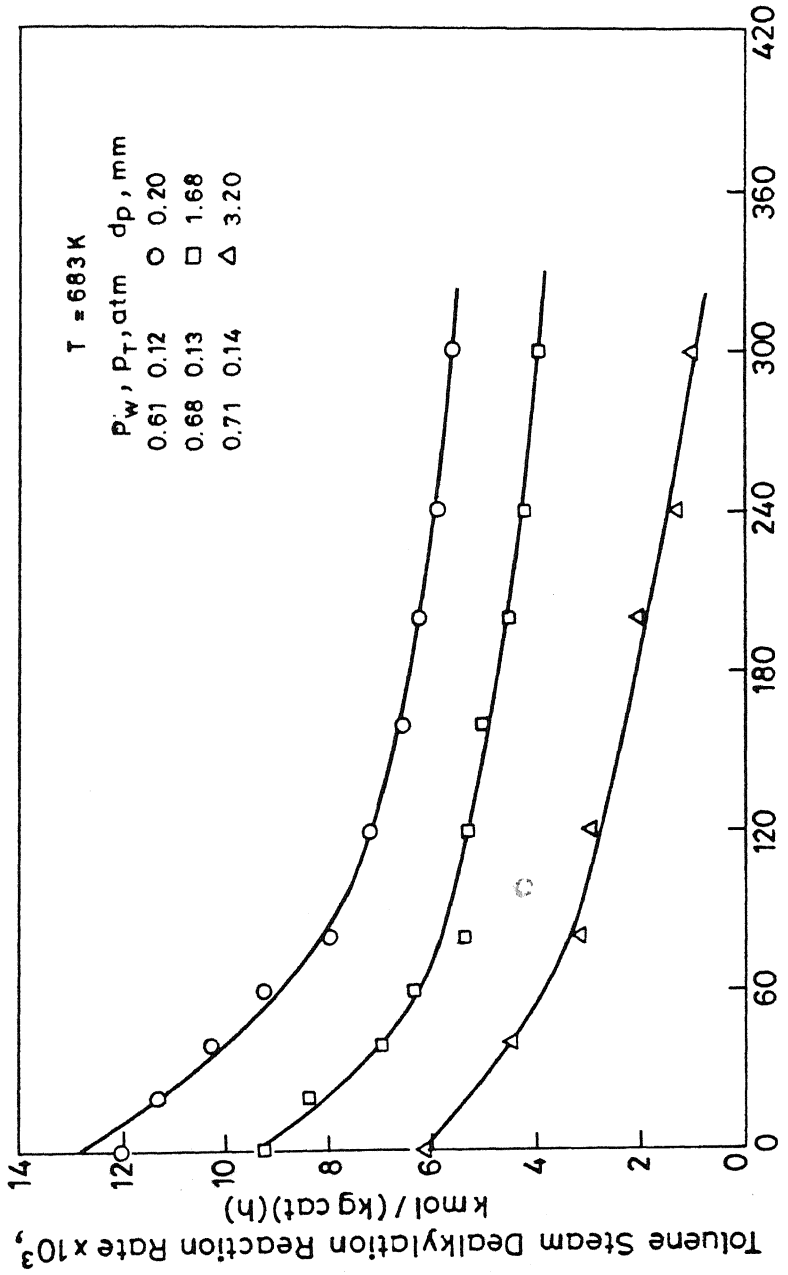

Fig. 4.34 Variation of rate of toluene steam dealkylation rate with catalyst size.

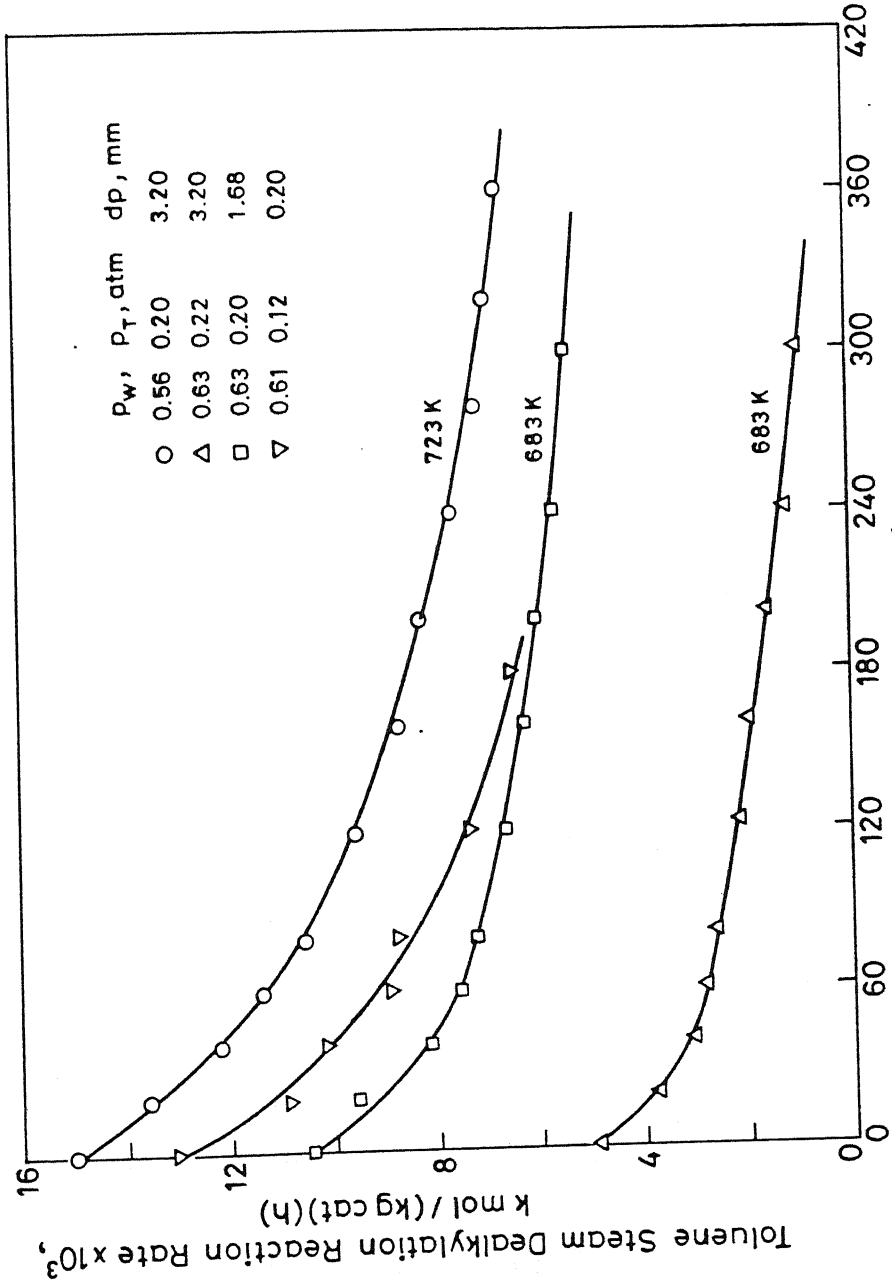

Fig. 4.35 Variation of toluene steam dealkylation reaction rate with catalyst diameter and temperature.

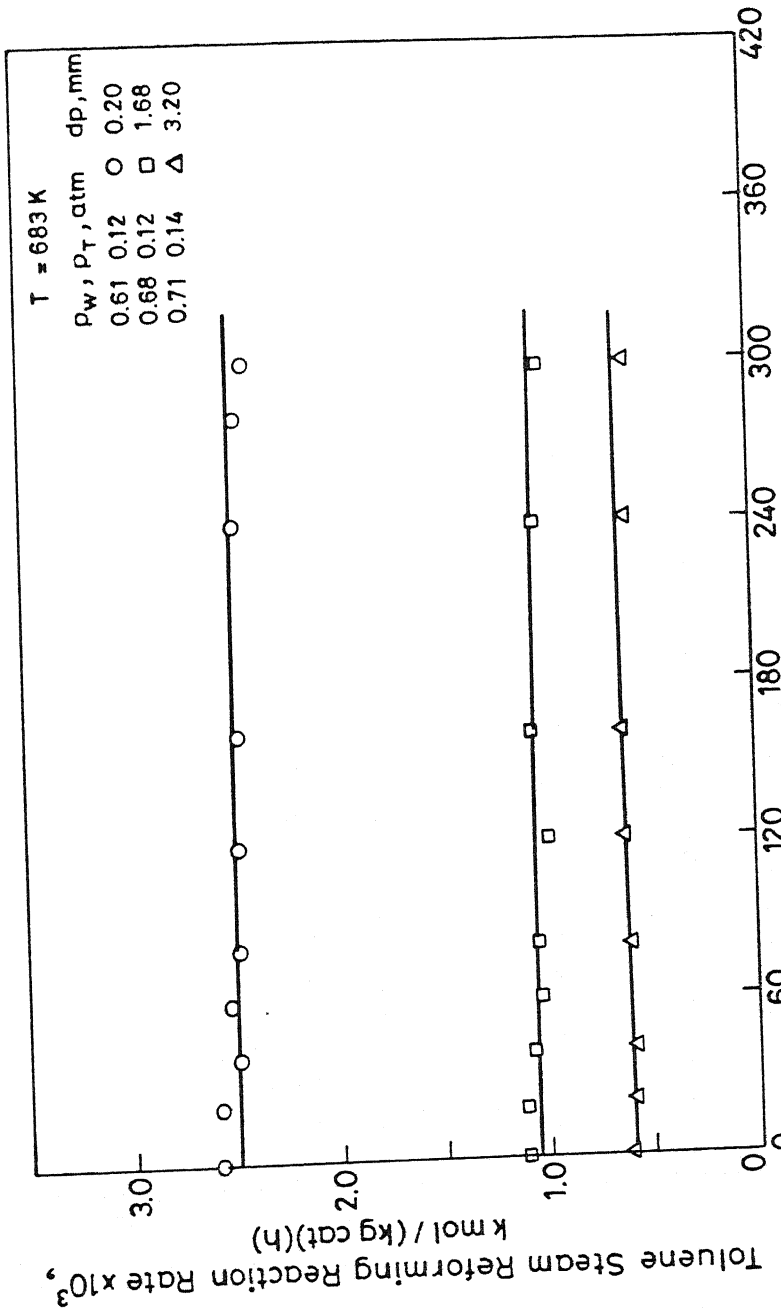

Fig. 4.36 Variation of rate of toluene steam reforming reaction with catalyst size.

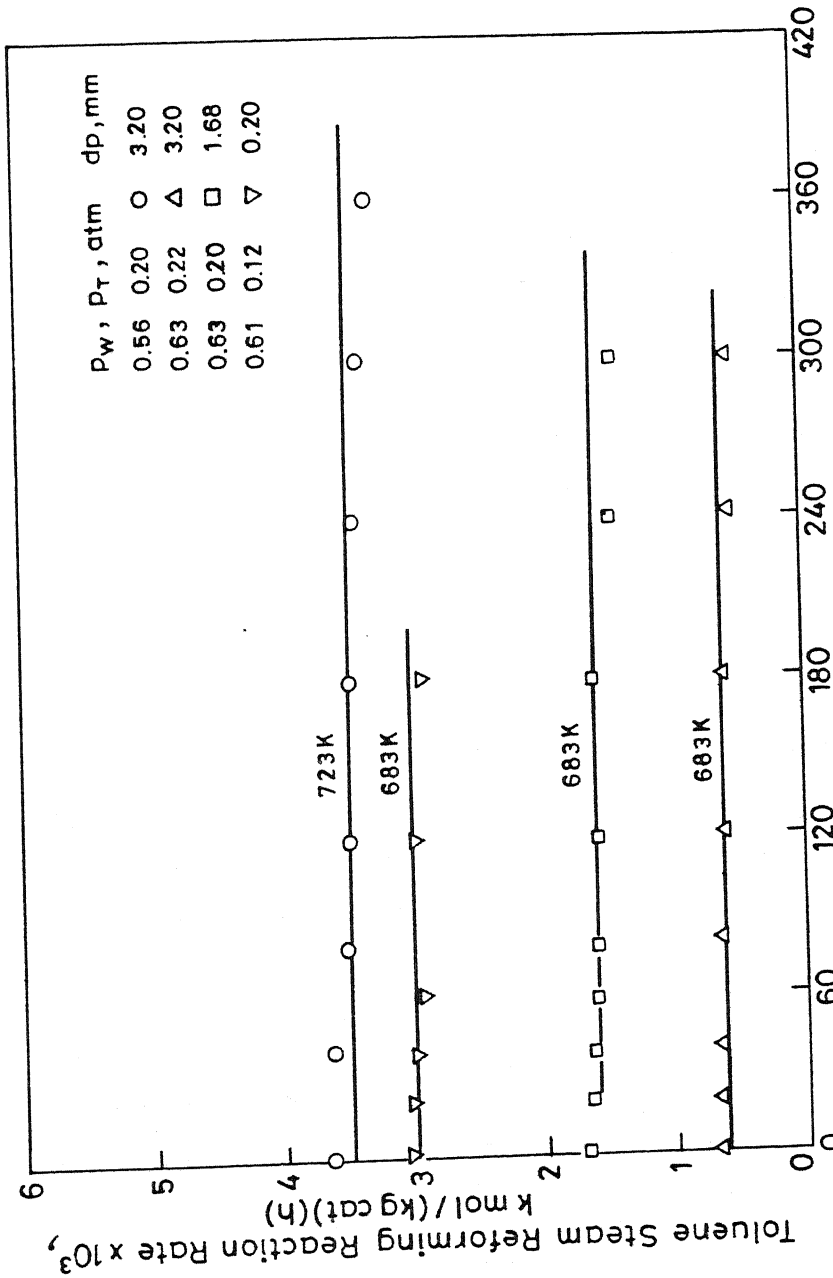

Fig. 4.37 Variation of rate of toluene steam reforming reaction with catalyst size and temperature.

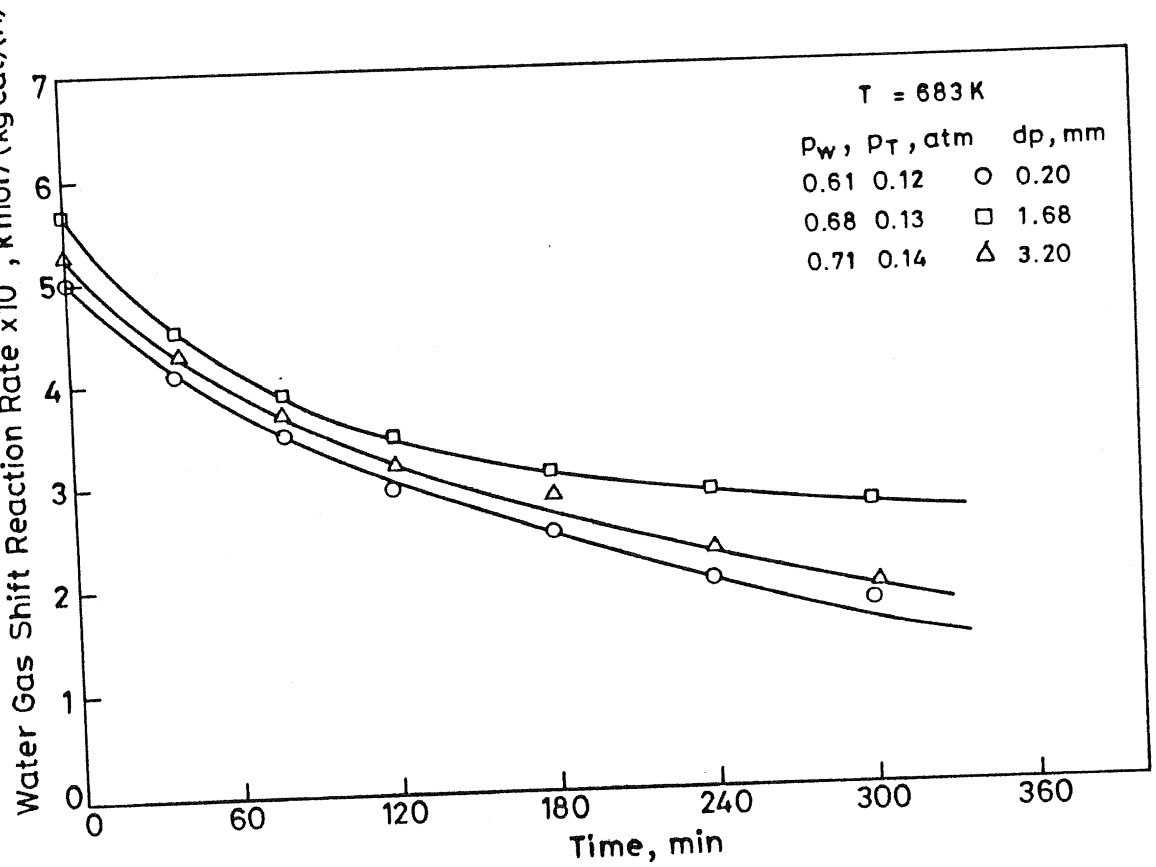

Fig. 4.38 Variation of rate of water gas shift reaction with catalyst size.

However, as can be seen from Figures 4.34,4.35,4.38 and 4.39, the rate of deactivation of toluene steam dealkylation reaction for 0.2 mm catalyst particles was higher and that for water gas shift reaction lower than that for the catalyst in which diffusional influences were present. As discussed in section (4.4.2) , the intrinsic deactivation kinetics for these two reactions depends on the partial pressures of water , toluene, benzene and carbon monoxide. Since carbon monoxide and benzene are products and water and toluene reactants, the observed deactivation for the pellets will be a complex function of the partial pressures . As reported by Kam et al. (1975), for simultaneous parallel and series deactivation , the catalyst deactivation behavior is governed by the relative magnitude of the individual rate constants of the deactivation equations. If the parallel fouling rate constant is much greater than that for series fouling, then the reaction system tends to reproduce parallel fouling behavior but on a reduced scale. However, the combined series/parallel deactivation mechanisms can show considerable deactivation compared to parallel deactivation alone when the rate constants are of same magnitude. The effect of introduction of Langmuir-Hinshelwood kinetics into the rate expression for the main reaction is to emphasize the importance of the deactivation (Wolf and Petersen, 1974).

For calculating the variation of the reaction rates, with time due to deactivation , a detailed model of the catalyst pellet is necessary and this is discussed below.

4.5.2 Modeling of Diffusion-Deactivation Interaction

To model the variation of reaction rates with time under diffusion-influenced conditions, the pellet mass balance equations

were combined with the intrinsic kinetics of the main and deactivation reaction. The following assumptions were made for the model development:

i) the catalyst pellet was considered to be of infinite length so that only one dimensional conservation equations were required. Dixon and Cresswell (1987) have shown that a finite cylindrical pellet can be approximated as an infinite pellet with mean hydraulic radius defined as

$$r_c = 2(V_p/S_x) \qquad (4.65)$$

where V_p is the total pellet volume and S_x is the total external area of the pellet. These authors found this approximation to be valid even for complex kinetics of a form very similar to that used in this study.

ii) Since the rates of deactivation were much smaller than the rates of the main reaction, the pellet was assumed to be operating under pseudo-steady state conditions.

iii) The interphase gradients were neglected . As discussed earlier (Section 4.1) , above an impeller speed of 2000 rpm, external mass transfer gradients were absent.

iv) The heat of reaction of the deactivation reaction was neglected. Since the rate of deactivation is slow, this assumption is justified.

v) The pellet was assumed to be isothermal. For a single reaction the effect of intraparticle heat transfer limitations inside the catalyst pellet depends upon the magnitude of the thermicity factor, β, defined as

$$\beta = \frac{(-\Delta H)\, D_{eff}\, C_{Ab}}{k_{eff}\, T_b} = \frac{(\Delta T)_{max}}{T_b} \qquad (4.6\text{ shift})$$

of

where $(-\Delta H)$ is the heat of reaction at the reaction temperature, D_{eff} is the effective diffusivity of the reactants, C_{Ab} is the bulk reactant concentration, k_{eff} is the thermal conductivity of the catalyst pellet and T_b is the bulk temperature.

For gas solid reactions, the range of β is usually in the range 0.001 to 0.3 (Lee , 1985), and for low values of β the pellet can be considered to be isothermal. For endothermic reactions, there is a decrease in temperature inside the pellet and since the rate decreases with temperature, the effect of heat transfer resistances in further diminished.

The above equation (4.66) is valid only for a single reaction. For complex reactions , the overall heat generated or consumed in the reactions will depend on the extent of the various reactions and will be a function of the product selectivities. For the reaction scheme proposed in this study, the overall heat of reaction per mole of water reacted, $(\Delta H)_{overall}$, was estimated based on the number of moles of water consumed in each of the 3 reactions. To check the assumption of pellet isothermality, an approximate value of β for this reaction, was calculated at an average benzene selectivity of 0.8 and an average carbon dioxide selectivity of 0.5 With these selectivities, the total moles of water consumed per mole of toluene reacted is 2.7 Thus, we have

$$(\Delta H)_{overall} = \frac{(\Delta H)_1 * 0.8 + (\Delta H)_2 * 0.2 + (\Delta H)_3 * 0.5}{2.7} \qquad (4.67)$$

where $(\Delta H)_1$, $(\Delta H)_2$, $(\Delta H)_3$ are the heats of reaction of toluene

steam dealkylation , toluene steam reforming and water gas shift reactions , respectively.

The value of β was calculated at an average temperature of 700 K. Using standard methods, (Reid et al., 1977)

$$(\Delta H)_{1 \text{ at } 700 \text{ K}} = 41,120 \quad \text{kcal/kmol of toluene reacted}$$

$$(\Delta H)_{2 \text{ at } 700 \text{ K}} = 219,320 \quad \text{kcal/kmol of toluene reacted}$$

$$(\Delta H)_{3 \text{ at } 700 \text{ K}} = -9,386 \quad \text{kcal/kmol of water reacted}$$

Hence $(\Delta H)_{overall}$ is = 26,691 kcal/kmol of water consumed.

To estimate β , D_{eff} was taken to be 0.011 m^2/h and k_{eff} as 149 cal/(h.m.K), respectively. With these values , β was -0.029 at 700 K. Thus, the assumption of pellet isothermality was justified. As discussed be Carberry (1976), for most gas-solid reactions, the pellet can be considered to be isothermal.

With these assumptions, the conservation equations for the cylindrical pellet can be written as (Hughes, 1984),

$$\frac{D_{eff,T}}{RT}\left[\frac{1}{r}\frac{dp_T}{dr}+\frac{d^2p_T}{dr^2}\right] = \rho_p\left[R_1^o a_1 + R_2^o a_2\right] \qquad (4.68)$$

$$\frac{D_{eff,B}}{RT}\left[\frac{1}{r}\frac{dp_B}{dr}+\frac{d^2p_B}{dr^2}\right] = -\rho_p\left[R_1^o a_1\right] \qquad (4.69)$$

$$\frac{D_{eff,W}}{RT}\left[\frac{1}{r}\frac{dp_W}{dr}+\frac{d^2p_W}{dr^2}\right]=\rho_p\left[R_1^o a_1+7R_2^o a_2+R_3^o a_3\right] \quad (4.70)$$

$$\frac{D_{eff,CO}}{RT}\left[\frac{1}{r}\frac{dp_{CO}}{dr}+\frac{d^2p_{CO}}{dr^2}\right]=\rho_p\left[-R_1^o a_1-7R_2^o a_2+R_3^o a_3\right] \quad (4.71)$$

$$\frac{D_{eff,C}}{RT}\left[\frac{1}{r}\frac{dp_C}{dr}+\frac{d^2p_C}{dr^2}\right]=-\rho_p\left[R_3^o a_3\right] \quad (4.72)$$

$$\frac{D_{eff,H}}{RT}\left[\frac{1}{r}\frac{dp_H}{dr}+\frac{d^2p_H}{dr^2}\right]=\rho_p\left[-2R_1^o a_1-11R_2^o a_2-R_3^o a_3\right] \quad (4.73)$$

where R is the gas constant, $D_{eff,i}$ is the effective diffusivity of component i and r is the radial coordinate.

The change in activity with time is obtained from the intrinsic kinetics as

$$-\frac{da_1}{dt}=\frac{k_{d1}P_{CO}+k_{d2}(P_T+P_B)}{(1+K''_W P_W)}a_1^2 \quad (4.62)$$

$$-\frac{da_2}{dt}=0 \quad (4.63)$$

$$-\frac{da_3}{dt}=k_{d3}P_{CO}P_W+k_{d4}(P_T+P_B) \quad (4.64)$$

In eqns. (4.68 to 4.73), R_1^o, R_2^o, and R_3^o are the intrinsic kinetics of the main equations and given by eqns. (4.43 - 4.45).

Since the experiments were conducted in a gradientless reactor, the partial pressures of the reaction components at the catalyst surface were the same as the reactor exit values. Thus the boundary conditions were

$$r = 0 , \quad \frac{dp_j}{dr} = 0 \qquad (4.74)$$

$$r = r_c \qquad p_j = p_j^e \qquad (4.75)$$

$$j = T, W, B, CO, C, H$$

p_j^e is the exit partial pressure of component j at the exit of the reactor. Eqn (4.73) was eliminated using equations (4.68) to (4.72) and the partial pressure of hydrogen at any position in the pellet could be expressed as:

$$p_H = -9(D_{eff,B}/D_{eff,H})(p_B - p_B^e) - 11(D_{eff,T}/D_{eff,H})(p_T - p_T^e)$$

$$+(D_{eff,C}/D_{eff,H})(p_C - p_C^e) + p_H^e \qquad (4.76)$$

The average reaction at any time for each of the 3 reactions in the pellet can be calculated by integrating the point rates across the pellet volume and can be expressed as:

$$\bar{R}_i(t) = \frac{2}{r_c^2} \int_o^{r_c} r\, R_i^o(r)\, a_i(r,t)\, dr \qquad i = 1,2,3 \quad (4.77)$$

To solve the above equations, the values of the effective diffusivities at the reaction temperature are needed. The effective diffusivity of hydrogen in the hydrogen-nitrogen mixture was measured experimentally using the gas chromatogarph method discussed by Valus and Schneider (1985).Calculations showed that the predominant mode of intraphase transport was by Knudsen diffusion. The effective diffusivities for the each of reaction components at temperature were calculated using the experimental results of the effective diffusivity of hydrogen in H_2-N_2 mixture (Lee, 1985) and could be expressed as:

$$D_{eff,j} = 1.9\times10^{-3}\sqrt{\frac{T}{M_j}} \qquad (4.78)$$

where $D_{eff,j}$ is in m^2/h , T is in K, M_j is the molecular weight of component j, ρ_p is the pellet density. The pellet density, ρ_p, was experimentally measured and found to be 956 kg/m^3. Equations (4.68) to (4.72) together with equations (4.62 - 4.64),(4.43 - 4.45) and (4.74 to 4.78) constitute the model equations for calculating the variation of the average rates of reaction with time in the diffusion-influenced pellets.

4.5.3 Model Solution

For a give set of reactor inlet conditions (W/F_{To} temperature, R), the solution requires an iterative calculation because the exit partial pressures are not known a priori. The method of solution consisted of the following steps:

1) For a given set of inlet reactor conditions, values of the exit

partial pressures were assumed.

2) For the assumed exit partial pressures, the partial pressure profiles in the pellet were determined by numerically solving eqns. (4.68 - 4.72) together with eqn. (4.76). For time zero, the activity of each of the three reactions was unity.

3) With the partial pressure profiles obtained in step (2) , the average reaction rates were calculated using eqn. (4.77)

4) With the average reaction rates calculated in step (3) , the exit molar flow rates of the reaction components were calculated using the reactor mass balance equation as follows:

$$F_T = F_{To} - (\bar{R}_1 + \bar{R}_2) \times W \qquad (4.79)$$

$$F_W = F_{Wo} - (\bar{R}_1 + 7\bar{R}_2 + \bar{R}_3) \times W \qquad (4.80)$$

$$F_B = \bar{R}_1 W + F_{Bo} \qquad (4.81)$$

$$F_{CO} = (\bar{R}_1 + 7\bar{R}_2 - \bar{R}_3) \times W + F_{CO,o} \qquad (4.82)$$

$$F_C = \bar{R}_3 W + F_{C,o} \qquad (4.83)$$

$$F_H = (2\bar{R}_1 + 11\bar{R}_2 + \bar{R}_3) \times W + F_{Ho} \qquad (4.84)$$

where $\bar{R}_1$, $\bar{R}_2$ and $\bar{R}_3$ are the average reaction rate of toluene steam dealkylation , toluene steam reforming and water gas shift reactions, respectively, W is the weight of catalyst , F_{To}, F_{Bo}, $F_{CO,o}$, $F_{C,o}$, F_{Ho} and F_{Wo} are the inlet flow rates of toluene , benzene , carbon monoxide, carbon dioxide, hydrogen and water, respectively. The new guess values for the exit partial pressures

were then found from

$$(p_j^e)_{new} = (F_j \Big/ \sum_{j=1}^{6} F_j).P \quad , \qquad (4.85)$$

where P is the total exit pressure and was always 1 atm.

5) The $(p_j^e,s)_{new}$ were compared with the partial pressure values assumed in step 1 and if the difference was above the tolerance limit, steps (2) to (4) were repeated with this new guess values . This was continued till convergence was obtained.

6) After the convergence was obtained for the first time interval, the new values of the activities inside the pellet for the next time interval were calculated using eqns. (4.62) to (4.64). It should be noted that the activities were a function of the radial position in the pellet. With these new values of the activities , steps (1) to (5) were repeated .

7) Steps (1) to (6) were executed for the required period of run time.

4.5.3.1 Numerical Solution of The Pellet Equations

The system of differential equations given by equations (4.68 to 4.72) was solved using a five point orthogonal collocation technique (Villadsen and Stewart,1967). In order to use this method, the radial coordinate was nondimensionalised with respect to the hydraulic radius, r_c. Using this technique, these differential equations were converted to a nonlinear set of 25 algebraic equations which can be expressed as:

$$\mathbf{C}.\bar{X} = \bar{D} \qquad (4.86)$$

where **C** is a 25x25 matrix such that

$$C_{ij} = C_{i+5,j+5} = C_{i+10,j+10} = C_{i+15,j+15} = C_{i+20,j+20} = B_{ij}$$

$$D(i) = \frac{\rho_p \, RT \, r_c^2}{D_{eff,C}} \left[- R_3^o \, a_3 - B_{i,6} \, P_C^e \right], \qquad i = 20,25 , \qquad (4.93)$$

These 25 nonlinear equations were solved using Brown method (1973) and the detailed computer listing of the programme is given in Appendix V.For starting the computation, the experimental values of the partial pressures were given as the guess values. The execution time for a run time of 4 hours was usually 15 minutes on a DEC1090 computer.

4.5.4 Model Results

For the comparison of the calculated and experimental results , 26 runs for a catalyst size of 3.2x3.2 mm and 7 runs for a 1.68 mm catalyst size were available (for details refer Appendix III).For all the runs, the above programme was executed and the results calculated using the above model were compared with the experimental data.

The comparison between the experimental and calculated results for two widely different conditions at each of the 4 temperatures, for the 3.2x3.2 mm cylindrical pellet, is shown in Figures 4.40 to 4.47. As can be seen from these figures, the agreement between the calculated and experimental rates was satisfactory at all the 4 temperatures. For most of the runs, the predicted rates were within ± 9 % of the experimental rates. However, for the some runs, the deviation was higher. This difference could be due to either the error in estimating the effective diffusivities or due to the experimental errors. The calculated rates for the toluene steam reforming reaction gradually increased with run time. This is because, the rate of

deactivation of toluene steam reforming reaction has been assumed to be zero and the exit partial pressure of reactants increased whereas those of the products decreased due to the deactivation of TSD and WGS reactions. However, this increase was marginal.

For both the TSD and WGS reactions, the activity profile decreased from the surface to the center of the particle . This profile was initially relatively flat and became steeper with increasing run time. If the deactivation was caused mainly by toluene partial pressure , then a decreasing profile would be observed, whereas if the deactivation was only dependent on the carbon monoxide and benzene partial pressures then an increasing profile would be obtained. The combination of both mechanisms lead to the actual activity profile.

The above model was also tested for a catalyst size of 1.68 mm average diameter and the results are shown in Figures 4.48 to 4.51. As can be seen from these figures, the calculated rates are in good agreement with the experimental values for this size also. The maximum deviation between the calculated and experimental rates was for the water gas shift reaction. For the sake of comparison, runs in which the exit partial pressures for the 3.2x3.2 mm pellet were nearly the same are also shown in these figures. The exit partial pressures in atm for run M3 were, p_T =0.15, p_W =0.71, p_B = 0.03, p_H = 0.07, p_{CO} = 0.03 and p_C = 0.02 whereas for run P3 p_T =0.20, p_W =0.64, p_B = 0.05, p_H = 0.09, p_{CO} = 0.03 and p_C = 0.02. Similarly, the partial pressures in the M2 run were p_T =0.08, p_W =0.80, p_B = 0.02, p_H = 0.06, p_{CO} = 0.03 and p_C = 0.02 whereas in run P5 were p_T =0.08, p_W =0.79, p_B = 0.03, p_H = 0.06, p_{CO} = 0.02 and p_C = 0.02

As shown in Figures 4.48 and 4.50, in both cases, the rate

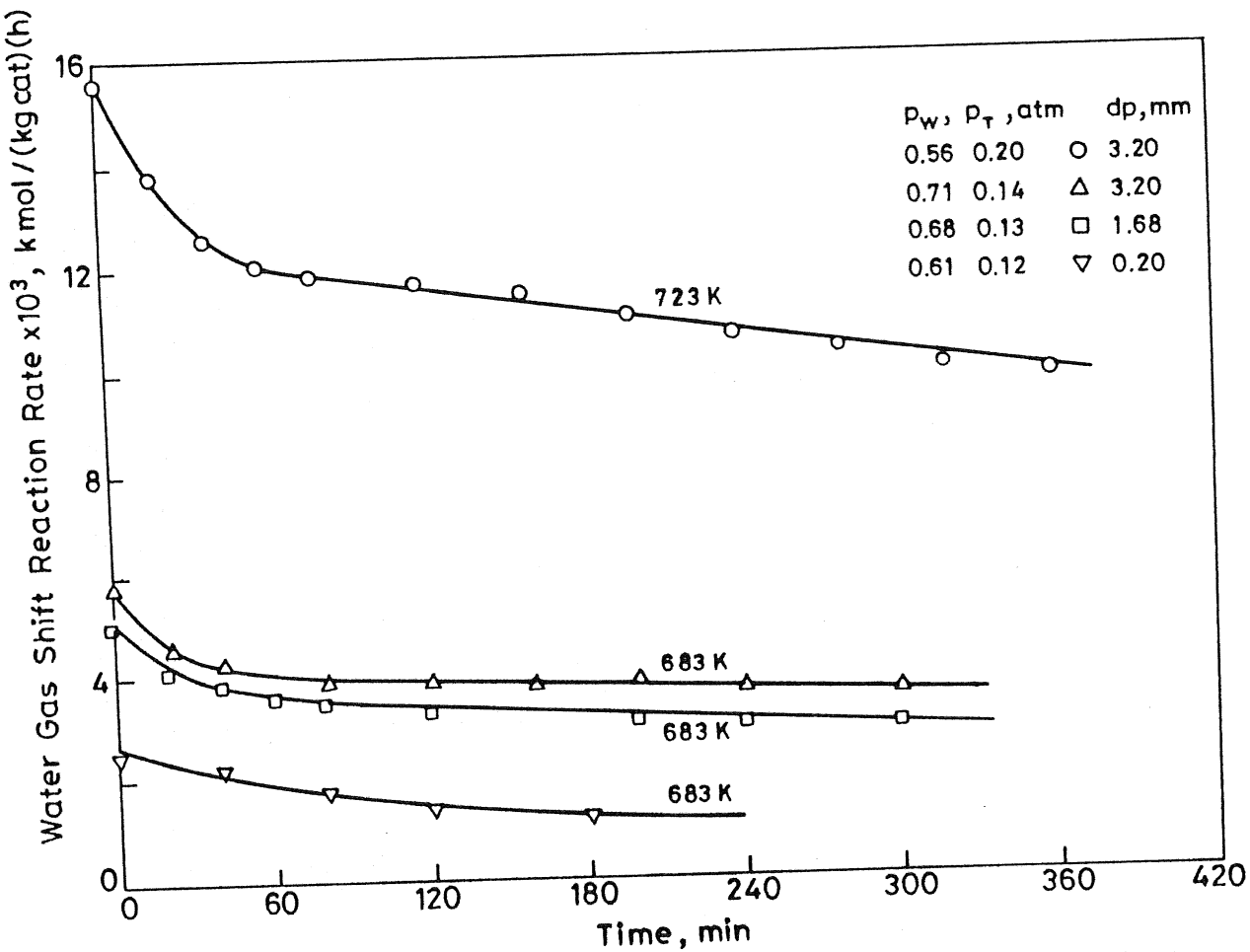

Fig. 4.39 Variation of rate of water gas shift reaction with catalyst size and temperature.

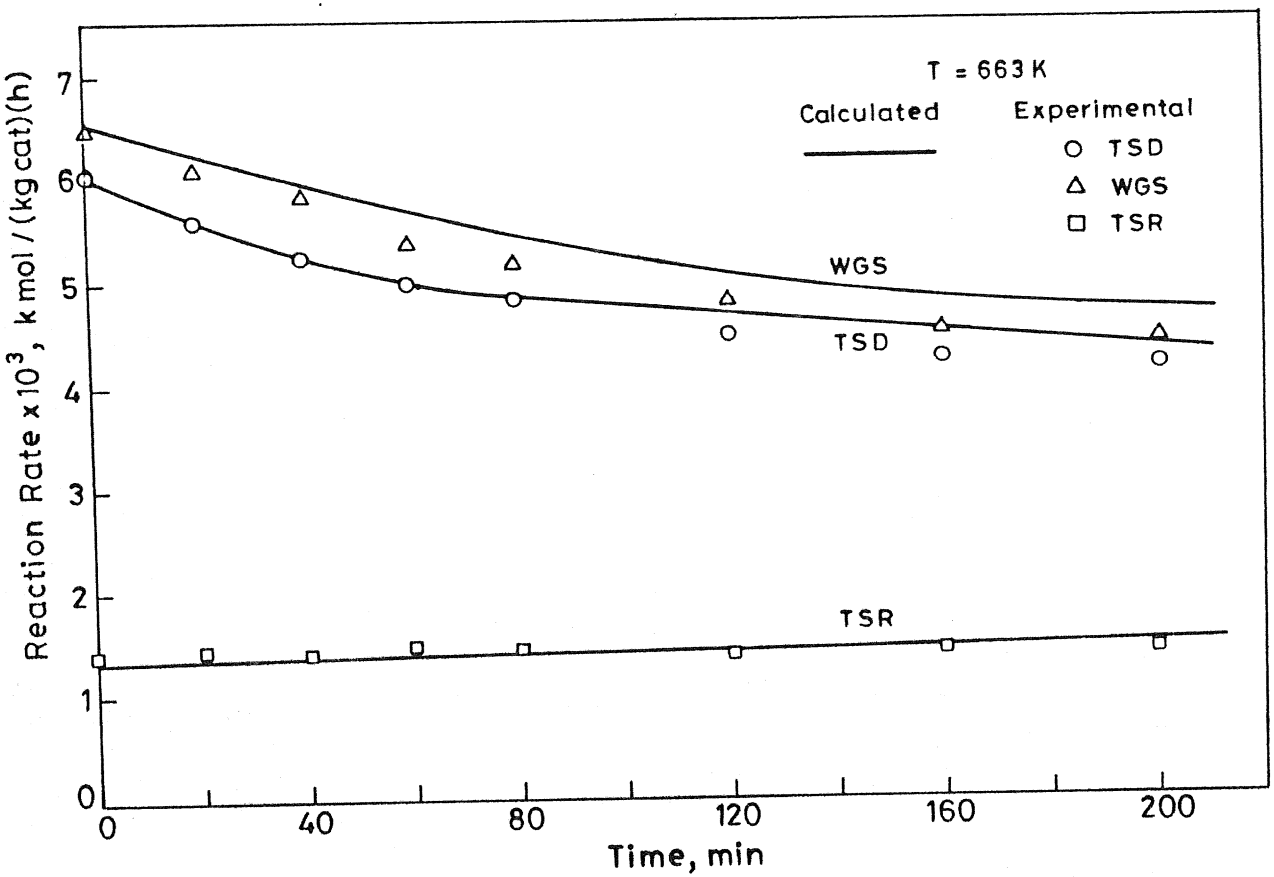

Fig. 4.40 Comparison between calculated and experimental results for diffusion influenced pellets (catalyst size : 3.2 x 3.2 mm, run no. L6)

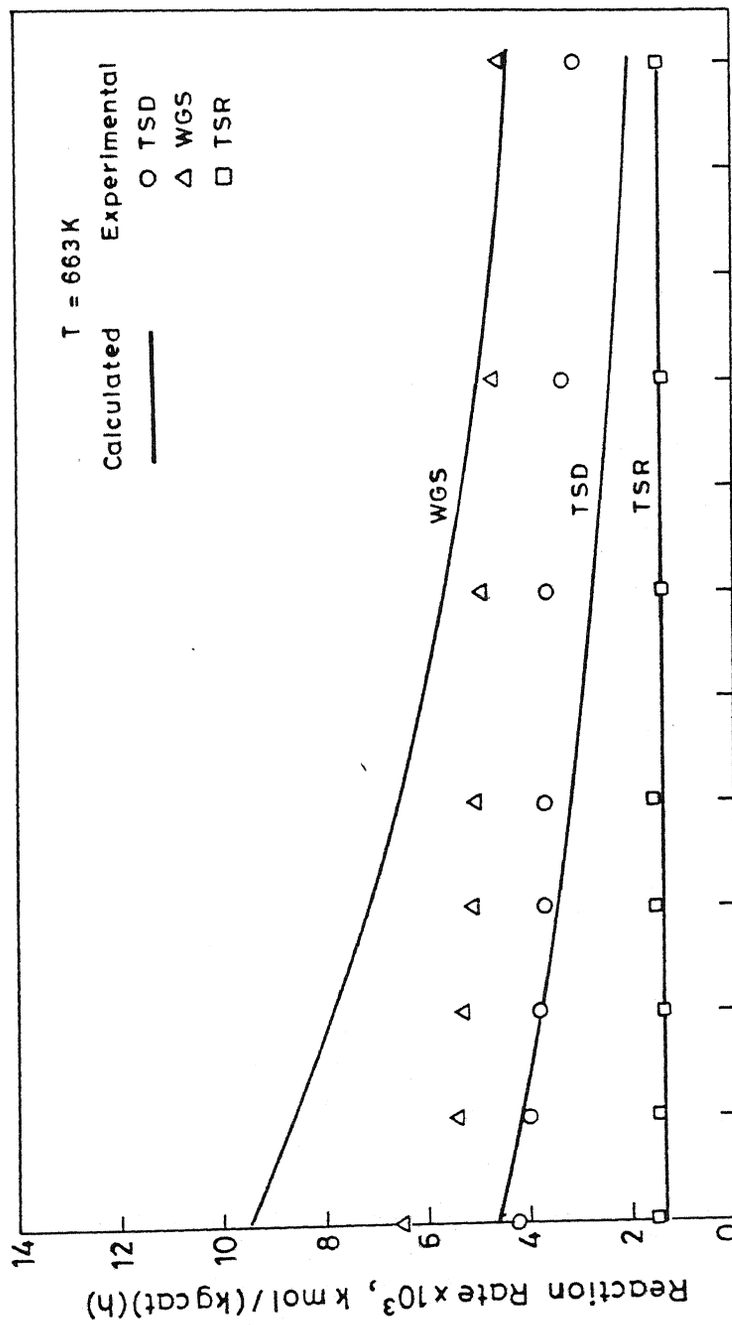

Fig. 4.41 Comparison between calculated and experimental results for diffusion influenced pellets (catalyst size: 3.2 x 3.2 mm, run no. L5)

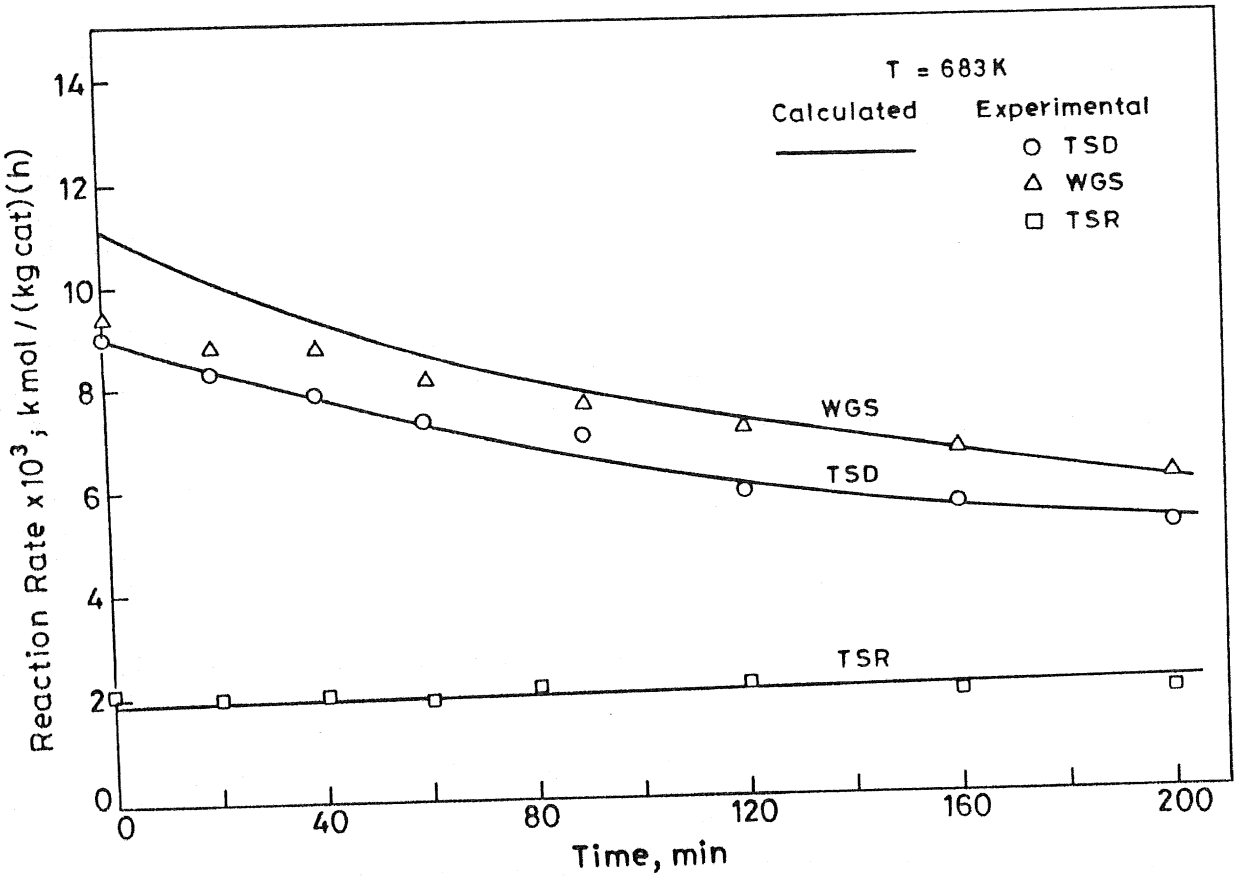

Fig. 4.42 Comparison between calculated and experimental results for diffusion influenced pellets (cat. size: 3.2 x 3.2 mm, run no. M2)

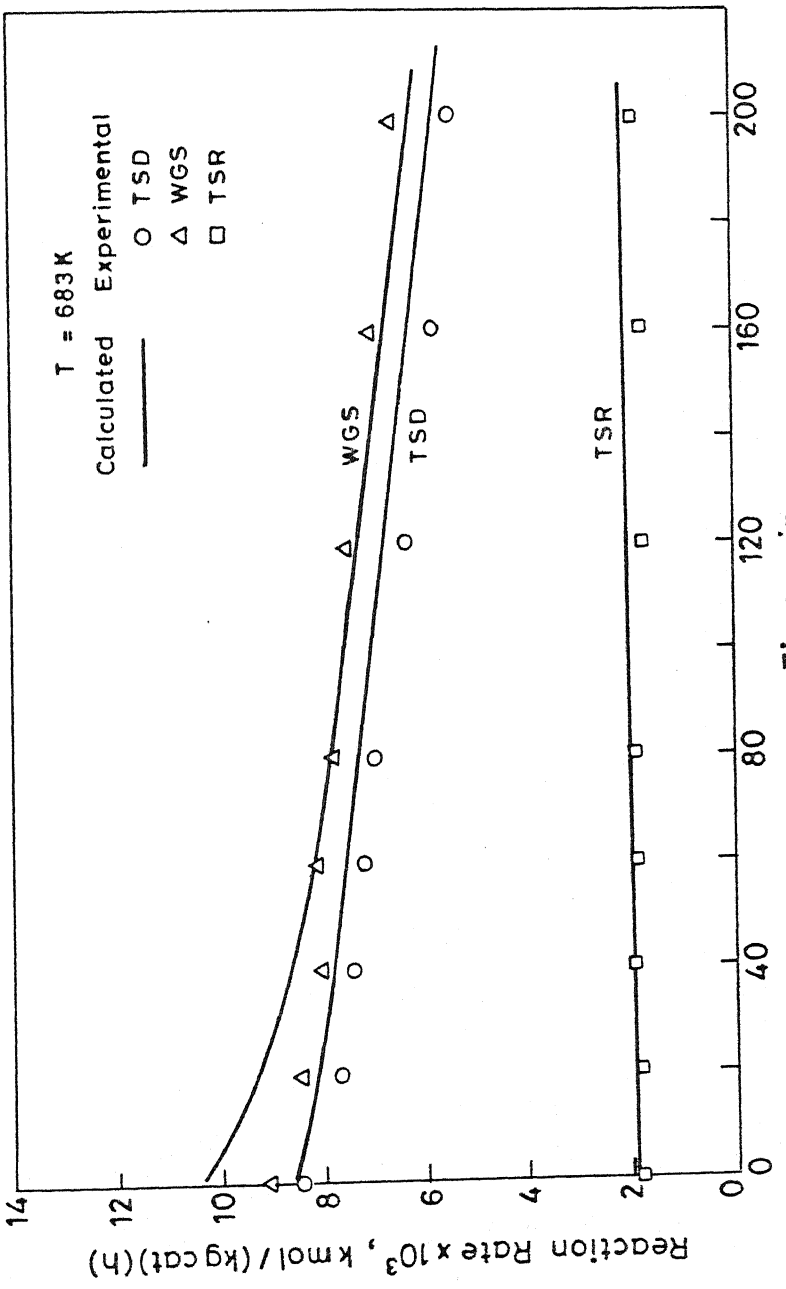

Fig. 4.43 Comparison between calculated and experimental results for diffusion influenced pellets (cat. size: 3.2 x 3.2 mm, run no. M7)

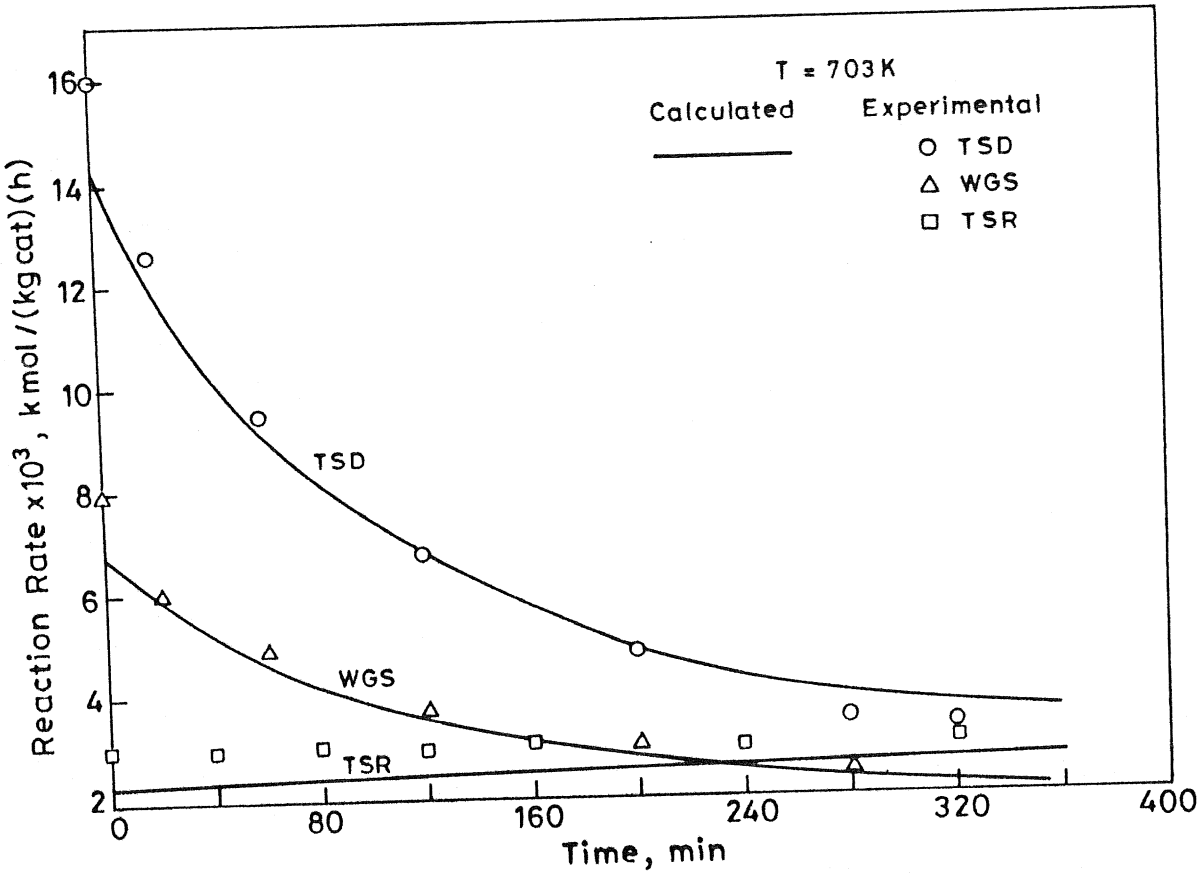

Fig. 4.44 Comparison between calculated and experimental results for diffusion influenced pellets (cat. size: 3.2 x 3.2 mm, run no. N1)

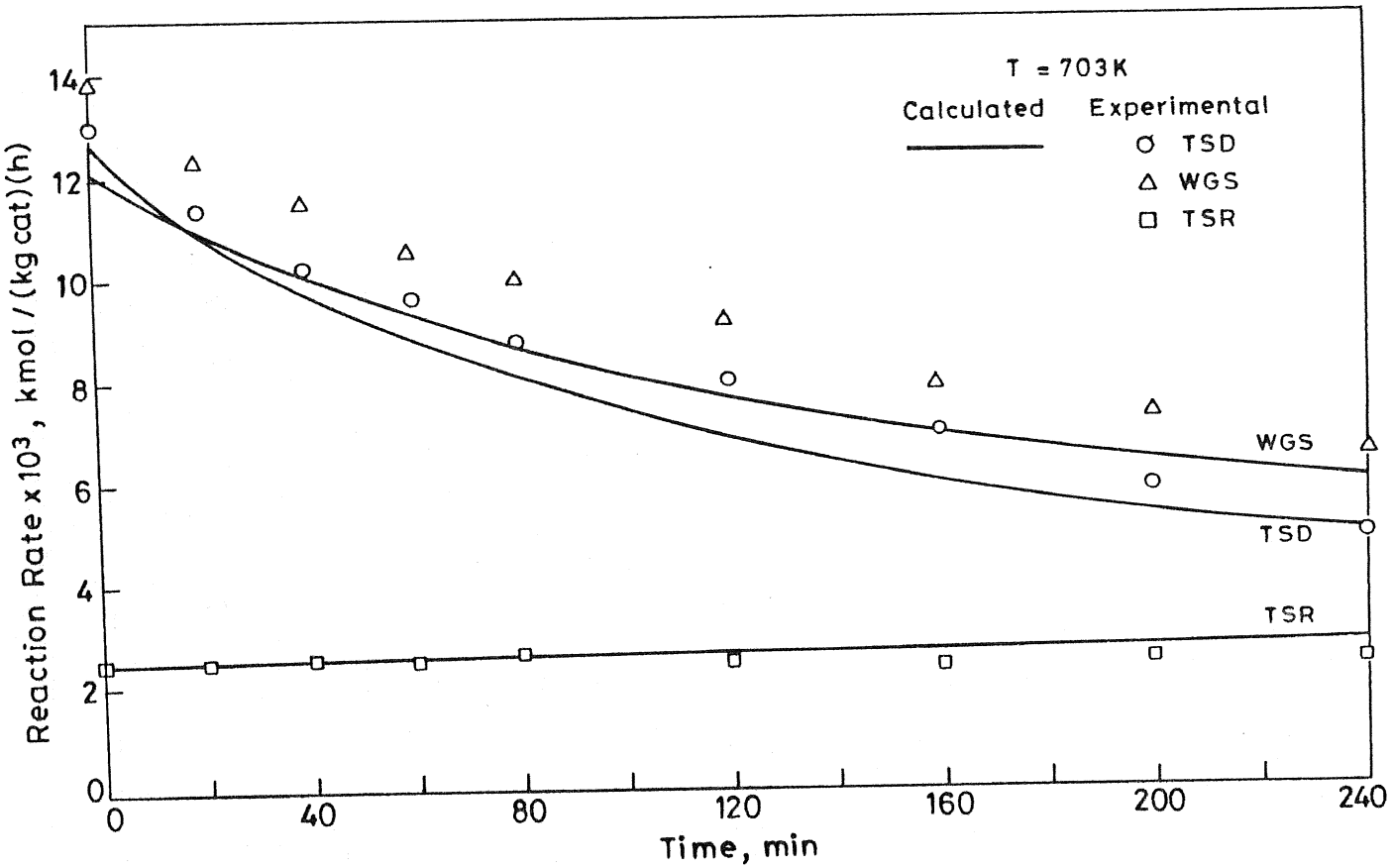

Fig. 4.45 Comparison between calculated and experimental results for diffusion influenced pellets (catalyst size: 3.2 x 3.2 mm, run no. N5)

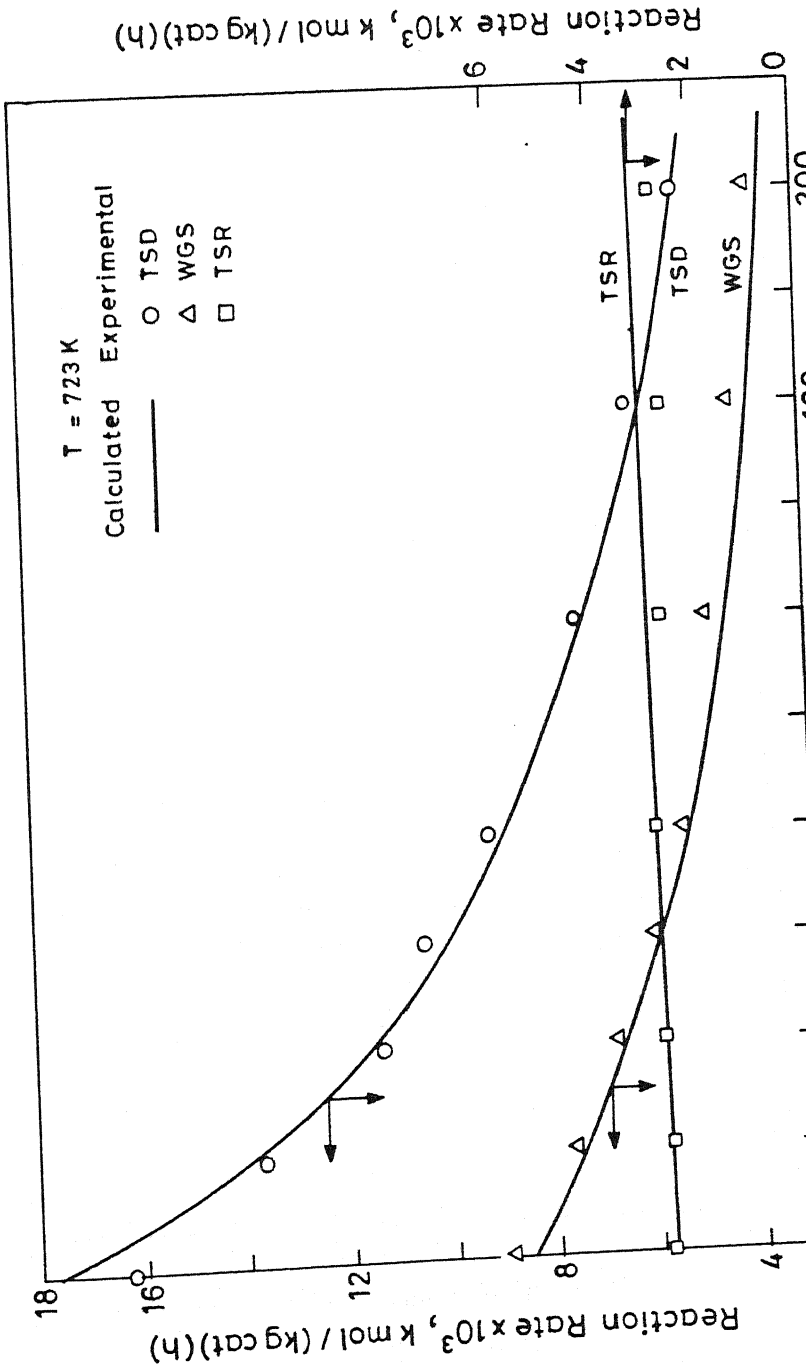

Fig. 4.46 Comparison between calculated and experimental results for diffusion influenced pellets (cat. size: 3.2 x 3.2 mm, run no. 06)

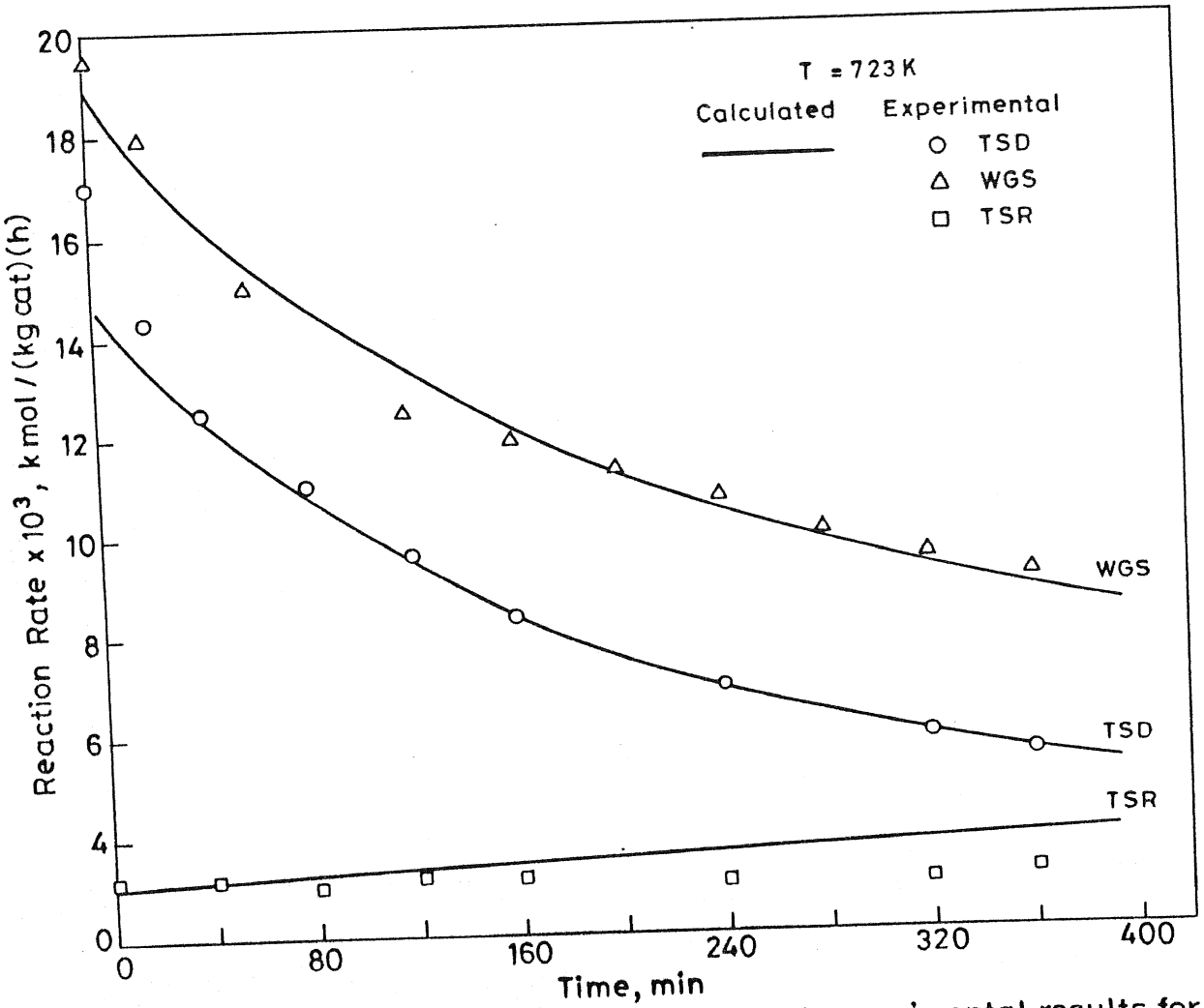

Fig. 4.47 Comparison between calculated and experimental results for diffusion influenced pellets (cat. size : 3.2 x 3.2 mm, run no. 03)

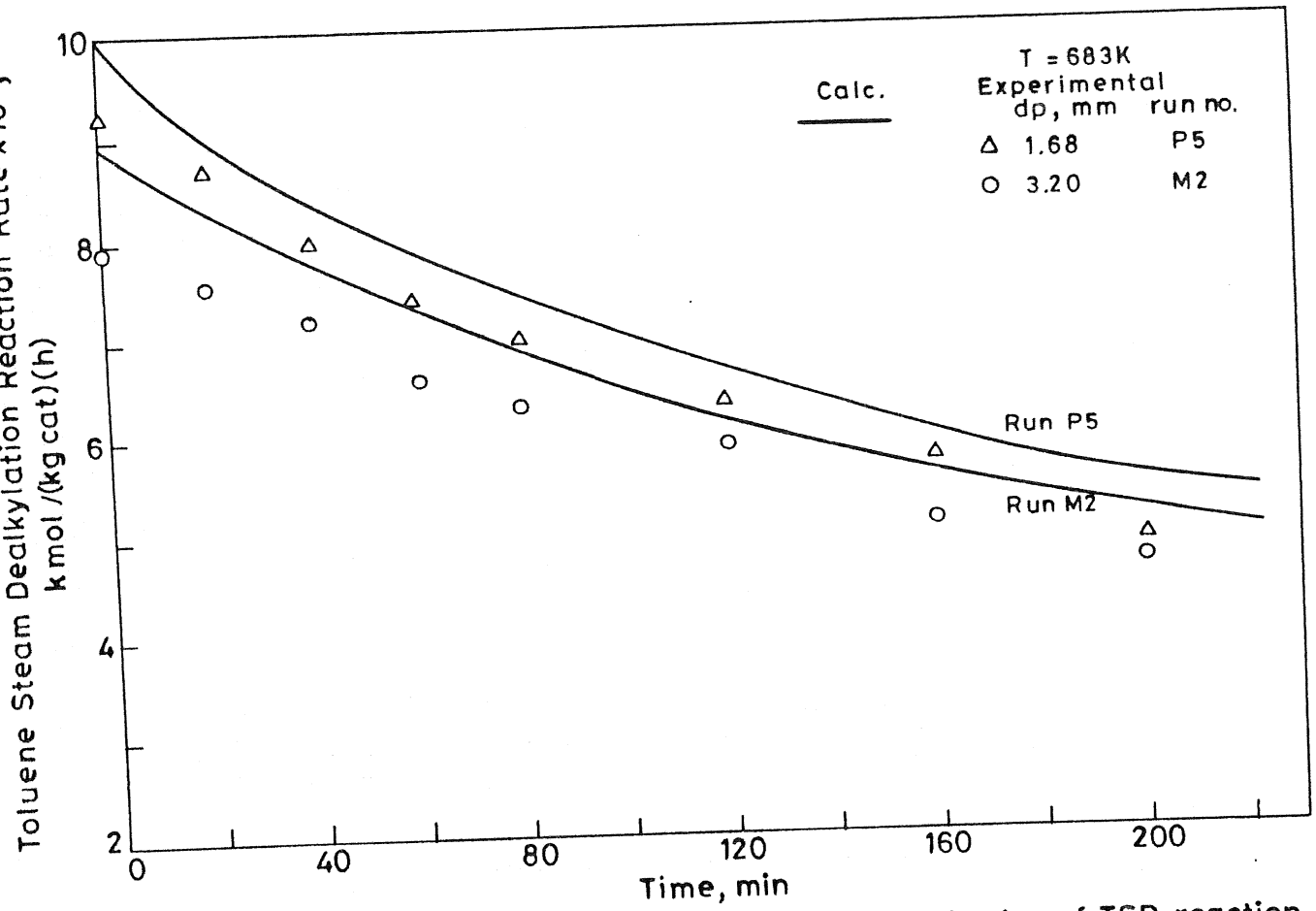

Fig. 4.48 Comparison of calculated and experimental rates of TSD reaction at different catalyst sizes.

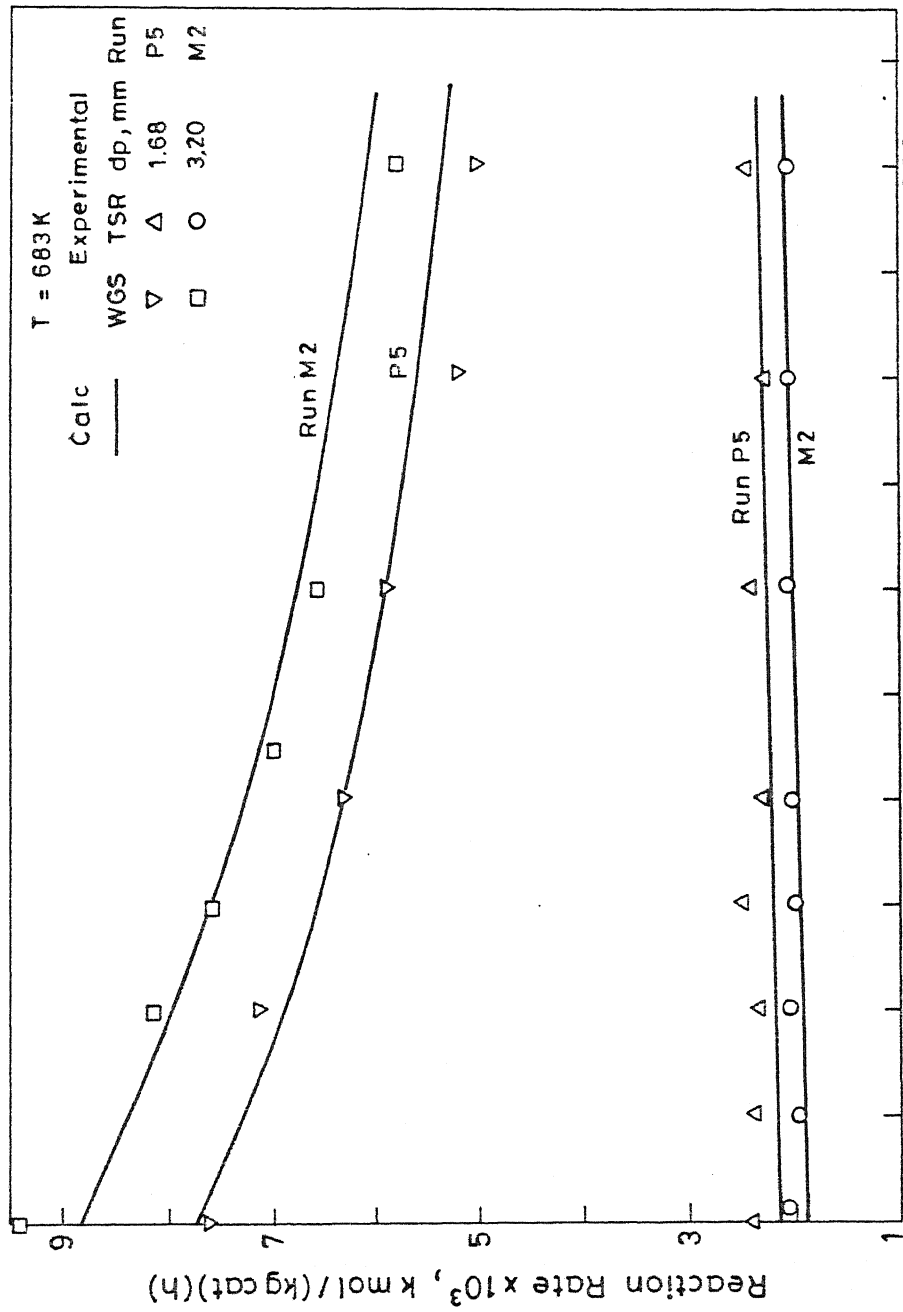

Fig. 4.49 Comparison of calculated and experimental rates of TSR and WGS reaction at different catalyst sizes.

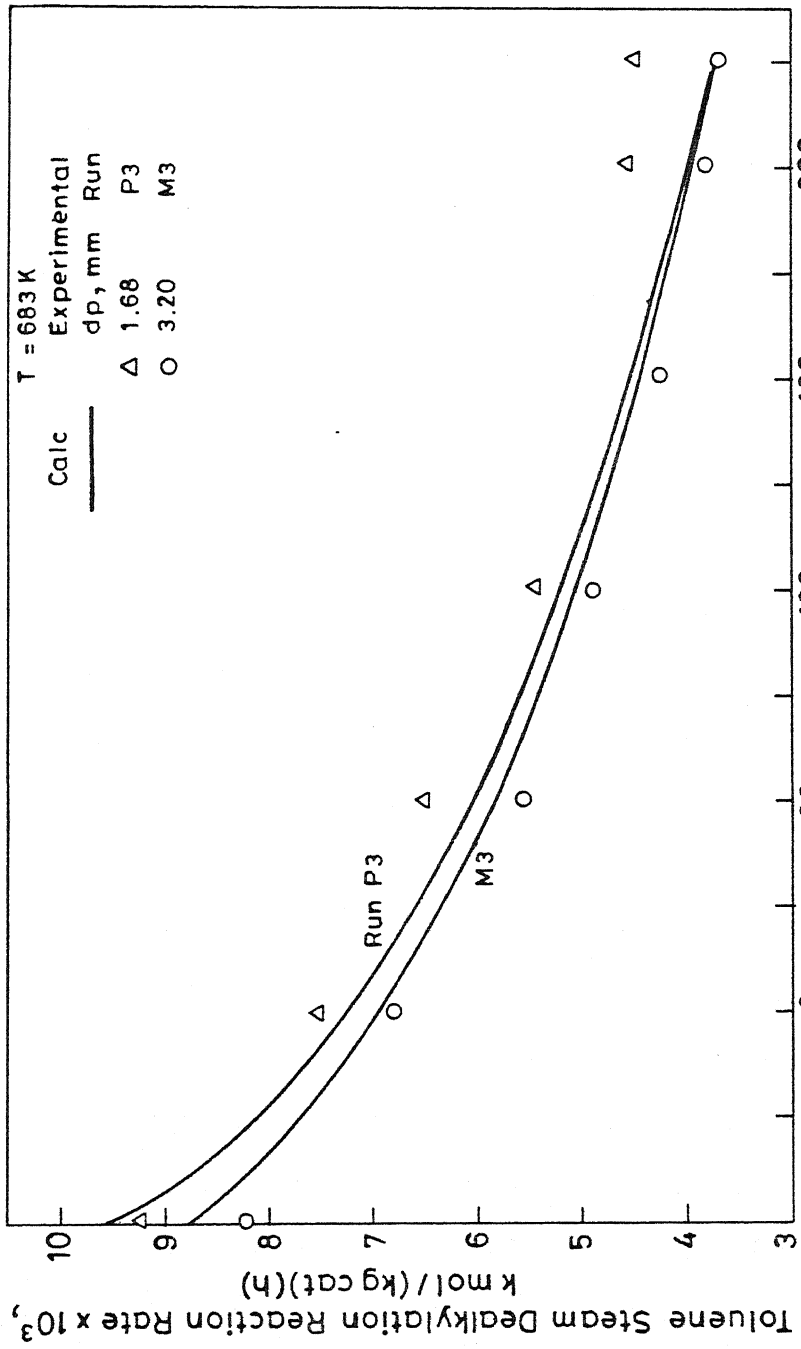

Fig. 4.50 Comparison of calculated and experimental rates of TSD reaction at different catalyst sizes.

of toluene steam dealkylation reaction was higher for the smaller size catalyst. In contrast, the rate of water gas shift reaction was higher for the larger size catalyst (Figs. 4.49 and 4.51). This is also in agreement with the experimental findings. The rate of water gas shift reaction is mainly dependent on the partial pressures of carbon monoxide and water and due to diffusional resistances, the partial pressure of CO is higher and that of water lower in the pellet. The data and model calculations suggest that for the intermediate size catalyst (1.68 mm) the combination of carbon monoxide and water partial pressures results in this behavior.

4.5.5 Model Sensitivity

In the model equations presented above, the effective diffusivity of the various components were not measured at the reaction conditions and therefore, the values used in the model, could be different from the actual values. To check the sensitivity of the model results, the effective diffusivities of the water, toluene and carbon monoxide were varied and the average rates recomputed. For this analysis, the effective diffusivity of only one component was varied at a time, keeping the other D_{eff} at the values computed using equation (4.78). The effect of increasing or decreasing $D_{eff,W}$ on the rates of TSD,TSR and WGS reactions for the same set of conditions is shown in Figures 4.52 and 4.53 . It should be mentioned that the values of $D_{eff,W}$ calculated using eqn. (4.78) was 0.146 m^2/h at 703 K. As shown in these figures,although onincreasing $D_{eff,W}$, the average reaction rates of the three reactions were higher, the percentage change in the average reaction rates on changing $D_{eff,W}$ by a factor of 4 was less than 2 %. With increasing $D_{eff,W}$, the rate

of deactivation of toluene steam dealkylation was also affected, especially for run times of less than 1 h. The effect of changing $D_{eff,T}$ on the average rates of the three reactions is shown in Figures 4.54 and 4.55 . As shown in these figures, with increasing $D_{eff,T}$, the average reaction rates for toluene steam dealkylation and toluene steam reforming reactions increased whereas the water gas shift reaction rate decreased. The increase in the TSD and TSR rates was marginal whereas the decreasein the water gas shift reaction rate was more pronounced. The decrease in water gas shift reaction rate is due to the inhibition of the intrinsic reaction rate with increasing partial pressure of toluene.

The effect of varying $D_{eff,CO}$ on the rates of the three main reactions is shown in Figures 4.56 and 4.57. With increasing $D_{eff,CO}$, the average reaction rates of toluene steam dealkylation and toluene steam reforming reactions increased whereas that of water gas shift reaction decreased. The increase in TSR rate was marginal compared to the increase in TSD reaction rate. However , the decrease in water gas shift reaction rate was significant (approximately, 17 %).

Form the analysis, it can be concluded that, this model is not very sensitive to changes in the effective diffusivities of the reactants but appreciable changes can take place due to change in the effective diffusivity of carbon monoxide.

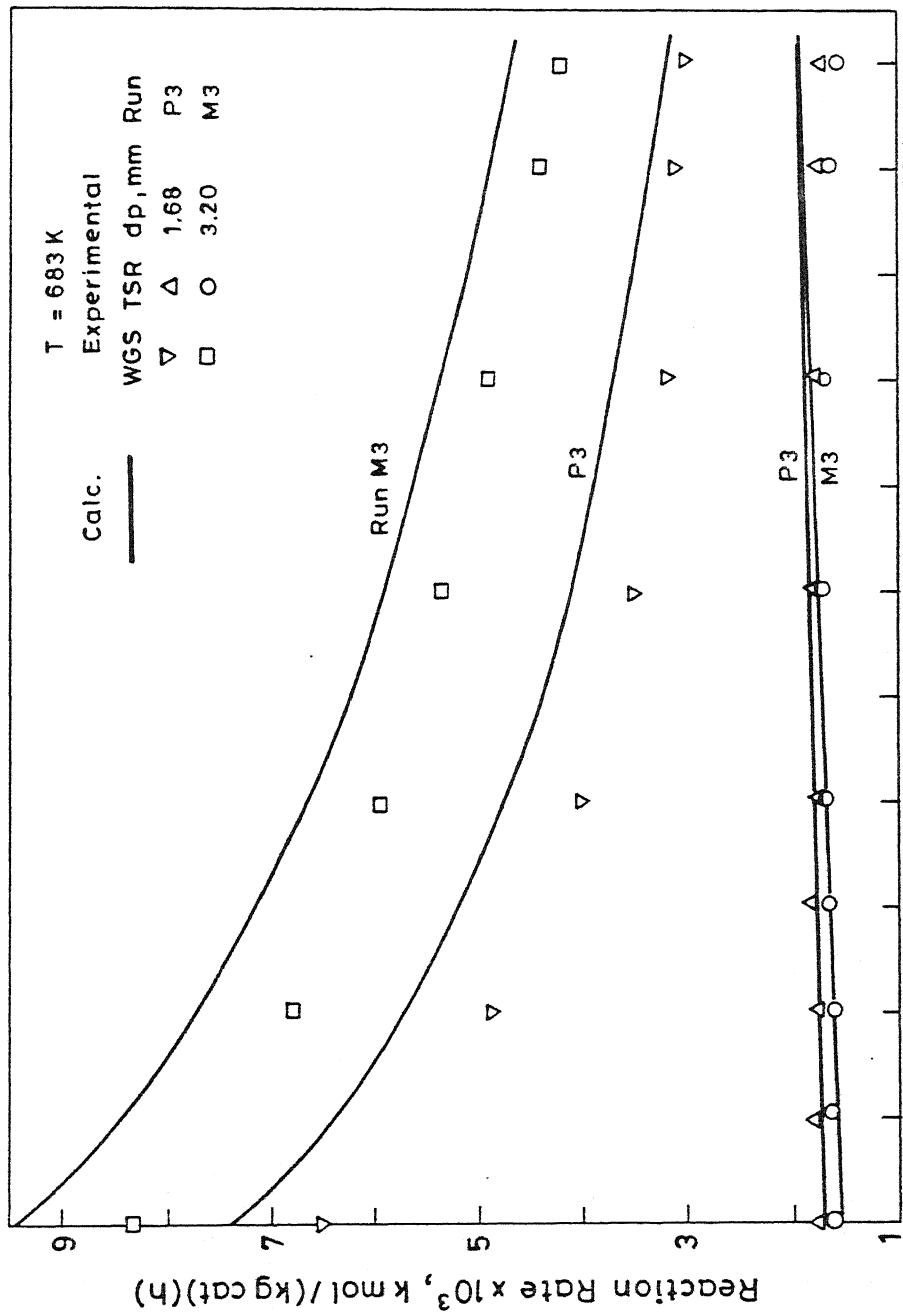

Fig. 4.51 Comparison of calculated and experimental rates of TSR and WGS reactions at different catalyst sizes.

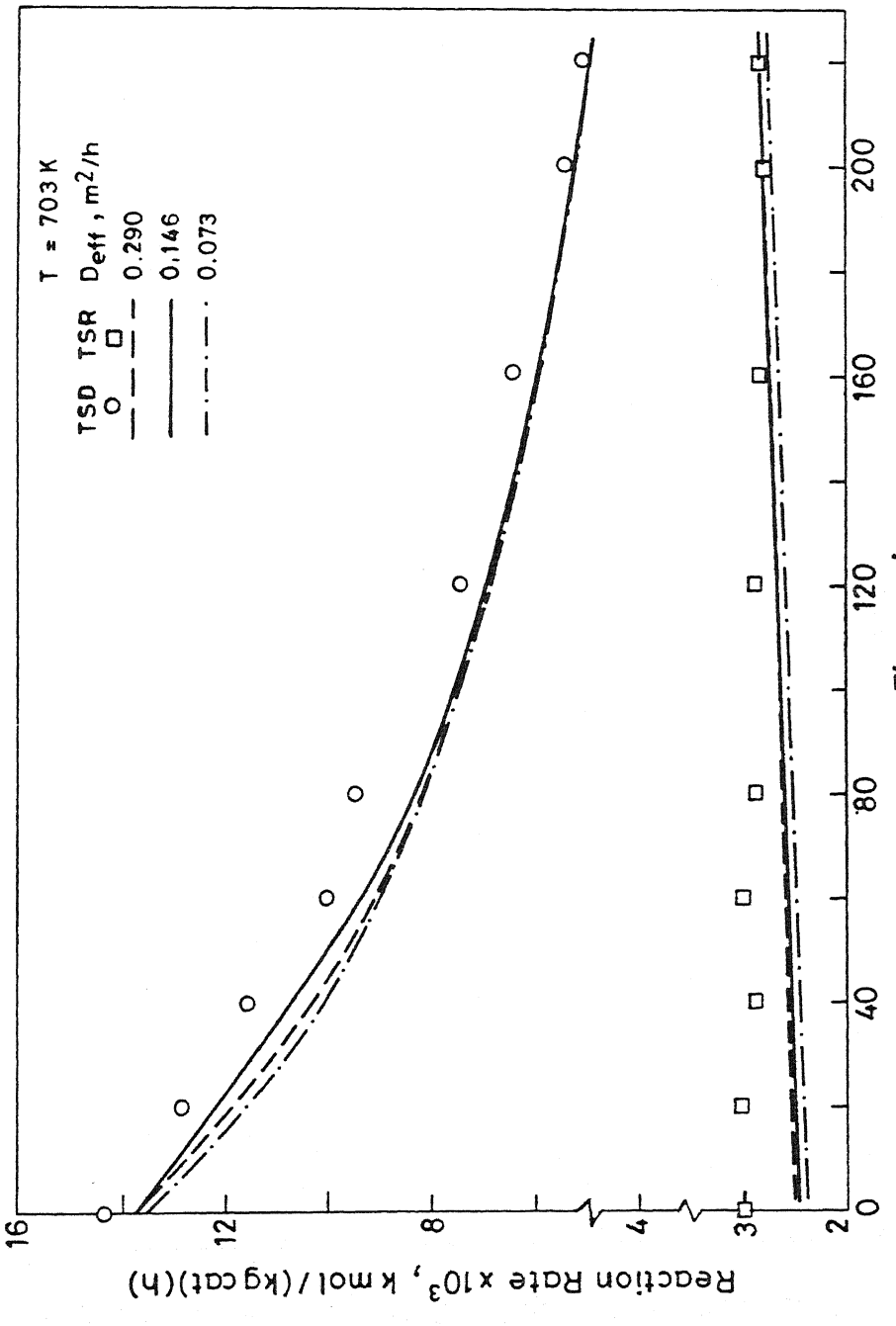

Fig. 4.52 Effect of diffusivity of water on TSD and TSR reaction (run: N6)

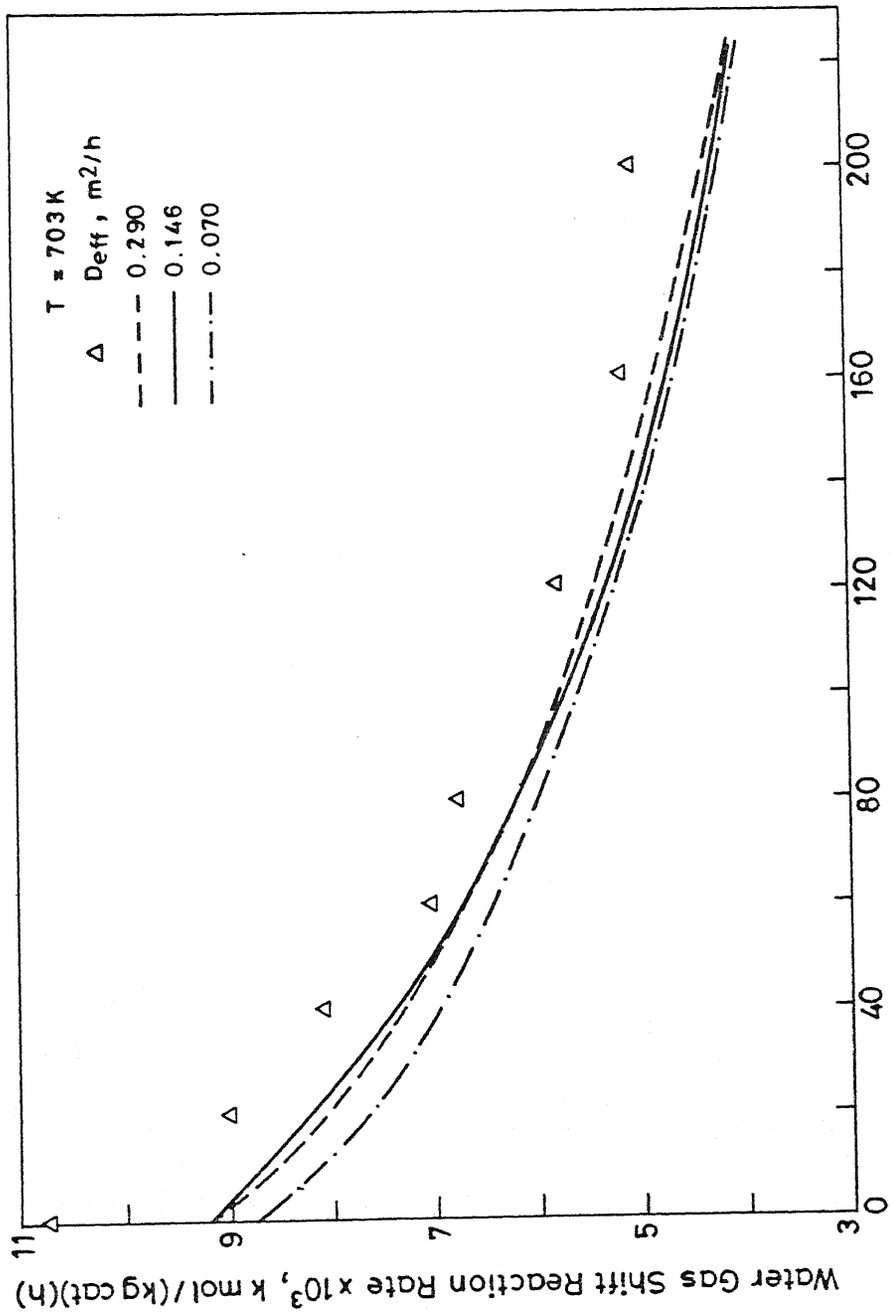

Fig. 4.53 Effect of diffusivity of water on water gas shift reaction (run: N6)

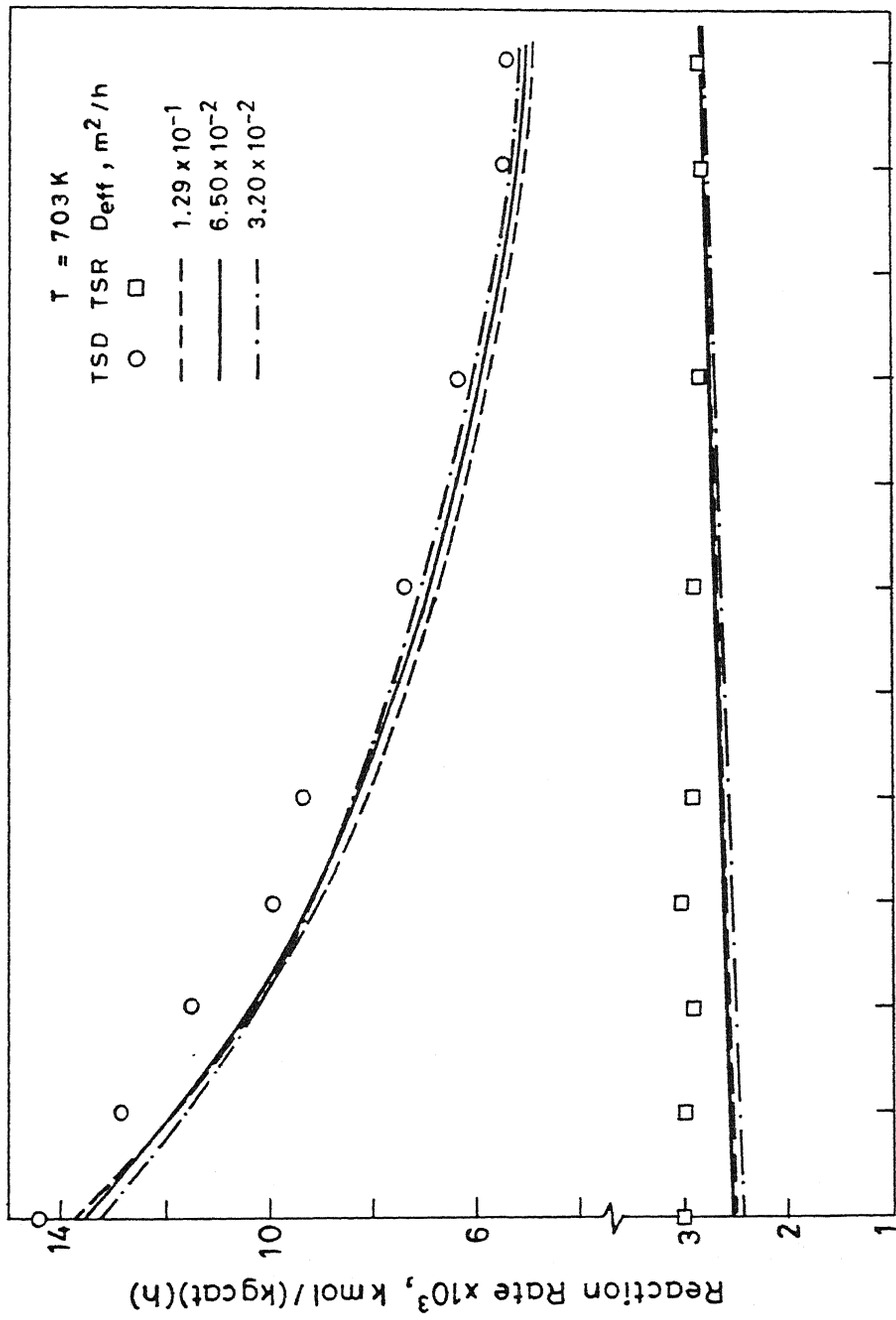

Fig. 4.54 Effect of diffusivity of toluene on TSR and TSD reactions (run: N6)

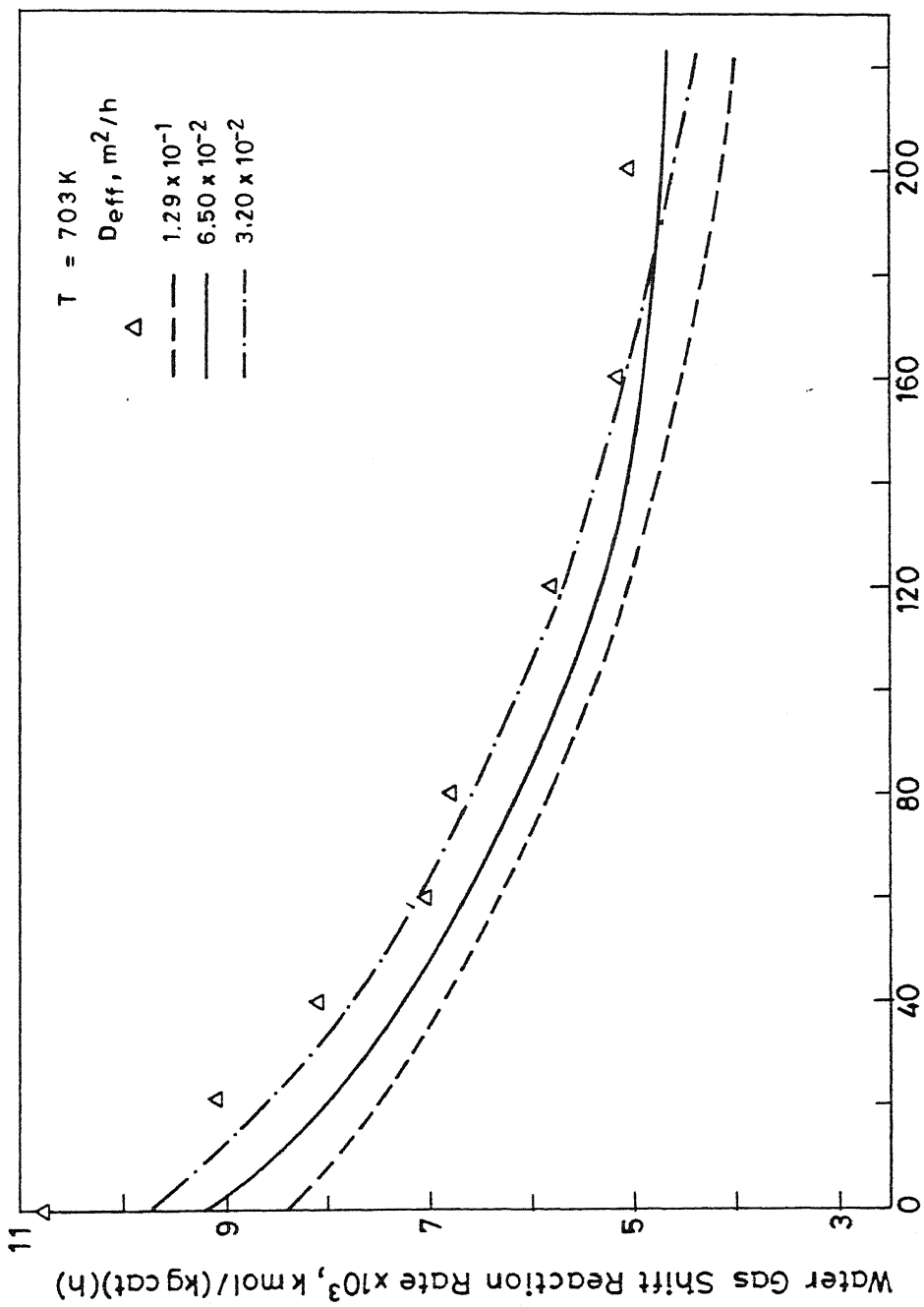

Fig. 4.55 Effect of diffusivity of toluene on water gas shift reaction (run: N6)

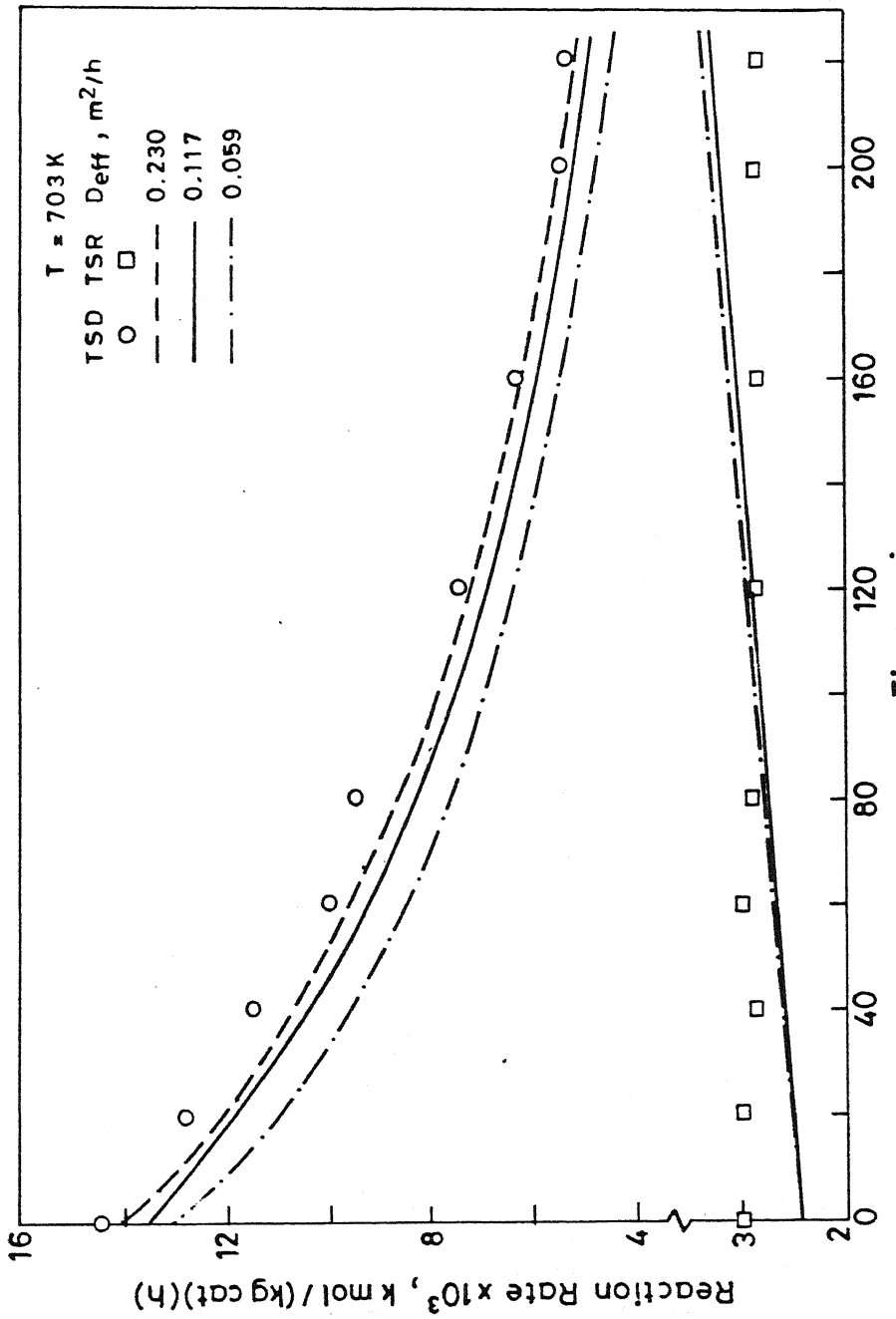

Fig. 4.56 Effect of diffusivity of carbon monoxide on TSD and TSR reactions (run: N6)

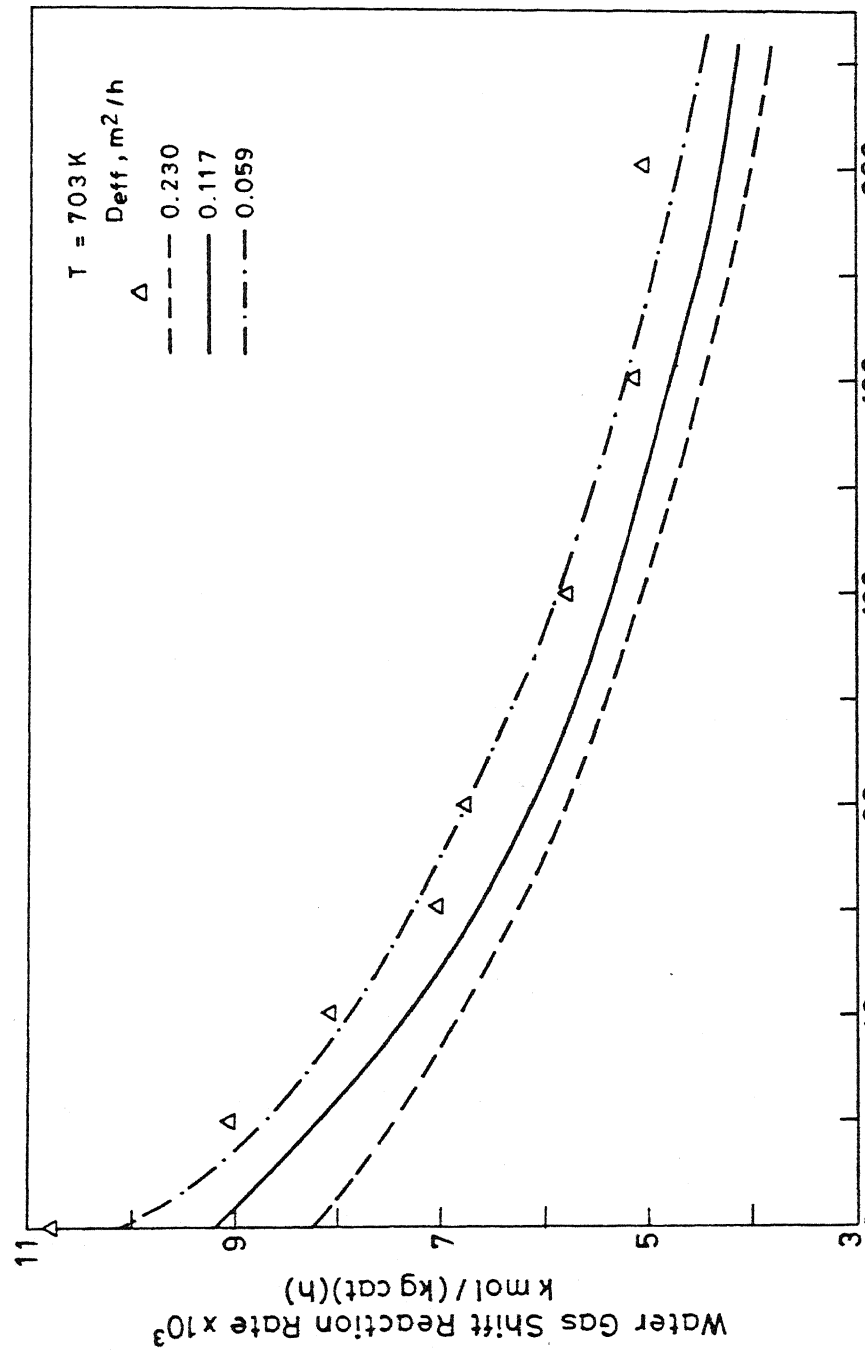

Fig. 4.57 Effect of diffusivity of carbon monoxide on water gas shift reaction (run no. N6)

Chapter 5

CONCLUSION AND RECOMMENDATIONS

5.1 CONCLUSIONS

From this study,it can be concluded that the water/toluene reaction over Rh/γ-Alumina catalyst could be satisfactorily represented by the following three reactions

$$C_6H_5CH_3 + H_2O \longrightarrow C_6H_6 + CO + 2H_2$$

$$C_6H_5CH_3 + 7H_2O \longrightarrow 7CO + 11H_2$$

$$CO + H_2O \rightleftharpoons CO_2 + H_2$$

The intrinsic rates of these reactions on a fresh catalyst can be modeled using Langmuir-Hinshelwood rate expressions based on the assumption that water and toluene adsorb on different types of active sites. The model for toluene steam dealkylation which gave the best fit assumes that the rate controlling step is the surface reaction of adsorbed water and adsorbed toluene. On the other hand, the model for the intrinsic kinetics of water gas shift reaction was derived assuming the controlling step was the transport and adsorption of the intermediate from the support site adjacent to the metal site . The intrinsic kinetics for the 3 reactions could be modeled as follows:

$$R_1^o = \frac{k_1 K_T K_W p_T p_W}{(1 + K_W p_W)(1 + K_T p_T + K_{CO}^2 p_{CO} + 1.7 p_R)}$$

$$R_2^o = \frac{k_2 K_T' K_W' P_T P_W^2}{(1 + K_W' P_W)(1 + K_T' P_T + K_{CO}' P_{CO} + 0.32 P_R)}$$

$$R_3^o = \frac{k_3 K_W' K_{CO}' (P_{CO} P_W - P_H P_{C/K})}{(1 + K' P_W)(1 + K_T P_T + K_{CO} P_{CO} + 0.32 P_R)}$$

The catalyst activity decreased with run time due to coke deposition. The deactivation kinetics of this complex system could be represented using aselective deactivation modelThe toluene steam reforming reaction showed a constant activity with run time.

$$-\frac{da_1}{dt} = \frac{k_{d1} P_{CO} + k_{d2}(P_T + P_B)}{(1 + K_W'' P_W)} a_1^2$$

$$-\frac{da_2}{dt} = 0$$

$$-\frac{da_3}{dt} = (k_{d3} P_{CO} \cdot P_W + k_{d4}(P_T + P_B)) a_3^2$$

The experimentally measured rates for diffusion-influenced catalysts could be satisfactorily predicted using a one-dimensional pseudo-steady state isothermal model. The experimental results as well as the calculated rates showed that the rate of toluene steam dealkylation and toluene steam reforming reactions increased as the catalyst pellet size was reduced. in contrast, the water gas shift reaction exhibited an opposite effect. In conclusion, this pellet model together with the intrinsic kinetics of the main and deactivation reations determined in this study, can be used to predict the effect of diffusion in this complex reaction.

5.2 RECOMMENDATIONS

The following recommendations are made for further study:

1) attempts should be made to measure the coke profiles in the catalyst pellet and correlated it with the catalyst activity.

2) the deactivation kinetics of toluene steam reforming reaction need to be investigated in more detail since at a temperature of 723 K, the reaction rate showed a slight decrease with run time, while this was not observed at the lower temperatures.

3) the effect of total pressure on the reaction rates should be investigated.

4) efforts should be made to operate the Berty reactor such that only one exit partial pressure can be varied at a time.

REFERENCES

Al-Alyed, O.S. and Kunzru,D., "Cyclohexane Dehydrogenation on a Nickel Catalyst: Kinetics and Catalyst Fouling", J.Chem.Tech. Biotechnol 1988,**43**,23.

Albright,L.F.and Baker,R.T.K.,"Coke Formation on Metal Surfaces", ACS Symposium Series,No. 202, Amer.Chem.Soc., Washington, 1982.

Amenomiya,Y.," Active Sites of Solid Acidic Catalyst. II Water Gas Conversion on Alumina and some other Catalyst," J.Catal.,1979,**57**,64.

Amenomiya,Y.," Active Sites of Solid Acidic Catalysts.III Infrared Study of the Water Gas Conversion Reaction on Alumina," J.Catal., 1978,**55**,205.

Aris,R. "The Mathematical Theory of Diffusion and Reaction in Permeable Catalysis",Clarendon Press,Oxford, 1975.

Appleby,W.G.,Gibbson,J.W andGood,G.M.,"Coke Formation in Catalytic Cracking "Ind.Eng.Chem.Proc.Des.Dev. 1962,**1**,102-115.

Baker,R.T.K,and Chludzinski,J.J., "Filamentous Carbon Growth on Nickel-Iron Surfaces : The Effect of Various Oxide Additives," J. Catal. 1980,**64**,464-478.

Bakulin,M.N.,Levinter,M.E. and Unger,P,"Composition of Products from Condensate During Reforming," Int.Chem. Eng. 1978, **18**, 89.

Barbier,J.,Marecot,P.,Martin,N.Elassal,L.and Maurel,R.,"Selective Poisoning by Coke Formation on Pt/Al_2O_3",in Catalyst Deactivation Editors, Delmon, B. and Froment, G. F.,1980, Elsevier,Amsterdam.

Bartholomew,C.H.," Carbon Deposition in Steam Reforming and Methanation," Catal. Rev. Sci.Eng. 1982,**24**,67-75.

Bartholomew,C.H.,"Catalyst Deactivation,"Chem.Engg.,1984,**12**,96-112

Berty,J.M.," Reactor for Vapor-Phase Catalytic Studies," Chem.Eng. Prog.,1974,**70**,78-84.

Bell,A.T,"Catalyst Deactivation ", Chemical Industries Ser. Vol. 30 Chapt.9, Editors, Petersen E.E. and Bell A.T., 1987.

Beltrame,P.,Freio,L.,Forni,L. and Torrazza,S.,"Activity of Various Supported Rh Catalyst for Toluene Steam Dealkylation",J.Catal., 1979,**60**,472-475.

Beltrame,P.,Ferino,I.,Maronglu,B. and Torrazza.S.,"Kinetics and Products Inhibition Effect in Toluene Steam Dealkylation over $Rh/-Cr_2O_3/\gamma-Al_2O_3$,",Ind.Eng.Chem.Process Des.Dev., 1984, **23**, 176-179.

Bernardo, C.A., and Lobo,L.S., "Kinetics of Carbon Formation From a Cetylene and 1-Butene on Cobalt", in Catalyst Deactivation,

Editors,Delmon,B and Froment,G.F.,Elsevier,Amsterdam. 409,1980.

Beuther,H.,Larson,O.H. and Perrotta,A.J.,"The Mechanism of Coke Formation on Catalysts",in Catalyst Deactivation, Editors, Delmon, B. and Froment,G.F., Elsevier,Amsterdam,1980.

Blanding,F.G.,"Reaction Rates in Catalytic Cracking of Petroleum. Ind.Eng.Chem. 1953,45,1186-1193.

Blue,R.W. and Engle,C.J.,"Hydrogen Transfer Over Silica-Alumina Catalysts,",Ind.Eng.Chem.,1951,43,494-501.

Bridger,G.W., in Catalyst Handbook, Wolf Scientific Books,1970.

Brown,K.,"Numerical Solution of System of Nonlinear Algebriac Equations",Byrne,G.D.and Hall,C.A.,Editors. Academic ,NY,1973

Butt J.B.,"Catalyst Deactivation", Adv.Chem.Ser. 1972,109,359-465

Butt,J.B., Delgado-Diaz, S. and Muno,W.K., " Effect of Coking on the Transport Properties of H-Mordenite," J.Catal. 1975,37,158-165

Butt,J.B.,Watcher,C.K. and Billimoria,R.M.," On The Separability Of Catalytic Deactivaiton Kinetics," Chem. Eng. Sci. 1978,33, 1321-1329.

Butt,J.B.,"Catalysis Science and Technology", Vol,6, Editors,

J.R.,Anderson and Boudart,M., Springer-Verlag, 1984.

Campbell,D.R., and Wojciechowski,B.W., "Theoretical Patterns of Selectivity in Aging Catalyst wiht Special Reference To the Catalytic Cracking of Petroleum,"Can.J.Chem. Eng.,1969,47,413-417.

Carberry,J.J.," Yield in Chemical Reactor Engineering," Ind. Eng.Chem. 1966,58,40-47.

Carberry,J.J., and Gorring ,R.L.,"Time-Dependent Pore Mouth Poisoning of Catalysts," J.Catal. 1966,5,529-534 .

Carberry,J.J., "Chemical and Catalytic Reaction Engineering",Mc-Graw-Hill Book Company,1976.

Carbucicchio,M.,Forzatti,P., Trifiro,F.,Tronconi,E. and Villa,P.L. " Deactivation of Silica Supported Fe_2O_3-MoO_3 Catalyst For The Oxidation of Methanol", in Catalyst Deactivation ,Editors, Delmon,B. and Froment.G.F.,Amsterdam 1980.

Cooper,B.J., Trimm, D.L., " The Coking of Platinum/Alumina Reforming Catalysts,", in Catalyst Deactivation ,Editors, Delmon,B. and Froment.G.F.,Amsterdam 1980.

Corella,J.and Asua,J.M.,"Kinetics of the Deactivation of a 10% Cu-0.5% Cr_2O_3/Asbestos Catalyst for Benzyl Alcohol Dehydrogenation " Chem.Eng.Sci. 1980,35,1447-1449.

Corella,J.and Asûa J.M., "Kinetics of Deactivation of a Solid Catalyst ina Nonsimple Reaction. Isobutene Oxidation in Gaseous Phase by a Parallel Reaction Network"Ind. Eng. Chem. Proc.Des.Dev. 1982,**21**,551-558.

Corella,J. and Asua,J.M.,"Kinetic Equations of Mechanistic Type with Nonseparable Variables for Catalyst Deactivation by Coke. Models and Data Analysis Methods", Ind. Eng. Chem. Proc.Des.Dev. 1982,**21**,55-61.

Corella,J.and Asûa J.M.,"Kinetics and Mechanism of Deactivation by Fouling of a Silica-Alumina Catalyst in the Gaseous Phase Dehydration of Isoamyl Alcohol",Can.J.of Chem.Eng. 1981, **59**, 506-510.

Corella,J.,Aznar,P.M. and Bilbao,J."Kinetics of Inseparable Variables in Catalyst Deactivation due to Blockage of Active Centers by Coke Produce by a Parallel Reaction. Mechanism and Method of Data Analysis," ,Int.Chem.Engg.,1985a,**25**,275-282.

Corella,J.,Bilbao,R.,Mollna,J.A., and Artigas,A., "Variation with Time of the Mechanism,Observable Order, and Activation Energy of the Catalyst Deactivation by Coke in the FCC Process," Ind.Eng.Chem.Process.Des.Dev. 1985b,**24**,625-636.

Corella,J., Monzon,A., Butt,J.B. and Absil,R.P.L., The Modeling of the Kinetics of Deactivation of a Commercial Hydrocracking Catalyst in the Reaction of Cumene Disproportionation", J. Catal. 1986,**100**,149-157.

Corella,J.,Fernandez,A.,and Santamaria,J.," Effect of the Kinetic Parameters of Catalyst Deactivation on The Variation of The Product Distribution With Time-On-Stream,"An.Quim.,1988,**84**,192-204

Corella,J.,Morales,F.G.,Provost,M.,Espinosa,A. and Serano,J., "The Selective Deactivation Kinetic Model Applied to The Kinetics of The Catalytic Cracking (FCC Process)",Inter.Conf. on Adv.In Chem. Eng., I.I.T., Kanpur,1989.

Davis,G.O.,"Coal Refining by Solvent Extraction and Hydrocracking" Chem.and Ind. 1978,560-571.

dePauw,R.P.and Froment,G.F.,"Deactivation of a Platinum Reforming Catalyst in a Tubular Reactor"Chem.Eng.Sci. 1975,**30**,789-801.

Dictor, R., " A Kinetic Study of the Water-Gas Shift Reaction Over Rh/Al_2O_3 Catalysts,", J.Catal., 1987,**106**,458-463.

Dixon,A.G. and Cresswell,D.L.,"Model Reduction for Two-Dimensional Catalyst Pellets with Complex Kinetics,",Ind.Eng.Chem.Res.,1987, 26,2306-2312.

Dumez,F.J.and Froment,G.F., " Dehydrogenation of 1-Butene into Butadiene Kinetics.Catalyst Coking and Reactor Design," Ind. Eng. Chem.Proc. Des.Dev. 1976,**15**,291-301.

Duprez,D.,Prerira,P.,Miloudi,A.and Maurel,R.,"Steam Dealkylation of Aromatic Hydrocarbons. Role of the Support and Kinetic Pathways of

Oxygenated Species in Toluene Steam Dealkylation over Group VIII Metal Catalysts," J.Catal. 1982,75,151-163.

Duprez,D.,Miloudi,A, and Tournayan,L.," New Evidence for The Support Effects in Toluene Steam Dealkylation of Toluene on Rhodium Alumina-Chromia Catalysts,"Appl.Catal. 1985a,14,333-342.

Duprez,D.,Mendez,M. and Little,J., "Evaluation of a Method for Characterizing Coked and Sulfided Rh/Al $_2$O$_3$ Catalysts: Study of the Space and Time Dependence of Sulfur Deposition on Rh/Al$_2$O$_3$ in Toluene Steam Reforming," Appl.Catal. 1986,27,145-160.

Dydykina,G.V.,Rabinovich,G.L. and Maslyankii,G.N.," Determination of The Composition of Products of Catalytic Demthylalkylation of Toluene," Kinet.Katal. 1972,14,57.

Eberly,P.E., Kimberlin,C.N., Miller,W.H. and Drushel,H.V., "Coke Formationn on Silica-Alumina Cracking Catalyst,"Ind. Eng.Chem. Proc.Des.Dev. 1966,5,193.

Forni,L.,Ferino,I.,Bruno,M. and Torrazza,S., "Activity and Structure ofRh/Cr$_2$O$_3$ Catalystfor Toluene Steam Dealkylation," J.Catal. 1984,85,169.

Francis,P.D.," Catalytic Steam Dealkylation of Alkyl Phenols," J. Catal. 1980,61,528-532.

Froment,G.F. and Bischoff,K.B.,"Non-steady State Behavior of Fixed Bed Catalytic Reactors Due to Catalyst Fouling,"Chem.Eng.Sci. 1961,16,189.

Froment,G.F. and Bischoff,K.B., Chem. Eng. Sci. 1962,17, 105

Froment,G.F. and Bischoff,K.B.,"Chemical Reactor Analysis and Design", J.Wiley, New York, 1979.
Froment,G.F.,"A Quantitative Approach of Catalyst Deactivation by Coke Formation," Proceeding of the International Symposium on Catalyst Deativation, Antwerp, 1980,1-18,Editors, Delmon,B., Froment, G.F, Elsevier,Amsterdam. 1980.

Froment,G.F.," The Kinetics of Complex Reactions,", Chem. Eng. Sci.,1987,45,1073-1087.

Gavalas,G.R.,"Fixed Bed Reactor With Regenerative Cooling ",Ind. Eng. Chem.Fundam.,1971,10, 71-74.

Grenoble,D.C.,"The Chemistry and Catalysis of the Water/Toluene Reaction. 1. The Specific Activities and Selectivities of the Group VIII Metals Supported on Al$_2$O$_3$," J.Catal. 1978,51,203-211.

Grenoble,D.C.,"The Chemistry and Catalysis of the Water/Toluene Reaction. 2. The Role of Support and Kinetic Analysis," J. Catal. 1978b,51,211-220.

Grenoble ,D.C.,Estadt,M.M., and Ollis,D.F., " The Chemistry and Catalysis of the Water Gas Shift Reaction. ,1. The Kinetics over Supported Metal Catalysts,"J.Catal.,1981,67,90-102

Hatcher,W.J.J.,"Cracking Catalyst Deactivation Models," Ind.Eng. Chem.Prod.Res.Dev., 1985,24,10-15.

Haldeman,R.G.,and Botty,M.C.,"On The Nature of The Carbon Deposit of Cracking Catalysts," J.Phys. Chem. 1959, 63, 489-498.

Hegedus,L.L. and McCabe, R.W., "Catalyst Poisoning,",in Catalyst Deactivation.,1980, Editors,Delmon, B. and Froment G.F.

Hosten,L.H.,Froment,G.F.," Isomerization of n-Pentane,", Ind. Eng. Chem. Proc.Des.& Dev.,1971,10,280-293.

Hughes,R.,"Deactivation of Catalysis",Academic Press,London, 1984.

Jacob S.M., Gross,B., Voltz S.E. and Weekman, V.W.,"A Lumping and Reaction Scheme For Catalytic Cracking",A.I.Ch.E.J,1976,22,701-713

Jodra,L.G.,Romero,A. and Corella,J., " Kinetics of The Catalytic Dehydrogenation of Benzylalcohol," An.Qium. 1976,72,823.

John, T. M., Pachovsky, R. A. and Wojciechowski, B. W.," Coke and Deactivation in Catalytic Cracking". Adv.Chem.Ser. 1974,133,422.

Jossens,L.W. and Petersen,E.E.," A Novel Reactor System That Permits The Direct Determination of Deactivation Kinetics for Heterogeneous Catalyst,", J.Catal., 1982a,73,366-376.

Jossens,L.W. and Petersen, E.E., " Fouling of a Platinum Reforming Catalyst a Ccompanying The Dehydrogenation of MethylCyclohexane," J.Catal., 1982b,377-387.

Kam,E.K.T.,Ramachandran,P.A. and Hughes,R.,"Isothermal Fouling of Catalyst Pellets," J.Catal.,1975,38,283-293.

Kam,E.K.T., Ramachandran,P.A.and Hughes,R., "The Effect of Film Resistances on The Fouling of Catalyst Pellets - I: Pseudo-Steady State Analysis,",Chem. Eng. Sci.,1977a,32,1307-1315.

Kam,E.K.T., Ramachandran,P.A.and Hughes,R.," The Effect of Film Resistances on The Fouling og Catalyst Pellets - II: Transient Analysis,",Chem. Eng. Sci.,1977b,32,1315-1325.

Khang,S.Z. and Levenspiel,O.," The Suitability of an nth Order Rate Form to Represent Deactivating Catalyst Pellet," Ind. Eng. Chem. Fundam., 1973,12,185.

Kim,C.J.,"Noble Metal Catalyzed Water-Hydrocarbon Reaction Paths," J.Catal., 1978,52,169.

Klugherz,P. and Harriott,P," Kinetics of Ethylene Oxidation on a Supported Silver Catalyst," A.I.Ch.E.J.,1971,17,856.

Kochloefl,K.,"Activity and Selectivity of Supported Noble Metals for Steam Dealkylation of Toluene" Proc.VIth.Int.Cong. Catal., London, The Chemical Society, II, 1976,.

Krishnaswamy,S. and Kittrel,J.R., " Diffusional Influences on

Deactivation Rates,"A.I.Ch.E.J. 1981,27,120-125.

Krishnaswamy,S. and Kittrel,J.R.,"Effect of External Diffusion on Deactivation Rates,"A.I.Ch.E.J., 1982,28,125-132.

Kumbilieva,K.,Kostyukovsky,M.M., Petrov,L. and Kiperman,S.L., "Joint Effects of Intraparticale Diffusion Resistance and Catalyst Deactivation,"in Catalyst Deactivation ,1987, Editors,Delmon,B.and Froment,G.F.,Elsevier Science Pub. Amsterdam., 1987.

Lambercht, G. C. N. and Froment, G. F., " Fouling of Platinum-Reforming Catalyst in Tubular Reactors,", Proc. 5th. Eur. Symp. on Chem. React. Eng.,Amsterdam,1972.

Langer,B.E. and Meyer,S.," The Mechanism of Coke Formation in The Reaction of Butadiene on a Calcined NaNH -Y,", in Catalyst Deactivation,Editors,Delmon,B.and Froment,G.F., 1980.

Lee,H.H., "Heterogeneous Reactor Design ", Butterworth Publishers, 1985.

Lee,J.W., Butt,J.B. and Downing,d.M.," Kinetic, Transport, and Deactivation Rate Interactions on Steady State and Transient Responses in Heterogeneous Catalysis," A.I.Ch.E.J.,1978,24,212-222

Lee,H.H,and Butt,J.B.,"Heterogeneous Catalytic Reactors Undergoing Chemical Deactivation," A.I.Ch.E.J,1982a.28,405-410.

Lee,H.H,and Butt,J.B.,Part II," Design and Analysis:Approach of Reactor Point Effectiveness," A.I.Ch.E.J,1982b.28,410-417.

Levenspiel,O.,Chemical Reaction Engineering.2nd edition, John Wiley,New york,1972.

Levinter,M.E., Panchenkov,G.M. and Taratarov,M.A., " Diffusion Factors in Coking Formation on a Silica-Alumina Catalyst,", Int. Chem. Eng.,1967,7,23-27.

Mahoney, J.M.," The Use of a Gradientless Reactor in Petroleum Reaction Engineering Studies ," J.Catal., 1974,32,247-253.

Marin,G.B. and Froment,F.G.," Reforming of C_6 Hydrocarbon on a Pt-Al_2O_3 Catalyst,".Chem. Eng. Sci. 1982,37,759-773.

Masamune,S. and Smith,J.M., " Performance of Fouled Catalyst Pellets," A.I.Ch.E.J., 1966,12,384-394.

McCarty,G.L and Wise J.S., " Hydrogenation of Surface Carbon on Alumina-Supported Nickel,",J. Catal.,1979, 57,406-416.

McLaughlin,K.W. and Anthony,R.G., "The Role of Zeolite Pore Structure During Deactivation by Coking," A.I.Ch.E.J., 1985, 31, 927-934.

Nemits G.S and Petersen,E.E,"Catalyst Fouling",in Catalyst Deactivation,Editors,Petersen, E.E. and Bell,A.T.,1987.

Deactivation,Editors,Petersen, E.E. and Bell,A.T.,1987.

Mills, G. A., Boedeker, E. R. and Oblad, A. G., " Chemical Characterization of Catalysts.I. Poisoning of Cracking Catalyst By Nitrogen Compounds and Potassium," J.Amer.Chem.Soc., 1950,**72**,1554

Mori,S. and Uchiyama,M., "Role of Urania as a Promoter of Support Rhodium in the Catalyzed Steam Dealkylation of Toluene," J.Catal. 1976,**42**,323-325.

Murakami,Y.K.,Hattori,T. and Masuda,M.," Effect of Intraparticle Diffusion on Catalyst Fouling",Ind.Eng.Chem.Fundam. 1968,**7**,599-605

Mori,S. and Maso,U.," Role of Urania as a Promoter of Supported Rhodium in the Catalyzed Steam Dealkylation of Toluene," J.Catal. 1976,**42**,323

Newson,E.J., " Catalyst Deactivation Due To Pore Pluging by Reaction Products," Ind.Eng. Chem.Proc. Des.Dev. 1975,**14**,27-33

Noda,H.,Tone,S. and Taok,O.J., " Kinetics of Isopentane Dehydrogenation on Chromia-Alumina Catalyst with Catalyst Fouling,"J.Chem. Engg.Japan 1974,**7**,110-116.

Onal,I. and Butt, J. B.," Kinetic Separability of Catalyst Poisoning," Proc. 7th. Int. Congr. Catalysis ,Tokyo,1981.

Ozawa,Y. and Bischoff,K.B., Coke Formation Kinetics on Silica-Alumina Catalyst,", Ind.Eng. Chem.Proc. Des.Dev.,1968,**7**,22-28.

Pachovsky,R.A., Best,D.A., Wojciechowski,B.W., " Application of The Time-on Stream Theory to Catalyst Decay", Ind. Eng. Chem. Proc. Des.Dev.,1973,**12**,254.

Parera, J.M., " Dehydration of MeOH Activity Centers of The Catalyst," J.Res.Inst.Hokkaido Univ.**16**,525.

Rabinovich,G.L.,Maslyankii,G.N. and Treiger,L.M., " Reaction Mechanism of Water Steam Alkylbenzene Dealkylation on The Group VIII Metal," Kinet.Katal.,1971,97-106 (pub. 1975) by Elsevier: Amsterdam.

Rabinovich, G.L.,Maslyanski G.N.,Vorobev,V.S. and Biryukova,L. "Demethylation of Toluene During Its Reaction With Water Vapor Under Pressure",Neftekhimiya, 1973,**13**,518-522.

Raddvic,L.R. and Vannice,M.A.," Sulfur Tolerance of Methanol Catalysts: Modeling of Catalyst Deactivation," ,Appl.Catal.,1987, 29,1-20.

Ramser,J.H.and Hill,P.B," Physical Structure of Silica-Alumina Catalysts", Ind.Eng.Chem.,1958,**50**,117-124.

Reid,R.C.,Prausnitz, J.M. and Sherwood,T.K.,"Properties of Gases and Liquids",3rd.Ed.,McGraw Hill Book Co.New York,1977.

Richardson,J.T.," Experimental Determination of Catalyst Fouling

Parameters", Ind.Eng.Chem.Proc.Des.Dev. 1972,**11**,8-14.

Romero,A., Bilbao,J. and Gonzalez-Velasco, J.R.," Calculation of Kinetic Parameters For the Deactivation of Heterogeneous Catalyst" Ind. Eng. Chem.Process Des.Dev.,1981,**20**,570-575.

Rostrup-Nielsen,J.,and Trimm,D.L.," Mechanism of Carbon Formation on Nickel Containing Catalysts," J.Catal.,1977,**48**,155-165.

Ruderhausen,C.G.,and Watson,C.C.," Variables Affecting Activity of Molybdena-Alumina Hydroforming Catalyst in Aromatization of Cyclohexane," Chem.Eng.Sci. 1954,**3**,110-121.

Sagara,M.,Masamune,S. and Smith,J.M., " Effect of Nonisothermal Operation on Catalyst Fouling," A.I.Ch.E.J.,1967,**13**,1226-1229.

Satterfield,C.N., "Mass Transfer in Heterogeneous Catalysis",M.I.T press Cambridge,Mass., 1970.

Schipper,P.H.,Graziani,K.R.,Choi,B.C.,Ramage,M.P.," The Extension of Mobil's Kinetic Reforming Model To Include Catalyst Deactivation," Proc. 8th.Int. Symp. Chem. React.Eng., Edingbuth 1984,p 33-44.

Solymosi, F., Erdohelyi,A. and Kocsis, M., " Surface Interaction Between H_2 and CO on Rh/Al_2O_3 Studied by Adsorption and Infrared Spectroscopic Measurements,", J. Catal., 1980, **65**,428-436.

Solymosi,F. and Pasztor,M., " Infrared Study of the Influence of CO on the Topology of Supported Rhodium,", J.Phys. Chem., 1985,**89**, 4789-4793.

Somorjai, G.A., and Blakely, D.W.,Nature,1975, **258**,580. Stejins,M. and Froment,G.F.,"Hydroisomerization and Hydrocracking. 3: Kinetic Analysis Rate Data for n-Decane and n-Dodecane,", Ind.Eng.Chem.Des.Dev.,1981,**20**,660.

Szepe,S. and Levenspiel,O.,"Proceedings Fourth European Syposium", Brussels,1968.

Takeuchi,M.,Ishige, T.,Fukumuro,T.,Kubota,H.,and Shindo,M. Kag.Kag. (Engl.ed.),1966, **4**,378.

Thiele,E.W., " Relation Between Catalyst Activity and Size of Particle," Ind.Eng.Chem.,1939,**31**,916.

Trimm,D.L.,"The Formation and Removal of Coke From Nickel Catalysts,"Catal.Rev.Sci,Eng. 1977,**16**,135-74.

Onuoha N.I.,"Copper Catalysts for The Hydrolysis of Acrylonitrile To Acrylamide: Deactivation and Cure",in Catalyst Deactivation, Editors,Delmon,B.and roment,G.F., Elsevier Science Publisher.

Trimm, D.L., " Catalyst Design for Reduced Coking,"Appl.Catal. 1983 ,**5**,263-290.

Uchida,S.,Osuda,S. and Shindo,M.," On the Dehydrogenation of n-Butane with the Deactivation of Alumina-Chromia Catalyst".Can. J.Chem.Eng.,1975 **53**,666-672.

Valus,J. and Schneider,P,"Transport Parameters of Porous Catalyst Via Chromatography With a Single Pellet String Column",Chem.Eng. Sci.,1985,**40**,1457.

Van Trimpont, P.A., Marin, G. B. and Froment, G. F.," Kinetics of Methylcyclohexane Dehydrogenation on Sulfided Commercial Platinum/ Alumina and Platinum -Rhenium/Alumina Catalysts," Ind. Eng. Chem. Fundam. 1986,**25**,544-553.

Van Trimpont,P.A., Marin,G.B. and Froment,G.F.," Reforming of C_7 Hydrocarbons on a Sulfided Commercial Pt/Al_2O_3 Catalyst," Ind.Eng. Chem.Res.,1988,**27**,51-57.

Villadsen,J.V. and Stewart,W.E.,"Solution of Boundary-Value Problems by Orthogonal Collocation",Chem.Eng.Sci.,1967,**22**,1483.

Voorhies,A.," Carbon Formation in Catalytic Cracking," Ind. Eng. Chem., 1945,**37**,318.

Wang, H.P. and Yates,J.T., " Spectroscopic Study of The Inter-conversion of Chemisorbed Surface Species: The Reaction $Rh^1(CO)$ + $CO \longrightarrow Rh^1(CO)_3$," J.Catal., 1984,**89**, 79-92.

Weekman,W,Jr.," A Model of Catalytic Cracking Conversion in Fixed, Moving and Fluid Bed reactors," Ind. Eng.Chem.Proc.Des.Dev. 1968,**7**,90.

Weekman, V.W. and Nace D.M., " Kinetics of Catalytic Cracking Selectivity in Fixed, Moving and Fluid Bed Reactors," 1970, A.I.Ch.E.J., 1970.**16**,397-405.

Weisz,P.B. and Hicks,J.B.," The Behavior of Porous Catalyst in View of Internal Mass and Heat Transfer Diffusion Effects," Chem. Eng. Sci.,1962,**17**,265-285.

Wheeler,A., "Reaction Rates and Selectivity in Catalyst Pores," Adv. Catal., 1951,**3**,250.

Wheeler,A., (Editors,Emmett,P.H.), Reinhold, NewYork, 1955, Vol.**2**,

White,H.L., " Indroduction to Industrial Chemistry", 1986, John Wiely Son. NY

Wojciechowski,B.W., " Theoretical Treatment of Catalyst Decay," Can.J.Chem.,1968,**46**,48.

Wojciechowski,B.W. and Pachovsky,R.A.,"Theoretical Interpretatin of Gas Oil Conversion Data on an X-Sieve Catalyst",Can. J.Chem. Eng.,1971,**49**,365-370.

Wojciechowski,B.W., " The Kinetic Foundation and The Practical Application of the Time on Stream Theory of Catalyst Decay," J

Catal.,Rev.Sci.Eng.,1974,9,79-113.

Wojciechowski,B.W. and Corma,A., Chemical Industries Ser.Vol 25 "Catalytic Cracking" Mercel Dekker,Inc. 1986.

Wolf,E. ,and Petersen, E.E.," On The Kinetics of Self Poisoning Catalyst Reactions," J.Catal. 1977a, 47,28-32.

Wolf,E. ,and Petersen, E.E.," Kinetic of Deactivation of Reforming Catalyst During Methylcyclohexane Dehydrogenation in a Diffusion Reaction," J.Catal. 1977b, 46,190-203.

Yates, J.,T., Duncan,J.T.M., Worley,S.D. and Vaughan, R.W.," Infrared Spectra of Chemisorbed CO on Rh,", J.Chem.Phys.,1979,70, 1219-1235.

Rabinovich, G.L., and Mozhaiko, V.N., Neftekhimiya,1975,15,373

APPENDIX I

Calibration Curves of Water/Toluene Reaction Components

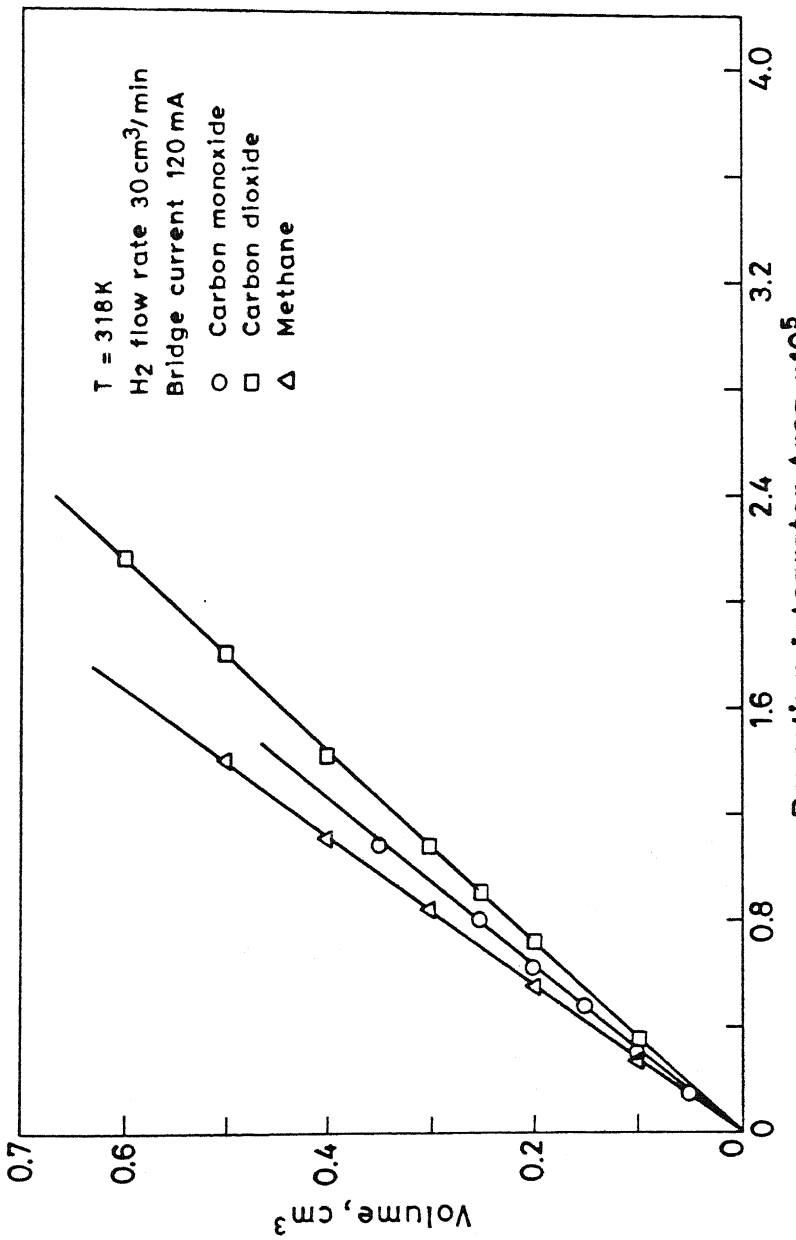

Fig. A1 CO, CO_2 and methane calibration curves.

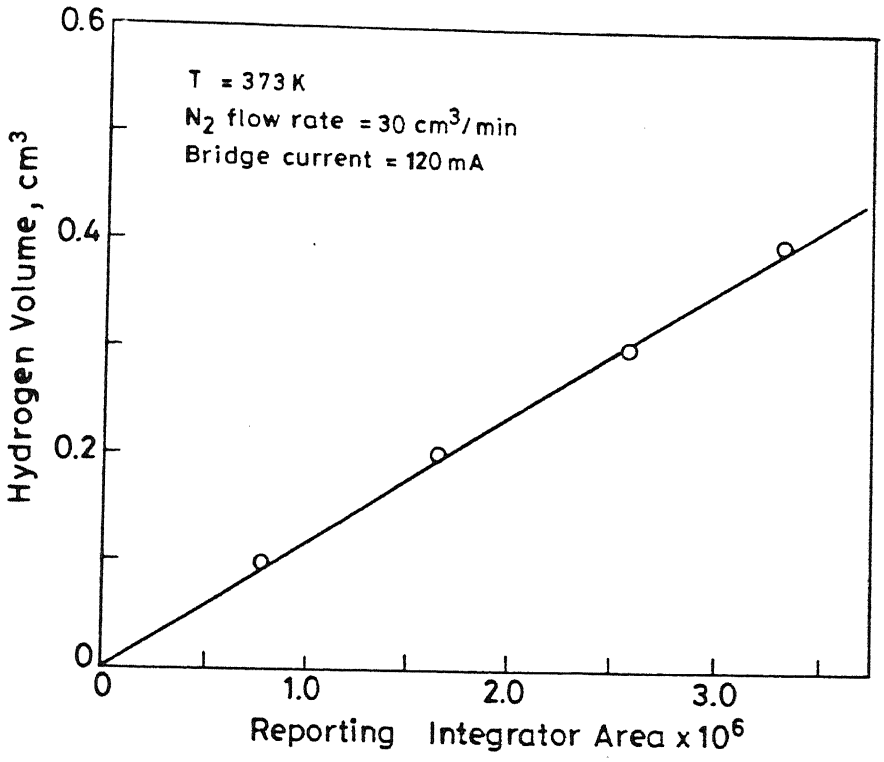

Fig. A2 Hydrogen calibration curve.

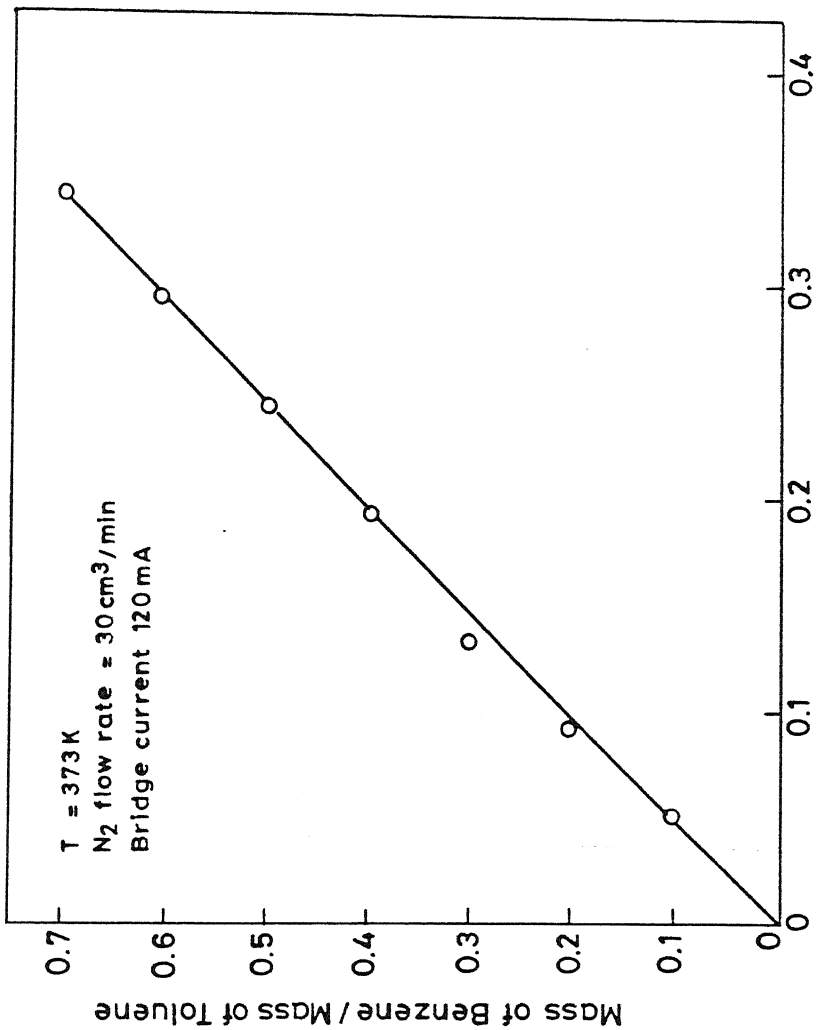

Fig. A3 Benzene/toluene ratio calibration curve.

Appendix II

Intrinsic Kinetic Data

SUMMARY OF RATE DATA FOR STEAM DEALKYLATION OF TOLUENE WATER REACTION

Partial pressures of reaction components,(atm).

r_i = (kmol)/(kgcat)(h). of ith reaction .,i = 1,2,3

Time min.	P_T	P_B	P_H	P_{CO}	P_{CO2}	P_W	$r_1 \times 10^3$	$r_2 \times 10^3$	$r_3 \times 10^3$
Run # 01			Average Temperature: 663 K						
W/F_{To}= 5.78									
00	0.35	0.013	0.053	0.032	0.009	0.53	5.00	1.3	8.1
40	0.36	0.008	0.047	0.025	0.008	0.54	4.20	1.3	5.8
80	0.37	0.007	0.045	0.023	0.007	0.55	3.20	1.3	4.6
Run # 02 ,W/F_{To}=16.41									
00	0.051	0.01	0.033	0.018	0.007	0.881	08.0	2.2	4.2
40	0.055	0.007	0.031	0.017	0.007	0.883	6.2	2.2	3.8
80	0.056	0.006	0.029	0.016	0.006	0.885	5.5	2.2	3.3
120	0.056	0.005	0.026	0.014	0.005	0.890	5.3	2.2	2.9
Run # 03 ,W/F_{To}= 8.67									
00	0.23	0.026	0.067	0.025	0.012	0.640	8.6	1.8	1.5
40	0.24	0.014	0.05	0.019	0.011	0.656	6.3	1.8	1.4
80	0.24	0.011	0.053	0.018	0.011	0.660	5.1	1.8	1.2
120	0.24	0.009	0.050	0.017	0.010	0.663	4.4	1.8	1.1
180	0.25	0.006	0.044	0.014	0.009	0.672	3.6	1.8	1.0
Run # 04 ,W/F_{To}= 17.34									
00	0.33	0.027	0.08	0.034	0.010	0.510	8.1	1.4	1.2
40	0.347	0.018	0.06	0.027	0.009	0.522	3.9	1.4	1.0
80	0.355	0.013	0.06	0.023	0.008	0.535	2.1	1.4	0.8
Run # 05 ,W/F_{To}= 9.34									

00	0.063	0.006	0.023	0.013	0.008	0.892	7.8	2.5	2.8
40	0.065	0.004	0.020	0.011	0.005	0.894	6.3	2.5	1.9
80	0.070	0.003	0.018	0.009	0.004	0.898	5.2	2.5	1.4
Run # 06 , W/F_{To}=15.59									
00	0.085	0.016	0.059	0.026	0.017	0.790	8.0	2.2	4.2
40	0.093	0.011	0.042	0.021	0.013	0.810	5.9	2.2	3.1
80	0.096	0.009	0.037	0.017	0.012	0.825	4.9	2.2	2.4
120	0.100	0.007	0.032	0.015	0.010	0.832	4.1	2.2	1.9
Run # 07 , W/F_{To}= 15.6									
00	0.115	0.020	0.047	0.022	0.015	0.780	9.1	2.3	2.6
40	0.121	0.013	0.042	0.021	0.011	0.786	5.9	2.3	1.8
80	0.126	0.009	0.034	0.018	0.010	0.795	4.6	2.4	1.4
Run # 08 , W/F_{To}=18.23									
00	0.140	0.030	0.078	0.031	0.017	0.700	9.0	2.0	2.6
40	0.160	0.017	0.065	0.023	0.014	0.720	5.3	2.0	2.1
80	0.162	0.014	0.062	0.020	0.013	0.726	4.2	2.0	1.7
120	0.165	0.013	0.058	0.019	0.013	0.735	3.9	2.0	1.4
180	0.170	0.012	0.050	0.016	0.012	0.742	3.4	2.0	1.2
Run # 09 , W/F_{To}= 17.34									
00	0.370	0.055	0.115	0.045	0.024	0.380	6.8	0.86	1.8
40	0.407	0.029	0.096	0.040	0.021	0.404	3.8	0.86	1.6
80	0.413	0.022	0.085	0.032	0.019	0.422	2.8	0.86	1.2
120	0.425	0.018	0.080	0.030	0.018	0.430	2.3	0.86	1.0

Average Temperatue 683 K

Run # P1, W/F_{To}= 15.6									
00	0.10	0.033	0.073	0.034	0.020	0.740	12.0	2.9	07.0
40	0.115	0.020	0.058	0.030	0.014	0.765	09.5	2.9	05.5

80	0.125	0.013	0.041	0.020	0.010	0.790	06.6	2.9	04.0
120	0.132	0.008	0.030	0.016	0.007	0.800	05.0	2.9	03.2
Run # P2, W/F_{To}= 14.45									
00	0.340	0.070	0.150	0.044	0.038	0.340	10.0	1.0	01.5
40	0.380	0.046	0.120	0.041	0.030	0.373	06.8	1.0	01.2
80	0.395	0.038	0.113	0.040	0.027	0.380	05.4	1.0	01.0
Run # P3, W/F_{To}= 08.2									
00	0.053	0.008	0.035	0.020	0.006	0.880	11.0	4.0	07.6
40	0.057	0.005	0.030	0.016	0.006	0.885	10.0	4.0	06.6
80	0.058	0.004	0.022	0.014	0.005	0.895	09.0	4.0	05.3
Run # P4, W/F_{To}= 4.34									
00	0.345	0.022	0.083	0.033	0.015	0.510	12.2	1.8	01.8
40	0.352	0.015	0.070	0.031	0.013	0.520	09.0	1.8	01.4
80	0.355	0.013	0.060	0.030	0.012	0.526	07.7	1.8	01.1
Run # P5, W/F_{To}= 7.23									
00	0.230	0.014	0.070	0.026	0.013	0.640	13.1	1.0	02.4
40	0.243	0.009	0.060	0.025	0.012	0.650	09.0	1.0	01.7
80	0.245	0.006	0.055	0.020	0.011	0.660	06.5	1.0	01.4
Run # P6, W/F_{To}= 32.42									
00	0.015	0.018	0.095	0.027	0.033	0.790	05.6	0.8	15.1
40	0.022	0.015	0.075	0.016	0.024	0.820	05.2	0.8	10.3
80	0.024	0.014	0.066	0.012	0.021	0.844	05.0	0.8	08.5
120	0.025	0.013	0.062	0.011	0.020	0.860	04.4	0.8	07.3
180	0.028	0.011	0.055	0.010	0.019	0.870	04.1	0.8	06.1
Run # P7, W/F_{To}= 13.76									
00	0.117	0.046	0.153	0.030	0.037	0.610	12.0	2.5	05.0
40	0.132	0.036	0.120	0.025	0.031	0.645	10.3	2.5	04.1
80	0.135	0.034	0.114	0.024	0.030	0.655	08.4	2.5	03.5
120	0.136	0.032	0.110	0.023	0.030	0.655	07.5	2.5	03.1

180	0.138	0.030	0.100	0.022	0.029	0.660	06.4	2.5	02.5
240	0.142	0.027	0.095	0.021	0.027	0.666	05.9	2.5	02.0
Run # P8, W/F_{To}= 15.6									
00	0.061	0.033	0.127	0.026	0.033	0.710	11.0	1.4	06.0
40	0.071	0.025	0.111	0.024	0.028	0.732	10.0	1.4	05.0
80	0.076	0.023	0.106	0.022	0.025	0.756	09.2	1.4	04.5
120	0.077	0.021	0.096	0.020	0.022	0.762	08.5	1.4	04.0
180	0.080	0.018	0.087	0.018	0.021	0.770	08.0	1.4	03.8
240	0.082	0.016	0.081	0.016	0.019	0.782	07.5	1.4	03.6
Run # P9, W/F_{To}= 9.36									
00	0.077	0.014	0.051	0.016	0.110	0.83	10.0	2.1	02.7
40	0.082	0.009	0.046	0.015	0.108	0.837	07.6	2.1	02.3
80	0.085	0.007	0.038	0.013	0.095	0.845	06.5	2.1	02.2
120	0.088	0.006	0.033	0.011	0.085	0.855	05.2	2.1	01.9
Run # P10, W/F_{To}= 12.31									
00	0.180	0.185	0.115	0.044	0.027	0.445	10.4	1.4	03.8
40	0.190	0.180	0.100	0.038	0.023	0.470	08.5	1.4	03.2
80	0.200	0.175	0.096	0.033	0.022	0.475	07.2	1.4	02.8
120	0.205	0.172	0.093	0.030	0.021	0.478	06.3	1.4	02.4
180	0.208	0.175	0.090	0.029	0.020	0.485	05.5	1.4	02.1
240	0.214	0.170	0.082	0.026	0.018	0.497	04.8	1.4	01.8
Run # P11, W/F_{To}= 11.11									
00	0.170	0.215	0.080	0.039	0.018	0.480	12.0	1.7	03.8
40	0.174	0.208	0.077	0.031	0.017	0.485	07.8	1.7	03.0
80	0.175	0.204	0.074	0.030	0.016	0.490	06.9	1.7	02.6
120	0.177	0.200	0.072	0.030	0.015	0.492	05.7	1.7	02.2
180	0.179	0.192	0.070	0.028	0.014	0.498	05.0	1.7	01.8
240	0.184	0.190	0.068	0.026	0.013	0.504	04.4	1.7	01.4
Run # P12, W/F_{To}= 9.56									

00	0.230	0.108	0.170	0.044	0.035	0.410	10.2	2.3	02.2
40	0.260	0.086	0.130	0.036	0.028	0.450	07.5	2.3	01.8
80	0.280	0.078	0.110	0.029	0.024	0.482	06.5	2.3	01.5
120	0.293	0.070	0.090	0.027	0.021	0.492	05.8	2.3	01.3
180	0.268	0.065	0.088	0.024	0.020	0.500	05.0	2.3	01.1
Run # P13, W/F_{To}= 18.14									
00	0.190	0.180	0.185	0.051	0.041	0.370	09.0	3.3	03.1
40	0.210	0.151	0.130	0.040	0.033	0.420	06.0	3.3	02.3
80	0.220	0.135	0.124	0.032	0.028	0.455	05.0	3.3	02.0
120	0.228	0.132	0.111	0.028	0.026	0.465	04.2	3.3	01.6
180	0.230	0.130	0.108	0.027	0.025	0.468	03.6	3.3	01.3
240	0.235	0.127	0.100	0.025	0.023	0.478	03.0	3.3	01.1
Run # P14, W/F_{To}=21.88									
00	0.051	0.030	0.100	0.025	0.022	0.760	12.0	3.4	08.1
40	0.055	0.024	0.091	0.021	0.018	0.772	9.7	3.3	06.8
80	0.059	0.019	0.082	0.017	0.015	0.783	7.3	3.4	05.2
120	0.061	0.016	0.072	0.014	0.013	0.792	5.5	3.4	04.7
Run # P15, W/F_{To}=12.47									
00	0.14	0.050	0.150	0.045	0.033	0.57	10.1	2.7	04.9
40	0.150	0.038	0.143	0.039	0.028	0.581	8.6	2.7	3.9
120	0.160	0.029	0.137	0.031	0.022	0.590	6.7	2.6	2.8

Average Temperature: **693 K**

Run # Q1, W/F_{To}=7.23									
00	0.220	0.023	0.096	0.030	0.018	0.610	15.6	2.7	03.1
40	0.226	0.018	0.088	0.027	0.017	0.620	10.8	2.7	02.5
80	0.228	0.016	0.085	0.026	0.016	0.625	08.8	2.7	02.2
120	0.230	0.015	0.081	0.025	0.015	0.632	07.5	2.7	01.7
Run # Q2 , W/F_{To}= 17.34									

00	0.260	0.070	0.180	0.044	0.036	0.390	12.0	0.9	03.0
40	0.282	0.050	0.170	0.042	0.033	0.410	08.4	0.9	02.5
80	0.291	0.044	0.165	0.039	0.031	0.421	06.7	0.9	02.2
120	0.300	0.039	0.160	0.036	0.030	0.426	05.2	0.9	01.8
180	0.305	0.036	0.155	0.032	0.029	0.431	04.0	0.9	01.6
Run # Q3, W/F_{To}= 5.78									
00	0.341	0.021	0.087	0.036	0.014	0.500	14.7	2.0	02.2
40	0.350	0.014	0.075	0.030	0.012	0.520	10.2	2.0	01.8
80	0.352	0.010	0.071	0.028	0.011	0.522	07.8	2.0	01.6
120	0.356	0.008	0.068	0.025	0.010	0.531	06.0	2.1	01.4
Run # Q4, W/F_{To}= 17.34									
00	0.325	0.080	0.165	0.048	0.035	0.330	10.8	0.9	01.7
40	0.356	0.056	0.155	0.045	0.034	0.350	07.1	0.9	01.5
80	0.361	0.047	0.150	0.043	0.033	0.362	05.2	0.9	01.3
120	0.366	0.046	0.146	0.041	0.031	0.366	04.0	0.9	01.1
Run # Q5, W/F_{To}= 15.6									
00	0.045	0.041	0.093	0.038	0.022	0.761	10.2	2.6	15.5
40	0.033	0.030	0.077	0.033	0.018	0.801	09.1	2.6	09.1
80	0.026	0.023	0.075	0.031	0.016	0.825	08.3	2.6	07.2
120	0.022	0.019	0.065	0.027	0.015	0.840	07.8	2.6	06.2
180	0.025	0.015	0.058	0.022	0.014	0.856	06.3	2.6	06.0
Run # Q6, W/F_{To}= 10.94									
00	0.048	0.012	0.031	0.017	0.007	0.880	13.3	4.1	08.3
40	0.056	0.007	0.030	0.016	0.007	0.885	10.6	4.1	06.1
80	0.059	0.006	0.026	0.015	0.006	0.890	09.3	4.1	05.2
120	0.060	0.005	0.025	0.015	0.006	0.892	08.2	4.1	04.2
180	0.060	0.004	0.024	0.013	0.005	0.896	07.3	4.1	03.4
Run # Q7, W/F_{To}= 15.95									
00	0.122	0.040	0.137	0.033	0.030	0.632	14.0	2.3	05.2

40	0.132	0.032	0.111	0.031	0.028	0.654	10.8	2.3	04.7
80	0.141	0.023	0.105	0.028	0.025	0.672	08.9	2.3	04.1
120	0.146	0.022	0.095	0.025	0.022	0.680	07.7	2.3	03.7
180	0.150	0.021	0.091	0.024	0.020	0.691	07.0	2.3	03.4
240	0.156	0.018	0.090	0.021	0.019	0.697	06.4	2.3	03.1

Average Temperature: **713 K**

Run # R1, W/F_{To}=15.61

00	0.072	0.050	0.145	0.043	0.033	0.675	16.2	3.1	13.8
40	0.089	0.037	0.115	0.035	0.022	0.703	12.5	3.1	10.3
80	0.096	0.032	0.102	0.030	0.019	0.721	10.8	3.1	08.9
120	0.099	0.028	0.090	0.027	0.017	0.735	09.3	3.1	07.2
180	0.113	0.020	0.076	0.023	0.015	0.755	08.2	3.1	06.3

Run # R2, W/F_{To}= 15.61

00	0.105	0.053	0.160	0.043	0.033	0.600	18.1	3.0	10.0
40	0.125	0.037	0.151	0.038	0.025	0.636	14.8	3.0	09.0
80	0.135	0.031	0.111	0.032	0.021	0.671	11.9	3.0	08.0
120	0.141	0.028	0.100	0.028	0.019	0.682	10.6	3.0	07.5
180	0.142	0.025	0.098	0.026	0.018	0.690	09.5	3.1	07.0
240	0.150	0.023	0.088	0.020	0.017	0.710	08.7	3.1	06.0

Run # R3, W/F_{To}= 15.61

00	0.121	0.051	0.148	0.039	0.030	0.562	18.5	2.7	07.6
40	0.132	0.042	0.136	0.036	0.026	0.580	14.6	2.7	06.6
80	0.141	0.035	0.121	0.032	0.023	0.600	12.7	2.7	05.9
120	0.147	0.031	0.113	0.031	0.021	0.610	11.2	2.7	05.4
180	0.152	0.025	0.103	0.030	0.020	0.622	09.3	2.7	04.9

Run # R4, W/F_{To}= 15.61

00	0.124	0.052	0.148	0.030	0.033	0.400	16.0	1.5	03.0
40	0.146	0.031	0.127	0.040	0.026	0.420	11.6	1.5	02.7

80	0.151	0.027	0.117	0.037	0.022	0.430	09.5	1.5	02.5
120	0.155	0.026	0.106	0.031	0.021	0.440	08.6	1.5	02.4
180	0.160	0.023	0.092	0.025	0.020	0.456	07.8	1.5	02.2
Run # R5, W/F_{To}= 15.61									
00	0.138	0.037	0.125	0.036	0.024	0.211	10.0	0.40	01.7
40	0.150	0.024	0.097	0.031	0.018	0.222	07.0	0.40	01.6
80	0.156	0.022	0.096	0.030	0.017	0.225	05.7	0.40	01.5
120	0.160	0.020	0.094	0.030	0.015	0.231	04.5	0.40	01.4
180	0.164	0.017	0.092	0.029	0.014	0.243	03.7	0.40	01.3
Run # R6 , W/F_{To}= 15.61									
00	0.170	0.021	0.053	0.015	0.012	0.170	10.0	0.40	00.9
40	0.18	0.015	0.043	0.011	0.009	0.185	06.8	0.40	00.9
80	0.182	0.011	0.040	0.101	0.008	0.188	05.0	0.40	00.8
120	0.185	0.009	0.038	0.009	0.008	0.190	03.9	0.40	00.8
Run # R7, W/F_{To}= 15.33									
00	0.057	0.012	0.047	0.015	0.011	0.854	20.0	5.0	09.0
40	0.062	0.008	0.038	0.013	0.008	0.871	17.0	5.0	07.2
80	0.064	0.007	0.033	0.012	0.007	0.880	13.9	5.0	06.4
120	0.066	0.006	0.030	0.011	0.006	0.885	12.2	5.0	05.6
180	0.068	0.005	0.028	0.010	0.005	0.889	10.3	5.0	04.7
Run # R8, W/F_{To}= 16.41									
00	0.051	0.025	0.090	0.039	0.013	0.784	09.1	3.4	11.0
40	0.061	0.020	0.060	0.025	0.009	0.800	07.4	3.4	08.4
80	0.066	0.016	0.040	0.016	0.007	0.860	06.3	3.4	06.3
Run # R9, W/F_{To}= 22.79									
00	0.040	0.040	0.150	0.034	0.036	0.691	13.5	2.8	14.5
40	0.053	0.030	0.133	0.031	0.031	0.717	11.8	2.8	13.0
80	0.055	0.027	0.125	0.027	0.030	0.721	10.2	2.8	10.9
120	0.056	0.026	0.118	0.026	0.029	0.732	09.1	2.8	10.2

180	0.059	0.024	0.110	0.024	0.027	0.755	08.1	2.8	09.9
240	0.067	0.020	0.086	0.020	0.021	0.788	07.3	2.8	08.9
Run # R10, W/F_{To}= 16.41									
00	0.031	0.071	0.031	0.013	0.008	0.910	16.0	4.7	08.2
40	0.036	0.005	0.024	0.011	0.005	0.920	14.5	4.7	05.7
80	0.039	0.003	0.020	0.009	0.003	0.930	13.4	4.7	04.5
Run # R11, W/F_{To}= 21.44									
00	0.170	0.050	0.145	0.035	0.032	0.440	16.0	2.0	03.4
40	0.185	0.035	0.128	0.033	0.024	0.471	12.6	2.0	03.0
80	0.195	0.030	0.113	0.026	0.022	0.485	09.8	2.0	02.7
120	0.200	0.026	0.097	0.019	0.020	0.508	08.6	2.0	02.4
180	0.204	0.022	0.095	0.019	0.019	0.510	07.5	2.0	02.0
Run # R12, W/F_{To}= 21.44									
00	0.260	0.067	0.165	0.050	0.032	0.410	18.0	1.8	04.2
40	0.298	0.044	0.150	0.043	0.030	0.430	12.9	1.8	03.4
80	0.302	0.039	0.145	0.036	0.030	0.440	09.5	1.8	02.9
120	0.312	0.035	0.135	0.031	0.029	0.455	07.8	1.8	02.7
180	0.317	0.032	0.127	0.029	0.028	0.465	06.9	1.8	02.2
240	0.321	0.030	0.116	0.028	0.026	0.481	06.1	1.8	01.9
run # R13 , W/F_{To}= 21.44									
00	0.072	0.020	0.087	0.026	0.019	0.510	16.9	2.2	03.3
40	0.080	0.013	0.075	0.021	0.016	0.522	14.5	2.2	03.0
80	0.085	0.012	0.051	0.009	0.013	0.550	12.8	2.2	02.8
120	0.087	0.011	0.047	0.008	0.011	0.560	11.8	2.2	02.6
Run # R14, W/F_{To}= 21.45									
00	0.130	0.033	0.116	0.024	0.029	0.467	17.8	2.0	03.3
40	0.142	0.021	0.103	0.025	0.021	0.468	14.0	2.0	02.9
80	0.150	0.016	0.090	0.024	0.019	0.500	12.2	2.0	02.8
120	0.156	0.014	0.075	0.016	0.017	0.506	11.2	2.0	02.5

180	0.162	0.010	0.060	0.009	0.016	0.522	09.6	2.0	02.2
Run # R15, W/F_{To}= 7.23									
00	0.14	0.017	0.390	0.051	0.018	0.360	13.8	1.1	04.1
40	0.147	0.013	0.37	0.049	0.018	0.363	10.2	1.1	03.8
80	0.151	0.010	0.375	0.047	0.017	0.370	08.2	1.1	03.3
120	0.155	0.009	0.375	0.045	0.016	0.375	07.0	1.1	03.2
Run # R16, W/F_{To}= 7.23									
00	0.157	0.024	0.103	0.037	0.016	0.431	17.2	2.0	06.0
40	0.160	0.019	0.097	0.032	0.014	0.452	14.4	2.0	05.0
80	0.163	0.014	0.085	0.029	0.013	0.455	11.6	2.1	04.2
120	0.167	0.012	0.076	0.028	0.011	0.462	09.8	2.1	03.8
180	0.171	0.010	0.069	0.021	0.010	0.476	08.0	2.0	03.3
Run # R17, W/F_{To}= 7.23									
00	0.150	0.027	0.220	0.050	0.010	0.440	15.9	2.0	08.0
40	0.166	0.018	0.195	0.041	0.008	0.465	13.2	2.0	06.5
80	0.171	0.013	0.190	0.032	0.007	0.478	09.6	2.0	05.0
120	0.175	0.009	0.181	0.024	0.006	0.492	07.6	2.0	04.0
180	0.182	0.007	0.175	0.016	0.005	0.510	06.2	2.0	03.2
Run # R18, W/F_{To}= 29.62									
00	0.034	0.110	0.250	0.072	0.068	0.270	05.6	0.6	06.6
40	0.046	0.107	0.190	0.046	0.041	0.360	03.9	0.6	05.8
80	0.052	0.100	0.170	0.035	0.037	0.390	03.1	0.6	05.3
120	0.056	0.100	0.155	0.032	0.036	0.400	02.5	0.6	04.5
180	0.059	0.097	0.145	0.030	0.034	0.411	01.8	0.6	03.9
240	0.061	0.095	0.134	0.028	0.031	0.421	01.3	0.6	03.3
Run # R19, W/F_{To}= 29.62									
00	0.049	0.340	0.068	0.044	0.019	0.480	10.5	1.4	17.4
40	0.058	0.35	0.041	0.032	0.012	0.510	08.2	1.4	13.0
80	0.062	0.352	0.027	0.023	0.008	0.531	06.5	1.4	10.7

120	0.065	0.356	0.023	0.019	0.006	0.535	05.4	1.4	09.6
Run # R20, W/F_{To}= 29.64									
00	0.037	0.038	0.200	0.06	0.055	0.350	08.0	1.0	06.0
40	0.045	0.031	0.176	0.055	0.054	0.355	07.3	1.0	05.2
80	0.047	0.030	0.167	0.051	0.044	0.371	06.9	1.1	05.0
120	0.051	0.029	0.157	0.042	0.038	0.391	06.5	1.0	04.8
180	0.054	0.026	0.154	0.040	0.037	0.400	05.6	1.0	04.1
240	0.058	0.024	0.142	0.033	0.035	0.420	05.0	1.1	03.6
300	0.062	0.023	0.130	0.027	0.033	0.440	04.7	1.0	03.2
360	0.063	0.022	0.122	0.021	0.030	0.451	04.0	1.0	02.9
420	0.064	0.021	0.120	0.020	0.030	0.455	03.5	1.0	02.2
Run # R21, W/F_{To}= 29.62									
00	0.020	0.165	0.230	0.085	0.072	0.280	10.2	0.7	06.7
40	0.023	0.161	0.210	0.074	0.062	0.285	09.0	0.7	06.2
80	0.030	0.160	0.20	0.065	0.058	0.292	07.6	0.7	05.8
120	0.036	0.16	0.187	0.062	0.052	0.33	06.7	0.7	05.3
180	0.044	0.160	0.165	0.050	0.044	0.370	05.4	0.7	05.0
240	0.051	0.160	0.145	0.036	0.038	0.400	04.5	0.7	04.4
300	0.054	0.160	0.120	0.020	0.032	0.440	03.8	0.7	04.1
Run # R22, W/F_{To}= 31.81									
00	0.040	0.020	0.068	0.022	0.015	0.830	16.8	4.2	14.0
40	0.047	0.013	0.057	0.018	0.009	0.856	13.8	4.2	11.4
80	0.049	0.011	0.051	0.017	0.008	0.861	11.6	4.3	09.2
120	0.051	0.010	0.048	0.016	0.008	0.870	09.3	4.2	08.1
180	0.053	0.009	0.046	0.015	0.008	0.870	07.8	4.2	07.0
Run # R23, W/F_{To}= 12.26									
00	0.072	0.050	0.146	0.045	0.030	0.650	16.0	2.9	14.0
40	0.090	0.040	0.111	0.035	0.021	0.690	1[illegible]2	2.9	11.2
80	0.099	0.030	0.098	0.029	0.019	0.720	13.4	2.9	09.5

120	0.106	0.023	0.085	0.026	0.017	0.730	11.6	2.9	08.4
180	0.108	0.022	0.083	0.025	0.016	0.744	09.9	2.9	07.2
Run # R24, W/F_{To}= 15.61									
00	0.048	0.044	0.17	0.037	0.046	0.640	14.0	2.5	11.0
40	0.060	0.034	0.15	0.036	0.037	0.680	10.9	2.5	09.0
80	0.066	0.030	0.124	0.026	0.031	0.711	09.8	2.5	07.9
120	0.071	0.027	0.115	0.025	0.029	0.73	08.7	2.5	07.1
180	0.076	0.023	0.108	0.022	0.025	0.741	08.1	2.5	06.4
240	0.078	0.020	0.096	0.020	0.023	0.755	07.4	2.5	06.1

Average Temperature **723 K**

Run # S1, W/F_{To}= 4.68									
00	0.115	0.090	0.040	0.021	0.055	0.785	26.0	5.9	06.3
40	0.136	0.026	0.025	0.012	0.027	0.821	23.6	5.9	04.1
80	0.142	0.006	0.012	0.006	0.013	0.842	20.8	5.9	03.3
Run # S2, W/F_{To}= 15.61									
00	0.071	0.053	0.177	0.036	0.044	0.641	20.0	3.4	08.1
40	0.085	0.037	0.130	0.030	0.028	0.660	15.3	3.4	07.2
80	0.100	0.026	0.102	0.028	0.024	0.710	13.5	3.5	06.7
120	0.108	0.020	0.090	0.024	0.020	0.735	10.6	3.5	05.9
180	0.111	0.016	0.007	0.023	0.016	0.770	08.7	3.5	05.2
Run # S3, W/F_{To}= 4.68									
00	0.066	0.020	0.021	0.10	0.002	0.890	12.2	6.3	06.4
40	0.069	0.009	0.017	0.09	0.002	0.900	11.1	6.3	04.5
80	0.070	0.002	0.009	0.007	0.001	0.911	09.4	6.3	04.0
run # S4, W/F_{To}= 4.68									
00	0.395	0.035	0.108	0.045	0.015	0.400	23.2	2.5	04.0
40	0.425	0.016	0.082	0.037	0.012	0.425	18.0	2.5	03.2
80	0.445	0.008	0.054	0.028	0.009	0.455	14.0	2.5	02.8

120	0.462	0.003	0.036	0.020	0.006	0.475	11.6	2.5	02.3
Run # S5, W/F_{To}= 5.06									
00	0.210	0.033	0.088	0.044	0.025	0.600	25.4	4.3	08.0
40	0.235	0.013	0.048	0.033	0.012	0.655	20.6	4.3	07.0
60	0.24	0.011	0.044	0.031	0.010	0.662	16.5	4.3	06.0
Run # S6, W/F_{To}= 4.34									
00	0.320	0.038	0.087	0.043	0.024	0.480	24.7	3.0	04.6
40	0.345	0.022	0.064	0.360	0.015	0.515	18.7	3.0	04.0
60	0.353	0.017	0.052	0.34	0.013	0.530	13.8	3.0	03.2
Run # S7, W/F_{To}= 2.89									
00	0.330	0.028	0.069	0.039	0.016	0.510	25.7	3.4	04.5
40	0.360	0.015	0.044	0.031	0.010	0.540	18.3	3.5	03.3
80	0.365	0.011	0.037	0.027	0.008	0.550	14.5	3.5	02.5
Run # S8, W/F_{To}= 5.3									
00	0.110	0.020	0.064	0.042	0.013	0.752	25.0	5.4	16.0
40	0.120	0.013	0.052	0.038	0.012	0.765	19.8	5.4	11.5
80	0.130	0.009	0.040	0.030	0.009	0.783	15.7	5.4	09.4
120	0.133	0.007	0.032	0.230	0.007	0.786	12.9	5.4	07.9
Run # S9, W/F_{To}= 7.8									
00	0.057	0.011	0.038	0.019	0.007	0.867	24.0	5.9	13.0
40	0.061	0.072	0.035	0.017	0.006	0.872	19.2	5.9	11.2
80	0.063	0.057	0.030	0.015	0.005	0.881	16.5	5.9	10.6
120	0.065	0.047	0.029	0.014	0.003	0.886	13.6	5.9	10.0
180	0.068	0.040	0.027	0.120	0.003	0.892	11.4	5.9	09.4
Run # S10, W/F_{To}= 3.74									
00	0.116	0.016	0.053	0.036	0.010	0.765	25.5	5.7	13.2
40	0.130	0.050	0.032	0.025	0.008	0.800	19.8	5.7	10.5
80	0.136	0.020	0.020	0.020	0.005	0.812	16.5	5.7	08.0
120	0.138	0.012	0.013	0.016	0.004	0.821	13.7	5.7	07.3

180	0.141	0.008	0.090	0.010	0.004	0.833	11.0	5.7	05.8
Run # S11, W/F_{To} = 18.23									
00	0.046	0.039	0.012	0.032	0.026	0.742	19.0	4.2	22.2
40	0.060	0.025	0.010	0.028	0.022	0.762	15.6	4.2	17.2
80	0.065	0.022	0.009	0.026	0.020	0.772	13.3	4.2	14.8
120	0.067	0.200	0.084	0.024	0.017	0.780	12.0	4.2	13.5
180	0.070	0.019	0.080	0.021	0.016	0.792	11.0	4.2	11.6
240	0.071	0.017	0.070	0.020	0.016	0.805	10.5	4.2	10.3
300	0.074	0.015	0.063	0.018	0.015	0.811	09.5	4.2	09.2
360	0.078	0.013	0.052	0.016	0.014	0.825	08.2	4.2	07.3
Run # S12, W/F_{To} = 14.81									
00	0.045	0.038	0.127	0.040	0.028	0.722	17.0	3.5	23.1
40	0.058	0.026	0.107	0.033	0.024	0.751	14.1	3.5	17.8
80	0.062	0.023	0.094	0.029	0.021	0.762	11.7	3.5	16.0
120	0.066	0.020	0.088	0.028	0.020	0.770	09.6	3.5	14.4
180	0.071	0.017	0.074	0.022	0.018	0.794	07.8	3.5	13.0
240	0.074	0.014	0.068	0.019	0.017	0.800	06.4	3.5	12.3
Run # S13, W/F_{To} = 10.26									
00	0.057	0.028	0.098	0.035	0.020	0.760	20.6	4.7	17.3
40	0.065	0.022	0.088	0.027	0.046	0.780	17.6	4.7	15.2
80	0.073	0.020	0.080	0.025	0.015	0.790	15.1	4.7	14.2
120	0.075	0.015	0.059	0.020	0.012	0.811	13.5	4.7	13.2
180	0.077	0.014	0.056	0.019	0.010	0.820	12.7	4.7	11.2
240	0.080	0.011	0.049	0.018	0.009	0.830	11.4	4.7	10.6
300	0.082	0.010	0.045	0.016	0.008	0.837	11.2	4.6	09.5
Run # S14, W/F_{To} = 8.2									
00	0.068	0.020	0.070	0.028	0.011	0.800	22.9	5.4	15.0
40	0.075	0.014	0.060	0.024	0.009	0.818	18.5	5.4	13.2
80	0.080	0.010	0.046	0.022	0.009	0.835	15.1	5.4	11.0

120	0.084	0.008	0.038	0.017	0.007	0.846	13.4	5.4	10.5
180	0.088	0.005	0.030	0.013	0.005	0.860	11.8	5.4	08.9
240	0.092	0.004	0.024	0.010	0.004	0.866	10.5	5.4	08.2
Run # S15, W/F_{To}= 4.56									
00	0.077	0.011	0.062	0.024	0.008	0.820	24.8	6.0	12.1
40	0.080	0.009	0.053	0.027	0.007	0.825	20.7	6.0	09.8
80	0.082	0.007	0.049	0.026	0.006	0.832	17.2	6.0	08.6
120	0.083	0.006	0.044	0.025	0.005	0.836	15.6	6.0	07.5
Run # S16, W/F_{To}= 6.34									
00	0.070	0.018	0.072	0.024	0.010	0.801	23.8	5.9	13.2
40	0.075	0.016	0.060	0.021	0.009	0.820	20.4	5.9	10.8
80	0.077	0.013	0.055	0.019	0.008	0.826	17.7	5.9	09.1
120	0.078	0.011	0.051	0.018	0.007	0.832	15.6	5.9	08.1
180	0.081	0.009	0.045	0.015	0.006	0.842	13.3	5.9	07.3
Run # S17, W/F_{To}= 6.10									
00	0.039	0.050	0.021	0.010	0.003	0.910	21.5	6.8	10.0
40	0.042	0.02	0.017	0.009	0.002	0.920	18.8	6.8	07.2
80	0.044	0.012	0.009	0.006	0.001	0.935	16.3	6.8	06.0
120	0.046	0.009	0.007	0.004	0.001	0.940	14.8	6.8	04.8
Run # S18, W/F_{To}= 4.34									
00	0.170	0.026	0.060	0.038	0.017	0.690	25.9	4.9	10.0
40	0.18	0.021	0.050	0.030	0.010	0.715	20.5	4.9	08.5
80	0.186	0.014	0.041	0.028	0.009	0.721	17.3	4.9	07.5
120	0.192	0.010	0.034	0.026	0.008	0.729	14.8	4.9	06.3
run # S19, W/F_{To}= 20.51									
00	0.030	0.049	0.150	0.044	0.042	0.671	17.0	4.9	24.0
40	0.044	0.037	0.137	0.034	0.034	0.711	15.5	4.9	19.8
80	0.052	0.032	0.115	0.028	0.029	0.741	13.6	4.9	17.5
120	0.058	0.030	0.094	0.023	0.023	0.770	12.8	4.9	15.4

180	0.062	0.027	0.082	0.021	0.021	0.784	12.1	4.9	13.7
240	0.067	0.022	0.075	0.018	0.018	0.797	11.6	4.9	10.3
300	0.073	0.018	0.065	0.017	0.016	0.805	09.6	4.9	09.8
360	0.076	0.014	0.058	0.016	0.015	0.821	07.8	4.9	08.7
420	0.078	0.012	0.050	0.014	0.013	0.830	06.4	3.9	06.7
Run # S20, W/F_{To}= 22.79									
00	0.031	0.046	0.180	0.045	0.033	0.73	17.7	3.1	31.0
40	0.058	0.027	0.110	0.030	0.030	0.745	14.1	3.1	26.0
80	0.060	0.022	0.100	0.026	0.022	0.751	11.8	3.1	21.3
120	0.065	0.022	0.096	0.025	0.020	0.771	10.0	3.2	18.1
180	0.068	0.020	0.086	0.022	0.018	0.787	08.9	3.2	15.7
240	0.073	0.016	0.075	0.017	0.016	0.800	07.7	3.1	13.5
300	0.077	0.014	0.066	0.015	0.014	0.815	06.3	3.2	12.2
Run # S21, W/F_{To}= 4.68									
00	0.055	0.007	0.027	0.011	0.004	0.897	24.6	6.1	08.0
40	0.059	0.003	0.021	0.009	0.003	0.906	20.2	6.1	05.8
80	0.064	0.001	0.009	0.005	0.001	0.920	16.8	6.1	04.7
120	0.059	0.001	0.007	0.003	0.001	0.930	14.9	6.1	03.9
run # S22, W/F_{To}= 4.68									
00	0.210	0.030	0.081	0.023	0.019	0.630	27.0	4.6	04.0
40	0.235	0.011	0.067	0.019	0.014	0.652	19.5	4.6	03.3
80	0.252	0.003	0.035	0.011	0.007	0.692	15.8	4.6	02.8
120	0.260	0.001	0.026	0.008	0.005	0.700	13.7	4.6	02.2
Run # S23, W/F_{To}= 4.49									
00	0.030	0.014	0.035	0.012	0.008	0.900	18.8	4.7	12.0
40	0.037	0.008	0.025	0.010	0.006	0.915	15.9	4.8	08.7
80	0.041	0.004	0.017	0.007	0.004	0.925	14.8	4.7	06.5
Run # S24, W/F_{To}= 3.61									
00	0.220	0.028	0.060	0.019	0.012	0.660	28.3	4.9	03.5

40	0.233	0.018	0.048	0.016	0.010	0.672	20.2	4.9	02.8
80	0.240	0.016	0.041	0.014	0.009	0.684	16.5	4.9	02.2
120	0.253	0.013	0.035	0.012	0.007	0.693	13.5	4.9	02.0
Run # S25, W/F_{To}= 8.02									
00	0.035	0.060	0.030	0.016	0.004	0.910	19.9	5.2	14.9
40	0.041	0.032	0.016	0.012	0.003	0.923	17.3	5.2	10.8
80	0.044	0.009	0.006	0.006	0.001	0.940	15.6	5.2	08.3
120	0.046	0.007	0.003	0.004	0.001	0.942	13.4	5.2	06.5
Run # S26, W/F_{To}= 10.9									
00	0.022	0.025	0.061	0.018	0.010	0.860	12.6	4.0	20.0
40	0.034	0.010	0.040	0.012	0.006	0.895	10.4	4.0	14.2
80	0.040	0.045	0.022	0.008	0.003	0.920	09.2	4.1	09.1
Run # S27, W/F_{To}= 12.26									
00	0.195	0.047	0.082	0.024	0.017	0.631	26.5	4.4	04.6
40	0.240	0.020	0.040	0.012	0.009	0.682	19.2	4.4	03.7
80	0.260	0.015	0.013	0.004	0.003	0.720	15.6	4.4	03.1
120	0.277	0.010	0.008	0.002	0.002	0.732	13.7	4.4	02.7
Run # S28, W/F_{To}= 2.46									
00	0.190	0.012	0.040	0.016	0.008	0.732	29.0	6.0	04.0
40	0.201	0.004	0.023	0.012	0.005	0.750	22.3	6.1	03.1
80	0.215	0.002	0.012	0.008	0.003	0.772	18.6	6.1	02.5
120	0.220	0.001	0.008	0.006	0.002	0.782	16.2	6.1	02.1
Run # S29, W/F_{To}= 15.6									
00	0.075	0.050	0.125	0.046	0.028	0.660	20.0	3.6	18.0
40	0.096	0.032	0.100	0.040	0.023	0.705	16.3	3.6	14.2
80	0.105	0.024	0.086	0.033	0.020	0.730	13.4	3.6	11.7
120	0.112	0.019	0.070	0.030	0.016	0.752	11.2	3.6	10.2
180	0.120	0.015	0.056	0.022	0.014	0.770	09.6	3.7	09.3
Run # S30, W/F_{To}= 18.23									

00	0.035	0.044	0.160	0.047	0.038	0.655	16.0	3.0	24.1
40	0.049	0.032	0.137	0.038	0.031	0.711	13.3	3.0	18.6
80	0.060	0.027	0.100	0.027	0.022	0.752	11.2	3.0	15.3
120	0.063	0.023	0.092	0.025	0.021	0.761	10.5	3.0	13.1
180	0.067	0.021	0.090	0.024	0.020	0.770	09.0	3.0	11.6
240	0.071	0.018	0.078	0.022	0.018	0.790	08.3	3.0	10.7
300	0.075	0.015	0.070	0.019	0.014	0.805	07.5	3.0	09.9
Run # S31, W/F_{To} = 20.61									
00	0.040	0.048	0.178	0.043	0.045	0.652	16.3	3.0	18.2
40	0.043	0.041	0.150	0.032	0.036	0.700	14.0	3.0	16.2
80	0.052	0.034	0.117	0.027	0.028	0.740	12.2	3.0	13.1
120	0.055	0.030	0.106	0.025	0.024	0.756	10.6	3.1	12.2
180	0.060	0.027	0.009	0.022	0.022	0.770	09.4	3.0	11.4
Run # S32, W/F_{To} = 10.11									
00	0.270	0.062	0.140	0.042	0.026	0.430	22.2	2.4	03.5
40	0.295	0.046	0.140	0.041	0.025	0.441	14.2	2.4	03.3
80	0.310	0.038	0.125	0.040	0.023	0.463	10.5	2.4	03.0
120	0.315	0.033	0.120	0.038	0.022	0.470	09.3	2.4	02.7
180	0.321	0.027	0.105	0.033	0.019	0.490	07.8	2.5	02.4
Run # S33, W/F_{To} = 17.34									
00	0.320	0.100	0.130	0.035	0.026	0.380	23.4	2.1	02.1
40	0.370	0.056	0.116	0.045	0.018	0.393	14.8	2.1	01.9
80	0.370	0.055	0.114	0.044	0.018	0.395	07.0	2.1	01.7
120	0.378	0.050	0.109	0.037	0.016	0.400	06.6	2.1	01.5
180	0.390	0.045	0.100	0.035	0.015	0.410	06.0	2.1	01.4
Run # S34, W/F_{To} = 22.78									
00	0.100	0.042	0.125	0.105	0.076	0.472	11.8	2.5	15.0
40	0.115	0.030	0.150	0.145	0.075	0.486	08.8	2.5	12.4
80	0.117	0.026	0.153	0.147	0.074	0.488	07.3	2.5	10.3

120	0.119	0.023	0.147	0.146	0.073	0.489	06.0	2.5	07.2
180	0.120	0.022	0.145	0.143	0.072	0.500	04.9	2.5	08.1
240	0.122	0.020	0.140	0.140	0.070	0.505	06.1	2.5	07.7
Run # S35, W/F_{To}= 24.52									
00	0.135	0.011	0.159	0.270	0.106	0.330	03.1	1.2	34.0
40	0.141	0.004	0.157	0.290	0.098	0.320	01.1	1.2	29.5
80	0.144	0.003	0.145	0.300	0.093	0.330	00.9	1.2	25.5
120	0.145	0.002	0.144	0.302	0.089	0.327	00.6	1.2	24.8
180	0.147	0.001	0.125	0.300	0.083	0.328	00.4	1.2	24.2
Run # S36, W/F_{To}= 10.12									
00	0.190	0.015	0.125	0.170	0.067	0.432	09.3	2.1	23.0
40	0.198	0.010	0.110	0.180	0.058	0.441	04.4	2.1	19.6
80	0.200	0.007	0.106	0.183	0.060	0.445	03.5	2.1	16.5
120	0.204	0.006	0.080	0.170	0.060	0.456	02.5	2.1	14.1
180	0.215	0.005	0.070	0.162	0.060	0.478	02.1	2.1	11.2
Run # S37, W/F_{To}= 23.12									
00	0.280	0.027	0.120	0.150	0.056	0.365	11.8	1.8	13.2
40	0.290	0.012	0.119	0.155	0.060	0.363	06.0	1.8	11.0
80	0.300	0.009	0.108	0.160	0.060	0.371	05.5	1.8	09.4
120	0.304	0.007	0.103	0.160	0.055	0.381	04.2	1.8	08.7
180	0.310	0.004	0.096	0.160	0.055	0.391	1.70	1.8	07.6
Run # S38, W/F_{To}= 21.67									
00	0.280	0.035	0.140	0.140	0.050	0.330	10.2	1.3	11.0
40	0.285	0.015	0.145	0.133	0.046	0.350	06.3	1.3	09.0
80	0.302	0.014	0.140	0.122	0.044	0.352	05.1	1.3	07.6
120	0.310	0.009	0.111	0.106	0.043	0.376	03.9	1.3	06.8
180	0.313	0.008	0.104	0.081	0.040	0.410	01.5	1.3	06.3
Run # S39, W/F_{To}= 28.9									
00	0.270	0.062	0.220	0.180	0.108	0.185	06.8	0.6	13.0

40	0.305	0.037	0.198	0.175	0.100	0.188	03.6	0.6	10.2
80	0.310	0.032	0.189	0.167	0.098	0.200	03.0	0.6	09.2
120	0.320	0.025	0.185	0.165	0.092	0.206	02.5	0.6	08.2
180	0.323	0.021	0.181	0.160	0.091	0.220	02.2	0.8	07.0

APPENDIX III

RATE DATA FOR DIFFUSION INFLUENCED-CATALYST

Catalyst patical diameter = 3.2 mm

W/F_{To} in (kgcat)/(kmol/h)

Time (min)	$R_1 \times 10^3$ kmol/ kgcat.h	$R_2 \times 10^3$ kmol/ kgcat.h	$R_3 \times 10^3$ kmol/ kgcat.h	P_T atm	P_B atm	P_H atm	P_{CO} atm	P_C atm	P_W atm
			Temperature = 663 K						
run # L1, W/F_{To} =39.24									
00	5.2	0.40	2.80	0.33	0.09	0.151	0.047	0.036	0.345
40	3.5	0.40	2.00	0.37	0.05	0.130	0.043	0.032	0.365
80	2.3	0.40	1.70	0.39	0.04	0.110	0.038	0.027	0.366
120	1.6	0.40	1.50	0.40	0.03	0.105	0.033	0.026	0.395
200	1.4	0.40	1.40	0.41	0.02	0.100	0.032	0.026	0.400
run # L2 W/F_{To} = 34.81									
00	3.3	0.50	5.10	0.32	0.04	0.100	0.030	0.021	0.488
40	2.9	0.50	4.50	0.34	0.02	0.081	0.026	0.017	0.513
80	2.5	0.50	4.40	0.35	0.01	0.077	0.025	0.017	0.515
120	2.2	0.50	4.30	0.35	0.01	0.075	0.023	0.016	0.517
200	2.0	0.50	4.20	0.36	0.008	0.070	0.022	0.015	0.521
240	1.8	0.50	4.00	0.36	0.007	0.070	0.021	0.014	0.530
run # L3 W/F_{To} = 45.94									
00	5.0	1.40	7.30	0.14	0.028	0.070	0.024	0.016	0.710
40	4.3	1.40	6.70	0.16	0.015	0.052	0.018	0.013	0.740
80	4.1	1.40	6.20	0.16	0.013	0.045	0.017	0.012	0.750
120	3.8	1.40	5.40	0.17	0.008	0.042	0.016	0.011	0.755
200	3.3	1.40	5.20	0.17	0.007	0.041	0.015	0.010	0.758
run # L4 , W/F_{To} = 46.03									
00	4.8	0.50	2.20	0.21	0.051	0.104	0.039	0.024	0.567
40	2.4	0.50	1.90	0.23	0.028	0.098	0.036	0.022	0.581
80	2.1	0.50	1.80	0.24	0.024	0.095	0.036	0.022	0.585

120	1.6	0.50	1.70	0.25	0.018	0.085	0.031	0.021	0.594
200	1.2	0.50	1.60	0.26	0.014	0.075	0.028	0.020	0.607

run # L5 , W/F_{To} = 56.75

00	4.2	1.50	6.50	0.10	0.028	0.075	0.021	0.017	0.750
40	4.0	1.50	5.30	0.11	0.016	0.073	0.020	0.017	0.755
80	3.8	1.50	5.10	0.12	0.015	0.070	0.020	0.016	0.760
120	3.6	1.50	4.95	0.12	0.012	0.062	0.020	0.015	0.762
200	3.4	1.50	4.70	0.13	0.010	0.050	0.017	0.014	0.780
240	3.2	1.50	4.60	0.13	0.009	0.045	0.015	0.013	0.785

run # L6 , W/F_{To} = 61.29

00	6.2	1.40	6.50	0.044	0.024	0.065	0.015	0.016	0.830
40	5.2	1.40	5.80	0.060	0.010	0.037	0.009	0.012	0.851
80	4.8	1.40	5.20	0.065	0.007	0.032	0.009	0.009	0.878
120	4.3	1.40	4.80	0.066	0.006	0.031	0.009	0.009	0.880
200	4.2	1.40	4.20	0.066	0.005	0.030	0.008	0.008	0.885

Temperature = 683 K

run # M1 , W/F_{To} = 15.54

00	9.0	1.20	4.0	0.046	0.097	0.020	0.006	0.004	0.894
40	7.2	1.20	3.2	0.065	0.081	0.016	0.005	0.003	0.901
80	6.5	1.20	3.0	0.066	0.071	0.015	0.005	0.003	0.902
120	5.9	1.20	2.7	0.068	0.050	0.012	0.004	0.002	0.904

run # M2 , W/F_{To} = 21.45

00	9.0	2.1	9.4	0.083	0.021	0.058	0.024	0.014	0.790
40	7.9	2.1	8.2	0.095	0.011	0.050	0.020	0.012	0.810
80	7.0	2.0	7.2	0.098	0.009	0.042	0.018	0.010	0.820
120	5.9	2.1	6.6	0.100	0.006	0.040	0.016	0.010	0.830
200	4.8	2.1	5.8	0.110	0.004	0.030	0.012	0.008	0.855

run # M3 , W/F_{To} = 22.95

00	8.1	1.7	8.3	0.145	0.026	0.074	0.030	0.017	0.710
40	6.8	1.7	6.8	0.160	0.013	0.065	0.026	0.015	0.715
80	5.5	1.7	5.9	0.162	0.011	0.060	0.025	0.015	0.721
120	4.9	1.7	5.4	0.170	0.009	0.050	0.020	0.012	0.732
200	3.8	1.7	4.4	0.174	0.007	0.044	0.016	0.010	0.752
240	3.3	1.7	3.9	0.177	0.006	0.042	0.015	0.010	0.760

run # M4 , W/F_{To} = 14.66

00	5.0	1.60	5.8	0.222	0.022	0.075	0.032	0.017	0.630
40	3.7	1.60	4.7	0.232	0.014	0.067	0.027	0.016	0.642
80	2.7	1.60	4.1	0.240	0.010	0.063	0.024	0.014	0.650
120	2.3	1.60	3.8	0.242	0.009	0.060	0.022	0.013	0.656
200	1.8	1.60	3.7	0.243	0.007	0.055	0.021	0.013	0.658
240	1.3	1.60	3.6	0.250	0.005	0.050	0.020	0.013	0.665

run # M5 , W/F_{To} = 14.61

00	7.9	1.0	2.6	0.330	0.037	0.062	0.032	0.013	0.520
40	7.2	1.0	2.0	0.348	0.022	0.060	0.028	0.011	0.532
80	6.3	1.0	1.9	0.354	0.018	0.055	0.024	0.010	0.535
120	5.9	1.0	1.8	0.356	0.017	0.050	0.023	0.010	0.544
200	4.7	1.0	1.6	0.360	0.014	0.044	0.020	0.008	0.555

run # M6 , W/F_{To} = 19.83

00	5.4	1.0	3.0	0.326	0.034	0.110	0.027	0.016	0.500
40	3.3	1.0	2.4	0.337	0.020	0.096	0.020	0.016	0.502
80	2.6	1.0	2.2	0.344	0.017	0.085	0.018	0.015	0.508
120	2.2	1.0	1.9	0.350	0.013	0.080	0.016	0.015	0.510
180	1.5	1.0	1.8	0.352	0.011	0.072	0.014	0.014	0.515
240	1.2	1.0	1.5	0.360	0.009	0.065	0.013	0.012	0.524

run # M7 , W/F_{To} = 19.03

00	8.4	1.8	9.2	0.350	0.062	0.154	0.055	0.030	0.344
40	7.6	1.8	8.2	0.375	0.040	0.140	0.050	0.024	0.370

80	7.0	1.8	7.8	0.382	0.034	0.130	0.046	0.024	0.375
120	6.4	1.8	7.5	0.390	0.033	0.125	0.038	0.023	0.381
180	5.4	1.8	7.0	0.400	0.028	0.110	0.030	0.020	0.394

Temperature 703 K

run # N1 , W/F_{To} = 5.78

00	16.0	3.0	08.1	0.300	0.041	0.141	0.050	0.027	0.440
40	11.0	3.0	05.4	0.310	0.033	0.128	0.044	0.023	0.460
80	08.2	3.0	04.3	0.318	0.030	0.124	0.040	0.022	0.463
120	06.7	3.0	03.7	0.320	0.026	0.123	0.033	0.022	0.465
200	04.8	3.0	03.1	0.323	0.024	0.116	0.033	0.022	0.470
240	04.3	3.0	02.5	0.323	0.023	0.114	0.032	0.021	0.475
300	03.4	3.0	02.0	0.330	0.021	0.104	0.032	0.020	0.480

run # N2 , W/F_{To} = 14.45

00	16.6	2.5	10.2	0.240	0.080	0.180	0.052	0.040	0.365
40	13.8	2.5	8.5	0.265	0.062	0.180	0.050	0.038	0.385
80	10.8	2.5	7.7	0.270	0.052	0.180	0.047	0.037	0.395
180	9.8	2.5	7.4	0.284	0.048	0.175	0.042	0.035	0.400
280	8.8	2.5	7.2	0.286	0.044	0.175	0.038	0.036	0.410
360	8.4	2.5	6.9	0.290	0.042	0.168	0.035	0.040	0.416

run # N3 , W/F_{To} = 9.35

00	9.3	6.3	24.5	0.060	0.007	0.085	0.015	0.020	0.815
40	8.0	6.3	23.2	0.061	0.006	0.060	0.013	0.015	0.840
120	7.4	6.3	22.4	0.064	0.005	0.055	0.013	0.014	0.846
180	6.9	6.3	22.1	0.062	0.005	0.054	0.012	0.014	0.846
240	6.8	6.3	22.0	0.061	0.005	0.048	0.012	0.013	0.847
360	6.6	6.3	21.7	0.063	0.004	0.041	0.010	0.011	0.850

run # N4 , W/F_{To} = 15.15

00	11.2	6.0	20.0	0.075	0.020	0.110	0.029	0.033	0.730

40	10.0	6.0	17.0	0.083	0.015	0.094	0.025	0.025	0.751
120	8.2	6.0	14.7	0.085	0.014	0.090	0.023	0.022	0.762
200	7.5	6.0	14.6	0.085	0.014	0.090	0.023	0.022	0.762
300	7.1	6.0	14.4	0.086	0.012	0.086	0.021	0.021	0.770
400	6.7	6.0	13.8	0.090	0.010	0.081	0.018	0.019	0.782
run # N5 , W/F_{To} = 14.31									
00	13.0	2.4	14.0	0.130	0.032	0.140	0.031	0.033	0.630
40	10.2	2.4	11.2	0.139	0.027	0.126	0.028	0.028	0.652
120	7.9	2.4	7.3	0.144	0.023	0.105	0.027	0.028	0.671
200	5.9	2.3	6.8	0.145	0.022	0.104	0.022	0.027	0.670
300	4.3	2.4	5.3	0.145	0.022	0.110	0.022	0.027	0.673
run # N6 , W/F_{To} = 8.87									
00	14.4	3.5	10.8	0.188	0.041	0.150	0.045	0.033	0.540
40	11.5	3.0	08.1	0.210	0.030	0.120	0.032	0.027	0.583
80	09.4	3.0	06.8	0.214	0.026	0.115	0.029	0.026	0.586
120	07.4	3.0	05.8	0.218	0.024	0.105	0.026	0.025	0.596
200	05.5	3.0	05.0	0.219	0.021	0.102	0.022	0.024	0.607
280	3.7	2.9	04.2	0.222	0.021	0.110	0.021	0.022	0.611
360	3.2	3.0	03.8	0.222	0.020	0.110	0.021	0.022	0.613
420	2.8	2.9	03.5	0.231	0.018	0.102	0.019	0.020	0.623
run # N7 , W/F_{To} = 17.48									
00	9.3	1.3	6.8	0.330	0.070	0.180	0.062	0.040	0.310
40	7.9	1.3	6.1	0.342	0.060	0.172	0.061	0.039	0.316
120	6.9	1.3	6.0	0.357	0.050	0.170	0.055	0.040	0.320
240	5.7	1.3	5.7	0.363	0.041	0.171	0.053	0.040	0.323
320	5.3	1.3	5.4	0.368	0.038	0.164	0.045	0.037	0.341
400	4.9	1.3	5.1	0.371	0.035	0.157	0.041	0.033	0.356

Temperature = 723 K

run # 01 , W/F_{To} = 17.39

00	4.0	4.0	19.5	0.035	0.003	0.050	0.016	0.013	0.885
40	3.8	4.0	16.2	0.035	0.003	0.048	0.015	0.013	0.885
200	3.7	4.0	14.5	0.035	0.003	0.047	0.014	0.013	0.887
280	3.4	4.0	14.0	0.036	0.003	0.038	0.013	0.012	0.900
360	3.1	4.0	13.6	0.038	0.002	0.035	0.010	0.010	0.907

run # 02 , W/F_{To} = 18.88

00	10.0	3.2	15.0	0.052	0.013	0.092	0.020	0.025	0.795
40	8.5	3.2	13.3	0.055	0.012	0.070	0.018	0.022	0.821
80	7.8	3.2	12.2	0.057	0.011	0.060	0.015	0.020	0.836
120	7.4	3.2	11.6	0.057	0.010	0.060	0.017	0.017	0.844
200	7.0	3.2	11.3	0.058	0.009	0.060	0.013	0.015	0.845
280	6.7	3.2	10.8	0.059	0.009	0.058	0.012	0.014	0.847
360	6.4	3.2	10.4	0.060	0.009	0.053	0.013	0.013	0.855

run # 03 , W/F_{To} = 15.59

00	17.1	3.3	19.5	0.051	0.036	0.161	0.058	0.050	0.658
40	12.6	3.3	16.5	0.061	0.030	0.153	0.045	0.043	0.666
80	11.0	3.3	15.0	0.067	0.027	0.147	0.038	0.041	0.683
120	09.6	3.3	12.5	0.068	0.025	0.146	0.035	0.041	0.688
240	06.9	3.3	10.7	0.073	0.018	0.142	0.028	0.041	0.688
320	05.9	3.3	10.0	0.075	0.015	0.141	0.027	0.040	0.690
420	4.8	3.3	09.1	0.077	0.013	0.137	0.025	0.038	0.697

run # 04 , W/F_{To} = 13.97

00	16.4	4.5	15.4	0.120	0.037	0.180	0.050	0.035	0.570
40	12.8	4.5	12.6	0.132	0.031	0.135	0.042	0.030	0.630
120	10.6	4.5	10.6	0.145	0.025	0.112	0.030	0.024	0.666
200	9.4	4.5	9.8	0.145	0.021	0.110	0.027	0.023	0.671
280	8.4	4.5	9.5	0.148	0.020	0.105	0.022	0.021	0.676
320	8.1	4.5	9.4	0.152	0.019	0.094	0.022	0.021	0.685

440	7.3	4.5	9.0	0.155	0.017	0.092	0.021	0.020	0.693

run # 05 , W/F_{To} = 8.88

00	15.0	3.7	15.6	0.200	0.033	0.131	0.046	0.031	0.560
40	12.3	3.7	12.7	0.207	0.037	0.123	0.046	0.028	0.570
80	9.7	3.7	11.8	0.212	0.028	0.122	0.043	0.027	0.581
120	8.8	3.7	11.5	0.218	0.021	0.110	0.038	0.026	0.586
200	8.3	3.7	11.1	0.220	0.019	0.106	0.031	0.023	0.600
280	7.3	3.7	10.5	0.224	0.016	0.098	0.027	0.022	0.610
360	6.9	3.7	9.8	0.226	0.015	0.094	0.025	0.021	0.616

run # 06 , W/F_{To} = 5.87

00	16.3	2.8	09.1	0.295	0.050	0.160	0.060	0.036	0.410
40	11.5	2.8	06.9	0.304	0.040	0.142	0.052	0.032	0.425
80	09.1	2.8	05.5	0.312	0.032	0.141	0.051	0.031	0.432
120	07.5	2.8	04.9	0.316	0.030	0.138	0.042	0.030	0.442
240	04.7	2.8	03.6	0.322	0.023	0.134	0.040	0.030	0.447

run # 07 , W/F_{To} = 14.36

00	14.1	1.7	10.8	0.255	0.070	0.212	0.065	0.042	0.353
40	13.2	1.7	9.9	0.256	0.062	0.210	0.061	0.045	0.355
120	12.7	1.7	9.8	0.265	0.060	0.201	0.062	0.044	0.362
240	12.3	1.7	9.4	0.266	0.058	0.196	0.044	0.042	0.372
360	11.6	1.7	9.0	0.270	0.056	0.190	0.041	0.043	0.391

Catalyst particle diameter = 1.68 mm

Temperature = 683 K

run # P1 , W/F_{To} = 18.87

00	9.5	0.5	3.7	0.326	0.092	0.133	0.040	0.026	0.372
40	6.3	0.5	2.5	0.365	0.056	0.101	0.040	0.020	0.384
80	5.4	0.5	2.3	0.395	0.044	0.100	0.035	0.018	0.410
120	5.0	0.5	2.1	0.400	0.041	0.090	0.034	0.017	0.425

180	4.7	0.5	2.0	0.403	0.040	0.085	0.032	0.016	0.428
240	4.4	0.5	1.9	0.408	0.035	0.080	0.029	0.016	0.433
run # P2 , W/F_{To} = 17.40									
00	9.9	0.6	4.0	0.297	0.061	0.102	0.036	0.018	0.486
40	6.2	0.6	2.6	0.316	0.042	0.090	0.032	0.017	0.500
80	5.4	0.6	2.2	0.334	0.034	0.083	0.029	0.016	0.509
120	4.8	0.6	2.1	0.335	0.030	0.074	0.025	0.015	0.520
240	4.1	0.6	2.0	0.341	0.026	0.066	0.024	0.014	0.528
run # P3 , W/F_{To} = 16.6									
00	09.2	1.8	6.5	0.200	0.050	0.086	0.024	0.018	0.635
40	7.5	1.8	4.9	0.210	0.036	0.085	0.023	0.017	0.639
80	6.5	1.8	4.0	0.215	0.031	0.080	0.022	0.016	0.640
120	5.4	1.8	3.5	0.220	0.029	0.070	0.021	0.014	0.655
200	4.6	1.8	3.1	0.228	0.024	0.060	0.020	0.012	0.660
run # P4 , W/F_{To} = 20.58									
00	09.2	0.6	5.7	0.125	0.041	0.095	0.023	0.020	0.688
40	6.4	0.6	4.5	0.148	0.025	0.067	0.022	0.015	0.722
80	5.3	0.6	3.8	0.152	0.021	0.063	0.021	0.014	0.726
120	5.1	0.6	3.4	0.156	0.020	0.057	0.018	0.012	0.752
240	4.3	0.6	3.0	0.165	0.015	0.044	0.011	0.010	0.756
run # P5 , W/F_{To} = 20.22									
00	09.2	2.4	7.6	0.077	0.028	0.058	0.018	0.016	0.798
40	8.9	2.4	7.0	0.088	0.015	0.053	0.017	0.013	0.811
80	7.0	2.3	6.3	0.091	0.014	0.050	0.017	0.012	0.817
120	6.4	2.4	5.9	0.094	0.012	0.041	0.015	0.010	0.830
200	5.8	2.4	5.1	0.097	0.010	0.032	0.011	0.008	0.842
240	4.9	2.3	4.5	0.100	0.010	0.028	0.011	0.007	0.845
run # P6 , W/F_{To} = 24.22									
00	10.9	1.5	6.2	0.030	0.011	0.028	0.009	0.006	0.914

40	6.6	1.5	5.0	0.034 0.007 0.024 0.008 0.005 0.921
80	5.6	1.5	4.6	0.035 0.006 0.022 0.007 0.005 0.925
120	5.1	1.5	4.3	0.035 0.006 0.021 0.007 0.005 0.928
180	4.4	1.5	4.0	0.037 0.005 0.017 0.006 0.004 0.930

run # P7 , W/F_{To} = 17.03

00	13.5	1.6	11.0	0.053 0.017 0.050 0.012 0.012 0.860
40	9.9	1.6	8.6	0.059 0.012 0.037 0.011 0.008 0.871
80	9.0	1.6	8.1	0.060 0.011 0.035 0.011 0.008 0.874
120	8.7	1.6	8.0	0.060 0.010 0.034 0.011 0.008 0.877
240	8.2	1.6	7.5	0.061 0.010 0.033 0.010 0.007 0.880

APPENDIX IV

NONLINEAR OPTIMIZAION COMPUTER PROGRAMME

This programme has been used to estimate the various reactions constants for the main and deactivation kinetics.

```
      ************************************************************
C        PARAMETERS:                        X(I)
C        NO OF EXPERIMENTAL POINTS (M) M
C        NO OF PARAMETERS (N)               N
C        DEPENDENT VARIABLES(1):            Y(I)
C        ************************************************888
C        STANDARD DEVIATION OF THE PARAMETERS : SD1
C      ------------------------------------------------------------
      DIMENSION FJAC(94,10),FVEC(94),G(1240),S(94),V(10,10),W(1240)
       DIMENSION IW(1240),Y(94),PC(94),PH(94),PCO(94),PW(94),T(94)
        DIMENSION A(10,10),X(10),YT(94),YC(94),PT(94),PB(94),YM(94)
         DIMENSION PRO(94),SSSQ(94)
         EXTERNAL LSQFUN,LSQMON
         COMMON Y,PT,PB,PH,PCO,PC,PW,T,PRO
         M=94
         N=10
         OPEN(UNIT=6,DEVICE='DSK',FILE='RES.DAT')
         WRITE(21,75)
         READ(39,*)(X(J),J=1,N)
         DO 120 I=1,M
         READ(39,*)Y(I),YT(I),YC(i),YM(I),PT(I),PB(I),PH(I),PCO(I),
         1PC(I),PW(I),T(I)
C        TYPE*, Y(I),YT(I),YC(i),YM(I),PT(I),PB(I),PH(I),PCO(I),
C        1PC(I),PW(I),T(I)
120      CONTINUE
C-------------------------------      ----------------------------
         WRITE(21,*) (X(J),J=1,N)
         LIW=1240
         LW=1240
         LJ=94
         LJC=94
         LV=10
         IPRINT=1
         MAXCAL=600*N
         ETA=.3
         XTOL=10.*SQRT(X02AAF(XTOL))
```

```
      STEPMX=100000.0
      IFAIL=1
      CALL E04FCF(M,N,LSQFUN,LSQMON,IPRINT,MAXCAL,ETA,XTOL,STEPMX,
     1X,FSUMSQ,FVEC,FJAC,LJ,S,V,LV,NITER,NF,IW,LIW,W,LW,IFAIL)
      WRITE(21,86) (X(J),J=1,N)
      WRITE(21,101) IFAIL
      WRITE (21,102) FSUMSQ
C     WRITE(21,*)(X(J),J=1,N)
      CALL LSQGRD(M,N,FVEC,FJAC,LJ,G)
      DO 121 I=1,N
      DO 121 J=1,N
      A(I,J)=0.0
C     DO 21 I=1,N
C     DO 21 J=1,N
      DO 122 KK=1,M
      A(I,J)=A(I,J)+FJAC(KK,I)*FJAC(KK,J)
122   CONTINUE
121   CONTINUE
      DO 600 I=1,N
600   WRITE(21,85) (A(I,J),J=1,N)
      CALL STADEV(X,A,N,M,FSUMSQ)
      WRITE(21,105)
      WRITE(21,191)
      RSS=0.0
      SSQ=0.0
      SUM=0.0
      DO 40 I=1,M
      PRO(I)=PB(I)+PC(I)+PH(I)
      C=693./T(I)-1.
     ANUU=(X(1)*EXP(-X(2)*C)*EXP(X(4)*C)*EXP(X(6)*C)*PT(I)*PW(I))
      DE1=((1.+X(3)*EXP(X(4)*C)*(PW(I))))
     DE2=((1.+X(5)*EXP(X(6)*C)*PT(I)+X(7)*EXP(X(8)*C)*(PCO(I)**2)
     1+X(9)*EXP(X(10)*C)*PRO(I)))
      SS=ANUU/(DE1*(DE2))
      FVEC(I)=SS-Y(I)
      ABBA=ABS(FVEC(I)/Y(I))/FLOAT(M)
      SSQ=(SSQ+ABBA/Y(I))/M
      SSSQ(I)=(SSSQ(I)+ABS(FVEC(I)/Y(I)))
```

```
      DE11=((1.+XC(3)*EXP(XC(4)*C)*(PW(I))))
      DE22=((1.+XC(5)*EXP(XC(6)*C)*PT(I)+XC(7)*EXP(XC(8)*C)*
     1(PCO(I)**2)
     1+XC(9)*EXP(XC(10)*C)*PRO(I)))
      RES=ANU/(DE11*(DE22))
      FVECC(I)=RES-Y(I)
20    CONTINUE
      RETURN
      END
C     ------------------------------------------------------------
      SUBROUTINE LSQMON(M,N,XC,FVECC,FJACC,LJC,S,IGRADE,NITER,NF,IW
     1,LIW,W,LW)
      DIMENSION FJACC(94,10),FVECC(94),S(94),W(1240),XC(10),IW(1240),
     1G(1240),T(94)
      COMMON Y,PT,PB,PH,PCO,PC,PW,T,PRO
      FSUMSQ=F01DEF(FVECC,FVECC,M)
      CALL LSQGRD(M,N,FVECC,FJACC,LJC,G)
      GTG=F01DEF(G,G,N)
C     WRITE(21,107) NITER,NF,FSUMSQ,IGRADE
      DO 20 J=1,N
C     WRITE(21,108)
C108  FORMAT(/8X,'X',20X,'G',11X,'SINGULAR VALUE'/)
C     WRITE(21,109) XC(J)
C109  FORMAT(/2X,'XC=',2X,E15.8)
20    CONTINUE
C107  FORMAT(//2X,'ITNS',4X,'FEVALS',10X,'SUMSQ',13X,'GRADE',
C     18X,I4,6X,I5,6X,E15.8,2X,I3)
      RETURN
      END
C     ++++++++++++++++++++++++++++++++++++++++++++++++++++++++++++
      SUBROUTINE LSQGRD(M,N,FVECC,FJACC,LJC,G)
      DIMENSION FJACC(94,10),FVECC(94),G(1240),LJC(94)
      DO 40 J=1,N
      SUM=0.0
      DO 20 I=1,M
      SUM=SUM+FJACC(I,J)*FVECC(I)
20    CONTINUE
      G(J)=SUM+SUM
```

```
40      CONTINUE
        RETURN
        END
C-------------------------------------------------------------------
C       THE FOLLOWING SUBROUTINE FINDS OUT STANDARD DEVIATION
C-------------------------------------------------------------------
        SUBROUTINE STADEV(X,FF,N,M,RSSQ)
        DIMENSION X(10),FF(10,10),FFT(10,10),FY(10)
        INDIC=-1
        DO 10 I=1,N
        DO 10 J=1,N
        FFT(I,J)=FF(I,J)
10      CONTINUE
        CALL MATINV(N,FFT,FY,-1,10)
        SIGMA1=RSSQ/(FLOAT(M-N))
        DO 15 I=1,N
        DO 15 J=1,N
        IF(I.EQ.J) GO TO 20
        GO TO 15
20      FFT(I,J)=SIGMA1*FFT(I,J)
        SD2=FFT(I,J)
        SD1=SQRT(ABS(FFT(I,J)))
        WRITE(21,456)
456     FORMAT(10X,'THE FINAL VALUE OF THE PARAMETER'/)
        WRITE(21,302) J,X(J),SD1,RSSQ
302     FORMAT (10X,'X(',I2,')=',E10.5,3X,'SD1=',E15.8,3X,'RSSQ='
        ,E15.8)
15      CONTINUE
        RETURN
        END
C-------------------------------------------------------------------

C       SUBROUTINE FOR INVERSION OF MATRIX
        SUBROUTINE MATINV(N,A,X,INDIC,NRC)
        DIMENSION IROW(10),JCOL(10),JORD(10),Y(10),A(10,10),X(10)
        EPS=1.E-25
        IF (INDIC.GE.0) MAX=N+1
        MAX=N
        IF(N.LE.20) GO TO 5
```

```
      GO TO 75
5     DETER=1.
      DO 18 K=1,N
      KM1=K-1
      PIVOT=0.0
      DO 11 I=1,N
      DO 11 J=1,N
      IF(K.EQ.1) GO TO 9
      DO 8 ISCAN=1,KM1
      DO 8 JSCAN=1,KM1
      IF(I.EQ.IROW(ISCAN)) GO TO 11
      IF(J.EQ.JCOL(JSCAN)) GO TO 11
8     CONTINUE
9     IF(ABS(a(i,j)).le.Abs(pivot)) GO TO 11
      PIVOT=A(I,J)
      IROW(K)=I
      JCOL(K)=J
11    CONTINUE
      IF(ABS(PIVOT).GT.EPS) GO TO 13
      GO TO 76
13    IROWK=IROW(K)
      JCOLK=JCOL(K)
      DETER=DETER*PIVOT
      DO 14 J=1,MAX
      A(IROWK,J)=A(IROWK,J)/PIVOT
14    CONTINUE
      A(IROWK,JCOLK)=1./PIVOT
      DO 18 I=1,N
      AIJCK=A(I,JCOLK)
      IF(I.EQ.IROWK) GO TO 18
      A(I,JCOLK)=-AIJCK/PIVOT
      DO 17 J=1,MAX
      IF(J.NE.JCOLK) A(I,J)=A(I,J)-AIJCK*A(IROWK,J)
17    CONTINUE
18    CONTINUE
      DO 20 I=1,N
      IROWI=IROW(I)
      JCOLI=JCOL(I)
```

```
      JORD(IROWI)=JCOLI
      IF(INDIC.GE.0) X(JCOLI)=A(IROWI,MAX)
20    CONTINUE
      INTCH=0
      NM1=N-1
      DO 22 I=1,NM1
      IP1=I+1
      DO 22 J=IP1,N
      IF(JORD(J).GE.JORD(I)) GO TO 22
      JTEMP=JORD(J)
      JORD(J)=JORD(I)
      JORD(I)=JTEMP
      INTCH=INTCH+1
22    CONTINUE
      IF(INTCH/2*2.NE.INTCH) DETER=-DETER
      IF(INDIC.LE.0) GO TO 26
      GO TO 77
26    DO 28 J=1,N
      DO 27 I=1,N
      IROWI=IROW(I)
      JCOLI=JCOL(I)
      Y(JCOLI)=A(IROWI,J)
27    CONTINUE
      DO 28 I=1,N
      A(I,J)=Y(I)
28    CONTINUE
      DO 30 I=1,N
      DO 29 J=1,N
      IROWJ=IROW(J)
      JCOLJ=JCOL(J)
      Y(IROWJ)=A(I,JCOLJ)
29    CONTINUE
      DO 30 J=1,N
30    A(I,J)=Y(J)
76    WRITE(21,303)
77    WRITE(21,305)
75    WRITE(21,301)
C     DO 45 I=1,N
```

```
      IF (I.EQ.J) GO TO 45
      GO TO 43
C45   WRITE(21,302)(A(I,J),J=1,N)
45    WRITE(21,302) A(I,J)
43    CONTINUE
301   FORMAT(/10X,'MATRIX INVERSE IS CALLED'/)
303   FORMAT(10X,'FIRST STATMENT')
305   FORMAT(10X,'THIRD STATMENT')
302   FORMAT(10X,10(4X,E15.8)/)
      RETURN
      END
```

APPENDIX V

COMPUTER PROGRAME TO SOLVE PELLET EQUATIONS USING ORTHOCOLLOCATION METHOD

```
C    PROGRAMME TO CALCULATE THE PARTIAL PRESSURES AS FUNCTION OF
C    PELLET RADIUS
C    NO OF COLLOCATION POINTS USED = 5
C  1    REFERES TO TOLUENE COMPONENT
C  2    REFERS TO WATER    COMPONENT
C  3    REFERS TO BENZENE COMPONENT
C  4    REFERS TO CO       COMPONENT
C  5    REFERS TO CO2      COMPONENT
C  6    REFERS TO H2       COMPONENT
C  M    NO OF REACTION COMPONENT =  6
C       FI(1)    TOLUENE FEED RATE (KG MOLE/HR)
C       FI(2)    WATER   FEED RATE (KG MOLE/HR)
C       WCT      CATALYST WEIGHT   (KG)
C       WT       WEIGHT OF RESIDUALS IN ORTHO-COLLOCATION
C       RC       HYDRAULIC RADIUS FOR CYLINDER = 4*(Vp/Sx)
C       TEND     TOTAL TIME AT THE RUN COMPLETION
C       DELT     TIME INCREMENT
C       ACT1     ACTIVITY FOR REACTION I
C       ACT3     ACTIVITY FOR REACTION III
C       PHIj A CONSTANT = PELLET DENSITY* GAS CONST.*TEMP./(RC)**2
C       Di       EFFECTIVE DIFFUSIVITY OF COMPONENT i
C  ------------------------------------------------------------
      DIMENSION F(5),WT(6)
      DIMENSION R10(6),R20(6),R30(6),PP(6,6),PE(6),FI(6),FOT(25)
      DIMENSION PPN(6,6),Y(210),B(6,6),PEN(6)
      DIMENSION DA1DT(6),DA3DT(6),AVGR(5),X(210),W(25,5)
      DIMENSION BBB(25)
      COMMON/SAM/PP,T,PE,N
      COMMON/OMAR/ACT1(6),ACT3(6),R10,R20,R30
      OPEN(UNIT=22,FILE='OUT.FOR')
      WT(1)=0.050
      wt(2)=0.104
      WT(3)=0.13
      WT(4)=0.121
      WT(5)=0.08
      WT(6)=0.014
      N=5
C     XTOL=10.*SQRT(X02AAF(XTOL))
```

```
      READ(31,*) FI(1),FI(2),PE(1),PE(2),PE(3),PE(4),PE(5),PE(6)
     1,WCT,T
C       ------------------------------------------------------------
       WRITE(22,*)  FI(1),FI(2),PE(1),PE(2),PE(3),PE(4),PE(5),PE(6)
     1,WCT,T
       WRITE(22,102)
102       FORMAT(5X,20('--'))
       TEND=5.0/60
       TIME=0.0
       DELT=1.0/60.0
       DO 919 K=1,N
       ACT1(K)=1.0
       ACT3(K)=1.0
919       CONTINUE
101       DO 70 J=1,6
70        PP(N+1,J)=PE(J)
401       DO 1013 I=1,N
       DO 1003 J=1,6
       PP(I,J)=PE(J)
1003      CONTINUE
1013      CONTINUE
201       DO 119 I=1,N
       X(I)=PP(I,1)
       X(I+N)=PP(I,2)
       X(I+2*N)=PP(I,3)
       X(I+3*N)=PP(I,4)
       X(I+4*N)=PP(I,5)
119       CONTINUE
       PRINT,EXECUTION IS ON DO NOT COME NEAR ME
       N1=5*N
       IPRINT=0
       NUMSIG=5
       MAXIT=200
       ASTER=1.0
       EPS=1.0E-03
       ND=22
       CALL NONLIN(N1,NUMSIG,MAXIT,IPRINT,X,EPS,ASTER,ND)
       DT=0.0234*SQRT((T/323.)*2/92.11)
       DW=0.0234*SQRT((T/323.)*2/18.0)
```

```
      DB=0.0234*SQRT((T/323.)*2/78.11)
      DC1=0.0234*SQRT((T/323.)*2./28.)
      DC=0.0234*SQRT((T/323.)*2/44.)
      DH=0.0234*SQRT((T/323.))
      RC=0.0127/12.0
      PHI=956.0*0.082*T*(RC)**2
      PHIT=PHI*1.0/DT
      PHIW=PHI/DW
      PHIB=PHI/DB
      PHIC1=PHI/DC1
      PHIC=PHI/DC
      PHIH=PHI/DH
      DO 112 I=1,N
      PP(I,1)=X(I)
      PP(I,2)=X(I+N)
      PP(I,3)=X(I+2*N)
      PP(I,4)=X(I+3*N)
      PP(I,5)=X(I+4*N)
      PP(I,6)=-9.*(DB/DH)*(PP(I,3)-PE(3))-11.*DT/DH*(PP(I,1)-PE(1))
     1  +DC/DH*(PP(I,5)-PE(5))+PE(6)
112   CONTINUE
      WRITE(22,1101)
1101  FORMAT(5X,'PP(I,1)',5X,'PP(I,2)',5X,'PP(I,3)',5X,'PP(I,4)',5X
     1,'PP(I,5)',5X,'PP(I,6)'/)
      WRITE(22,202)
202   FORMAT(5X,20('--'))
      DO 1009 I=1,N+1
1009     CONTINUE
C     CALCULATION OF AVERAGE RATES BY NUMERICAL INTEGRATION
C     ------------------------------------------------
      AR1=0.0
      AR2=0.0
      AR3=0.0
      DO 15 I=1,N
      AR1=AR1+2.*(R10(I)*WT(I)*ACT1(I))
      AR2=AR2+2.*(R20(I)*WT(I))
      AR3=AR3+2.*(R30(I)*ACT3(I)*WT(I))
      PRINT *, AR1,AR2,AR3
```

```
15    CONTINUE
      WRITE(22,901)
901 FORMAT(5X,'AVERAGE RATE RXN I.=',5X,'AVEG.RATE RXN II=',5X
  1    ,'AVEG.RATE RXN III='/)
      WRITE(22,92) AR1,AR2,AR3
92    FORMAT(10X,E15.8,10X,E15.8,10X,E15.8)
C     MASS BALANCE ON FLOW RATES + DISAPPEARANCE AND REACTION RATES
C     WCT = WEIGHT OF CATALST IN Kg
      FOT(1)=FI(1)-(AR1+AR2)*WCT
      FOT(2)=FI(2)-(AR1+7.*AR2+AR3)*WCT
      FOT(3)=(AR1)*WCT
      FOT(4)=(AR1+7.*AR2-AR3)*WCT
      FOT(5)=(AR3)*WCT
      FOT(6)=(2.*AR1+11.*AR2+AR3)*WCT
C     ------------------------------------------------------------
C     FINDING PARTIAL PRESSURE OF REACTION COMPONENTS
      FOUT=0.0
      DO 16 I=1,6
      FOUT=FOT(I)+FOUT
16    CONTINUE
C     ------------------------------------------------------------
C     OBJECTIVE FUNCTION 2 FOR PARTIAL PARTIAL PRESSURES
      OBJ2=0.0
      DO 17 I=1,6
      PEN(I)=FOT(I)/FOUT
      PRINT 999,PEN(I)
999   FORMAT(3X,'PEN=',F10.8)
      WRITE(22,907) PEN(I)
907   FORMAT(5X,'PEN(I)=',F10.6)
      OBJ2=OBJ2+(PEN(I)-PE(I))**2
      IF (PEN(I).LE.0.0) PEN(I)=0.0
17    CONTINUE
      IF (OBJ2.LE.0.00001) GO TO 500
      GO TO 600
600   DO 18 I=1,6
      PE(I)=PEN(I)
   PP(I,6)=-9.*(DB/DH)*(PP(I,3)-PE(3))-11.*DT/DH*(PP(I,1)-PE(1))
  1   +DC/DH*(PP(I,5)-PE(5))+PE(6)
```

```
18    CONTINUE
      GO TO 401
500 WRITE (22,777)
777 FORMAT(5X,'PARTIAL PRES(PEN) BASED ON MOLES,AVG.RATES,ACT,'/)
      WRITE(22,302)
302   FORMAT(5X,40('--'))
      DO 311 I=1,N
      PRINT ,AR1,AR2,AR3
      WRITE(22,778) PEN(I),AR1,AR2,AR3
778   FORMAT(5X,6(10X,E15.8))
311   CONTINUE
C     ------------------------------------------------------------
      TIME=TIME+DELT
      IF (TIME.GE.TEND) GO TO 700
      GO TO 707
707   CONTINUE
      AKD1=1.164E2*EXP(-3855/(1.987*T))
      AKD2=1.183E3*EXP(-9137/(1.987*T))
      AKD3=14.13*EXP(-1194/(1.987*T))
      AKD4=57.06*EXP(-6423/(1.987*T))
      AAKW=0.096*EXP(3039/(1.987*T))
      DO 19 I=1,N
      DA1DT(I)=(AKD1*PP(I,4)+AKD2*(PP(I,1)+PP(I,3)))*(ACT1(I))**2
     1 /(1.+AAKW*PP(I,2))
      DA3DT(I)=(AKD3*PP(I,4)*PP(I,2)+AKD4*(PP(I,1)+PP(I,3)))
     1 *(ACT3(I)**2)/(1.+AAKC1*PP(I,4))
      ACT1(I)=ACT1(I)-DA1DT(I)*DELT
      ACT3(I)=ACT3(I)-DA3DT(I)*DELT
19    CONTINUE
C     WRITE(22,404)
404   FORMAT(5X,'ACTIVITY ONE',10X,'ACTIVITY THREE'/)
C     WRITE(22,405) ACT1,ACT3
405   FORMAT(15X,F7.5,15X,F7.5)
      GO TO 201
700   STOP
      END
C     ++++++++++++++++++++++++++++++++++++++++++++++++++++++++++++
      SUBROUTINE AUXFCN(X,FVECK,M)
```

```
C     NNN= NUMBER OF EQUATION TO BE SOLVED =5*N
C     X  = GUESS VALUES OF PP(I,J)
      DIMENSION FVEC(210),PP(6,6),RES(210),C(25,25),
     1  B(6,6),BBB(25),WT(6)
      DIMENSION R10(6),R20(6),R30(6),PE(6),X(210)
      COMMON/SAM/PP,T,PE,N
      COMMON/OMAR/ACT1(6),ACT3(6),R10,R20,R30
      IFLAG=0
      DO 911 I=1,N
      PP(I,1)=X(I)
      PP(I,2)=X(I+N)
      PP(I,3)=X(I+2*N)
      PP(I,4)=X(I+3*N)
      PP(I,5)=X(I+4*N)
911   CONTINUE
C     CALCULATION OF DIFFUSIVITIES FOR DIFFERENT COMPONENTS
      DT=0.00468*SQRT((T/323.)*2/92.11)
      DW=0.0234*SQRT((T/323.)*2/18.0)
      DB=0.0234*SQRT((T/323.)*2/78.11)
      DC1=0.0234*SQRT((T/323.)*2./28.)
      DC=0.0234*SQRT((T/323.)*2/44.)
      DH=0.0234*SQRT((T/323.))
      RC=0.0127/12.0
C     UNIT OF RC= METER = DIXON AND CRESSWELL APPROXIMATION
C     CALCULATION OF RIGHT HAND CONSTANT= Rp*R*T/Diff*RC**2
      PHI=956.0*0.082*T*(RC)**2
      PHIT=PHI*1.0/DT
      PHIW=PHI/DW
      PHIB=PHI/DB
      PHIC1=PHI/DC1
      PHIC=PHI/DC
      PHIH=PHI/DH
C     WEIGHT OF RESIDUSLS FROM COLLOCATION  PROGRAMME
C     ------------------------------------------------------------
      DO 23 I=1,N
      R10(I)=0.
      R20(I)=0.
      R30(I)=0.
```

```
23    CONTINUE
      A=37.471-3*ALOG(T)
      D=(16.748/2)*.001*T+0.23917-8.08*1.E-06*T*T
      FA=9542.03*(1./T-1./298.)
      EQ=EXP((1.0/1.987)*(A+D+FA))
      RK1=3.054E5*EXP(-22307./(1.987*T))
      RK2=3.180E3*EXP(-18176./(1.987*T))
      RK3=4.003E9*EXP(-32910./(1.987*T))
      AKW=3.90E-2*EXP(5940./(1.987*T))
      AKW2=0.5900*EXP(4502./(1.987*T))
      AKT=9.10E-2*EXP(8709./(1.987*T))
      AKT2=0.030*EXP(10217./(1.987*T))
      AKC1=2.111*EXP(7583./(1.987*T))
      AKC2=3.09E-8*EXP(26989./(1.987*T))
      AKR=1.69
      AKR2=0.32
      AKWT=AKT*AKW
      AKWT2=AKT2*AKW2
104   DO 4 I=1,N
      PP(I,6)=-9.*(DB/DH)*(PP(I,3)-PE(3))-11.*DT/DH*(PP(I,1)
     1  -PE(I))+DC/DH*(PP(I,5)-PE(5))+PE(6)
      SITE1=(1.+AKW*PP(I,2))
      SITE11=(1.+AKW2*PP(I,2))
      SITE2=(1.+AKT*PP(I,1)+AKC1*(PP(I,4)**2)+AKR*(PP(I,3)
     1 +PP(I,5)+ PP(I,6)))
      SITE22=(1.+AKT2*PP(I,1)+AKC2*(PP(I,4))+AKR2*(PP(I,3)
     1 +PP(I,5)+ PP(I,6)))
      R1O(I)=R1O(I)+RK1*AKWT*PP(I,1)*PP(I,2)/(SITE1*SITE2)
      R2O(I)=R2O(I)+RK2*AKWT2*PP(I,1)*(PP(I,2)**2)/(SITE11*
     1SITE22)
      R3O(I)=R3O(I)+RK3*AKW2*AKC2*(PP(I,4)*PP(I,2)-(PP(I,6)
     1 *PP(I,5)/EQ))/(SITE11*SITE22)
4     CONTINUE
      PRINT *,R1O,R2O,R3O
      DO 5 I=1,N
      BBB(I)=PHIT*(R1O(I)*ACT1(I)+R2O(I))-B(I,N+1)*PP(N+1,1)
5     CONTINUE
      DO 6 I=N+1,2*N
```

```
      BBB(I)=PHIW*(R10(I-N)*ACT1(I-N)+7*R20(I-N)+R30(I-N)
     1   *ACT3(I-N))-B(I-N,N+1)*PP(N+1,2)
6     CONTINUE
      DO 7 I=2*N+1,3*N
      K=2*N
      BBB(I)=-PHIB*(R10(I-K)*ACT1(I-K))-B(I-K,N+1)*PP(N+1,3)
7     CONTINUE
      DO 8 I=3*N+1,4*N
      KK=3*N
      BBB(I)=-(PHIC1*(R10(I-KK)*ACT1(I-KK)+7*R20(I-KK)
     1  -R30(I,KK) *ACT3(I-KK)))-B(I-KK,N+1)*PP(N+1,4)
8     CONTINUE
      DO 9 I=4*N+1,5*N
      KL=4*N
      BBB(I)=-PHIC*(R30(I-KL)*ACT3(I-KL))-B(I-KL,N+1)*PP(N+1,5)
9     CONTINUE
      NNN=5*N
      DO 75 I=1,NNN
      RES(I)=0.0
75    CONTINUE
      DO 111 I=1,NNN
      DO 112 J=1,NNN
      RES(I)=RES(I)+C(I,J)*X(J)
112   CONTINUE
111   CONTINUE
      DO 951 I=1,NNN
      FVEC(I)=RES(I)-BBB(I)
951   CONTINUE
      FVECK=FVEC(M)
      RETURN
      END
C     For maximum efficiency order your functions in AUXFCN so that
C      the linear functions come first. Then the functions
C      become progresssively-
C      more nonlinear with most nonlinear function coming last.
      SUBROUTINE  NONLIN(N,NUMSIG,MAXIT,IPRINT,X,EPS,ASTER,ND)
C      This subroutine solves a system of N simultanious nonlinear
C     equations.The method used is at least quadratically convergent
```

```
C    and requires only (N**2/2+3*N/2) function evaluations per
C    iterative step as compared with (N*2+N) evaluations for
C     NEWTON'S method.
C     This results in a savings of computational effort for
C      sufficiently
C     complicated functions. The method does not require the userto
C     furnish any deratives.
C     INPUT PARAMETERS FOLLOW :
C     N = Number eqations (= number of unknowns)
C     NUMSIG = Number of significant digits desired.
C     MAXIT = Maximum number of iterations to be used.
C    IPRINT = Output option,output if =1;hower,failure indications
C     are always output;MAXIT exceed and singular Jacobian.
C     X  = Vector of initial guesses.
C     EPS = Convergence criterion.Iteration will be terminated if
C     ABS(F(I)).LT.EPS,I=1,...,N,where F(I) denoates the I th
C     funtion in the system.
C     Convergence criterion is considered to be met if either
C     the numbr of the function values is satisfied. To force the
C     iteration to be terminated by one of the criteria,simply set
C     the other one to be
C     very stringent.
C     OUTPUT PAPAMETERS FOLLOW :
C     NIT = Number of iterations used.
C     X  = Solution of the system (or best approximation therto).
C     DOUBLE PRECISION X,Y,PART,TEMP,COE,BOE
      DIMENSION  X(210),PART(210),TEMP(210),COE(22550)
      DIMENSION Y(210)
C     DOUBLE PRECISION RELCON,F,FACTOR,HOLD,H,FPLUS,DERMAX,TEST

C     DOUBLE PRECISION FMAX
      DIMENSION  ISUB(210),LOOKUP(210),BOE(210)
C DELTA WILL BE A FUNCTION OF THE MACHIENE AND THE PRECESSION USED
      DELTA = 1.E-7
      RELCON = 10.E+0**(-NUMSIG)
      JTEST  = 1
      DO 700 M =1,MAXIT
```

```
      IQUIT = 0
      IFLAG=1
      FMAX = 0.
      M1 = M-1
      IF(IPRINT.NE.1)  GO TO 9
      OPEN(UNIT=ND,FILE='OUT.FOR')
49    FORMAT(I5,7E18.8/(E23.8,6E18.8)/)
102   FORMAT(I5,7E18.8/(E23.8,6E18.8)/)
9     DO  10 J=1,N
10    LOOKUP(J)=J
C     The array LOOKUP permits a partial effect without having to
C     phisica interchange rows or columns.
C     PRINT 130,N
130   FORMAT(1X,'N=',I3)
      DO 500  K=1,N
      IF(K-1) 134,134,131
131   KMIN=K-1
C     PRINT 132,KMIN
132   FORMAT(1X,'KMIN=',I3)
      CALL BACK(KMIN,N,X,ISUB,COE,BOE,LOOKUP)
C     Set up partial deratives of Kth function..
134   CALL AUXFCN(X,F,K)
      FMAX= AMAX1(FMAX,ABS(F))
      IF(ABS(F) .GE.EPS) GO TO 1345
      IQUIT=IQUIT+1
      IF(IQUIT.NE.N)  GOTO 1345
      GOTO 725
1345  FACTOR = .001E+00
135   ITALLY = 0.
      DO 200 I=K,N
      ITEMP = LOOKUP(I)
      HOLD = X(ITEMP)
      PREC = 5.E-6
C     PREC IS THE FUNCTION OF THE MACHINE SIGNIFICANCE,SIG,AND
C      SHOULD   C    BE COMPUTED AS PREC = 5.*(-SIG+2).IN THIS
C      INSTANCE WE WERE DEALING WITH AN 8 DIGIT MACHINE.
      ETA = FACTOR*ABS(HOLD)
      H = AMIN1(FMAX,ETA)
```

```
      IF(H.LT.PREC)  H=PREC
      X(ITEMP) = HOLD+H
      IF(K-1)  161,161,151
151    CALL BACK(KMIN,N,X,ISUB,COE,BOE,LOOKUP)
161    CALL  AUXFCN(X,FPLUS,K)
      PART(ITEMP)  = (FPLUS-F)/H
      X(ITEMP) = HOLD
      IF(ABS(PART(ITEMP)).LT.DELTA)  GOTO 190
      IF(ABS(F/PART(ITEMP)).LE.1.E+15)  GOTO 200
190    ITALLY = ITALLY+1
200    CONTINUE
      IF(ITALLY.LE.N-K)  GOTO 202
      FACTOR = FACTOR*10.0E+00
      IF(FACTOR.GT.11)  GOTO 775
      GOTO  135
202    IF(K.LT.N)  GOTO 203
      IF(ABS(PART(ITEMP)).LT.DELTA)  GOTO  775
      BOE(N) = 0.0E+00
      KMAX = ITEMP
      GOTO  500
C     Find partial deratives of largest absolute value.
203    KMAX  = LOOKUP(K)
      DERMAX = ABS(PART(KMAX))
      KPLUS = K+1
      IJ=K
      DO 210  I=KPLUS,N
      JSUB = LOOKUP(I)
      TEST = ABS(PART(JSUB))
      IF(TEST.LT.DERMAX)  GOTO 210
      DERMAX = TEST
      IJ=I
      KMAX = JSUB
210    CONTINUE
      IF(IJ.EQ.K)  GOTO 205
      IG=IJ+KPLUS
      DO 209 I=KPLUS,IJ
      IS=IG-I
209     LOOKUP(IS)=LOOKUP(IS-1)
```

```
205     IF(ABS(PART(KMAX)).EQ.0.0) GOTO 775
C     Set up coefficients for Kth row of triangular linear system
C     used to back-solve for the first K values ofX(I)
      LOOKUP(K)=0
      ISUB(K) = KMAX
      BOE(K) = 0.0E+00
      LAG=(K-1)*(N-FLOAT(K)/2)-K
      DO 220 J = KPLUS,N
      L=LAG+J
      JSUB = LOOKUP(J)
      COE(L)=-PART(JSUB)/PART(KMAX)
      BOE(K)=BOE(K)+PART(JSUB)*X(JSUB)
220     CONTINUE
500     BOE(K)=(BOE(K)-F)/PART(KMAX)+X(KMAX)
C      Back substitute to obtaiin next approximation to X.
      X(KMAX) = BOE(N)
      IF(N.EQ.1)  GOTO 610
      CALL  BACK(N-1,N,X,ISUB,COE,BOE,LOOKUP)
610     IF(M-1)  650,650,625
C        Test for convergence.
625    DO 630 I=1,N
      IF(ABS(TEMP(I)-X(I)).GT.ABS(X(I))*RELCON)  GOTO 649
630    CONTINUE
      JTEST = JTEST + 1.
      IF(JTEST-3)  650,725,725
649    JTEST = 1
650    DO 660 I = 1,N
660    TEMP(I) = X(I)
700    CONTINUE
C      OPEN(UNIT=ND,FILE='OUT.FOR')
      WRITE(ND,1753)
1753 FORMAT(5X,'NO CONVERGENCE.MAXIMUM NUMBER OF ITERATIONS USED')
      ASTER=1.
      PRINT  334
334 FORMAT(/5X,'NO CONVERGENCE.MAXIMUM NUMBER OF ITERATIONS USED.')
      IF(IPRINT.NE.1) GOTO 800
      WRITE(ND,1763)
1763 FORMAT(5X,'FUNCTION VALUES AT  LAST APPROXIMATION FOLLOW.:'/)
```

```
      PRINT 335
335 FORMAT(5X,'FUNCTION VALUES AT  LAST APPROXIMATION FOLLOW :'/)
      IFLAG = 1
      GO TO 7777
725   IF(IPRINT.NE.1)  GOTO 800
7777 DO 750 K = 1,N
      CALL  AUXFCN(X,PART(K),K)
750    CONTINUE
      IF(IFLAG.NE.1) GOTO 8777
C     WRITE(ND,7788)  (PART(K),K = 1,N)
7788   FORMAT(6E20.8)
C       PRINT  336, (PART(K),K=1,N)
C336    FORMAT(6E20.8)
      GOTO  800
8777   WRITE(ND,751)
751    FORMAT(//'CONVERGENCE BEEN ACHIEVED.THE FUNCTION VALUES.')
      WRITE(ND,7515)  (PART(K),K = 1,N)
7515 FORMAT(5X,'AT THE FINAL APPROXIMATION FOLLOW:'//(6E20.8)/)
      ASTER=2.
      GOTO  800

775   CONTINUE
752    FORMAT(//5X,'MODIFIED JACOBIAN IS SINGULAR.TRY A DIFFERENT')
      WRITE(ND,7525)
 7525 FORMAT(5X,'INITIAL APPROXIMATION.')
      ASTER=3.
800    MAXIT = M1+1
      RETURN
      END
      SUBROUTINE  BACK(KMIN,NM,X,ISUB,COE,BOE,LOOKUP)
C     DOUBLE PRECISION X,COE,BOE
C     Thid subroutine back-solves the first KMIN rows of a triangu-
C     laa rized linear system for improved X values in terms of
C     previous ones.
      DIMENSION  X(210),COE(22550),BOE(210)
      DIMENSION  ISUB(210),LOOKUP(210),DUMMY(210)
      KBACK=KMIN
      PRINT 81,KBACK
81    FORMAT(1X,'KBACK=',I3)
```

```
      N=NM
      KZA=KMIN+1
      DO 30 I=KZA,N
30    DUMMY(I)=LOOKUP(I)
      DO  200 KK = 1,KMIN
      KM = KMIN-KK+2
      KMAX = ISUB(KM-1)
      X(KMAX) = 0.0E+00
      LAG=(KM-2)*(N-FLOAT(KM-1)/2)-(KM-1)
      IC=0
      DO 100 J=KM,N
      L=LAG+J
      IF(KM.EQ.KZA) GOTO 20
      IF(IC.EQ.1) GOTO 20
      IF(J.EQ.N) GOTO 25
      JSUB=DUMMY(J+1)
      IF(JSUB.LT.ISUB(KM)) GOTO 15
      IC=1
25    JSUB=ISUB(KM)
15    DUMMY(J)=JSUB
      GOTO 10
      JSUB=DUMMY(J)
10    X(KMAX)=X(KMAX)+COE(L)*X(JSUB)
100   CONTINUE
      X(KMAX) = X(KMAX)+BOE(KM-1)
200    CONTINUE
      RETURN
      END
```

```
C       This programme is used to calculate Orthogonal-collocation
C       Points which are used in the earlier computer programme.

      SUBROUTINE COLL(A,B,Q,X,W,ND,N,AA)
C     IMPLICIT REAL *8 (A-H,O-Z)
      DIMENSION A(ND,ND),B(ND,ND),Q(ND,ND),X(ND),W(ND)
      DIMENSION QINV(10,10),Z(10),C(10,10),D(10,10)
      COMMON/ONE/X1(20)
      N1=N+1
C     THIS SUBROUTINE COMPUTES THE  MATRICES FOR ORTHOGONAL
C     COLLOCATION   USING SYMMETRIC POLYNOMIALS
      DO 57 I=1,N
      X(I)=X1(I)
57    CONTINUE
      X(N1)=1.0
      DO 30 I=1,N1
      AI=I
      Z(I)=1./(2.*AI+AA-2.)
30    CONTINUE
      DO 35 I=1,N1
      Q(I,1)=1.
      QINV(I,1)=1.
      DO 35 J=2,N1

      Q(I,J)=X(I)**(2*J-2)
35    QINV(I,J)=Q(I,J)
      DO 40 J=1,N1
      CA=2.*J-2.
      DA=(2.*J-2.)*(2.*J+AA-4.)
      DO 40 I=1,N1
      C(I,J)=CA*X(I)**(2*J-3)
      D(I,J)=DA*X(I)**(2*J-4)
40    CONTINUE
      CALL INVR (QINV,N1,10)
      DO 50 I=1,N1
      W(I)=0.0
```

```
      DO 50 J=1,N1
      A(I,J) =0.0
      b(i,j)=0.0
      DO 45 K=1,N1
      A(I,J)=A(I,J)+C(I,K)*QINV(K,J)
      B(I,J)=B(I,J)+D(I,K)*QINV(K,J)
45    CONTINUE
      Q(I,J)=QINV(I,J)
      W(I)=W(I)+Z(J)*QINV(J,I)
50    CONTINUE
C     WRITE(60,12) (X(I),I=1,N1)
12    FORMAT(3E16.5)
13    FORMAT('BIJ VALUES ARE ')
      WRITE(60,13)
      WRITE(62,55)((B(I,J),I=1,N1),J=1,N1)
55    FORMAT (9E16.5/)
      RETURN
      END
      SUBROUTINE INVR(A,N,NI)
C     IMPLICIT REAL *8 (A-H,O-Z)
      DIMENSION A(NI,NI),B(20),C(400)
      DO 5 J=1,N
      IND=N*(J-1)
      DO 5 I=1,N
      C(IND+I)=A(I,J)
5     CONTINUE
      CALL INVERT(N,1,C,B,1)
      DO 20 J=1,N
      DO 10 I=1,N
10    B(I)=0.
      B(J)=1.
      CALL INVSW(N,1,C,B,1)
      DO 15 I=1,N
      A(I,J)=B(I)
15    CONTINUE
20    CONTINUE
      RETURN
      END
```

```
      SUBROUTINE INVERT(N,NE,A,B,ITYPE)
C     IMPLICIT REAL *8 (A-H,O-Z)

      DIMENSION A(1000,3),B(N),A1(1000),B1(1000),C1(1000)
      GO TO (5,10,15),ITYPE
5     CALL DECOMP(N,A)
      RETURN
10    NP=(N-1)/NE+1
      PAUSE 14
      CALL LUDECO(NP,NE,A)
      RETURN
15    DO 20 K=1,N
      A1(K)=A(K,1)
      B1(K)=A(K,2)
      C1(K)=A(K,3)
20    CONTINUE
      CALL INVTRI(N,A1,B1,C1)
      DO 25 K=1,N
      A(K,1)=A1(K)
      A(K,2)=B1(K)
      A(K,3)=C1(K)
25    CONTINUE
      RETURN
      ENTRY INVSW
      GO TO (30,35,40) ,ITYPE
30    CALL SOLVE(N,A,B)
      RETURN
35    CALL FAS(NP,NE,N,A,B)
      RETURN
40    CALL SWEEP(N,A1,B1,C1,B)
      RETURN
      END
      SUBROUTINE SING(I)
      GO TO (5,15),I
5      WRITE(60,10)
10    FORMAT('MATRIX WITH ZERO ROW DECOMPOSE')
      RETURN
15    WRITE(60,20)
```

```
20    FORMAT('SINGULAR MATRIX IN DECOMPOSE. ZERO IN SOLVE ')
      RETURN
      END
      SUBROUTINE DECOMP(N,A)
C     IMPLICIT REAL *8 (A-H,O-Z)
      DIMENSION A(N,N)
      COMMON /DENSE/ IPS(201),SC(201)
      IF (N .EQ. 1) RETURN
      DO 25 I=1,N
      IPS(I)=I
      ROWNRM=0.0
      DO 10 J=1,N
      IF (ROWNRM-ABS(A(I,J))) 5,10,10
5     ROWNRM =ABS(A(I,J))
10    CONTINUE
      IF (ROWNRM) 15,20,15
15    SC(I)=1./ROWNRM
      GO TO 25
20    CALL SING(1)
      SC(I)=0.
25    CONTINUE
      NM1=N-1
      DO 65 K=1,NM1
      BIG=0.
      DO 35 I=K,N
      IP=IPS(I)
      SIZE=ABS(A(IP,K)*SC(IP))
      IF (SIZE-BIG) 35,35,30
30    BIG=SIZE
      IDXPIV=I
35    CONTINUE
      IF (BIG) 45,40,45
40    CALL SING(2)
      GO TO 65
45    IF (IDXPIV-K) 50,55,50
50    J=IPS(K)
      IPS(K)=IPS(IDXPIV)
      IPS(IDXPIV)=J
```

```
55    KP=IPS(K)
      PIVOT=A(KP,K)
      KP1=K+1
      DO 60 I=KP1,N
      IP=IPS(I)
      EM=-A(IP,K)/PIVOT
      A(IP,K)=-EM
      DO 60 J=KP1,N
      A(IP,J)=A(IP,J)+EM*A(KP,J)
60    CONTINUE
65    CONTINUE
      KP=IPS(N)
      IF (A(KP,N)) 75,70,75
70   CALL SING(2)
75    CONTINUE
      RETURN
      END
      SUBROUTINE SOLVE(N,A,B)
      DIMENSION A(N,N),B(N)
      COMMON /DENSE/ IPS(201),SC(201)
      IF (N .GT. 1) GO TO 5
      B(1)=B(1)/A(1,1)
      RETURN
5     CONTINUE
      NP1=N+1
      IP=IPS(1)
      SC(1)=B(IP)
      DO 15 I=2,N
      IP=IPS(I)
      IM1=I-1
      SUM=0.
      DO 10 J=1,IM1
      SUM=SUM+A(IP,J)*SC(J)
10    CONTINUE
      SC(I)=B(IP)-SUM
15    CONTINUE
      IP=IPS(N)
      SC(N)=SC(N)/A(IP,N)
```

```
      DO 25 IBACK=2,N
      I=NP1-IBACK
      IP=IPS(I)
      IP1=I+1
      SUM=0.
      DO 20 J=IP1,N
      SUM=SUM+A(IP,J)*SC(J)
20    CONTINUE
      SC(I)=(SC(I)-SUM)/A(IP,I)
25    CONTINUE
      DO 30 I=1,N
30    B(I)=SC(I)
      RETURN
      END
      SUBROUTINE FAS(NP,NE,NT,A,B)
      DIMENSION A(NP,NP,NE),B(NT)
      NP1=NP
      DO 10 L=1,NE
      DO 10 I=2,NP1
      I2=(L-1)*(NP-1)+I
      S=0.
      I1=I-1
      DO 5 J=1,I1
      J2=I2-I+J
      S=S+A(I,J,L)*B(J2)
5     CONTINUE
      B(I2)=B(I2)-S
10    CONTINUE
      DO 25 L1=1,NE
      L=NE-L1+1
      IF (L.NE.NE) GO TO 15
      B(NT)=B(NT)/A(NP,NP,NE)
15    N1=NP-1
      DO 25 K=1,N1
      I=N1+1-K
      I2=(L-1)*(NP-1)+I
      M=I+1
      N2=N1+1
```

```
      S=0.
      DO 20 J=M,N2
      J2=(L-1)*(NP-1)+J
20    S=S+A(I,J,L)*B(J2)
      B(I2)=(B(I2)-S)/A(I,I,L)
25    CONTINUE
      RETURN
      END
      SUBROUTINE LUDECO(NP,NE,A)
      DIMENSION A(NP,NP,NE)
      N1=NP-1
      DO 10 L=1,NE
      DO 5 K=1,N1
      K1=K+1
      DO 5 I=K1,NP
      S=A(I,K,L)/A(K,K,L)
      A(I,K,L)=S
      DO 5 J=K1,NP
      A(I,J,L)=A(I,J,L)-S*A(K,J,L)
5     CONTINUE
      IF  (L.EQ.NE) RETURN
      A(1,1,L+1)=A(NP,NP,L)
10    CONTINUE
      END
      SUBROUTINE INVTRI(N,A,B,C)
C     IMPLICIT REAL *8 (A-H,O-Z)
      DIMENSION A(N),B(N),C(N)
      DO 5 L=2,N
      S=A(L)/B(L-1)
      B(L)=B(L)-S*C(L-1)
5     A(L)=S
      RETURN
      END
      SUBROUTINE SWEEP(N,A,B,C,D)
C     IMPLICIT REAL *8 (A-H,O-Z)
      DIMENSION A(N),B(N),C(N),D(N)
      DO 5 L=2,N
5     D(L)=D(L)-A(L)*D(L-1)
```

```
      D(N)=D(N)/B(N)
      DO 10 L=2,N
      K=N-L+1
10    D(K)=(D(K)-C(K)*D(K+1))/B(K)
      RETURN
      END
```